

**REDUCTION, ANALYSIS, AND
INTERPRETATION OF DATA COLLECTED
IN THE LAGUNA MADRE BY
CONRAD BLUCHER INSTITUTE
1994 - 1998**



An employee-owned company

Document No 991034
PBS&J Job No 449708

HYDROGRAPHIC MONITORING IN THE LAGUNA MADRE:

**REDUCTION, ANALYSIS, AND
INTERPRETATION OF DATA COLLECTED BY
CONRAD BLUCHER INSTITUTE
1994 - 1998**

**Prepared for:
USACE, Galveston
2000 Fort Point Road
Galveston, Texas 77550**

**Prepared by
PBS&J
206 Wild Basin Road
Suite 300
Austin, Texas 78746-3343
and**

**Dr. George Ward, CRWR
The University of Texas at Austin
10100 Burnet Road
Austin, Texas 78758**

September 1999

Printed on Recycled Paper

TABLE OF CONTENTS

<u>Section</u>	<u>Page</u>
Executive Summary	ii
List of Figures	iv
List of Tables	viii
Preface	xi
1 0 <u>INTRODUCTION</u>	1-1
1 1 STUDY AREA AND BACKGROUND	1-2
1 2 STUDY DISCUSSION	1-4
2 0 <u>FIELD DATA COLLECTION</u>	2-1
2 1 MONITORING PLATFORMS AND INSTRUMENTATION	2-1
2 1 1 <u>Description of Monitoring Platforms</u>	2-5
2.1.2 <u>Platform Maintenance</u>	2-8
2.1 3 <u>Instrumentation</u>	2-8
2 2 OTHER AVAILABLE DATA	2-11
3 0 <u>DATA VALIDATION AND SCRUBBING</u>	3-1
3.1 DATA ACQUISITION AND SCREENING	3-1
3.2 IDENTIFICATION AND TREATMENT OF DATA ANOMALIES	3-4
3 3 SUMMARY OF DATA SETS	3-10
4 0 <u>THE HYDROGRAPHIC ENVIRONMENT</u>	4-1
4 1 WIND	4-1
4 2 WATER LEVEL	4-6
4 3 FREQUENCY DOMAIN ANALYSIS OF WIND AND WATER LEVEL	4-19
4 4 TEMPERATURE AND SALINITY	4-45
5.0 <u>CURRENTS</u>	5-1
5.1 GENERAL FEATURES OF CURRENTS IN THE LAGUNA MADRE	5-1
5.2 THE CURRENT VECTOR	5-14
5.3 FREQUENCY DOMAIN ANALYSIS	5-47
6 0 <u>SEDIMENTS AND THEIR RESUSPENSION</u>	6-1
7 0 <u>INTERACTION IN THE LAGUNA MADRE</u>	7-1
7 1 HYDROGRAPHIC INTERACTIONS AND SUSPENDED SEDIMENT	7-1
7 1 1 <u>Summer Conditions</u>	7-1
7 1 2 <u>Winter Frontal Conditions</u>	7-7
7 1.3 <u>TSS and Currents</u>	7-12

TABLE OF CONTENTS (Concluded)

<u>Section</u>		<u>Page</u>
7.2	PREDOMINANT CIRCULATIONS AND PREFERENTIAL TRANSPORT DIRECTIONS	7-22
7.3	HYDROGRAPHIC PROCESSES AND SEDIMENT TRANSPORT	7-35
8.0	<u>CONCLUSIONS AND RECOMMENDATIONS</u>	8-1
9.0	<u>REFERENCES</u>	9-1
	Appendix SR - Event chronologies	
	Appendix WR - Annual and Monthly Wind Roses	
	Appendix WF - Annual and Monthly Wind Speed Spectra	
	Appendix LF - Annual and Monthly Water Level Spectra	
	Appendix CS - Scatter Plots of Currents	
	Appendix CR - Annual and Monthly Current Roses	
	Appendix CS - Scatter Plots of Current	
	Appendix CF - Monthly Current Speed Spectra	
	Appendix TF - Frequency of Occurrence of Suspended Solids Concentrations	
	Appendix TF - TSS Data Summary	
	Appendix TS - Total Suspended Solids Time Series Plots	
	Appendix A - Time Series Plots of Air Temperature at Corpus Christi NAS, Harlingen International Airport, and Brownsville International Airport	
	Appendix B - Annotated Time-Series Plots of Raw Data and Screening Results	

LIST OF FIGURES

<u>Figure</u>		<u>Page</u>
1-1	Study Area	1-3
2-1	Lower Laguna Madre Map	2-2
2-2	Upper Laguna Madre Map	2-3
2-3	Photograph of Monitoring Platform LLM1	2-6
3-1	Display Screen for Program INSPECT	3-5
4-1	Monthly Wind Rose at TCOON Station - Arroyo Colorado	4-7
4-2	Monthly Wind Rose at TCOON Station - S Bird Island	4-9
4-3	Annual Wind Rose at TCOON Station - Arroyo Colorado	4-11
4-4	Annual Wind Rose at TCOON Station - S. Bird Island	4-12
4-5	Water Levels at Arroyo Colorado	4-13
4-6	Water Levels at S Bird Island	4-14
4-7	Seasonal Variations in Water Levels at Arroyo Colorado	4-16
4-8	Seasonal Variations in Water Levels at South Bird Island	4-17
4-9	Annual Wind Spectra at TCOON Station - Arroyo Colorado	4-20
4-10	Annual Wind Speed Spectra at TCOON Station - South Bird Island	4-22
4-11	Monthly Wind Speed Spectra at TCOON Station - Arroyo Colorado	4-25
4-12	Monthly Wind Speed Spectra at TCOON Station - Arroyo Colorado	4-26
4-13	Monthly Wind Speed Spectra at TCOON Station - Arroyo Colorado	4-27
4-14	Monthly Wind Speed Spectra at TCOON Station - Arroyo Colorado	4-28
4-15	Monthly Wind Speed Spectra at TCOON Station - South Bird Island	4-29
4-16	Monthly Wind Speed Spectra at TCOON Station - South Bird Island	4-30
4-17	Monthly Wind Speed Spectra at TCOON Station - South Bird Island	4-31
4-18	Monthly Wind Speed Spectra at TCOON Station - South Bird Island	4-32
4-19	Annual Water Level Spectra at TCOON Station - Arroyo Colorado	4-33
4-20	Annual Water Level Spectra at TCOON Station - South Bird Island	4-35
4-21	Monthly Water Level Spectra at TCOON Station - Arroyo Colorado	4-37
4-22	Monthly Water Level Spectra at TCOON Station - Arroyo Colorado	4-38
4-23	Monthly Water Level Spectra at TCOON Station - Arroyo Colorado	4-39
4-24	Monthly Water Level Spectra at TCOON Station - Arroyo Colorado	4-40
4-25	Monthly Water Level Spectra at TCOON Station - South Bird Island	4-41
4-26	Monthly Water Level Spectra at TCOON Station - South Bird Island	4-42
4-27	Monthly Water Level Spectra at TCOON Station - South Bird Island	4-43
4-28	Monthly Water Level Spectra at TCOON Station - South Bird Island	4-44

LIST OF FIGURES

<u>Figure</u>		<u>Page</u>
4-29	Squared Coherency between South Bird Island and Arroyo Colorado Water Levels	4-46
4-30	Squared Coherency between Wind Speed and Water Level at Arroyo Colorado	4-47
4-31	Squared Coherency between Wind Speed and Water Level at South Bird Island	4-48
5-1	Annual Current Rose at LLM1 Station	5-16
5-2	Annual Current Rose at LLM2a/N Station	5-17
5-3	Annual Current Rose at LLM3N Station	5-18
5-4	Annual Current Rose at ULM1 Station	5-19
5-5	Annual Current Rose at ULM2 Station	5-20
5-6	Annual Current Rose at ULM3 Station	5-21
5-7	Scatter Plots of Currents at Station LLM1	5-22
5-8	Scatter Plots of Currents at Station LLM1	5-23
5-9	Scatter Plots of Currents at Station LLM1	5-24
5-10	Scatter Plots of Currents at Station LLM1	5-25
5-11	Scatter Plots of Currents at Station LLM2a/N	5-26
5-12	Scatter Plots of Currents at Station ULM1	5-27
5-13	Scatter Plots of Currents at Station ULM1	5-28
5-14	Scatter Plots of Currents at Station ULM1	5-29
5-15	Scatter Plots of Currents at Station ULM2	5-30
5-16	Scatter Plots of Currents at Station ULM3	5-31
5-17	Scatter Plots of Currents at Station ULM3	5-32
5-18	Monthly Current Rose at LLM1 Station	5-33
5-19	Monthly Current Rose at LLM1 Station	5-34
5-20	Monthly Current Rose at LLM1 Station	5-35
5-21	Monthly Current Rose at LLM1 Station	5-36
5-22	Monthly Current Rose at LLM2a/N Station	5-37
5-23	Monthly Current Rose at ULM1 Station	5-38
5-24	Monthly Current Rose at ULM1 Station	5-39
5-25	Monthly Current Rose at ULM1 Station	5-40
5-26	Monthly Current Rose at ULM2 Station	5-41
5-27	Monthly Current Rose at ULM3 Station	5-42
5-28	Monthly Current Rose at ULM3 Station	5-43
5-29	Amplitude Spectrum Plots Lower Laguna Madre, September 1994	5-48
5-30	Amplitude Spectrum Plots Lower Laguna Madre, June 1995	5-49

LIST OF FIGURES

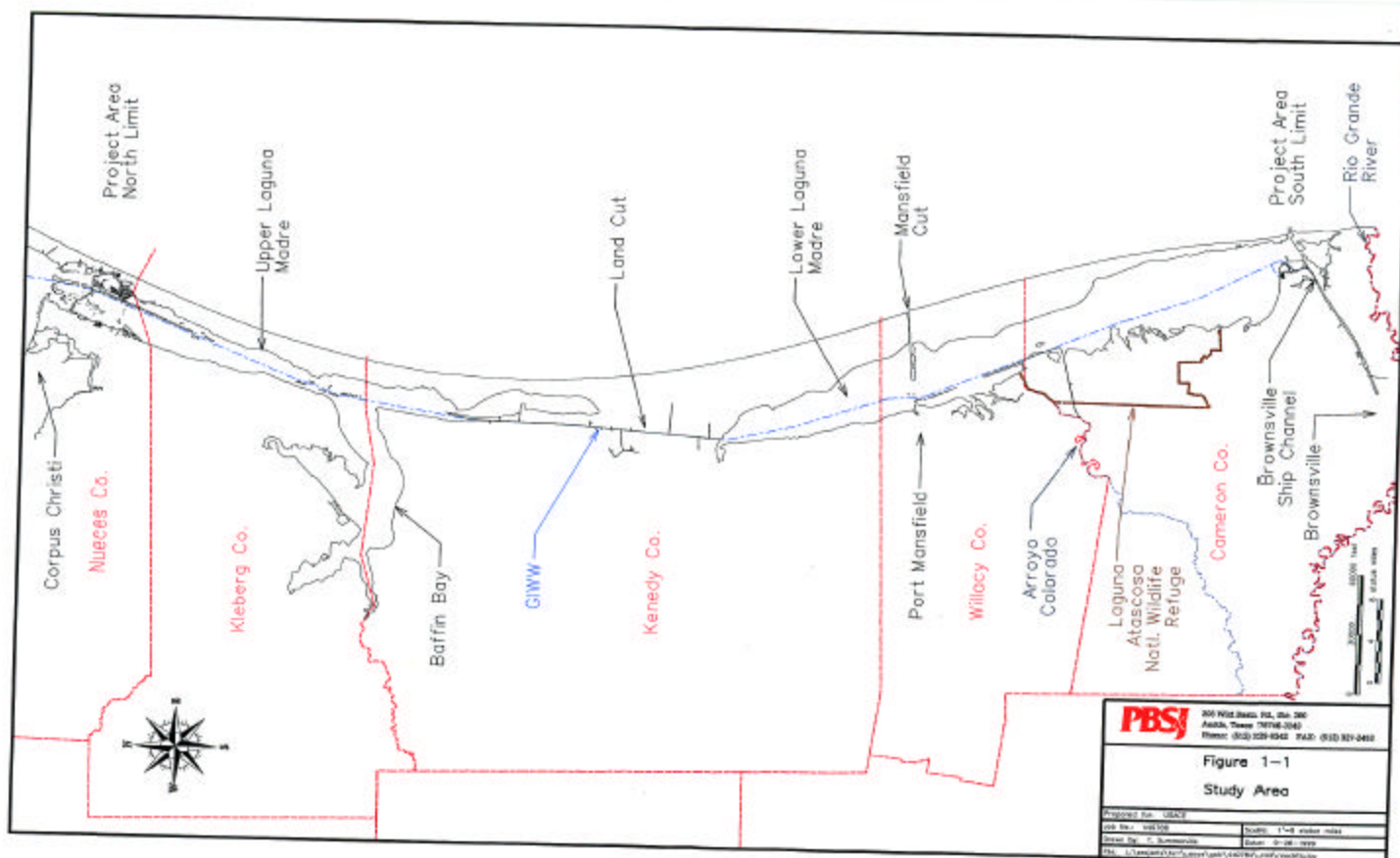
<u>Figure</u>		<u>Page</u>
5-31	Monthly Current Speed Spectra at Lower Laguna Madre Station 1	5-50
5-32	Monthly Current Speed Spectra at Lower Laguna Madre Station 1	5-31
5-33	Monthly Current Speed Spectra at Lower Laguna Madre Station 1	5-52
5-34	Monthly Current Speed Spectra at Lower Laguna Madre Station 1	5-53
5-35	Monthly Current Speed Spectra at Lower Laguna Madre Station 2A	5-54
5-36	Monthly Current Speed Spectra at Upper Laguna Madre Station 1	5-55
5-37	Monthly Current Speed Spectra at Upper Laguna Madre Station 1	5-56
5-38	Monthly Current Speed Spectra at Upper Laguna Madre Station 1	5-57
5-39	Monthly Current Speed Spectra at Upper Laguna Madre Station 2	5-58
5-40	Monthly Current Speed Spectra at Upper Laguna Madre Station 2	5-59
5-41	Monthly Current Speed Spectra at Upper Laguna Madre Station 2	5-60
5-42	Monthly Current Speed Spectra at Upper Laguna Madre Station 3	5-61
5-43	Monthly Current Speed Spectra at Upper Laguna Madre Station 3	5-62
5-44	Monthly Current Speed Spectra at Upper Laguna Madre Station 3	5-63
5-45	Monthly Current Speed Spectra at Upper Laguna Madre Station 3	5-64
6-1	Total Suspended Solids Levels at LLM Stations	6-4
6-2	Total Suspended Solids Levels at ULM Stations	6-6
7-1	LLM1 Water Level, Current, Turbidity, TSS and Wind Speed during Tidally-Dominated Flow	7-2
7-2	ULM1 Water Level, Current, Turbidity, TSS and Wind Speed during Tidally-Dominated Flow	7-4
7-3	ULM2 Water Level, Current, Turbidity, TSS and Wind Speed during Tidally-Dominated Flow	7-5
7-4	ULM3 Water Level, Current, Turbidity, TSS and Wind Speed during Tidally-Dominated Flow	7-6
7-5	LLM1 Water Level, Current, Turbidity, TSS and Wind Speed during Frontal Passage	7-8
7-6	ULM1 Water Level, Current, Turbidity, TSS and Wind Speed during Frontal Passage	7-9
7-7	ULM2 Water Level, Current, Turbidity, TSS and Wind Speed during Frontal Passage	7-10
7-8	ULM3 Water Level, Current, Turbidity, TSS and Wind Speed during Frontal Passage	7-11
7-9	Time Series of TSS and Current Components at LLM1	7-13
7-10	Time Series of TSS and Current Components at ULM1	7-14

LIST OF FIGURES

<u>Figure</u>		<u>Page</u>
7-11	Time Series of TSS and Current Components at ULM2	7-15
7-12	Time Series of TSS and Current Components at ULM3	7-16
7-13	Time Series of TSS at LLM1 and Wind Speed at Arroyo Colorado	7-18
7-14	Time Series of TSS at ULM1 and Wind Speed at S. Bird Island	7-19
7-15	Time Series of TSS at ULM2 and Wind Speed at S. Bird Island	7-20
7-16	Time Series of TSS at ULM3 and Wind Speed at S. Bird Island	7-21
7-17	TSS Versus Current Components and Wind Speed at LLM1	7-23
7-18	TSS Versus Current Components and Wind Speed at ULM1	7-24
7-19	TSS Versus Current Components and Wind Speed at ULM2	7-25
7-20	TSS Versus Current Components and Wind Speed at ULM3	7-26
7-21	Time Plot of Component Currents and Water Level at LLM2, March 1998	7-28
7-22	Scatterplot of LLM2 Currents for March 1998, Differentiating Before and After 12-17 March Outage	7-29
7-23	Scatterplot of LLM1 Currents for December 1994, Differentiating 6 December Transition	7-31
7-24	Computed Slope of Straight-Line Fit to Current Scatterplot by 25-hour Intervals, LLM1, December 1994	7-32
7-25	Computed Slope of Straight-Line Fit to Current Scatterplot by 25-hour Intervals, LLM1, November 1995	7-32
7-26	Computed Slope of Straight-Line Fit to Current Scatterplot by 25-hour Intervals, ULM1, July 1995	7-33
7-27	Computed Slope of Straight-Line Fit to Current Scatterplot by 25-hour Intervals, ULM2, July 1995	7-33
7-28	Lower Laguna Madre Showing High Maintenance Reach and Current Tragedy Proposed by James et al. (1977)	7-36

LIST OF TABLES

<u>Table</u>		<u>Page</u>
2-1	Platform Information	2-4
3-1	Comparison of Paired MSI and CBI Data for Temperature and Salinity	3-8
3-2	Summary of Laguna Madre Data Files	3-12
4-1	Frequency, Mean and Standard Deviation of Wind Speed at Arroyo Colorado	4-3
4-2	Frequency, Mean and Standard Deviation of Wind Speed at S Bird Island	4-4
4-9	Statistics of Temperature Data - Lower Laguna Madre	4-49
4-10	Statistics of Temperature Data - Upper Laguna Madre	4-50
4-11	Statistics of Salinity Data - Lower Laguna Madre	4-51
4-12	Statistics of Salinity Data - Upper Laguna Madre	4-52
5-1	Statistics of Current Data from Station LLM1	5-4
5-2	Statistics of Current Data from Station LLM2a/2N	5-6
5-3	Statistics of Current Data from Station LLM3	5-7
5-4	Statistics of Current Data from Station ULM1	5-8
5-5	Statistics of Current Data from Station ULM2	5-10
5-6	Statistics of Current Data from Station ULM3	5-12
6-1	Summary of Statistics for Total Suspended Solids	6-8



Because of concerns about the impacts of dredging and placement of maintenance material from the Gulf Intracoastal Waterway (GIWW) in the Laguna Madre, an Interagency Coordination Team (ICT) was formed to determine areas where there was inadequate information to address concerns. In August 1994, at the request of the ICT and through a Memorandum of Agreement between the U.S. Army Corps of Engineers (USACE), Galveston District and the Texas A&M Research Foundation, personnel from the Conrad Blucher Institute for Surveying and Science (CBI) at Texas A&M University-Corpus Christi (TAMU-CC), the Marine Science Institute of the University of Texas (UTMSI), and the Center for Coastal Studies (CCS) of TAMU-CC initiated a multi-disciplinary, multi-year study (the CBI Study), the first year of which has been described in Brown and Kraus (1997) and Militello *et al.* (1997).

The CBI study included the collection (and, originally, the reduction and interpretation) of the following types of data: current velocity, turbidity, salinity, pH, temperature, dissolved oxygen, chlorophyll-a, incident and underwater light irradiance (photosynthetically active radiation or PAR), total suspended solids (TSS), particle-size distribution, and, for the most recent data set, water-level data. These data were supplemented by water-level and wind measurements from Texas Coastal Ocean Observation Network (TCOON) platforms located at Port Isabel, Arroyo Colorado, and South Padre Island. The objectives of this multidisciplinary study were to assess water flow and sediment transport conditions and to identify possible modifications of the dredging practice to both reduce environmental impacts and to minimize the cost and frequency of dredging.

The CBI Study has collected an enormous volume of measurements, but the project has suffered from three inter-related problems: failure or questionable validity of portions of the data record, a consequence of the experimental nature of the equipment; lack of consistent data-recovery and pre-processing protocols, and substantial changes in personnel at CBI leading to discontinuity in staffing of the project. Previous reports developed in the CBI project, in addition to the two Year-1 reports cited above, include two data reports Brown (1997) and Ussery (1997, with an addendum, Ussery, 1998).

In April 1998, the ICT authorized, via a USACE Contract, the reduction and interpretation of the data from the CBI Study by PBS&J and Dr. George Ward (Present Study). Therefore, all available data collected from fixed-platform stations installed and maintained by CBI for the period of September 1994 through May 1998 have been retrieved, subjected to QA/QC analysis, and processed. The analysis of these processed data, including those discussed in the Year-1 reports, constitutes the basis for the present report. This report is therefore a composite effort of many contributors, including the previous reports Brown and Kraus (1997), Militello *et al.* (1997), Ussery (1997) and Brown (1997), from which text has been used where appropriate, and represents the efforts of these earlier investigators, the present staff of CBI,

especially Ms. Sara Ussery and Dr. Robert Benson, and the staff of PBS&J and Dr. Ward. The project study area description in this chapter and the original platform and instrument array (Chapter 2), in particular, are taken largely from Brown and Kraus (1997) and Militello *et al* (1997)

Because we have a larger base of data at our disposal, the data interpretation is new, even with respect to the Year-1 data, since, as described in detail in Chapter 3, during the Q/A effort for the present study, data problems emerged that were not accounted for in the earlier reports of Brown and Kraus (1997), Brown (1997), and Militello *et al* (1997). The present report does not, however, replace these earlier reports. Some of the chapters in Brown and Kraus (1997), Brown (1997), and Militello *et al* (1997) either (1) were only first year activities and are not included in the scope of the present project (e.g., the chapter concerned with the dredging-event sampling) or (2) are being reported separately by others (e.g., chapters on light attenuation and seagrass distribution) Brown and Kraus (1997), Brown (1997), Militello *et al* (1997), or Dunton (in preparation) should be consulted for that information.

1.1 STUDY AREA AND BACKGROUND

The Laguna Madre is a shallow, coastal embayment extending approximately 200 km (125 miles) southward from Corpus Christi Bay to Port Isabel, Texas, near the border with Mexico (Figure 1-1). The hypersaline conditions of the Laguna Madre are primarily attributed to the limited water exchange with the Gulf of Mexico, negligible fresh water inflow, and high evaporation rate (Breuer, 1962; Ward, 1997). Exchange between the Laguna Madre and the Gulf of Mexico is limited to three permanent openings: Brazos Santiago at the southern terminus of the Laguna Madre, Mansfield Pass, and Aransas Pass at the northern terminus via Corpus Christi Bay.

Based on area, the Laguna Madre comprises only 20% of the coastal embayments of Texas, but it contains approximately 80% of its seagrasses. Seagrass meadows cover most of the bottom of the Laguna Madre due to a combination of shallow depth and relatively low allochthonous inputs of suspended particles and nutrients (Quammen and Onuf, 1993). The high productivity of the Laguna Madre, inferred from finfish catch, has been well correlated with the presence of the extensive seagrass beds (TDWR, 1979).

The Laguna Madre is subdivided into two basins each with an average depth of about 1 m, referred to as the Upper Laguna Madre (ULM) and the Lower Laguna Madre (LLM). The basins are separated by a wind-tidal flat, the Saltillo Flats, about 40 km in length. The GIWW, with project dimensions of 4 m depth, 38 m bottom width, and 64 m top width, was dredged through the entire length of the Laguna Madre, from Corpus Christi Bay to Port Isabel in the 1940s. The Galveston District of the USACE completed the GIWW along the south Texas coast in 1949, connecting the upper and lower basins via the channel cut through Saltillo Flats, known as the Middle Ground (a.k.a., Land Bridge, Mudflats, Land Cut).

The construction of the GIWW is considered to have moderated the hypersaline conditions in the Laguna Madre. In the lower Laguna Madre, prior to the construction of the GIWW, salinities greater than 60 parts per thousand (ppt) were measured routinely. Subsequent to the construction of the GIWW, salinities rarely exceed 40 ppt (Quamman and Onuf, 1993). The ULM has no major stream tributaries. The lack of fresh water input coupled with the semi-arid climate (so that evaporation exceeds precipitation) has caused historical hypersaline conditions. Prior to the opening of the GIWW salinity values reached 100 ppt (Collier and Hedgpeth, 1950). Since opening of the GIWW through the ULM in 1949, salinity levels have been reduced and rarely reach the extremes observed prior to its opening. Salinity in the Upper Laguna Madre south of Baffin Bay did not rise above 60 ppt from 1967 to 1989 (Quamman and Onuf, 1993).

The predominant forcings responsible for the resuspension and transport of sediments include wind-induced currents, waves, tidal currents, and vessel-induced motions. Other factors that affect sediment transport, perhaps indirectly, are water depth, fetch, bottom morphology, sediment type (mineralogy, organic material), grain-size distribution, and bottom coverage of aquatic plants. During periods of strong winds, wave action and strong currents apply stress to the bottom, which, in turn, resuspend sediments into the water column. Once suspended, the sediment particles are transported by the currents to another, lower energy location where they are deposited. Some of these factors are examined in this report, while others are included in other reports for the ICT (Dunton, in preparation, EH&A 1998a, b, Lee Wilson Associates, 1998, Morton *et al* , 1998; Sheridan, 1998).

Several areas of environmental concern have been identified by these studies, especially with regard to seagrass health, relating to adverse effects of sediment resuspension and deposition. These include the reduction of light available through the water column, and burial or sediment coatings on seagrasses. The light reduction and sediment coatings reduce the capability of seagrasses to perform photosynthesis and can degrade the health of the seagrass beds. An assessment of increased turbidity and suspension of solids into the water column in relation to dredging provides information that can be applied to maintenance dredging operations and material placement locations and methods.

1.2 STUDY DISCUSSION

While the overall purpose of the CBI Study was to provide measurements that would yield information on the impacts from dredged material placement in the Laguna Madre and data necessary for the models that were being developed for the ICT, the original locations of the platforms in the ULM and LLM were designed for other specific objectives relative to dredging activities.

1. Encroachment of sediment on seagrass beds,
2. Resuspension of sediment in dredged material placement areas,

- 3 Reduction of light within the water column,
4. Transport of dredged material back into the GIWW and loss of material from placement sites,
5. Understanding of cause-and-effect relations between hydrodynamic forcing and sediment movement.

The ICT authorized CBI to continue to collect data to better understand the hydrography and sediment transport in the Laguna Madre and to provide input into the hydrographic and sediment transport models being developed for the ICT by the Waterways Experiment Station

The objective of the present work is to subject all data collected in the CBI project to a unified data-recovery process, by which is meant acquisition, Q/A screening, and processing. The work is conveniently subdivided according to geography, viz. the ULM and LLM systems. The focus of this work is on “hydrographic” data, i e., the digital records from:

- 1 acoustic doppler velocimeter (ADV) - three components of current velocity,
- 2 electromagnetic current sensor - two horizontal components of current velocity,
3. conductivity - internally converted to salinity in practical salinity units (PSU) equivalent to parts per thousand (ppt),
- 4 temperature - degrees Celsius,
- 5 turbidity - measured by an optical backscattering probe and reported in NTUs (nephelometric turbidity units),
- 6 water level - high resolution variation in water-surface elevation derived from pressure measurement

These hydrographic data sets were supplemented by additional data, including TSS determinations on water samples, field and laboratory measurements of salinity, and data logs from proximate TCOON platforms, especially water level (“tide”) and meteorological observations (wind, pressure, air temperature)

As matters developed, the original platform instrument packages used for the Laguna Madre did not include water level. In data interpretation (see Chapter 4), the ancillary environmental data obtained from proximate TCOON stations included water level, but this, of course, did not provide a direct measurement of wave activity at the measurement platform. For the new instrument packages (data collected after October 1997), pressure (i e., water level) is included in the array. During this same re-instrumentation the earlier ADV current sensors were replaced with the electromagnetic sensors.

Additional detail on the instrumentation and deployment is given in Chapters 2 and 3. Various analyses of the measurements are treated in Chapters 4 through 6, addressing the hydrographic environment, currents, and suspended sediments, respectively. Interactions among these variables and interpretation of the results are reserved for Chapter 7. A summary of the findings of this data reduction and analysis effort, plus conclusions and recommendations, is presented in Chapter 8.

Overall, the field data collection consisted of sustained long-term *in-situ* monitoring of physical, chemical, and biological parameters from six fixed platforms, and collection of water samples for laboratory analysis. Instrumentation and associated support equipment were installed beginning in August, 1994. This data recovery project is concerned only with the hydrodynamic and hydrographic components. This chapter describes the automatic monitoring component of the study, including instrument deployment information (deployment dates and location), equipment utilized, and calibration and maintenance procedures. This chapter also describes the platforms and the instrumentation and equipment installed on them, together with the general data-collection process.

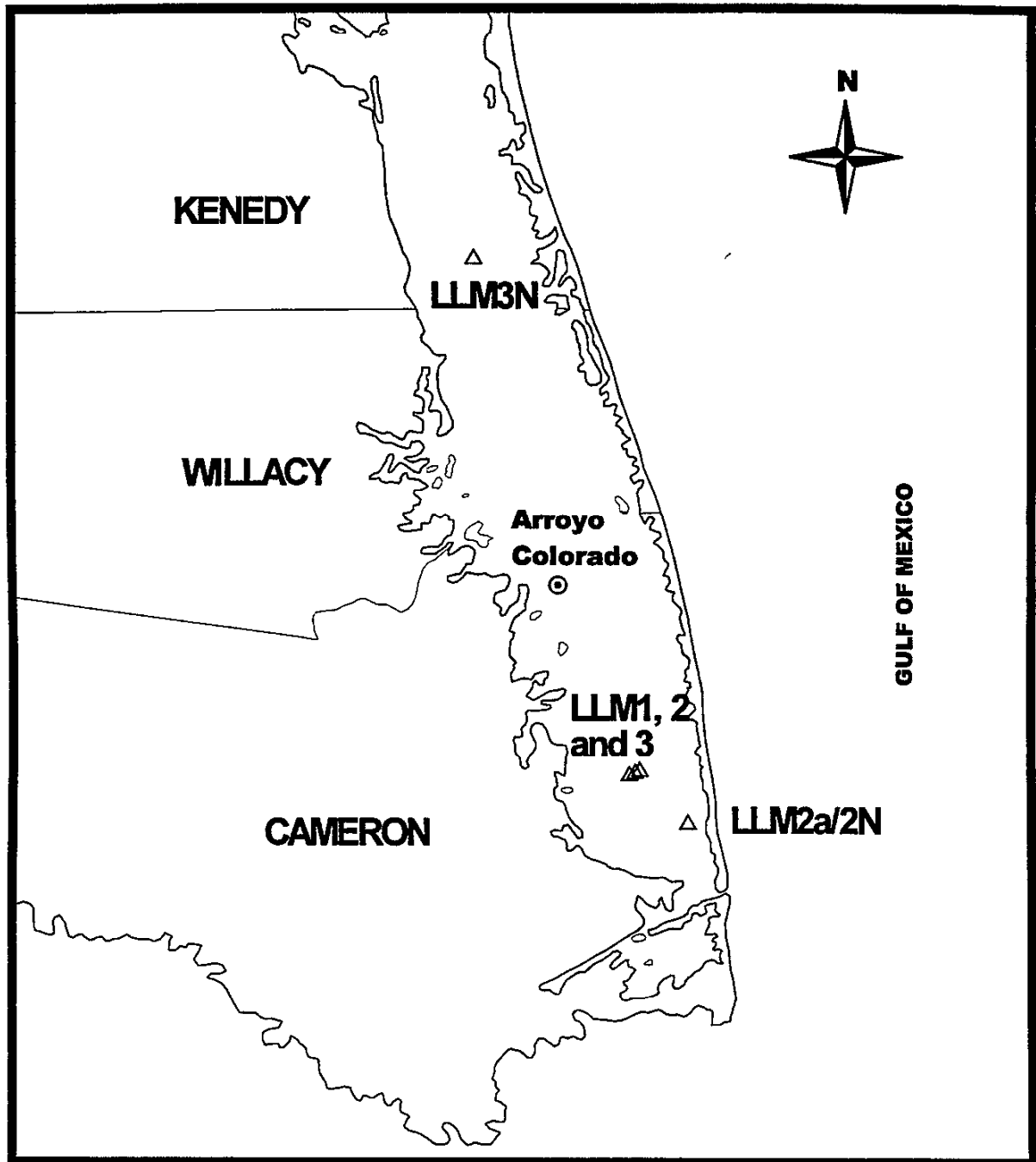
MONITORING PLATFORMS AND INSTRUMENTATION

Locations of the monitoring platforms are shown in figures 2-1 and 2-2, and coordinates and dates of installation for each platform are provided in Table 2-1. The original three fixed platforms in the LLM, denoted as LLM1, LLM2, and LLM3 (FIX 1, FIX 2, and FIX 3 in Brown and Kraus, 1997), were installed along a line running transverse to the GIWW at Channel Marker 91 in the Lower Laguna Madre, see Figure 2-1, and were operated until June 1996. At that time, LLM2 and LLM3 were dismantled. LLM2 was moved to a seagrass meadow east of the GIWW and designated LLM2a, which became LLM2N with the installation of the new instrumentation in 1997 (Figure 2-1). LLM3 was re-established at LLM3N, near Port Mansfield, in May 1997 but no data were collected and it was removed in July 1997. This platform was re-installed at this same location, still designated LLM3N, in November 1997 with new instrumentation. Like LLM2a/LLM2N, it was moved to collect data from a variety of locations with differing amounts and types of seagrasses.

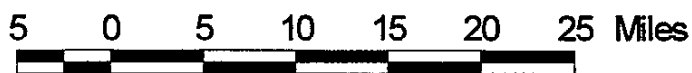
The northern-most platform, designated as ULM1, was located in Corpus Christi Bay (Figure 2-2) near the northern terminus of the ULM approximately 0.4 km east of the GIWW. This platform was intended to provide data from the vicinity of dredging sites on the southern side of Corpus Christi Bay. Platform ULM2 was placed in the Upper Laguna at the mouth of Baffin Bay, approximately 0.8 km west of the GIWW. The southernmost ULM platform, ULM3, was located approximately 10.2 km south of ULM2, and 0.3 km east of the GIWW, near the northern limit of the Mudflats. Both ULM2 and ULM3 were intended to provide information in the vicinity of dredging sites along the GIWW near the mouth of Baffin Bay. An additional purpose for these platforms was to provide data on physical processes and water quality for Baffin Bay, a relatively unstudied site.

FIGURE 2-1

CBI AND TCOON STATIONS IN LOWER LAGUNA MADRE



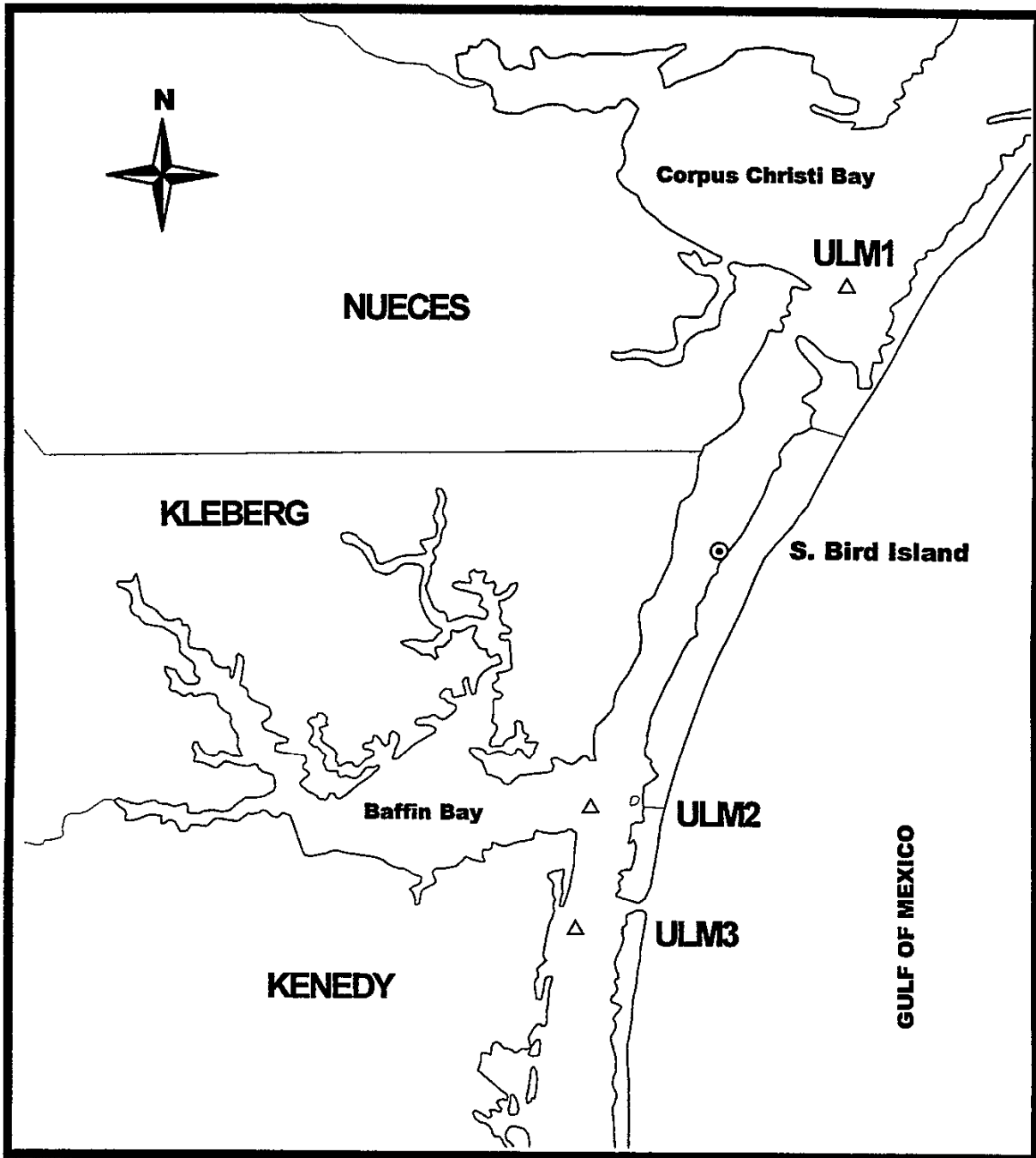
I:\projects\hco\449708\cad\figure2-1 ar



- ⊙ TCOON Stations
- △ CBI Stations

FIGURE 2-2

CBI AND TCOON STATIONS IN UPPER LAGUNA MADRE



f:\projects\hc1\coe\449708\cad\figure2-2 ai

5 0 5 10 15 20 Miles

⊙ TCOON Stations
△ CBI Stations

TABLE 2-1

PLATFORM INFORMATION

Platform Name	Date of Installation	Date of Removal	Latitude	Longitude
LLM1	28-30 August 1994	12 March 1998	26° 10' 45.2" N	97° 15' 36.2" W
LLM2	28-30 August 1994	4 June 1996	26° 10' 50.9" N	97° 15' 36.2" W
LLM3	28-30 August 1994	4 June 1996	26° 10' 58.1" N	97° 15' 04.3" W
LLM2a/2N	4 June 1996	2 April 1998	26° 08' 05" N	97° 12' 28" W
LLM3N	28 February 1997	5 March 1998	26° 39' 00" N	97° 24' 00" W
ULM1	1 November 1994	7 May 1998	27° 41' 27.5" N	97° 12' 17.8" W
ULM2	4 November 1994	7 April 1998	27° 17' 08.2" N	97° 24' 56.9" W
ULM3	4 November 1994	9 March 1998	27° 11' 32.7" N	97° 25' 42.2" W

The platforms were constructed using 6 in-square 15-ft treated wooden posts, which were embedded approximately 1.2 to 1.5 m (4 to 5 ft) into the bottom using a jet-pump. For LLM1, a pile driver had to be used to drive the legs through an apparent layer of shell located approximately 1 m below the bottom of the lagoon. Elevated platforms were constructed, with a deck located approximately 1.5 m above the mean water level to reduce exposure of the equipment to waves and salt spray. The exception was ULM3, which used an existing USACE platform refurbished for this study, a tri-leg wood structure 10-ft on one side and 8-ft on the other sides with a deck and railing. The platforms and equipment were originally installed during the period of August 28-31, 1994 (LLM) and November 1-4, 1994 (ULM), and the stations became fully operational when data-collection commenced on August 31, 1994 (LLM) and November 4, 1994 (ULM).

The full complement of automatic monitoring equipment at this time included current velocity sensor, electrometric probes for conductivity and temperature, fluorometer for chlorophyll-a, and optical turbidity. In some equipment packages at some platforms for some periods, measurements of pH, dissolved oxygen, pressure (which could be converted to water level) and radiation in the photosynthetically available radiation (PAR) bandwidth were included as well. The specific equipment varied over the course of the program. Originally, the instrumentation array at platforms LLM1, ULM1, ULM2, and ULM3 was comprised of: Sontek acoustic doppler velocimeter (ADV), Chelsea Fluorometer, Hydrolab conductivity/temperature probes, and Li-Cor turbidity sensor, together with equipment that logged, stored, and transmitted the data. Two PAR sensors were located at each platform, one above the water surface and one approximately one m below mean sea level. In addition to *in situ* measurement sensors, the platforms were equipped with ISCO automatic water samplers.

Figure 2-3 (from Brown and Kraus, 1997) shows the early main monitoring platform, LLM1, which was equipped with two environmental enclosures to minimize exposure of electronics and equipment to salt water, rain, and spray. One environmental enclosure housed the batteries, and the other enclosure contained the data collectors, signal processing units, and radio communications equipment. Power was supplied to the station by two gel cell batteries, which were charged by four solar panels. LLM1 was originally the principal platform for the Lower Laguna. The stations LLM2 and LLM3 served a supplementary purpose, and were equipped only with ISCO water samplers. These samplers collected water at specified times (here, twice daily as described below) and stored the water samples until they were retrieved and taken to CBI for analysis of total suspended solids (TSS) and particle size distribution.

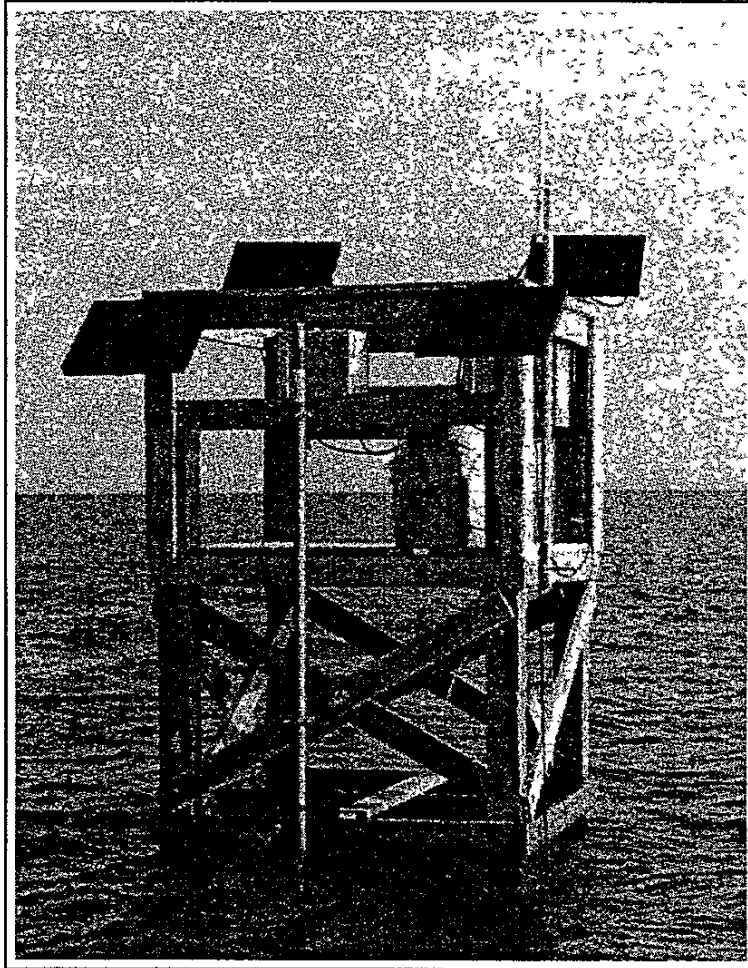


Figure 2-3. Photograph of Monitoring Platform LLM1

All sensors with the exception of the PAR sensors were logged with a specially-designed, low-power consumption micro-computer. The data collector had on-site storage capacity of approximately 14 days of data at the sampling rates used. As noted above, LLM2 and LLM3, in this stage of data collection, were only used for water-sample collection. When LLM2 and LLM3 were moved to LLM2a/LLM2N and LLM3N, respectively, they were equipped with the full suite of data collection equipment, which included Sontek ADV, Sea-Tec Fluorometer, Druck Pressure sensor, Seapoint Turbidity sensor, and an ISCO sampler. However, no data were collected from LLM3N with this instrument array.

The status of the data-collection system was checked remotely and data were transmitted to CBI via packet radio-modem connection. Originally, data were downloaded from LLM1 via a high-speed packet radio connection between the data-collection platform and a radio tower located in Los Fresnos, Texas, which then relayed the files to CBI via a modem/phone line connection. Subsequently, the data were downloaded via a high-speed packet radio connection between the data-collection platform and the University of Texas - Pan American Coastal Studies Laboratory located in the Town of South Padre Island, and then the data were transferred to CBI via an Internet connection. Once at CBI, the data were decoded and imported into the CBI Environmental Database where six-minute averages of all parameters were computed and stored. The data were then imported into the project database, where individual parameters were plotted and inspected.

The three monitoring platforms for the ULM were each equipped with one environmental enclosure, as noted above, to minimize exposure of electronics to the external environment. Each environmental enclosure housed the data collectors, signal processing units, radio communications controller, and batteries. The instruments and data loggers were powered by two 4-amp/hr gel cell batteries that were charged by two 30-watt solar panels. A low-power consumption microcomputer of 6-amp/hr/day yielded an on-site data storage capacity of approximately 13 days. Each station employed a packet controller, consisting of a radio and modem, which provided remote communication with the data-collection system from CBI. ULM1 had a UHF omnidirectional antenna which allows direct connection with CBI. Each of ULM2 and ULM3 had a UHF whip-antenna affixed to the platform. The data generated at these platforms were relayed from a radio tower located in Riviera, Texas, to CBI. Once at CBI, as with the LLM stations, the data were decoded and imported into the CBI Environmental Database where six-minute averages of all parameters were stored.

In Fall 1997, the Laguna Madre platforms were completely re-equipped with new sensors and dataloggers. The new instrument array consisted of the Applied Microsystems Ltd Smart Pack™, which measures pressure, temperature, conductivity, turbidity, and u and v current speed, using an electromagnetic (Marsh-McBirney) sensor.

2.1.2 Platform Maintenance

The installation and maintenance of the data-collection platforms proved to be more labor intensive than anticipated. During the one-year period from August 1994 through September 1995, there were approximately 100 days of field work. A chronology of events, including servicing of the platform, for the entire data collection period is presented in Appendix SR. Early on, regular maintenance of the fixed platforms was performed approximately once a week, as weather permitted, with duties including inspection of the data-collection and power systems, field cleaning of the ADV and fluorometer; weekly exchange of the Hydrolab unit with a laboratory-calibrated unit and post-calibration of the instrument returned from the field, replacement of the sample bottles in the automated samplers; replacement of batteries and desiccant, as needed and replacement of a polyethylene bag that protected the subsea PAR sensor. In addition, electronically acquired data were downloaded and taken back to CBI to be uploaded into the database. Upon removal from the automated water sampling unit, sample bottles were labeled and transported to CBI for analysis.

On February 8, 1995, radio contact was lost with ULM1. It is believed that a vessel had tied up to the platform during a storm the previous day and had uprooted the station. Repairs were made, and the station was back on line by February 15, 1995. An ADV was lost in this event. University of Texas Marine Science Institute (UTMSI) personnel maintained the PAR sensors and associated dataloggers, which were checked at monthly intervals, with preliminary data inspection carried out in the field. Additionally, sensor maintenance trips were scheduled so that the biofouling bag over the sensor was replaced every 2 to 3 weeks.

2.1.3 Instrumentation

Three components of water velocity (north-south u , east-west v , and vertical w) were measured continuously by Acoustic-Doppler Velocimeters (ADV) manufactured by SonTek (San Diego, California, USA), which is a new type of current meter that is reported to be highly accurate (even at weak water velocities) and robust against drift due to aging and biofouling. The ADV acoustically measures the three components of flow velocity at a point based on the Doppler-shift principle. The ADV has a centrally-located transmitting transducer surrounded by three receiving transducers mounted on arms orientated at 120-degree angles. The transmitting transducer emits periodic short acoustic pulses that are scattered back by material in the water column, such as bubbles and suspended material, assumed to move at the speed of the water flow. These acoustic echoes are detected by the receivers. By knowledge of the orientation of the acoustic beams and the principle that the frequency of the echo is Doppler shifted according to the relative motion of the scattering material, the orthogonal components of current velocity are computed. The ADV has a resolution of 0.1 mm/s over the range of 0 to 2.5 m/s and an accuracy the greater of $\pm 0.25\%$

or ± 0.25 cm/s (Kraus, *et al* 1994). In this study, the sampling rate of the ADV was 1 Hz with 6-min averages of each component of the water velocity, signal-to-noise ratio, and correlation coefficients stored in the on-site datalogger. The signal-to-noise ratio and correlation coefficients were used to determine the quality of the velocity data and to identify problems associated with the hardware, such as misaligned receivers or biofouling of the transmitters or receivers. The position and distance for the transmitter and each of the receivers were correlated against preset factory values of their positions. The ADVs were mounted at mid-depth with the probe oriented in such a manner that positive flow components (u, v, w) were directed toward the north, west, and upward, respectively.

The ADV sensors were originally developed as an ultra-precise high-resolution current sensor for laboratory measurements, intended to compete with laser doppler anemometers (LDAs). Adoption of the ADV technology for the hostile field environment was one of the primary objectives of the data collection program. The advantages of the technology, if it could be successfully applied in the field, would allow direct measurements of many processes that have heretofore been categorized as "turbulent". Moreover, if measurements of turbidity could be made at comparable time resolutions, then turbulent fluxes of sediment could be directly computed. Even if these experiments failed, the technology was expected to yield much more resolved details on estuarine currents than had been capable of measurement before.

The ADVs proved to be as sensitive and precise in field application as in the laboratory, but they also proved to be difficult to maintain and susceptible to damage. Calibration can be problematic. Each sensor has its own unique calibration which is established in precise laboratory testing by the manufacturer. Installation and maintenance are not "user-friendly" but require training and expertise with the technology. During the first 6 months of data collection, the range setting for the ADVs was set incorrectly. The ADV range settings were corrected in May, 1995. This incorrect setting caused parts of the ADV data to be invalid and unrecoverable. Because of this problem, ADV data analyzed in this report are those collected after June, 1995. The exact alignment of the transducers is critical to maintaining proper calibration. Their exact installation is crucial, and any later encounters with flotsam or massive objects floating in the water column, such as an errant mullet, can distort the data. It was discovered, for example, in using the same equipment in a platform in Lavaca Bay that a slight misalignment of the sensor at installation could produce anomalously large vertical components of current.

After November 1997 for ULM2 and December 1997 for all other sites, a different sensor was used, namely an electromagnetic sensor manufactured by Marsh-McBirney and comprising part of an integrated sensor package, the Smart Pack™ from Applied Microsystems Ltd. (As noted above, this package also includes sensors for pressure, temperature, conductivity, and turbidity.) This sensor is less precise and sensitive than the ADV and cannot, therefore, yield the turbulent fine structure, but it is a sensor designed for field work, with a long record of satisfactory performance in rugged, hostile coastal settings. The range

of the instrument is 0 - 3 m/s and the accuracy is rated by the manufacturer at ± 5 cm/s or better, with a resolution of 0.1 cm/s or finer

Water-quality parameters for most of the data collection period were monitored using a H20™ Water Quality Multiprobe (Hydrolab™ Corporation, Austin, Texas, USA), equipped with turbidity, water temperature, conductivity, pH, and dissolved oxygen sensors. The Hydrolab unit sampled every 2 min and data were logged using the Blucher Data Collector. The Hydrolab units deployed in the field were calibrated in the laboratory prior to deployment, with approximately weekly change-out of instruments. The specific conductance, pH, and turbidity sensors were calibrated using standard solutions. The pH and turbidity sensors were calibrated using a slope-calibration method and the conductivity sensor was calibrated using a one-point calibration with a standard solution having a conductivity similar to that observed in the field. The turbidity sensor, which uses an optical backscatter sensor, was calibrated using 0.2- μ m filtered, deionized water and 90 NTU formazin standard. The dissolved oxygen sensor was air calibrated at atmospheric pressure. The temperature sensor was calibrated by the manufacturer during fabrication and is considered stable for 3 years. The calibration procedure followed for the conductivity probe was such that an error of ± 3 ppt was typical for the resultant salinity data. In 1996, some problems with the salinity data were discovered (Kraus, pers. comm., 1996) and improvements to the calibration procedure were reported being made.

The re-equipment of the instrument packages in late 1997 included replacement of the Hydrolab probes with those that were part of the Applied Microsystems Ltd Smart Pack™, including sensors for pressure, temperature, conductivity, and turbidity. The temperature sensor is a pressure protected precision thermistor with a time constant of 350 ms. The range of operation is -2 to 32°C, with an accuracy rated at ± 0.005 °C or better and a resolution of 0.001°C or finer. The conductivity sensor is a platinumized electrode cell. Operating range is 0 - 6.5 S/m with an accuracy of ± 0.01 mS/cm or better, and resolution 0.003 mS/cm or finer. The turbidity sensor, like its predecessor, uses optical backscatter (OBS) technology, with operating range of 0 - 2000 NTUs, and resolution of 0.1 NTU or finer.

The OBS technology was probably the greatest disappointment of this project. The sensor proved to be exceedingly sensitive to biofouling on the optical surface. Even minute growth of marine periphyton and bacteria was sufficient to substantially increase light absorption, and register an apparent but fictitious increase in turbidity. The OBS data records display an exponentially growing turbidity, which appeared to be reset to a small value whenever the sensor was cleaned or replaced. At the outset of the project, it was acknowledged by all involved that this was untried technology, particularly in shallow, highly productive waters such as those of the Laguna Madre, and the potential for difficulties was recognized. The value of being able to monitor turbidity at the fine time resolution and with the accuracy afforded by the OBS justified experimenting with its use in this field application. Although no useful data were obtained, the

experience acquired in using this technology represents a major advance in the adaptation of the method to field environments typical of the Texas coast. CBI personnel are continuing to experiment with the technology and have recently developed some means of using transparent biocides to control biofouling (Benson, pers. comm, 1998), which may offer promise for use of the sensor in the future.

Mid-depth water samples were collected twice daily at 6 00 AM and 6 00 PM (local time) using a Model 2700 Portable Sampler™ (ISCO, Lincoln, Nebraska, USA). During approximately weekly routine servicing, the samples were removed from the water sampler and transported to CBI for analysis. The samples were analyzed for total suspended solids and particle-size distribution of the suspended solids. Total suspended solids concentration was determined by filtering a known volume of the sample twice, using two pre-weighed filters, a 1- μ m glass fiber filter and a 0.45- μ m cellulose filter, which were then dried at 65°C to constant weight. The volume of sample filtered was typically 500 mL; however, if the sample contained a relatively large amount of sediment, as determined visually, the volume filtered was reduced to 250-300 mL. Once the concentration of total suspended solids was determined, the filters were archived in labeled bags.

2.2 OTHER AVAILABLE DATA

This monitoring effort was supplemented by other instrumentation located in the region, including water-level, air temperature and wind-measurement systems operated by CBI as part of the Texas Coastal Ocean Observation Network (TCOON) and additional PAR sensors, operated by the National Biological Survey (NBS) and UTMSI. The TCOON real-time measurements are collected at approximately 40 stations along the Texas coast and stored in a database at CBI. Data from TCOON stations at S. Bird Island, for the ULM, and Arroyo Colorado, for the LLM were used in the present project for analyzing the tidal and meteorological components of variations in physical and water-quality parameters. Six-minute water-level data provided by the TCOON tide stations are collected according to National Ocean Service Standards and reported to an accuracy of 0.1 ft. Wind speed (average wind speed and gust) and direction data are collected hourly with average wind speed based on a 5.5-min average sampled at 1 Hz and the gust was defined as the highest 5 sec sustained wind speed in the 5.5-min sampling period. The wind measurements are of particular significance for understanding the role of the physical driving forces for the resuspension and transport of sediment.

Before the hydrographic data collected by the ICT project could be subjected to analysis, it first had to be screened for anomalies, these anomalies reconciled, corrected or eliminated, then the data compiled into seamless "scrubbed" data files. As noted in Chapter 1, data collection on this project in the Laguna Madre has been carried out over a nearly 4-year period by the Conrad Blucher Institute CBI), during which the Institute operations, field procedures and equipment have undergone major modifications, creating heterogeneous data records. For purposes of planning data transfer and screening, it was convenient to subdivide the CBI data sets into four classes:

Data Set I — Data analyzed in the "Year 1" reports, Brown and Kraus (1997) and Brown (1997). These data were collected in the period September 1994 through August 1995. The Brown and Kraus (1997) report also included a small amount of data through December 1995.

Data Set II — Continued data collection by the same personnel as involved in Data Set I, presumed to have been carried in conformity with the same Q/A and reduction protocols as Data Set I. Data collection period extended generally from September 1995 to September 1996.

Data Set III — Hydrographic data collected under interim management at CBI, from approximately October 1996 through early spring 1997.

Data Set IV — Hydrographic data collected by the present CBI personnel, from late fall 1997 through early spring 1998, utilizing completely new equipment and re-designed data recovery protocols.

The precise dates for Data Sets III and IV vary from station to station. As matters developed, the distinction between Data Set II and Data Set III proved to be unnecessary, because these data sets were generally in the same form and level of pre-processing, and therefore were operationally indistinguishable.

In the original project work plan, the data-recovery effort was conceived to be prosecuted in three main task efforts:

Task 1 - For Data Sets I, II and IV, acquisition of data files from CBI and their combination into a common data base for further analysis

Task 2 - Data acquisition, Q/A pre-processing and data compilation, Data Set III.

Task 3 - Data processing and analysis

Task 1 was intended to include performing a Q/A inspection, primarily to insure the integrity of the data transfer. As the project developed, the frequency and variety of data anomalies proved to be much greater than originally anticipated, including Data Set I (which had already been analyzed and reported in the Year-1 reports), so a concomitantly greater effort was necessary to complete the data scrubbing process. The work on Task 2 was somewhat ill-defined at the outset of the data-recovery effort, pending an assessment of the actual status of the Data Set III data files. As the project evolved, CBI staff were able to carry out the data processing exactly as with the other data sets (the primary anomalous aspect of Data Set III proved to be prolonged gaps in the data streams), and the Task 2 effort was folded into Task 1. Task 3 began with the screened and scrubbed data files in consistent formats, and addressed the actual data processing. The Interagency Coordination Team (ICT) specified that this was to focus on statistics of currents and associated hydrodynamic variables and was to follow the protocols and format of the Year-1 report, including scatter plots and directional statistics, time series plots, and spectral analyses. This chapter addresses Tasks 1-2, viz data acquisition, Q/A preprocessing and compilation.

In any sort of data-collection enterprise like this, electronic aberrancies in the data streams, i.e., lost records, data outages, calibration drifts and slippages, etc., are unavoidable and must be anticipated in data management. For example, some of the probes are subject to fouling over time, creating a degraded signal quality that varies as a function of time in an unknown manner, thereby causing loss of calibration. The final objective of Tasks 1 and 2 can be simply stated as the determination of which measurements are physically valid.

Downloading, re-formatting and transmission of the data were carried out with industry and patience by the staff of CBI. As data was received by this project team, the files were subjected to preliminary review, and any anomalies were drawn to the attention of CBI. The entire process took place over a six-month period, and in several instances necessitated CBI staff completely re-constructing data files from raw sensor output files. For example, it was discovered that some of the data files for ULM3 proved to contain data from ULM1 (except for January, April, July and October for both 1995 and 1996, which appear to be all right), apparently due to an errant file overwrite that occurred at some point early in the processing stream. This duplication was in fact present in the data files analyzed in the ULM data report (Brown, 1997), but this was overlooked in the review of that report.

A catastrophic crash of the RAID (Redundant Array of Inexpensive Devices) data storage network at CBI occurred in summer 1997, and all of the 1996-97 files had to be re-built by CBI staff from the original platform downloads, where this data survived. Some files are evidently gone forever. (This event, which the RAID strategy is supposed to prevent, has motivated changes in the procedure for archiving data at CBI.) Some piecemeal replacement files have been re-generated by CBI. These include January - June 1996 for ULM1, and the missing months in 1995 and 1996 for ULM3. For ULM1, only January and February 1997 are extant, the data from July - December 1996 being lost. The data record for ULM2 is complete through February 1997. The data record for ULM3 is piecemeal through February 1997.

The ULM3 replacement files posed an additional problem. Each month of data was given as three separate files, containing, respectively, (1) three components of current velocity, (2) hydrographic variables salinity, temperature, and turbidity, (3) chlorophyll-a (whose analysis was beyond the scope of this project). Merger of these files was made difficult because the data were not given at consistent times across the files (reason unknown). Some attempt was made to automate a merging procedure, but there were too many irregularities in the file structures. At last, we had to bite the bullet, and modify each of the data files manually using spreadsheet software.

Once the data files passed the preliminary screening process, the next step was to work through the entire data set month by month and platform by platform, carefully inspecting the data for several characteristic anomalies, and in the process to construct an inventory of data measurements, including periods of suspicious data and record breaks. Thus, it was necessary to *manually* inspect all of this data, and identify occurrences in the data streams of:

- (1) data gaps
- (2) anomalous records, e.g., short records (less than eight variable fields), missing entries (two or more tabs in a row without intervening characters), or nonnumeric entries
- (3) zero values (see discussion below)
- (4) discontinuities in the time entry
- (5) anomalous or "freak" values for the parameter being measured (e.g., current speeds greater than 10 m/s, salinities greater than 50, temperatures below 0, etc.)
- (6) physically unrealistic jumps in the sequence of measurements for a parameter, e.g., an abrupt shift in the salinity record of several ppt
- (7) "flatlines", i.e. a sustained dwelling of the measurement on one value

- (8) anomalous time patterns, e.g., exponential decreases or increases in value suggestive of fouling of the sensor, or physically peculiar time variation in a parameter

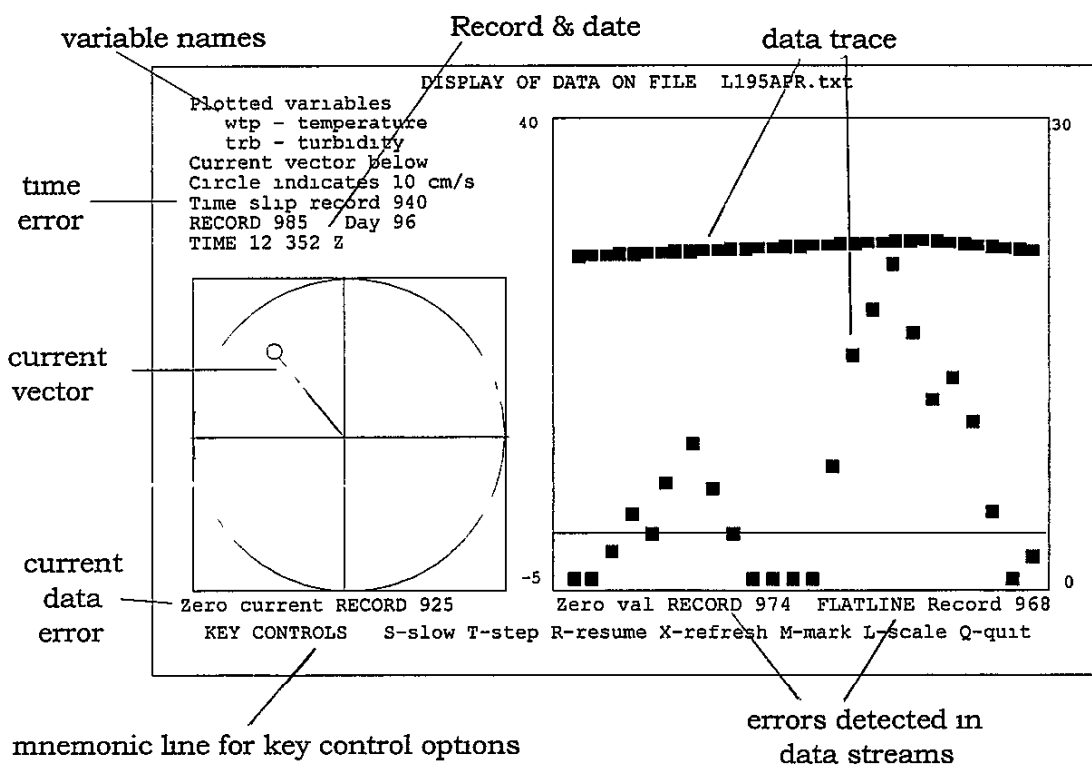
To facilitate this inspection task (which is tedious, soporific and onerous), a special-purpose program was developed, named INSPECT, that reads and displays a moving time history graph of two parameters (chosen by the user) along with a vector display of the simultaneous horizontal current. A mockup of the screen display of INSPECT is shown in Figure 3-1. The user controls the display of the data, which may be slowed, sped up, or stepped point by point. The plot axes may be re-scaled as the magnitudes of the variables change.

This automated processing relieved some of the tedium of manually inspecting such huge data files, but the task is still mind-numbing. As the program INSPECT marches through the data files, it automatically checks for many of the anomalies listed above, namely (1), (2), (3), (4) and (7). It displays the detection of these anomalies in garish colors at various spots on the screen (as shown in Figure 3-1) accompanied by the production of appropriate noises to alert the user, who might otherwise be staring slackjawed at the screen, drooling on the keyboard. The other anomalies cannot be detected automatically, but can be spotted in the display by an attentive user.

3 2 IDENTIFICATION AND TREATMENT OF DATA ANOMALIES

Screening the data sets with the INSPECT software is, in effect, a preliminary interpretation of the data, at least insofar as suggesting plausibility of apparently anomalous behavior of the data. The simultaneous display of current velocity serves the purpose of assisting the user in interpreting the behavior of the two parameters displayed. The INSPECT program cannot, of course, identify physically unreasonable behavior of the data—that is the job of the user who fixedly watches the data display. Notes on possible data anomalies are entered by the user from the keyboard into an output log file while the display program INSPECT is operating. After each such output file was completed, it was opened with a spreadsheet program, along with the corresponding data file, so that the two could be cross-compared. To facilitate this process, a hardcopy graphic display was produced, as described below. Each anomaly logged in the output file was examined and a determination made of whether it was of significance or not, whether it was likely to be real, and if not what corrective actions might be necessary. CBI provided a log of time history of each instrument/platform, including maintenance checks, instrument adjustments, exchange of sensors, etc., that greatly facilitated identification of plausible explanations for some of the anomalies. (This log has been edited and provided as Appendix SR.)

Fig. 3-1 Display screen for program INSPECT (see text)



As noted above, some data anomalies are to be anticipated in an automated collection program. We were surprised to discover a large number of such anomalies, including flatlines, zero dwells, and freak points. This was true even for the Year-1 data sets (Data Set I), and apparently these aberrant values were included in the analysis of the earlier reports (Brown and Krause, 1997, Brown, 1997) We also found occurrences of spurious data that evidently were introduced by the data handling, rather than originating at the platform These include data out of chronological order, duplicated records, and irregular time steps.

Given ample time, the optimum approach to resolving these anomalies would be to explore the origin of each and modify the individual data point appropriately Under the present time constraint, we can only implement obvious corrections, and expunge large blocks of suspicious data One has to be attuned to the principle of diminishing returns Isolated anomalous data points, i.e. physically suspicious ("freak") parameter magnitudes, whose values are not orders of magnitude out of the acceptable range might be safely retained in the data set, because combined with thousands of valid points, these will have little impact on the analysis of the data On the other hand, large blocks of anomalous data, such as flatlines, can have a substantial corrupting effect on statistics (We note that, as matters turned out, large blocks of spurious data were included in those data sets analyzed in the Year-1 reports These have been expunged in the present work)

The philosophy followed in general was to treat the screened data files as archival, so that no modifications were made to these files. Instead, each file was copied, and this copy served as a "corrected file" A complex graphical display on 11x17 pages (C-size) of the time series of various parameters was prepared showing companion meteorological data, anomalies logged by INSPECT, and maintenance or other actions taken with the platform according to the CBI logs Each such graph was limited to a few weeks in order to resolve the time variation of the measurements (These graphical displays form a detailed—and voluminous—record of the data sets before data scrubbing was instituted, and are provided as an archival appendix, bound separately as Appendix B)

These graphics allowed the ready identification of data anomalies and an immediate interpretation as to cause Each data file was worked through using the graphic as a guide Any anomalous data points that could not be reasonably interpreted were deleted in the "corrected" file. Freak data points were the most obvious to treat. These are isolated in the data stream and are very high or very low magnitudes compared to the pattern in that parameter. Flatline behavior is similarly obvious, and any such data sequences that we believed to be due to the instrument no longer responding to variation in the measured parameter were deleted Note that flatline behavior can be manifested in salinity and temperature, at least for several hours, under quiescent conditions, and may therefore be reasonably encountered in these data. On the other hand, flatline current speeds of any substantial duration are unlikely.

Zero values were another of the anomalies examined. These can result from the sensor malfunctioning while the data-logging process continues. Of course, any of these hydrographic parameters, even current speed, can be zero under the right conditions. Zero values of current, in particular, may be reasonable depending upon how the tide and wind were behaving. (Note that we are referring to zero current *speed*, not a zero in an individual component) Individual zeroes that are embedded in a sequence of otherwise substantial current speeds were generally deleted, unless these were clearly associated with reversal of current, e g , turn of the tide, or a pattern of diminishing then increasing current. A long duration of zero current speed (which is a special case of a flatline), in contrast, was compared to wind and water level data recorded at nearby CBI TCOON stations (for which the downloads from the CBI web page were carried out) Any zero values that could not be otherwise justified were expunged.

The three anomalies, quantum shifts in parameter values, drifts in value of a parameter, and peculiar time variation in a parameter, are really different manifestations of the same anomaly, *viz* excursions of parameter magnitude as a function of time that seem physically unlikely. (A gap in data can create what appears to be a quantum shift in the parameter, so before taking any corrective action, the technician always verified whether a timeslip occurred at that point in the data stream) There is a twofold problem in treating these anomalies First is the problem of establishing whether the measured behavior is plausible and should remain in the data set Second is the problem of how to correct a corrupted data point.

Some parameters like temperature or salinity do exhibit quantum jumps in magnitude if parcels of water with very different properties are carried past the point of measurement. The best clue to whether a quantum jump in the data may be real is the corresponding hydrographic data Is there a correlated variation in temperature or turbidity? Are there high values or sudden shifts of current speed, or water level? Was there a wind-shift, such as a frontal passage? Thus it was necessary to examine the data records around the same time of the other hydrographic variables as well as the downloaded TCOON data. It is also necessary to examine whether such anomalous behavior is associated with a non-physical event, notably a maintenance visit to the platform

A direct measurement at the platform can settle the question for temperature, salinity or turbidity. Unfortunately, CBI does not include *in situ* measurements as a part of its platform maintenance protocols During the first year, the University of Texas Marine Science Institute, as a part of its maintenance of PAR measurement equipment, made occasional measurements of salinity and temperature measurements at some of the ULM and LLM stations. We were provided copies of these measurements by Dr Ken Dunton of MSI. These measurements along with the corresponding values from the CBI platform are given in Table 3-1 Most of the data compare very well. A few of the salinity measurements evidence large departures. We have no means of determining which is more likely to be correct, so we simply note that these differences occasionally exist (It is of course possible that such paired measurements are correct, but the difference was

TABLE 3-1
COMPARISON OF PAIRED MSI AND CBI DATA

Date	Temperature (°C)		Salinity (‰)	
	MSI	CBI	MSI	CBI
Station: LLM1				
10/12/94	20 0	21 5		
02/16/95			31 6	32 8
03/06/95	16 0	16 4	31 7	34 3
03/27/95	26 0	25 5	32 5	32 1
04/18/95	24 5	25 1	31 6	31 2
05/24/95			39.6	32.9
06/30/95			36 5	34 3
07/27/95	29 0	30 3	37 7	35 8
08/08/95	30 0	30 4	37 3	36 8
09/19/95	30 0	30 8	38 4	
10/26/95	25 5	26 2	33 7	32 9
12/13/95	17 0	16 9	25 6	24 7
01/23/96	18 0	19 0	30 1	31 4
09/23/96			36 2	33 6
01/27/97	19 5	19 6		
02/25/97			31 6	28 9
Station: ULM1				
01/31/97	13.5	11.0	34 2	36 0
02/24/97	16 4	16 4	32 3	32 9
Station: ULM2				
09/10/96	30 0	29 5	50.1	45.5
09/25/96	29 5	30 2	45 5	45 0
10/15/96	25 7	25 3	44.2	49.7
11/26/96	14 0	13 2	47 4	47 5
12/17/96	14 4	14 2	46 0	48 4
01/31/97	13 0	12 6	38.8	48.8
02/24/97	15 4	16 7	32.0	42.6
Station: ULM3				
09/10/96	28 5	29 6	34.1	45.6
09/25/96		30 2	41 3	44 4
10/15/96	25 3	25 4	42 7	46 9
01/31/97	12 5	12 5	44 6	47 7
02/24/97	16 3	16 7	41 4	42 6

Note Bolded data indicate a greater than 10% difference between the MSI and CBI data

incurred due to timing of the measurement when salinity was changing abruptly, or depth differences in the presence of transient stratification.)

For those variations of a parameter with time that are determined to be spurious, the second problem is how to implement a correction. For quantum shifts, the key question is the magnitude of the shift: if it is not egregiously large, it may be possible to ignore the shift in the data analyses. For peculiar time variation, e.g., random wandering of the parameter over a range that is physically unlikely, there may be no recourse but to delete the entire sequence. If such behavior is bounded by maintenance visits at the platform, then this can be considered a dead giveaway that the problem is instrumental, hence spurious. One special type of peculiar time variation is clipping, in which the parameter varies normally up to a certain threshold value, but exhibits frequent flatlines at that threshold, and never shows an excursion beyond the threshold. A data stream can be clipped above or below. Once a clipping threshold is identified, then any occurrences of this value in the data stream should be deleted. A special case is when one of the current components is clipped. For example, inspection of some of the 1998 data from the LLM station revealed that some of the x-component is clipped for positive (eastward) values.

A quantum shift needs to be examined in the context of a longer series of data. Is there a companion shift in the opposite direction later? If not, the quantum shift may be evidence of a calibration drift, addressed in the next paragraph. Are the times of quantum shift bounded by maintenance visits? If the variation of the parameter seems realistic but the *magnitudes* are displaced upward or downward, then the obvious correction is to shift the displaced sequence by the appropriate amount. If, however, the *variation* is also suspicious, e.g., numerous flatline periods or a different variance than exhibited in this parameter before and after the period of the quantum shift, then it will be better to simply delete it.

Drifts are the most complex anomalies to be corrected. A slow drift in a parameter, due to gradual loss of calibration, is most likely to be manifested by an apparent quantum shift that corresponds to a maintenance visit. Probably the only feasible correction is to apply a linear compensation starting at the last known correct value, and extending to the time at which the quantum shift occurred. Although we were prepared to correct for these anomalies, fortunately we had none of these to deal with.

The sequence in which these anomalies were addressed began with the largest such anomalies and worked toward the smallest. This allowed disposal of the more significant aberrancies before being overtaken by the law of diminishing returns.

We emerged from this process with sets of data files, organized by platform and by month, in which most of the above-listed anomalies, and *all* of those with sufficient magnitude or frequency to potentially corrupt the data analysis, have been deleted. The "corrected" files still include data gaps in

time. These irregularities in the time dimension do not affect the various descriptive statistics, such as means, vector-means, variances, and current roses. On the other hand, irregularities in time interval greatly affect the determination of spectra, because 99% of the extant spectral models—and *all* of the commercial software products—assume a data file uniformly sampled in time. We followed the traditional approach to treating missing data in spectral analysis of "zero-padding", in which the missing data are replaced by zero values, which is a default option for the spectral-analysis software employed in this project (This is derived from the philosophy that such zero padding, though influencing the statistics of the data, will not affect the frequency content. If the missing data happen to occur at a consistent periodicity, there are methods for correcting the computed spectrum, see Bloomfield, 1976, and Priestley, 1981, and references therein, though this was not encountered in these data sets.) Therefore, in fact two different sets of "corrected" data files were used, depending upon the specific analyses. For statistics and vector roses, the "corrected" data files with data gaps were used. For spectral analyses, the "corrected" zero-padded data files were used.

3.3 SUMMARY OF DATA SETS

To summarize, the data sets collected during the CBI Laguna Madre project, as originally classified in the proposal and work plan, and their status are:

Data Set I — Data collected September 1994 through August 1995 and analyzed in the "Year 1" reports. The original data sets contained numerous anomalies, which have now been detected and removed from the data. The ULM3 data files proved to contain data from ULM1 (except for January, April, and July, 1995). CBI was able to reconstruct the missing months from the archived raw data downloads.

Data Set II — Data collected from September 1995 - fall 1996 by the same CBI personnel. Again, numerous anomalies were detected, including flatlines, zero dwells, and freak points, were detected and have been corrected. An additional station was installed in the Lower Laguna Madre in June 1996 in a seagrass meadow east of the GIWW, designated LLM2a. While including ADV current data, salinity and temperature were not monitored at this station. As with Data Set I, the ULM3 data files proved to contain data from ULM1 (except for October 1995, and January, April, July and October, 1996, which were okay).

Data Set III — Hydrographic data collected under interim management at CBI, from approximately fall 1996 through summer 1997. A major hard disk crash occurred at CBI in July 1997, and several of the Laguna Madre data files were lost. Despite valiant efforts by the CBI staff, it proved impossible to recover data taken after February 1997. Other data files were unrecoverable as well. For ULM1, only January and February 1997 are extant, the data from July - December 1996 being lost. The data record for ULM3 is piecemeal through February 1997, although all months are represented.

Data Set IV — Hydrographic data collected by the present CBI personnel, from late fall 1997 through early 1998. In addition to being taken by new personnel with new protocols, the equipment was different from that used in the earlier collections (see Chapter 2). Data were provided by CBI as 30-minute means (compared to the 6-minute means from the earlier data). The raw data from Data Set IV proved to be significantly cleaner than the data from Data Sets I-III. The predominant problems in Data Set IV involve time slips and data gaps. Data Set IV also has very few zero currents and flat lines in comparison to Data Sets I-III.

Table 3-2 is an inventory of all of the data files presently on hand and their status. Data files from the two TCOON stations, from which water level and wind data were obtained, are included as well. However, these data were not subjected to any Q/A procedures.

TABLE 3-2
SUMMARY OF LAGUNA MADRE DATA FILES

Year	Month	File Description Codes for Laguna Madre Stations								
		LLM1	LLM2a	LLM2N	LLM3N	ULM1	ULM2	ULM3	Arroyo Colorado	S Bird Island
1994	SEP	CWST6				x	x	x	WiL60	WiL60
	OCT	CWST6				x	x	x	WiL60	WiL60
	NOV	CWST6				_WST6	x	x	WiL60	WiL60
	DEC	CWST6				_WST6	_WST6	_WST6	WiL60	WiL60
1995	JAN	CWST6				CWST6	_WST6	_WST6	WiL60	WiL60
	FEB	CWST6				CWST6	_WST6	CWST6	WiL60	WiL60
	MAR	CWST6				CWST6	CWST6	CWST6	WiL60	WiL60
	APR	CWST6				CWST6	CWST6	CWST6	WiL60	WiL60
	MAY	CWST6				CWST6	CWST6	CWST6	WiL60	WiL60
	JUN	CWST6				CWST6	CWST6	CWST6	WiL60	WiL60
	JLY	CWST6				CWST6	CWST6	CWST6	WiL60	WiL60
	AUG	CWST6				CWST6	CWST6	CWST6	WiL60	WiL60
	SEP	CWST6				CWST6	CWST6	CWST6	WiL60	WiL60
	OCT	CWST6				CWST6	CWST6	CWST6	WiL60	WiL60
	NOV	CWST6				CWST6	CWST6	CWST6	WiL60	WiL60
	DEC	_WST6				CWST6	CWST6	M	WiL60	WiL60
1996	JAN	CWST6				CWST6	CWST6	CWST6	WiL60	WiL60
	FEB	CWST6				CWST6	CWST6	CWST6	WiL60	WiL60
	MAR	CWST6				CWST6	CWST6	CWST6	WiL60	WiL60
	APR	CWST6				CWST6	CWST6	CWST6	WiL60	WiL60
	MAY	CWST6				CWST6	CWST6	CWST6	WiL60	WiL60
	JUN	CWST6				CWST6	CWST6	CWST6	WiL60	WiL60
	JLY	CWST6				M	CWST6	CWST6	WiL60	WiL60
	AUG	CWST6				M	CWST6	M	WiL60	WiL60
	SEP	CWST6	CW__30			M	CWST6	CWST6	WiL60	WiL60
	OCT	CWST6	CW__30			M	CWST6	CWST6	WiL60	WiL60
	NOV	CWST6	CW__30			M	CWST6	CWST6	WiL60	WiL60
	DEC	CWST6	CW__30			M	CWST6	CWST6	WiL60	WiL60
1997	JAN	CWST6	CW__30			CWST6	CWST6	CWST6	WiL60	WiL60
	FEB	CWST6	CW__30			CWST6	CWST6	CWST6	WiL60	WiL60
	MAR									
	OCT									
	NOV	x		x	x	x	C,PST30	x	WiL60	WiL60
	DEC	CPST30		CPST30	CPST30	CPST30	CPST30	CPST30	WiL60	WiL60
1998	JAN	CPST30		CPST30	CPST30	CPST30	CPST30	CPST30	WiL60	WiL60
	FEB	CPST30		CPST30	CPST30	CPST30	x	CPST30	WiL60	WiL60
	MAR	CPST30		CPST30	CPST30	CPST30	CPST30	CPST30	WiL60	WiL60
	APR			CPST30		CPST30	CPST30		WiL60	WiL60
	MAY					CPST30			WiL60	WiL60

Key to Data Descriptors

C	X and Y Current Data	-	Missing Data	6	6 Minute Time Step
W	Vertical Current Component	M	Missing All Data	30	30 Minute Time Step
P	Pressure	x	No Data Collected	60	60 Minute Time Step
S	Salinity	Wi	Wind Data		
T	Temperature	L	Water Level		

In the Laguna Madre, the hydrodynamic parameters wind, water level, and current are closely related, and to a great extent the hydrographic environment can be characterized by their behavior. Wind exerts a direct stress on the waters of the Laguna creating a current, whose integrated effect in moving water about results in altered water levels. Water level is also influenced by the variation of water level in the Gulf of Mexico communicated to the Laguna Madre through the inlets. This Gulf water-level variation, in turn, may originate from the astronomical tide in the Gulf or from the action of wind (and, to a lesser extent, atmospheric pressure gradients) on the sea surface. In addition, the hydrographic parameters of temperature and salinity are important, because together they determine water density, which has a direct hydrodynamic effect, and analytically because they identify water masses, and can allow inference of transport and mixing processes. Current velocity is the central hydrographic variable for this study, because it is the primary mechanism in the suspension, transport and settling of sediment. As noted in Chapter 2, it is also the major parameter upon which the field measurements were focused. For this reason, the current data from this study are considered separately in the following chapter. In this chapter, the behaviors of wind, water level, and water characteristics of temperature and salinity, as inferred from the data records, are presented for the 1994 to 1998 monitoring period.

4.1

WIND

Wind is a forcing function. It has both a direct and an indirect effect on currents, thence on sediment transport. The direct effect of wind is local production of currents, through exertion of a stress at the water surface. There is a spectrum of scales of current response to wind stress. At the smallest space-time scales, the effect of wind stress is manifested in the production of short period capillary and gravity waves. With increasing wind speeds, these overtop and break, creating intense patchy turbulence distributed through the water column and contributing to the vertical mixing of parameters, including suspended sediment. This turbulence also extends to the bottom in shallow systems like the Laguna Madre, directly mobilizing sediment particles from the bed. Numerous investigations in shallow-water systems similar to Laguna Madre suggest that wind-generated waves are a dominant mechanism for resuspension of sediment in these environments (e.g., Ward, *et al*, 1984, Pejrup, 1986, Onuf, 1994, and Schoellhamer, 1995).

At larger space-time scales, wind stress forces a direct current resulting in movement of water (and any materials in suspension or solution). Under a sustained wind, this stress-induced movement produces depletion and accumulation of water volume manifested as changes in water level across the Laguna, referred to as denivellation, or, more colloquially, "set up" and "set down". A sudden change in wind in either speed or direction (or both) results in a corresponding movement of water and variation in

the water level. Frontal passages, in particular, produce rather sudden, and frequently dramatic water level responses (see below)

Indirect effects on currents and water level in the Laguna Madre can be summarized as the response of the Laguna to direct effects of wind on adjacent waterbodies. The larger the surface area of the waterbody (more specifically, the larger the fetch) and the shallower the depths, the greater the response to wind stress, and therefore the greater the potential for the resultant change in water level to affect the Laguna. The filter through which this effect is passed is the inlet(s) connecting the Laguna and the adjacent waterbody. The Gulf of Mexico is the most important such adjacent waterbody, but Corpus Christi Bay and Baffin Bay can be important in local regions of the Laguna Madre. Ward (1997) and references therein discuss the mechanics of a co-oscillating bay in communication with a larger waterbody through a narrow inlet, and likens the response of the bay to a stilling well, in the way that longer period variations pass through the inlet, but shorter period variations are filtered out.

To a first approximation, the wind regime in the Texas coastal zone can be characterized as a sustained onshore flow from the Gulf of Mexico modulated by the sea-land breeze circulation, and interrupted by frontal passages. The seabreeze cycle is a solenoidal circulation produced by the diurnal variation in density of the lower atmosphere resulting from the surface temperature differential of the land and sea (Ward, 1997). It is ultimately caused by the difference in thermodynamics of sea water and land surface, and is most pronounced along their boundary, i.e. the coastline. In the coastal zone itself, the seabreeze is manifested as a diurnal variation in wind velocity superposed on the normal onshore flow from the Gulf of Mexico. The familiar freshening of winds in the afternoon and the increase of short-crested windwaves (chop) are well-known features of summer hydrography in these bays attending the seabreeze. Although a seabreeze circulation is capable of being developed at any time in the year when conditions are favorable, the best conditions are under intense insolation in quiescent synoptic conditions when the onshore flow is weak. Thus, the seabreeze is best developed in conditions typical of summer. There is an inertial lag of the solenoidal circulation behind the daily change in sea-air temperature difference, and as the solenoidal circulation develops, the rotation of the earth (the Coriolis acceleration) produces a longshore component that turns the seabreeze component clockwise (Ward, 1997).

Two TCOON wind stations were selected to characterize wind climatology in the Lower and Upper Laguna Madre regions, respectively the Arroyo Colorado and South Bird Island anemometers. The selection was based upon period of record available, situation of the anemometer station as central as possible in the region, and minimal interfering structures (such as a barrier island). Tabulated in tables 4-1 and 4-2 are the frequencies of occurrence, mean, and standard deviation of the wind speed at Arroyo Colorado and S Bird Island, respectively. In the statistics of tables 4-1 and 4-2, zero values are identified as calms, and represent a separate category of wind speed. Some of the months exhibit an anomalously high

TABLE 4-1
FREQUENCY, MEAN AND STANDARD DEVIATION OF WIND SPEED AT ARROYO COLORADO

Month	Frequency of Occurrence (%) for Wind Speed (m/s) Range						# Data	# Missing	Wind (m/s)		
	Calm	0 - < 3	3 - < 6	6 - < 9	9 - < 12	>= 12			Mean	Std	Dev
09/94	3.5	30.5	45.5	19.4	1.1	0.0	712	8	4.0	2.2	
10/94	2.1	11.9	36.3	37.4	11.9	0.4	720	24	5.9	2.6	
11/94	0.9	8.5	29.4	42.0	16.7	2.5	671	49	6.6	2.7	
12/94	3.0	24.2	38.4	27.3	6.4	0.6	627	117	4.8	2.7	
01/95	2.9	20.6	32.9	25.9	15.5	2.1	611	133	5.6	3.2	
02/95	2.0	16.9	37.7	29.9	11.2	2.3	652	20	5.6	2.9	
03/95	1.8	11.4	31.3	34.8	16.5	4.1	683	61	6.5	3.1	
04/95	22.3	5.5	17.5	26.5	23.9	4.4	641	79	5.9	4.1	
05/95	0.1	3.3	18.2	41.9	30.5	6.1	738	6	8.0	2.6	
06/95	0.4	11.9	27.5	40.9	18.8	0.4	706	14	6.5	2.8	
07/95	0.4	12.8	26.5	38.6	18.9	2.7	697	47	6.6	2.9	
08/95	1.3	24.7	39.8	30.6	3.5	0.1	742	2	4.8	2.7	
09/95	1.8	21.1	46.6	26.2	2.9	1.3	714	6	4.8	2.5	
10/95	35.0	14.4	27.1	16.3	4.8	2.2	722	22	3.4	3.5	
11/95	99.9	0.0	0.0	0.0	0.1	0.0	701	19	0.0	0.3	
12/95	45.0	6.5	21.4	14.0	11.1	2.0	709	35	3.5	3.9	
01/96	2.8	11.9	43.0	21.7	12.9	7.7	653	90	6.2	3.5	
02/96	0.5	5.2	31.6	32.5	26.0	4.1	630	66	7.1	2.9	
03/96	0.2	8.2	31.4	37.4	19.0	3.9	649	95	6.9	2.9	
04/96	2.0	8.6	20.0	33.1	27.3	9.0	664	56	7.6	3.3	
05/96	0.0	0.4	3.8	37.8	56.0	2.0	744	0	9.1	1.6	
06/96	0.7	4.2	23.2	51.5	20.2	0.3	717	3	7.1	2.2	
07/96	1.0	5.6	22.3	46.7	24.0	0.4	732	12	7.2	2.5	
08/96	0.4	6.2	34.4	41.5	16.3	1.1	723	21	6.5	2.5	
09/96	4.8	9.3	37.1	36.9	10.3	1.6	669	51	5.8	2.7	
10/96	3.9	13.5	32.7	32.7	13.3	3.9	727	17	6.0	3.2	
11/96	0.9	8.8	38.6	34.6	13.9	3.2	682	38	6.4	2.7	
12/96	4.2	21.5	38.6	24.7	6.9	4.1	734	10	5.3	3.1	
01/97	3.3	12.3	34.7	27.4	16.0	6.3	700	44	6.3	3.4	
02/97	0.9	8.2	40.2	31.1	16.3	3.3	662	10	6.3	2.8	
03/97	2.3	11.1	30.9	37.4	15.0	3.3	738	6	6.4	2.9	
04/97	0.3	5.3	35.7	34.0	20.4	4.3	583	137	6.9	2.8	
05/97	0.8	7.0	26.4	45.8	19.2	0.7	738	6	6.7	2.5	
06/97								720			
07/97								744			
08/97								744			
09/97	4.2	18.4	37.6	37.0	2.9	0.0	663	57	5.1	2.4	
10/97	4.0	13.4	35.6	32.9	10.8	3.2	744	0	5.8	3.0	
11/97	0.7	9.3	44.3	30.6	12.3	2.8	709	11	6.0	2.7	
12/97	7.4	16.0	39.8	24.4	10.8	1.7	538	206	5.2	3.0	
01/98	1.8	11.6	42.2	35.5	8.2	0.7	552	192	5.6	2.4	
02/98	1.4	12.5	40.1	27.3	11.6	7.1	663	9	6.2	3.2	
03/98	1.7	5.6	27.0	32.7	24.7	8.3	712	32	7.4	3.3	
04/98	1.8	6.4	29.9	36.7	23.1	2.2	720	0	6.8	2.8	
05/98	0.0	1.8	20.0	53.7	23.8	0.7	735	9	7.5	2.0	
06/98	0.4	0.3	9.3	39.2	47.9	2.9	699	21	8.8	2.0	
07/98	0.3	3.4	22.9	50.3	23.0	0.1	739	5	7.3	2.2	
08/98	1.2	10.4	36.0	40.9	11.2	0.3	741	3	6.0	2.5	
09/98	0.0	0.0	25.0	45.8	29.2	0.0	24	0	7.5	1.9	

TABLE 4-2
FREQUENCY, MEAN AND STANDARD DEVIATION OF WIND SPEED AT S. BIRD ISLAND

Month	Frequency of Occurrence (%) for Wind Speed (m/s) Range						# Data	# Missing	Wind (m/s)		
	Calm	0 - < 3	3 - < 6	6 - < 9	9 - < 12	>= 12			Mean	Std	Dev
09/94	3.4	19.7	60.9	14.7	1.1	0.0	699	21	4.2	1.8	
10/94	2.3	14.7	47.7	29.6	5.7	0.1	707	37	5.2	2.3	
11/94	0.8	7.7	41.8	37.0	11.4	1.3	622	98	6.1	2.4	
12/94	3.2	16.7	53.7	20.1	6.2	0.1	708	36	4.8	2.3	
01/95	3.7	15.7	45.9	25.4	7.9	1.4	630	114	5.1	2.7	
02/95	3.4	17.0	52.0	19.4	6.5	1.6	613	59	4.9	2.6	
03/95	2.0	10.9	37.7	31.1	15.6	2.6	685	59	6.1	3.0	
04/95	1.2	10.4	38.5	37.5	10.6	1.8	680	40	6.1	2.6	
05/95	0.4	5.2	34.1	44.6	14.4	1.2	744	0	6.6	2.3	
06/95	0.8	14.5	38.5	39.3	6.7	0.1	712	8	5.5	2.3	
07/95	2.6	16.8	46.0	26.4	7.5	0.7	743	1	5.1	2.6	
08/95	3.7	27.5	51.2	16.4	1.1	0.1	737	7	4.0	2.1	
09/95	4.9	25.3	56.6	11.6	0.7	0.7	671	49	3.8	2.1	
10/95	2.8	21.9	40.3	23.7	9.2	2.0	704	40	5.1	2.9	
11/95	4.8	23.7	38.1	22.8	8.7	1.9	670	50	5.0	3.0	
12/95	3.7	18.0	43.5	24.5	8.7	1.6	699	45	5.1	2.8	
01/96	4.3	17.1	38.6	22.2	13.2	4.6	720	24	5.6	3.3	
02/96	1.4	12.3	41.2	32.4	10.3	2.5	651	45	5.8	2.7	
03/96	4.6	13.4	36.8	32.8	8.9	3.5	722	22	5.8	3.0	
04/96	3.2	13.1	32.3	36.3	11.6	3.4	708	12	6.0	3.1	
05/96	0.0	1.8	14.0	69.4	14.8	0.0	677	67	7.3	1.7	
06/96	0.6	7.1	39.2	46.7	6.4	0.1	720	0	6.0	2.1	
07/96	1.4	8.9	37.5	45.1	7.2	0.0	741	3	5.9	2.2	
08/96	0.9	9.1	50.8	33.5	5.6	0.1	693	51	5.5	2.1	
09/96	4.1	19.5	47.5	21.3	6.3	1.3	686	34	4.8	2.6	
10/96	4.2	19.2	39.4	23.2	8.5	5.5	715	29	5.3	3.2	
11/96	2.9	8.3	35.7	36.7	14.7	1.7	712	8	6.2	2.8	
12/96	13.6	18.8	36.6	20.7	8.1	2.3	707	37	4.5	3.2	
01/97	10.1	15.2	32.6	23.3	12.7	6.1	656	88	5.6	3.7	
02/97	3.7	14.3	36.7	30.9	13.0	1.4	622	50	5.7	2.9	
03/97	5.7	17.1	37.9	28.6	7.3	3.5	742	2	5.3	3.1	
04/97	0.7	7.5	38.3	32.6	19.8	1.1	708	12	6.4	2.6	
05/97	1.4	8.5	43.5	39.6	6.4	0.7	738	6	5.8	2.2	
06/97	0.8	8.3	49.4	35.7	5.5	0.1	708	12	5.6	2.1	
07/97	1.4	6.1	56.4	34.3	1.9	0.0	738	6	5.4	1.8	
08/97	3.4	6.0	44.1	38.3	8.2	0.0	619	125	5.7	2.3	
09/97	6.3	19.5	53.2	20.1	0.9	0.0	632	88	4.2	2.1	
10/97	5.3	16.4	41.5	28.0	7.3	1.5	715	29	5.1	2.8	
11/97	7.2	15.3	39.1	27.7	8.9	1.7	704	16	5.2	3.0	
12/97	12.1	19.9	32.2	23.7	10.7	1.4	738	6	4.8	3.3	
01/98	3.9	16.4	48.6	24.8	6.0	0.3	714	30	4.9	2.4	
02/98	3.2	16.9	39.2	28.3	10.6	1.8	661	11	5.5	3.0	
03/98	2.3	9.2	28.7	44.1	13.5	2.2	728	16	6.4	2.8	
04/98	1.7	9.2	40.3	33.9	13.7	1.3	717	3	6.0	2.6	
05/98	0.0	2.9	42.4	49.1	5.6	0.0	729	15	6.2	1.8	
06/98	0.1	2.1	19.9	57.2	19.5	1.1	699	21	7.4	2.0	
07/98	0.3	4.4	39.2	48.0	8.2	0.0	735	9	6.2	1.9	
08/98	1.9	9.9	50.8	32.0	5.2	0.2	618	5	5.3	2.2	

proportion of zero values. These data are as reported in the TCOON files. It is our feeling that for some of these months, the zeroes are, in fact, missing values. Certainly months 10/95-12/95 at the Arroyo Colorado must be largely missing values, as calms between 50% and 100% of the data are unrealistic. Although CBI employs a separate character as an identifier of missing data, this character was not entered in these records. Once we embark on the strategy of deleting zero values, we encounter the dilemma of differentiating real zeros elsewhere in the record, and become forced to make a data-point by data-point review. Rather than descend into this processing nightmare, we instead simply identify and qualify such zero values of wind. (Zeroes of current speed are a different matter, however, and are treated more carefully in the data scrubbing, see Chapter 3.)

As a rule, the late summer-early fall period evidences the lowest maximum speeds, with the wind predominantly out of the southeast quadrant. Because of the reduced frequency of high winds, and the minimal fetch associated with the easterly wind direction, there is generally reduced wave energy. During September, 1994, for example, the wind speed was predominantly less than 6 m/sec (13 mph) (80% of the time), with wind speeds rarely exceeding 9 m/sec (20 mph) (<1%), and the monthly mean wind speed was 4 m/sec (9 mph).

Monthly wind roses were generated using data collected for the period from September 1, 1994, to June 30, 1998, at these two TCOON stations. Figures 4-1 and 4-2 show example monthly wind roses for each month in 1996, for the Lower Laguna (Arroyo Colorado) and Upper Laguna (S. Bird Island), respectively. The entire suite of monthly wind roses are provided in Appendix WR. Note that the wind directions associated with these wind roses are reversed from their usual convention, that is, they are defined here as the direction to which the wind is blowing ("blowing toward") instead of the direction from which the wind blows ("blowing from."), to be more consistent with the vector character of the wind velocity. For these displays, the wind directions were sorted into 45° bins centered on the primary compass directions. Missing data undermines the representativeness of a few of these years, from which individual months had to be excluded because of missing measurements. The most complete years of data for both anemometers together were 1995 and 1996.

The prevailing SE wind is readily apparent at both stations. Typically, 50 cold fronts traverse the Laguna Madre region each year (Morgan *et al.*, 1975). The first front of the winter season generally traverses South Texas in late September or October. Frontal passages continue through the region, increasing in frequency during the winter months, and occurring in the spring typically through March or April. The wind usually increases in speed from the Gulf of Mexico with the approach of the front, then abruptly shifts to the northern quadrant with the frontal passage. For example, in the 1994-1995 winter season, the first front passed through the study area on October 8, 1994, with accompanying average wind speeds reaching 13 m/sec (29 mph). High north wind speeds prevail for a variable period from a day to over

a week, generally declining in speed over time and veering in direction. These short-duration, strong wind events figure importantly in the mechanism for sediment resuspension and transport.

The winter northerlies are more frequent at the northern S. Bird Island station than at the southern Arroyo Colorado station. While the frequency of north winds is around 10% at the former, the prominence of the occurrence of speeds greater than 12 m/s should be noted. The monthly wind roses of figures 4-1 and 4-2 display the shift from predominantly southeasterly wind regimes to alternating southeasterly and northerly—the bimodal rose—tracking the passage of seasons from summer to winter. The prevalence of high wind speeds from the SE in May should be especially noted. This is a result of late-spring frontal passages which enhance the normal onshore southeasterly winds, but have weak and variable north winds so contribute little to the wind rose.

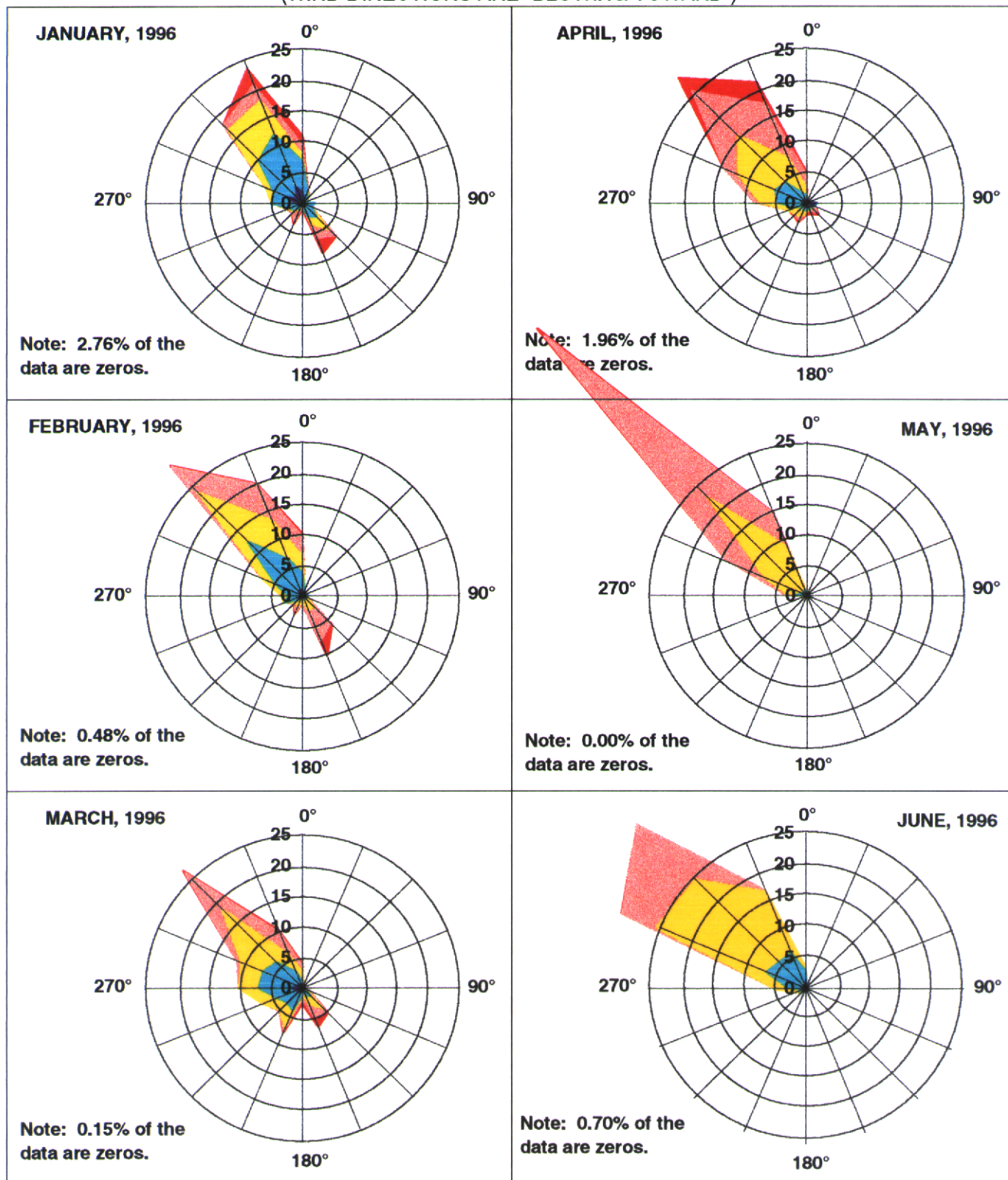
General prevailing wind conditions are presented by the annual wind roses for separate years in the study period. These are shown in figures 4-3 and 4-4, for the Lower Laguna (Arroyo Colorado) and Upper Laguna (South Bird Island), respectively. A close inspection of tables 4-1 and 4-2 also discloses that there is considerable year-to-year variation, as well as substantial differences between the wind statistics in the upper and lower segments of the Laguna, also exemplified graphically by figures 4-3 and 4-4. (Note that the records are incomplete for some years, so the resulting wind rose has to be appropriately interpreted.)

4.2 WATER LEVEL

Water level (a.k.a. “tide” level) is the hydrodynamic variable that is simplest to measure, so the data base on the Texas coast for water level is comparatively rich. The TCOON system, in particular, is a valuable archive of digital water-level data, but agencies such as the USACE, National Ocean Service, U.S. Geological Survey, Texas Water Development Board, and National Weather Service have monitored water levels at permanent tide stations on the Texas coast for many years (the USACE, in particular, having done so since the mid-Nineteenth Century).

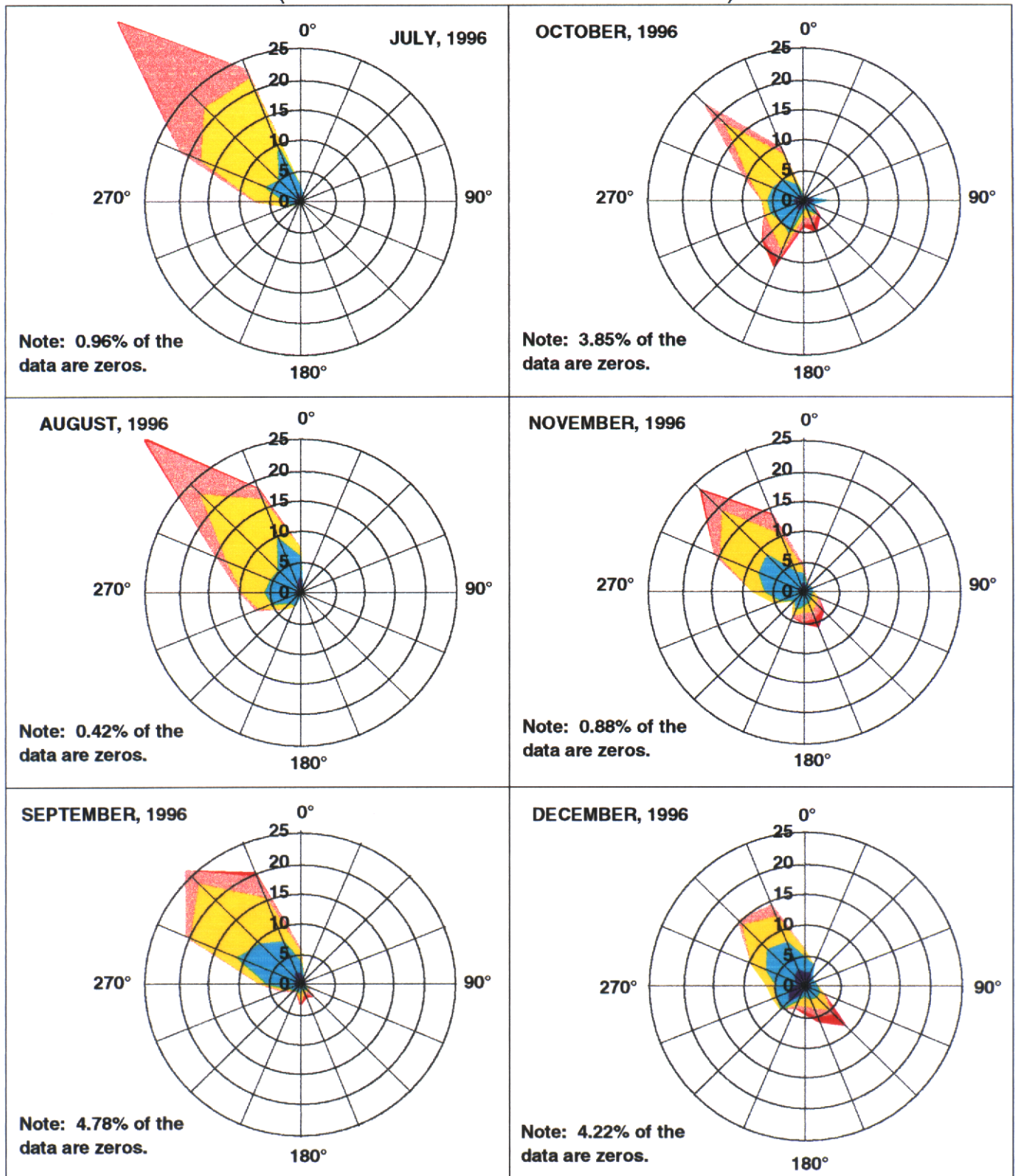
Water-level, as a hydrodynamic variable, is both a responder and a forcer. It responds to the movement of water due to wind stress and due to exchanges between the Laguna and adjacent waterbodies. But spatial gradients in water level entail pressure gradients that accelerate the water thereby producing currents. Variation in water level is a direct index, therefore, to currents that mobilize and transport sediment. As noted above, there is a spectrum of time-space scales of variation of water level. Figures 4-5 and 4-6 display the water-level time series at both TCOON stations, the Arroyo Colorado and South Bird Island, for the entire study period, along with low-pass 3-day sliding means. At this level of compression

FIGURE 4-1
MONTHLY WIND ROSE AT TCOON STATION - ARROYO COLORADO
(WIND DIRECTIONS ARE "BLOWING TOWARD")



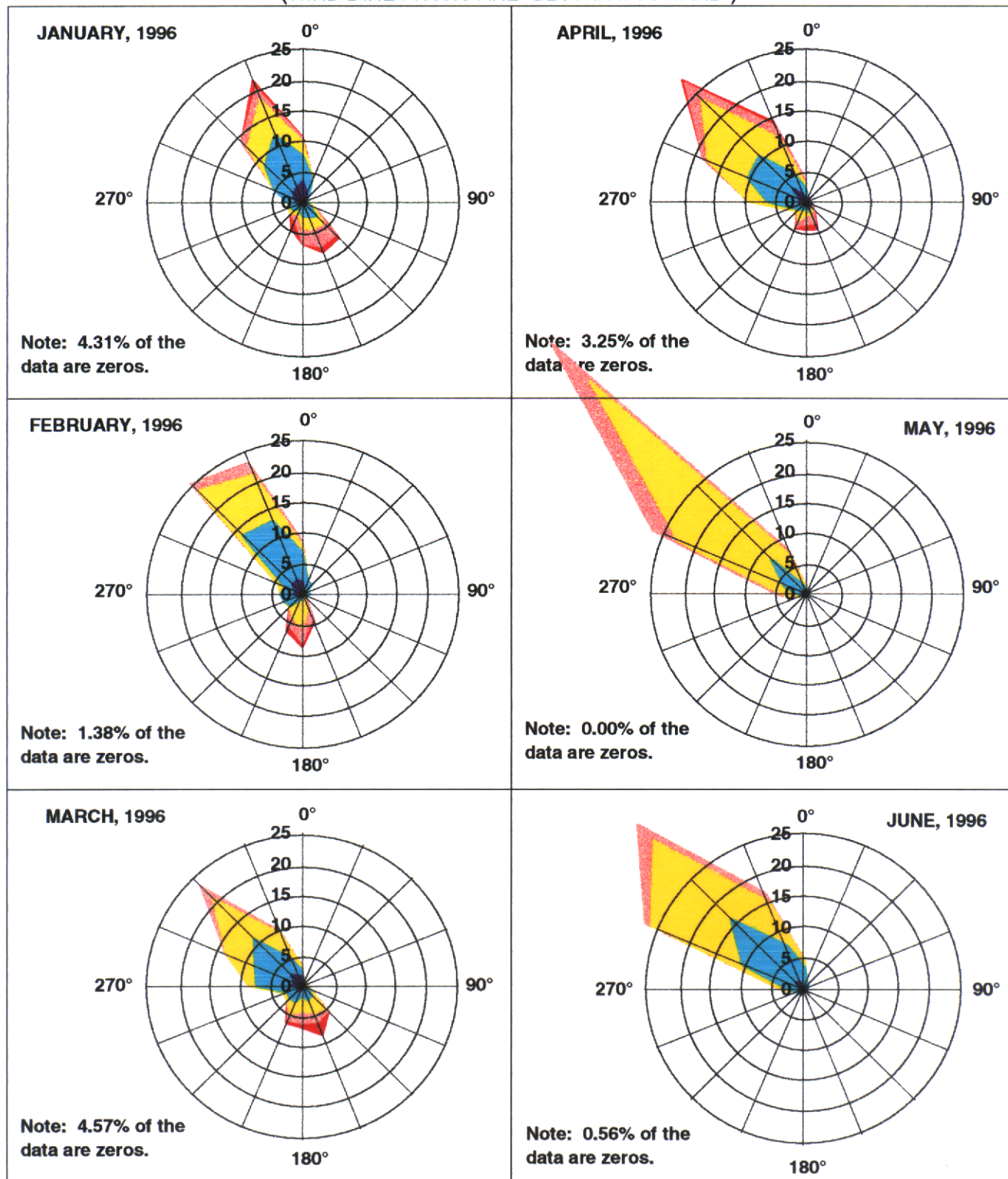
Wind Speed (m/s): ■ ≥ 12 ■ 9-12 ■ 6-9 ■ 3-6 ■ 0-3

FIGURE 4-1 (Continued)
MONTHLY WIND ROSE AT TCOON STATION - ARROYO COLORADO
(WIND DIRECTIONS ARE "BLOWING TOWARD")



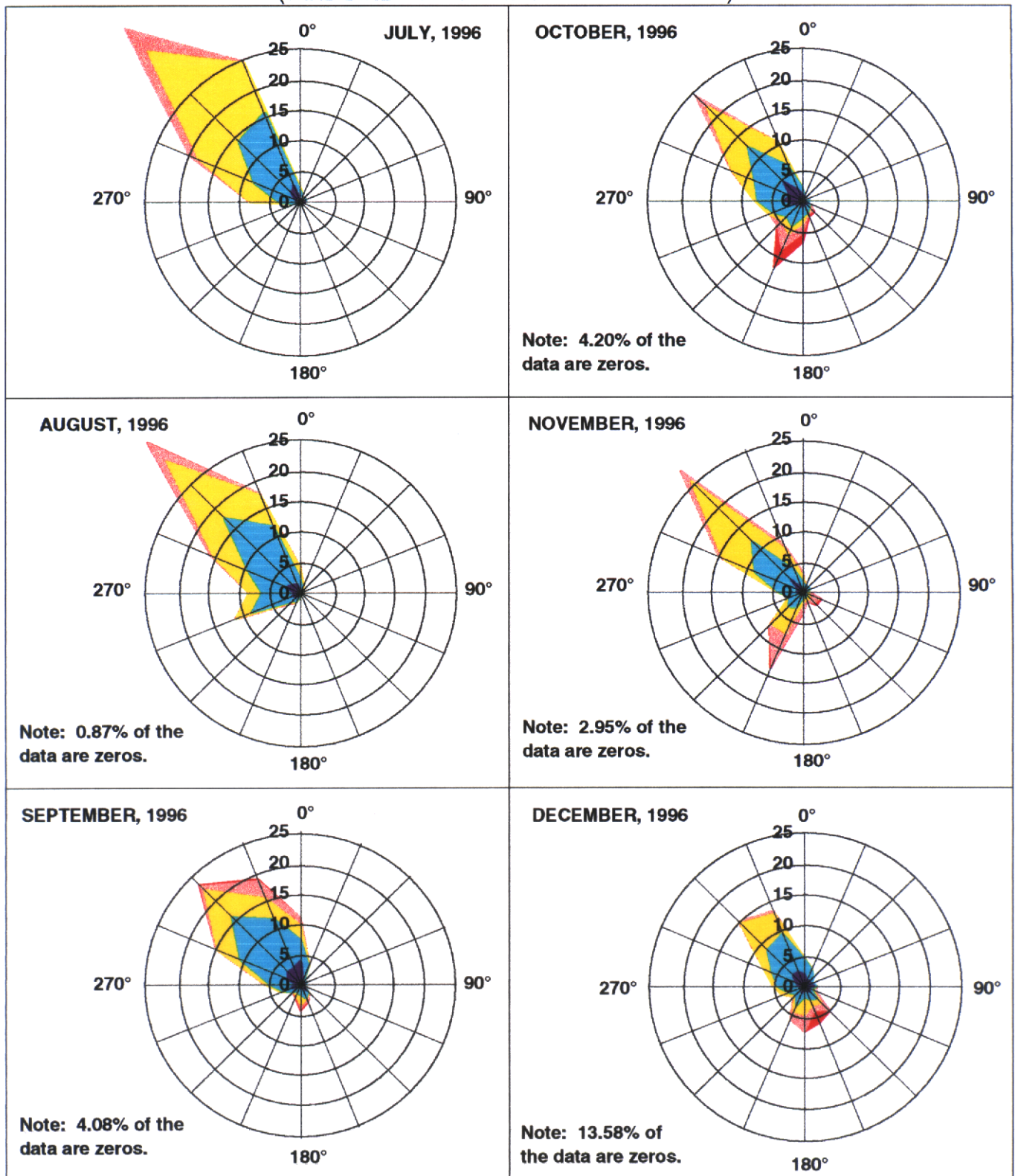
Wind Speed (m/s): ■ ≥ 12 ■ 9-12 ■ 6-9 ■ 3-6 ■ 0-3

FIGURE 4-2
MONTHLY WIND ROSE AT TCOON STATION - S. BIRD ISLAND
(WIND DIRECTIONS ARE "BLOWING TOWARD")



Wind Speed (m/s): ■ ≥ 12 ■ 9-12 ■ 6-9 ■ 3-6 ■ 0-3

FIGURE 4-2 (Continued)
MONTHLY WIND ROSE AT TCOON STATION - S. BIRD ISLAND
(WIND DIRECTIONS ARE "BLOWING TOWARD")



Wind Speed (m/s): ■ ≥ 12 ■ 9-12 ■ 6-9 ■ 3-6 ■ 0-3

FIGURE 4-3
ANNUAL WIND ROSE AT TCOON STATION - ARROYO COLORADO
(WIND DIRECTIONS ARE "BLOWING TOWARD")

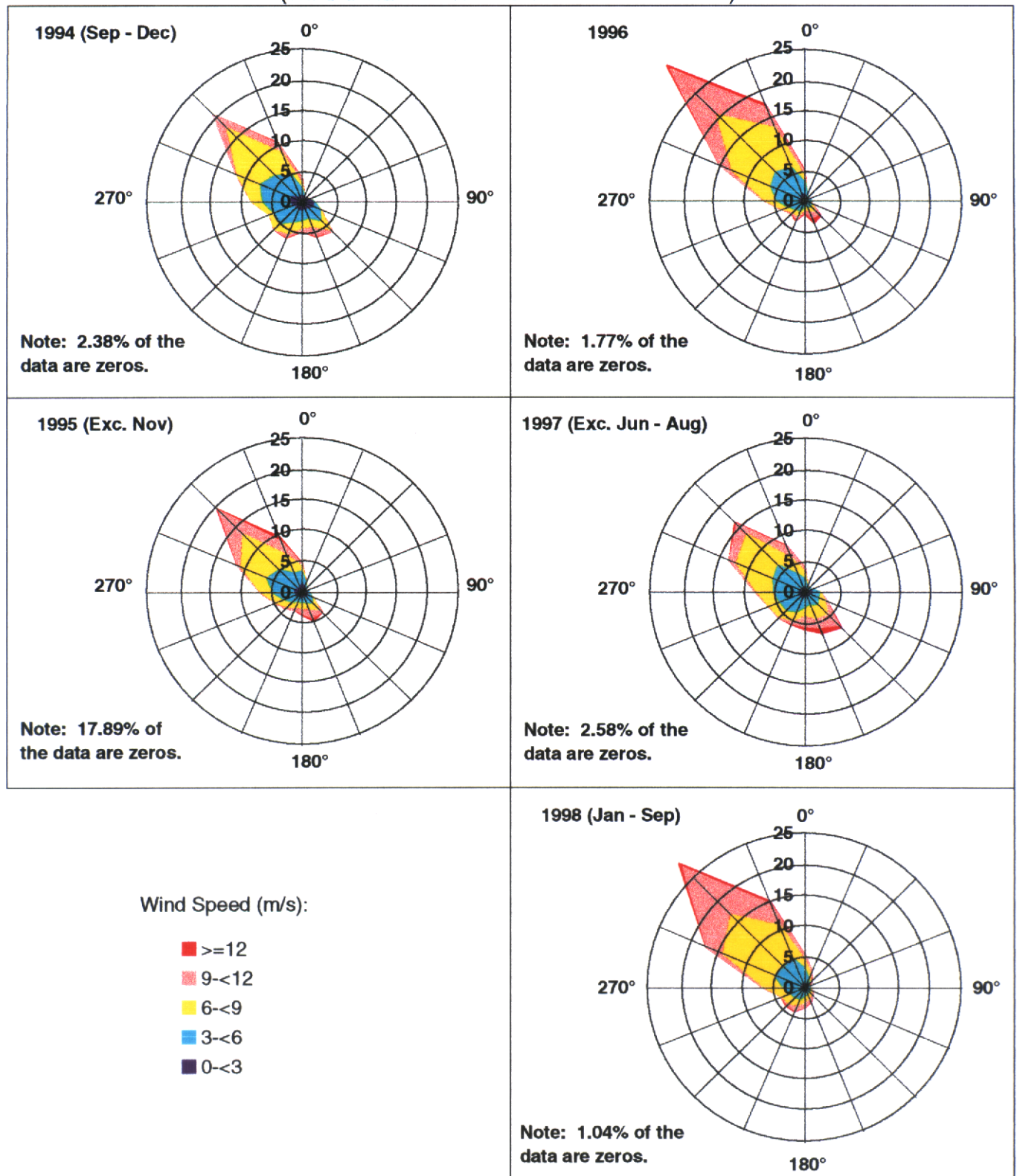


FIGURE 4-4
ANNUAL WIND ROSE AT TCOON STATION - S. BIRD ISLAND
(WIND DIRECTIONS ARE "BLOWING TOWARD")

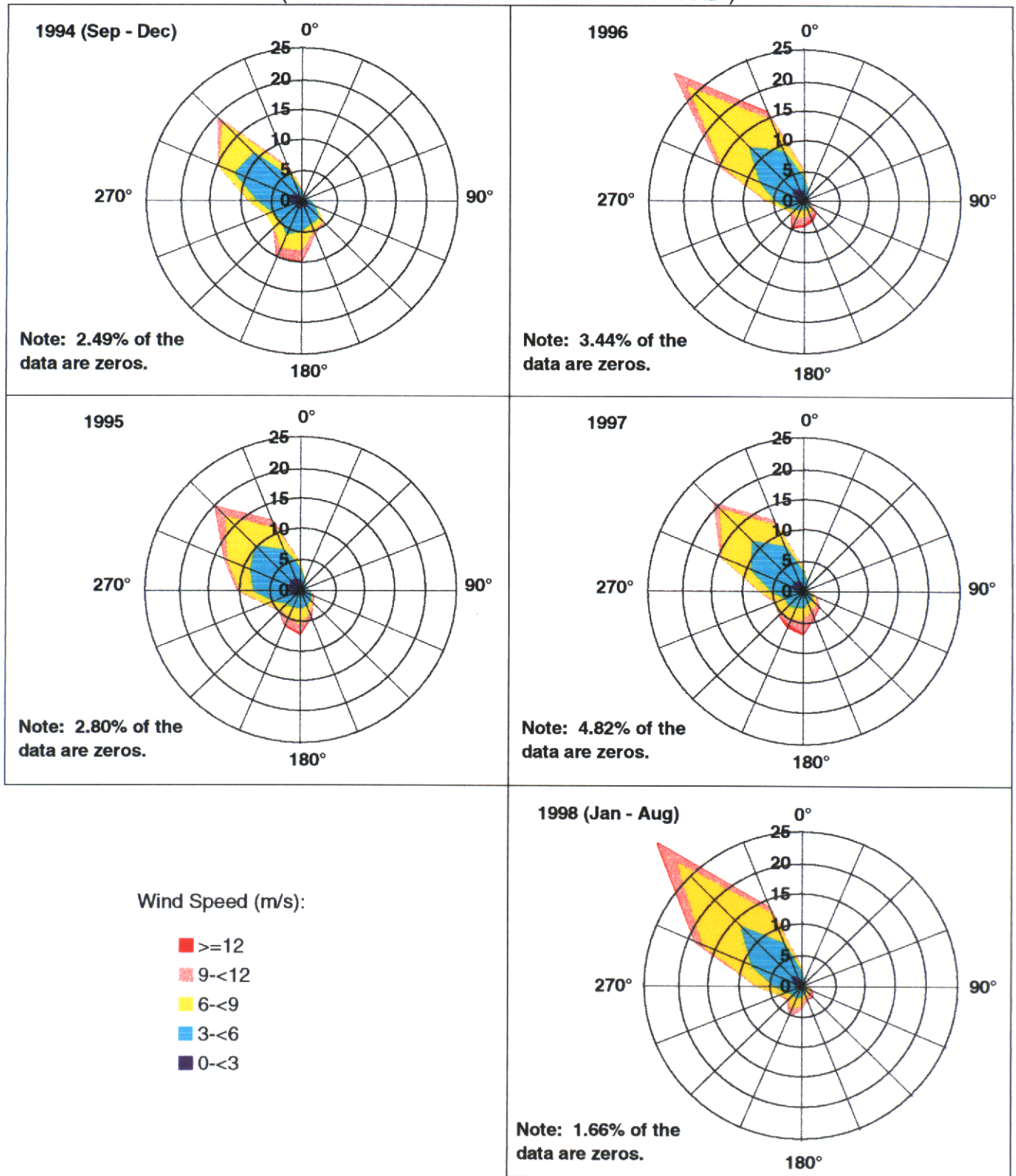


FIGURE 4-5
WATER LEVELS AT ARROYO COLORADO

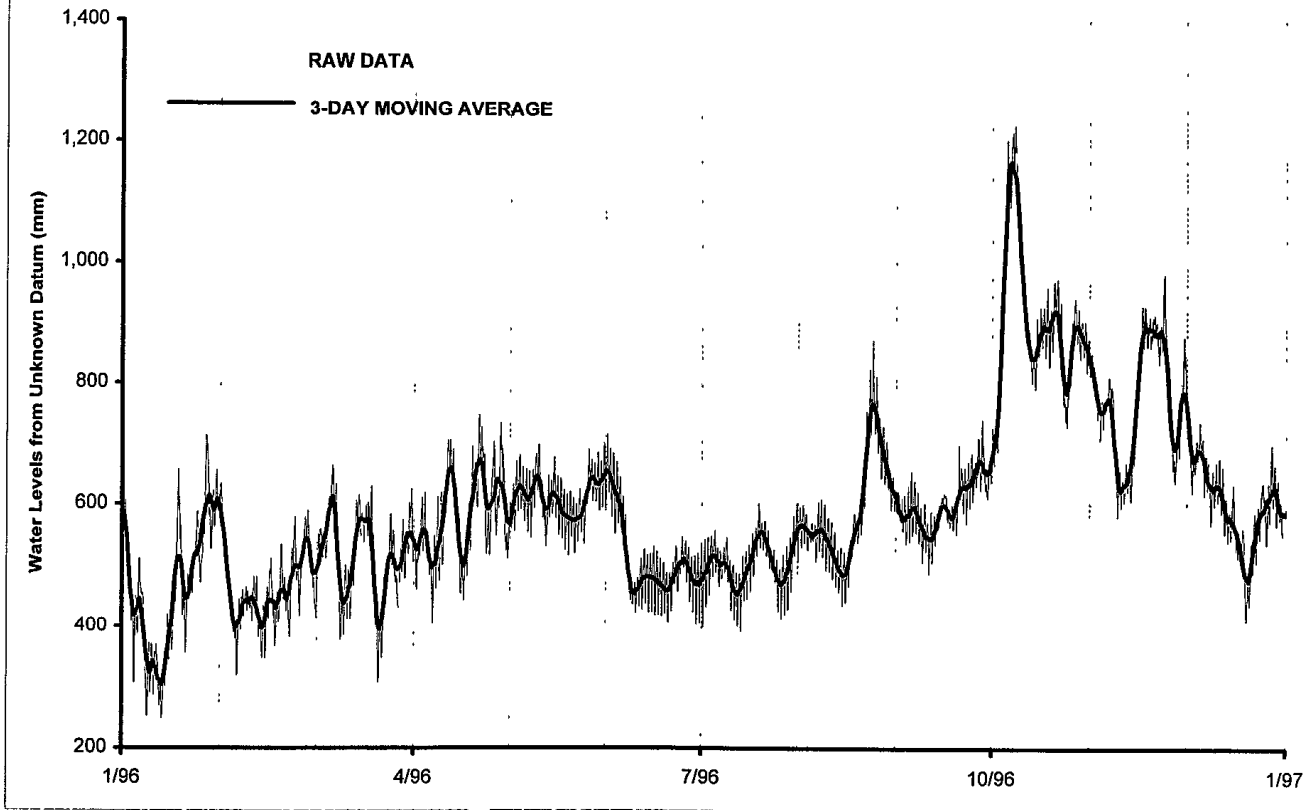
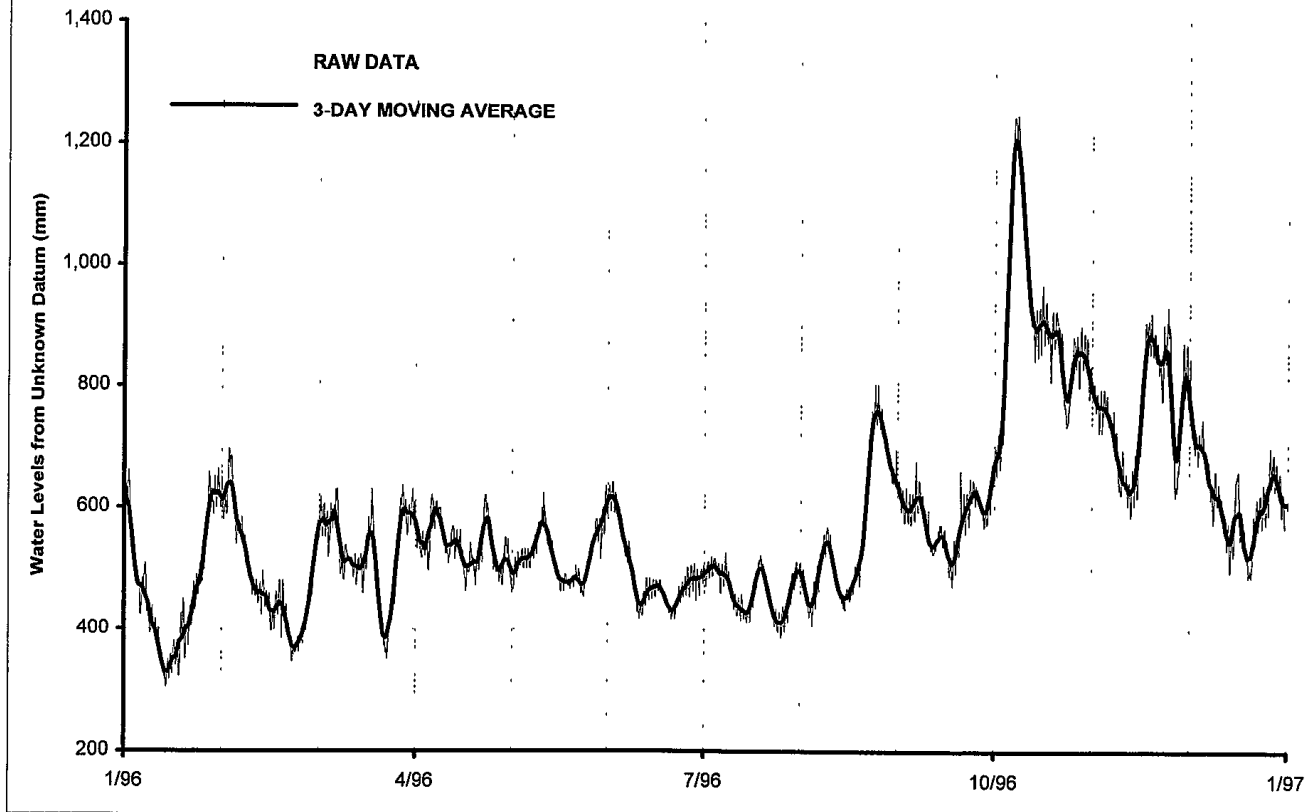


Fig4-5&7 Chart 5 6/30/99 9 16 AM KEM

PBS&J

FIGURE 4-6
WATER LEVELS AT S. BIRD ISLAND



of the time axis, only the peak excursions in water level are discernible in the plot, but the presence of long-period variation is clear. The coherency of these two records at these two stations for longer period variations (weeks to months) should be especially noted

At the largest scale, beyond even the record shown in figures 4-5 and 4-6, there is a long-period historical increase in water level along the Texas coast and in the Laguna Madre. This is the coastal response to a combination of global change in water level on the earth (eustatic change), local changes in water level, and rising or falling (subsidence) of land. Lyles, *et al.* (1988) determined that the mean water ("sea") level at the NOS tide gauge at Port Isabel averaged over 1945-1970 is 1.29 m (4.24 ft), and averaged over 1971-1986 is 1.38 m (4.52 ft), indicated the magnitude of the recent net increase in water level. Militello and Kraus (1994) estimated that over a 50-year period (1945-1994), the water level in the lower Laguna Madre would have risen 15.5 cm (0.5 ft), and suggest that this long-term change in depth would have implications for light attenuation and seagrass distribution.

In the Laguna Madre, one of the dominant variations in water level is the semi-annual secular rise and fall of sea level (Smith 1978, Ward, 1997). While this is evident in figures 4-5 and 4-6, it is exposed even more in a time-series of the low-pass filtered (with a cutoff period of 60 days) hourly water levels at the respective stations, figures 4-7 and 4-8. These figures reveal a semi-annual rise and fall of sea level of approximately 0.3 m (1 ft) within considerable interannual variation, with maximum water elevations occurring in spring (April-May) and Fall (October), and minimum levels occurring in late winter (January or February) and mid-summer (July). Various theories have been proposed to account for this variation, including seasonal heating of the water column, climatology of onshore versus offshore winds, and interaction with circulation vortices in the Gulf of Mexico, but there is no satisfactory physical explanation yet proposed. What is important is that this very low frequency signal propagates through the inlets into the Laguna practically without attenuation and is the main contributor to the net annual excursion in water level. The degree of interannual variation in the long-term water level variation is displayed by the 180-day sliding average in these figures. It will be recalled that the October 1996 fall high-water received considerable media attention because of water inundating part of the JFK Causeway (an event blamed widely, and incorrectly according to Ward, 1997, on a minor tropical storm that happened to be at large in the Gulf of Mexico at this time.)

For shorter-period (higher frequency) signals than the seasonal semi-annual component, there is a degree of filtering upon passage of the signal from the Gulf of Mexico through the inlets. Important (astronomical) tidal components include the fortnightly (~14 days) associated with the cycle of lunar declination, the diurnal (24.8 hrs) driven by the lunar day, and the semi-diurnal (12.4 hrs) of the lunar half-day. The higher the frequency, i.e. shorter the period, the greater the degree of filtering experienced by the signal on passing from the Gulf of Mexico into the Laguna. Moreover, the effect of frictional dissipation

FIGURE 4-7
SEASONAL VARIATIONS IN WATER LEVELS AT ARROYO COLORADO

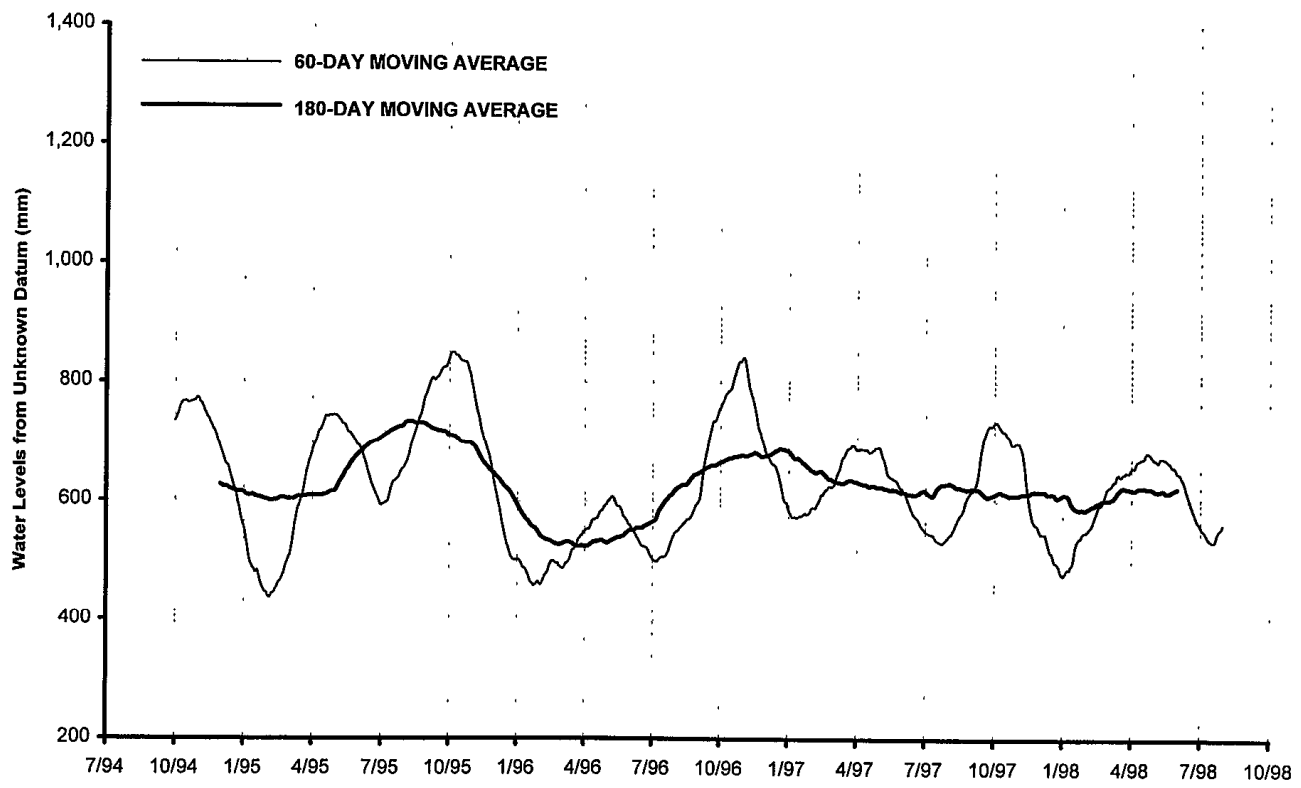
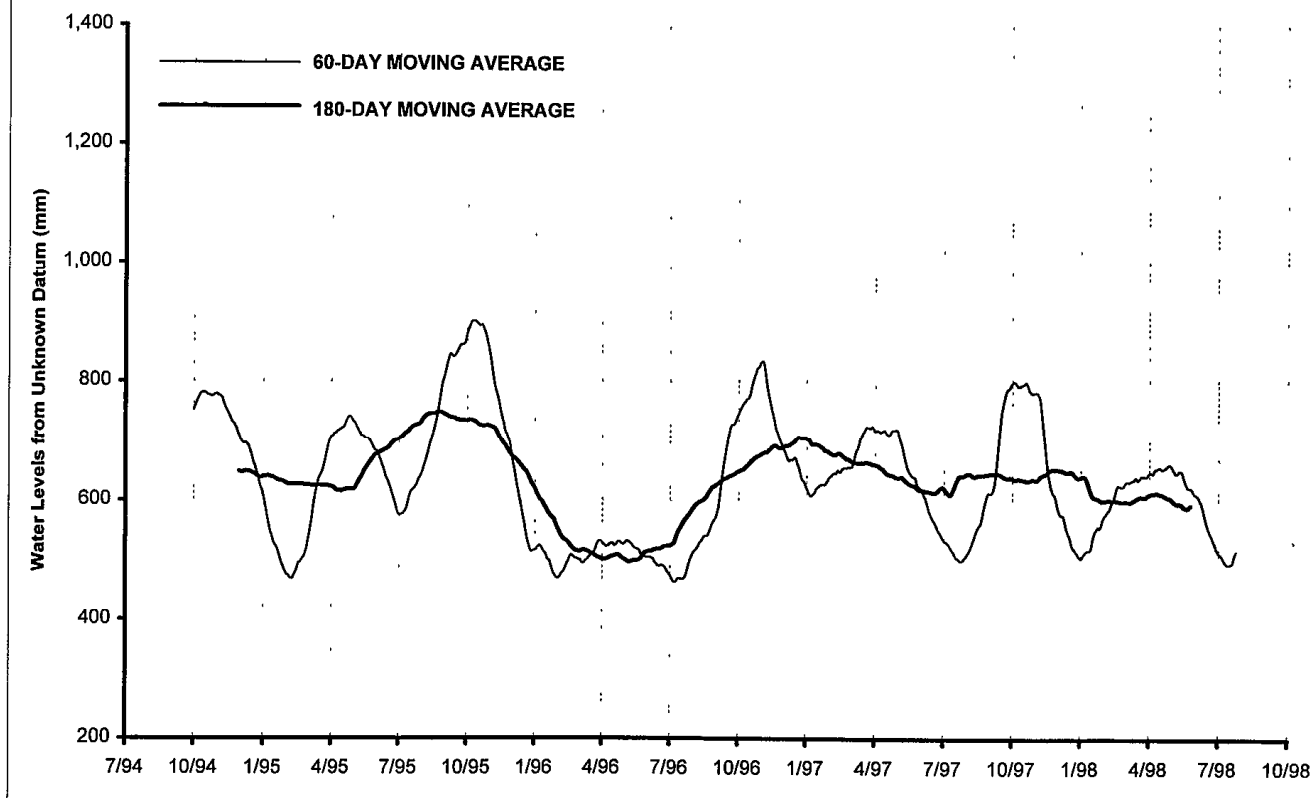


FIGURE 4-8
SEASONAL VARIATIONS IN WATER LEVELS AT S. BIRD ISLAND



is to further diminish the higher frequency components of the tide. For this reason, the 14-day component receives relatively little attenuation, but the diurnal component is substantially reduced, and the semi-diurnal is nearly eliminated. Because the usual 12.4 and 24.8-hr tidal signals are so attenuated within the Laguna, the Laguna Madre is classified as micro-tidal, with the mean tidal range varying from approximately 0.3 m (1 ft) in the vicinity of connections with the Gulf of Mexico to a few centimeters in the interior portions of the Laguna.

The Year-1 fixed measurement platforms in the Lower Laguna (LLM1, LLM2, LLM3) were located approximately 16 km (10 miles) north of Brazos Santiago Pass and approximately 35 km (22 miles) south of Mansfield Pass. The tidal signal propagates through Brazos Santiago Pass with relatively little attenuation. The mean diurnal tidal range is 43 cm (1.4 ft) outside the jetties at Brazos Santiago Pass and 40 cm (1.3 ft) inside the pass at Port Isabel (NOAA, 1983). However, as the tidal signal propagates approximately 27 km (17 miles) northward into the Laguna Madre, it is attenuated to a mean range of approximately 10 cm (0.3 ft) at Arroyo Colorado. In contrast to Brazos Santiago, the tidal signal propagating through Mansfield Pass is substantially attenuated by the small inlet and long, narrow channel and as a result little tidal signal reaches the Laguna Madre. In the Laguna Madre at Port Mansfield the mean range is approximately 7 cm (0.2 ft). Brown and Kraus (1997) attribute the attenuation of the semi-diurnal signal from Port Isabel into the Lower Laguna as the result of frictional effects associated with the shallow water. This is certainly a factor. Another is the dynamics of the co-oscillation of the shallow Laguna with the Gulf of Mexico. The deep Brownsville Ship Channel through Brazos Santiago allows propagation of the ocean tide to Port Isabel. The inlet filtering effect is really exerted across a section roughly coinciding with the old causeway to South Padre.

Meteorological systems impose additional variation in water level, primarily through the effects of wind stress, which in some cases exhibit significant periodicity. Seabreeze circulations contribute a 24-hr component (in addition to the tidal component induced by the sun), and frontal passages, especially during the winter, can introduce energy in the 3-7 day components, depending upon the season. Exchange between the embayments, the nearshore, and adjacent coastal shelf driven by meteorological forcing is a dominant mechanism for these low frequency variations (Smith, 1978, Ward, 1997). In addition, local meteorological forcing results in local set-up and set-down of the water. The magnitude of the seasonal and low-frequency variations in water elevation in the study area is shown by figures 4-5 and 4-6.

Ward (1997) distinguishes between two types of cold fronts, equinoctial and polar-outbreak, which differ primarily in the energy of the controlling synoptic system, therefore the extent to which the continental air behind the front overruns the Gulf of Mexico. Equinoctial fronts effect a pronounced wind shift, but do not substantially affect water levels in the adjacent Gulf of Mexico, so their influence is largely the direct wind stress response of the Laguna. Polar outbreak fronts, primarily a phenomenon of winter,

entail major incursions of polar air across the coastal plain and over the Gulf of Mexico, and result in the major set-up and set-down responses characteristic of intense "northers." From an analysis of frontal responses of Corpus Christi Bay, Ward (1997) drew the following conclusions concerning frontal passage response

- For a given front, the magnitude of water volume exchanged between a component bay and the adjacent system (ultimately the Gulf of Mexico) is generally greater than the internal cross-bay transport of water,
- The cross-bay transports are about the same magnitude for both equinoctial and polar-outbreak fronts, however, the influx volume is much greater for the polar-outbreak fronts;
- The frontal response of the Gulf of Mexico is the single most important factor determining the response of the bay,
- The frontal influx is on the same order as the great declination tidal prism, and for the outer bays is generally larger than the great-declination tidal prism;
- The time-scale of response to a frontal windshift for the influx is on the order of a day; the larger responses—to polar-outbreak fronts—take place over a longer time frame, perhaps 2-4 days.

4.3 FREQUENCY DOMAIN ANALYSIS OF WIND AND WATER LEVEL

To identify the periodic components of variations in wind, as well as water level and current (to be presented below), spectral analyses were performed for subsets of the complete time series. Wind is a vector quantity, but the spectrum is a scalar concept (a facile avoidance of the concept of directional spectrum, a topic which is beyond the scope of this study). Spectra were computed for three scalars that characterize the wind velocity: the two components (E-W and N-S), and the magnitude of the vector wind (i.e., the wind speed). Wind velocity time series data were grouped by study year and the spectra for each year are presented in Figure 4-9 for the Arroyo Colorado anemometer and Figure 4-10 for South Bird Island anemometer. The most obvious feature of these spectra is the prominent spike at exactly 1(cpd), i.e. period 24 hours. This is the signal from the seabreeze.

FIGURE 4-9
ANNUAL WIND SPEED SPECTRA AT TCOON STATION
ARROYO COLORADO

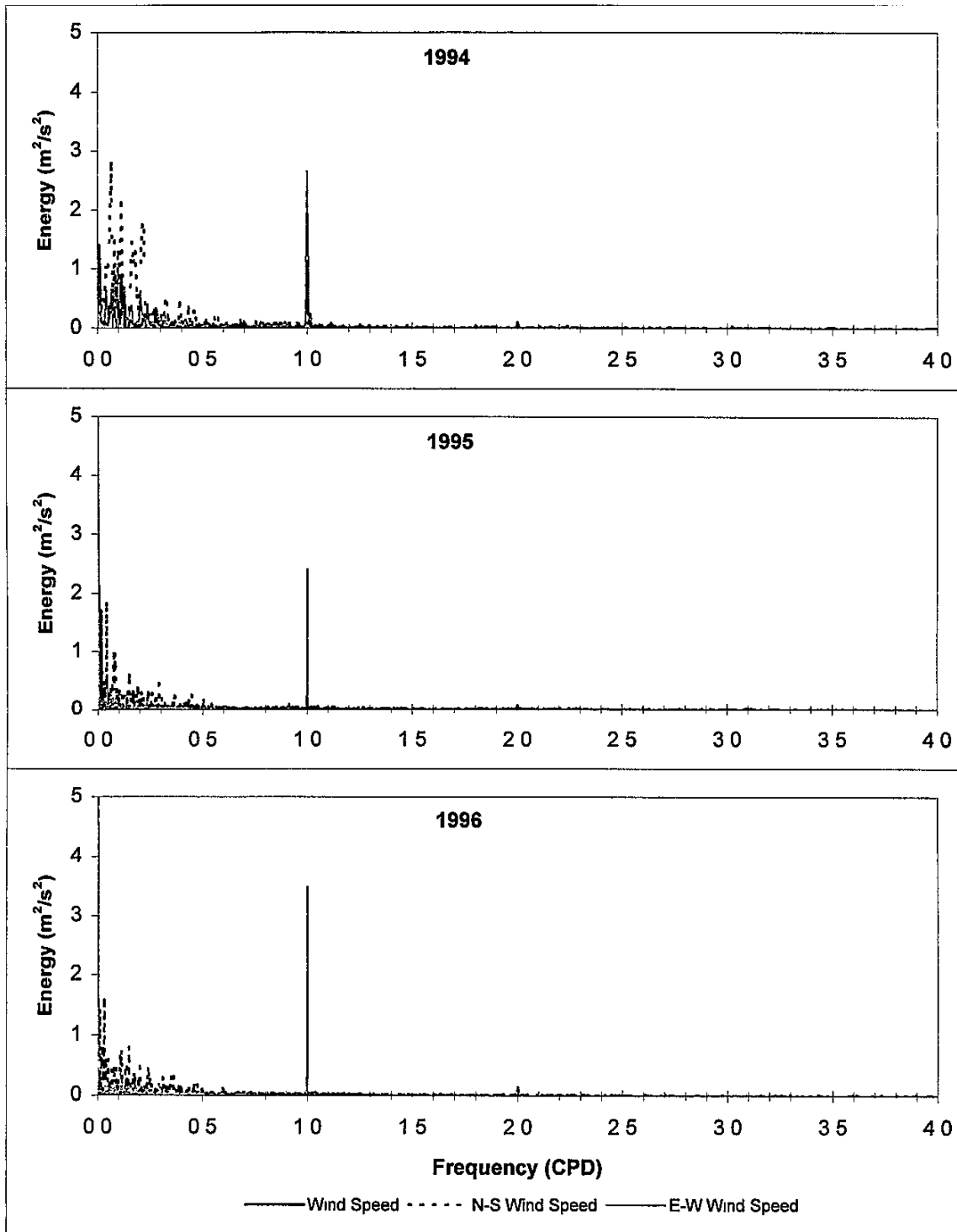


FIGURE 4-9 (Continued)
ANNUAL WIND SPEED SPECTRA AT TCOON STATION
ARROYO COLORADO

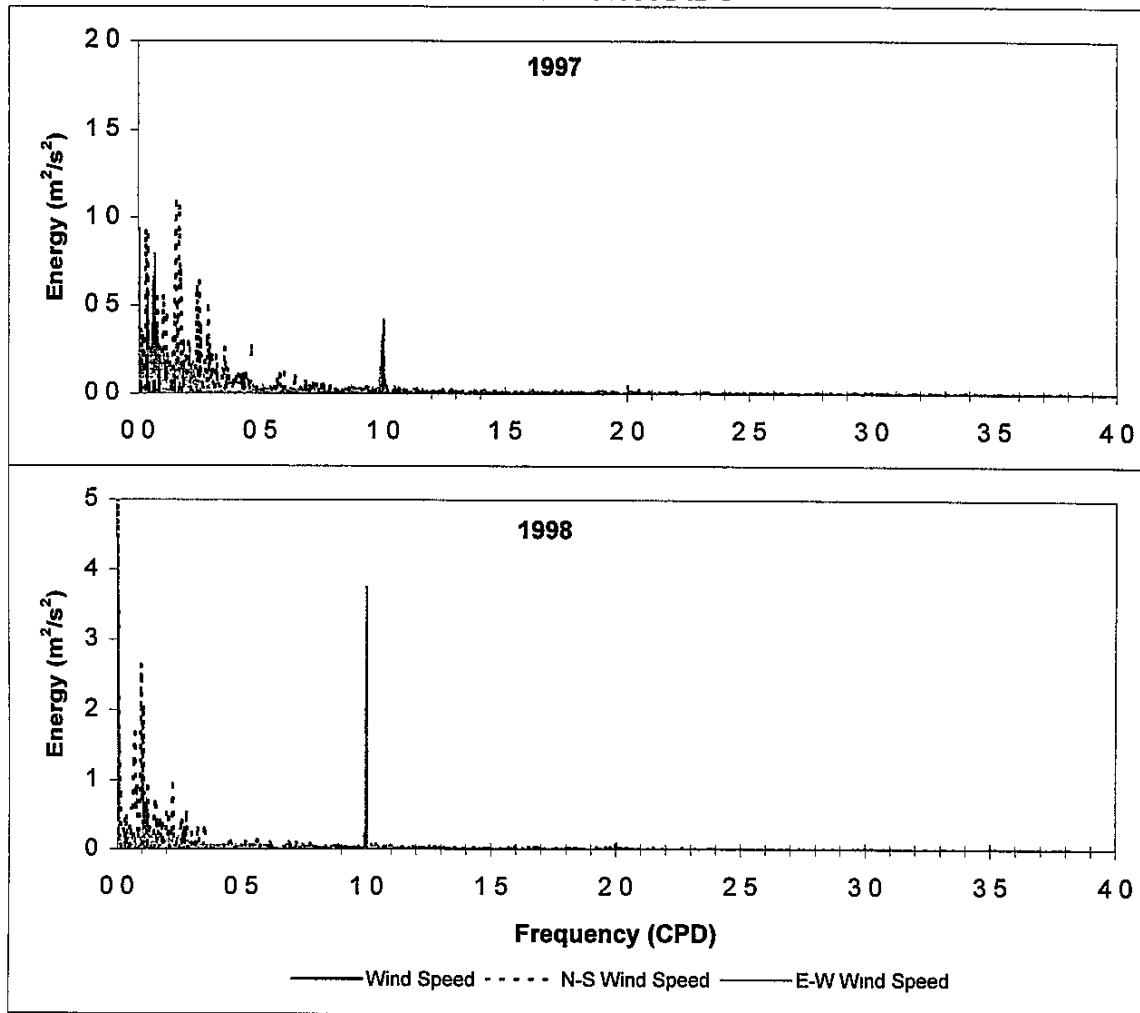


FIGURE 4-10
ANNUAL WIND SPEED SPECTRA AT TCOON STATION
SOUTH BIRD ISLAND

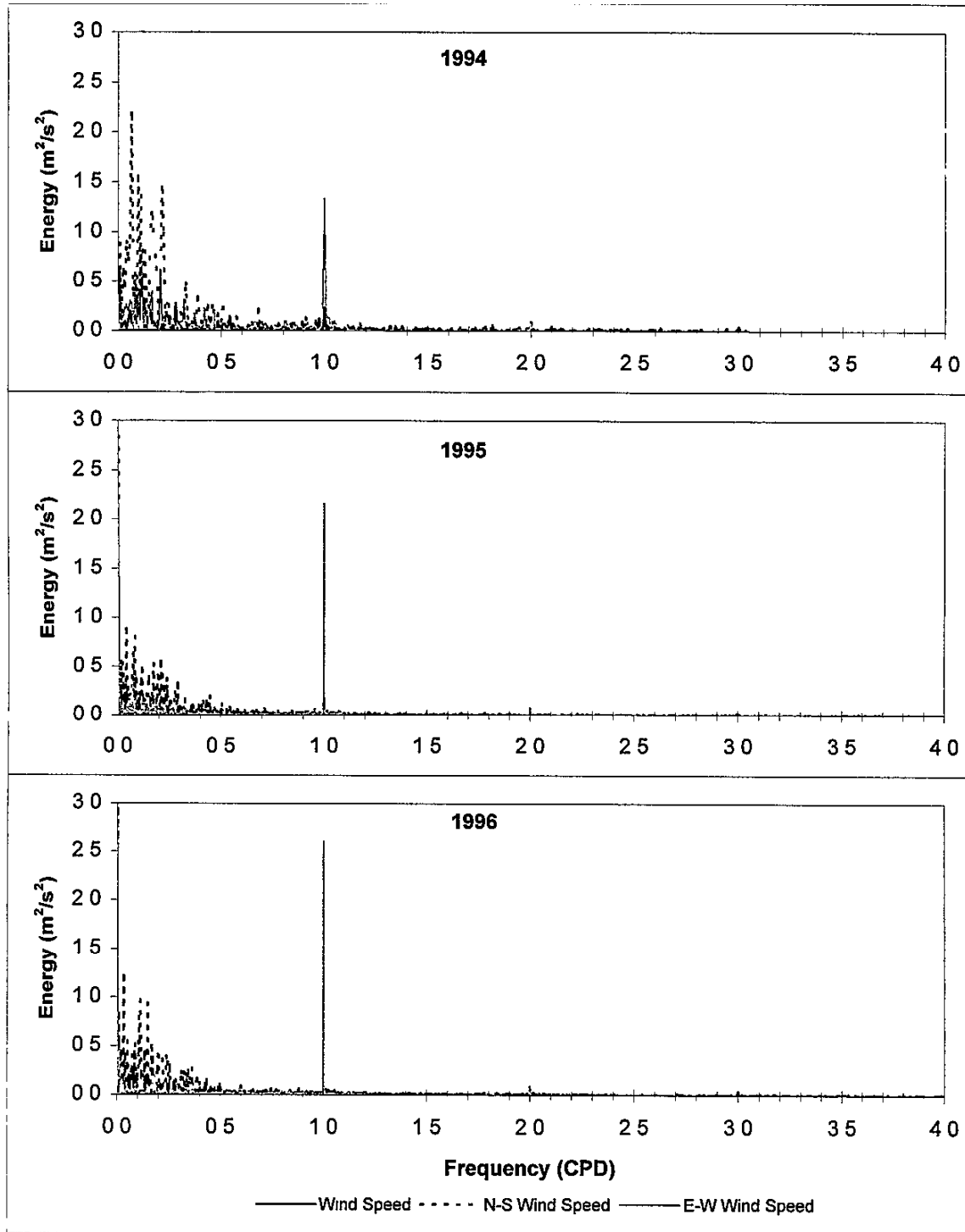
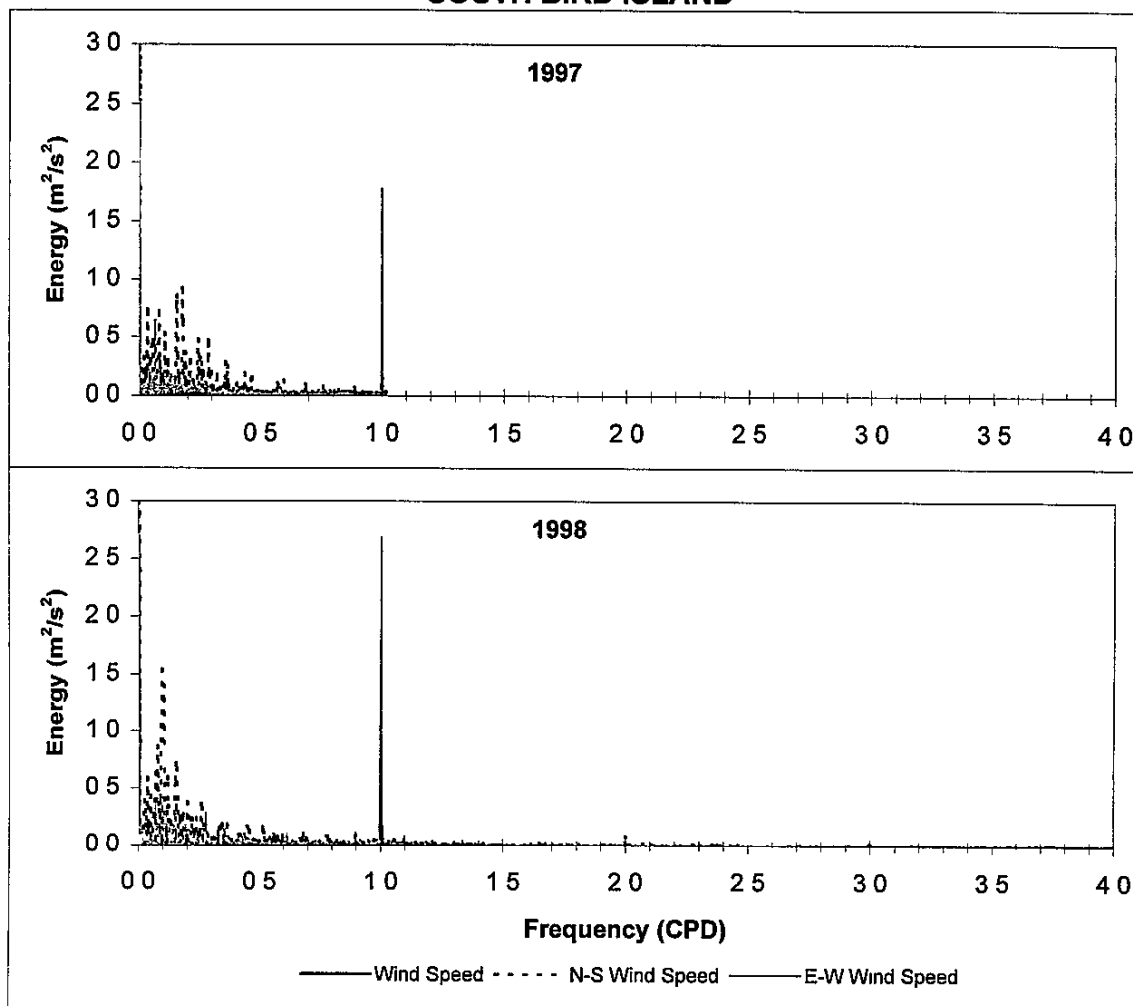


FIGURE 4-10 (Continued)
ANNUAL WIND SPEED SPECTRA AT TCOON STATION
SOUTH BIRD ISLAND



The annual spectra are useful as a general summary, but do not illuminate the seasonal variation in the spectrum. To display this, the time series were grouped month-by-month and the corresponding spectra computed. The complete set of monthly spectra are presented in Appendix WF. For present purposes, we display a representative selection. For this purpose, we chose 1996, because in this year fairly complete data sets existed for all of the hydrographic variables in both the Upper and Lower Laguna, thereby facilitating both month-to-month continuity and intercomparisons. The monthly spectra for the two anemometers are shown in figures 4-11 through 4-18. We note the following:

- 1 The seabreeze spike is present, but minimal, during the winter months, increasing in energy to maximal values in the period June - September
- 2 The greatest seabreeze energy is in the E-W component, i.e. the component transverse to the coastline.
- 3 Several lower frequency signals appear in the fall through spring period, being maximal in winter. The periodicities of around 3 and 6 days are particularly prominent. These are the result of frontal passages during the winter and equinoctial seasons.
4. Most of the energy of the frontal-passage periodicities is in the N-S component

Water level is subject to forcing by both wind and tides, directly and indirectly, so we anticipate the spectrum to be complex. Figures 4-19 and 4-20 display the annual spectra for 1994-1998 (That is, the spectra computed from the time series grouped by year, some of which, e.g., 1998, are incomplete.) In all of these annual spectra, there are prominent peaks at frequencies of periods of 12, 12.4, 24 and 25.5 hrs (2, 1.94, 1, and 0.94 cpd, respectively). These are power spectra. Some of the analyses presented by Brown and Kraus (1997) are amplitude spectra. The differences between the two are discussed in Chapter 5.

Examples of monthly spectra of water levels are presented in figures 4-21 through 4-24 for the Lower Laguna (Arroyo Colorado) and in figures 4-25 through 4-28 for the Upper Laguna (South Bird Island). There are fewer data points in a month so the resolution of the spectra is coarser than the annual spectra, but the variation with season and climatology is evident. In these graphs, the same spectra are plotted at two different scales, to better display the smaller components of their structure. The right-hand axis is the expanded scale and applies to the broken curve. There is a seasonal increase of the 24-hr component into the summer and early fall, which is very prominent in the Lower Laguna. Also, at these resolutions there is practically no discernible power in the semidiurnal components.

FIGURE 4-11
MONTHLY WIND SPEED SPECTRA AT TCOON STATION
ARROYO COLORADO

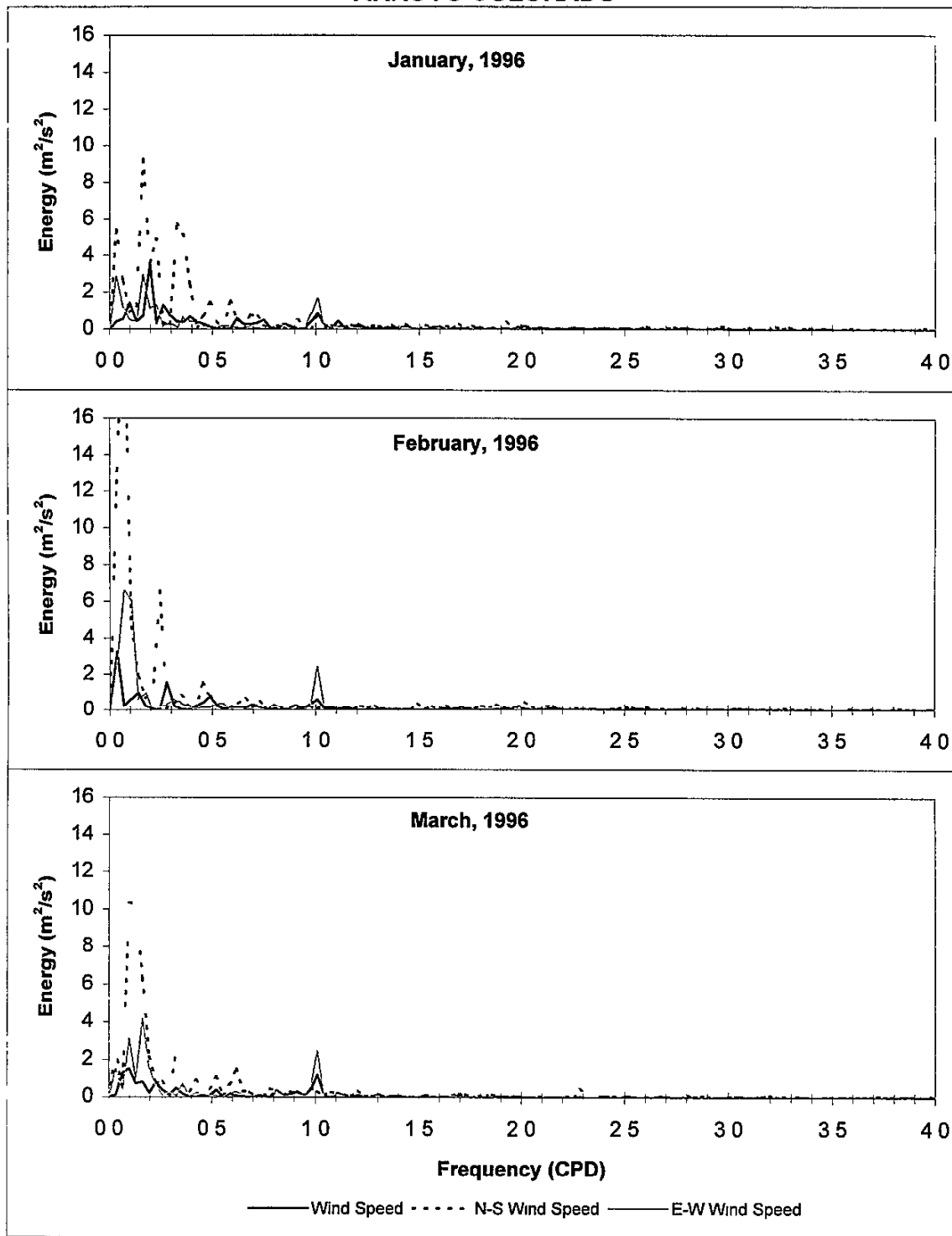


FIGURE 4-12
MONTHLY WIND SPEED SPECTRA AT TCOON STATION
ARROYO COLORADO

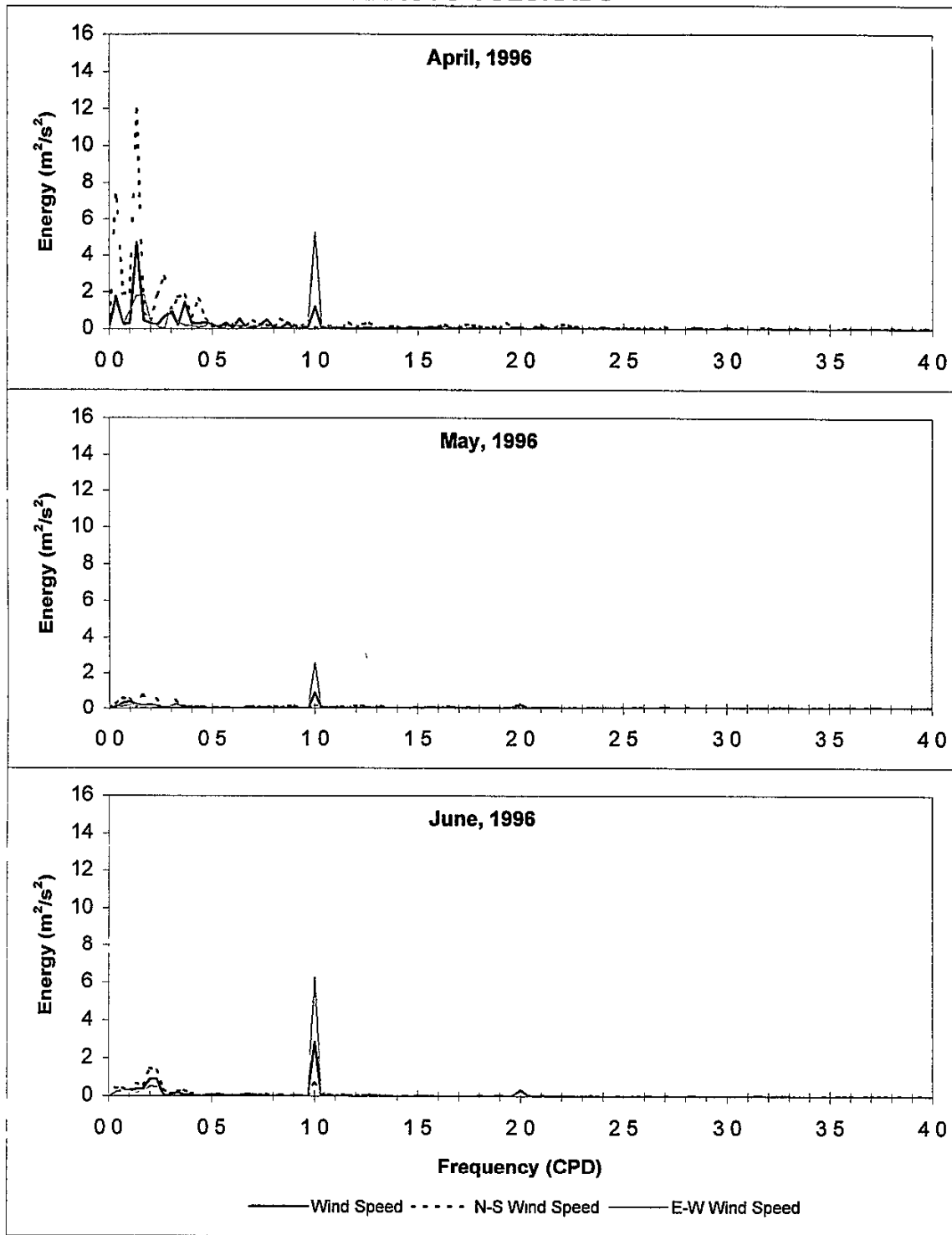


FIGURE 4-13
MONTHLY WIND SPEED SPECTRA AT TCOON STATION
ARROYO COLORADO

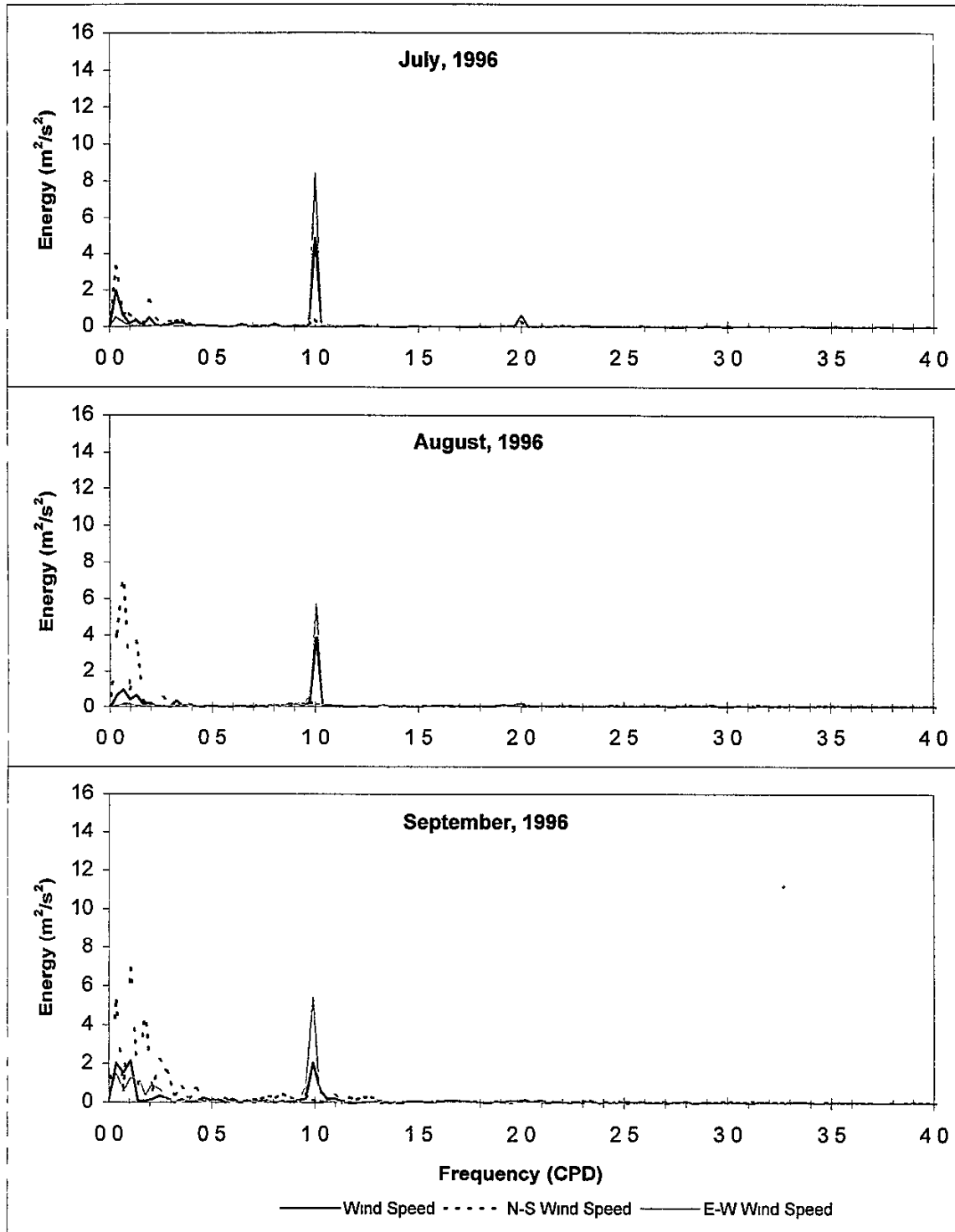


FIGURE 4-14
MONTHLY WIND SPEED SPECTRA AT TCOON STATION
ARROYO COLORADO

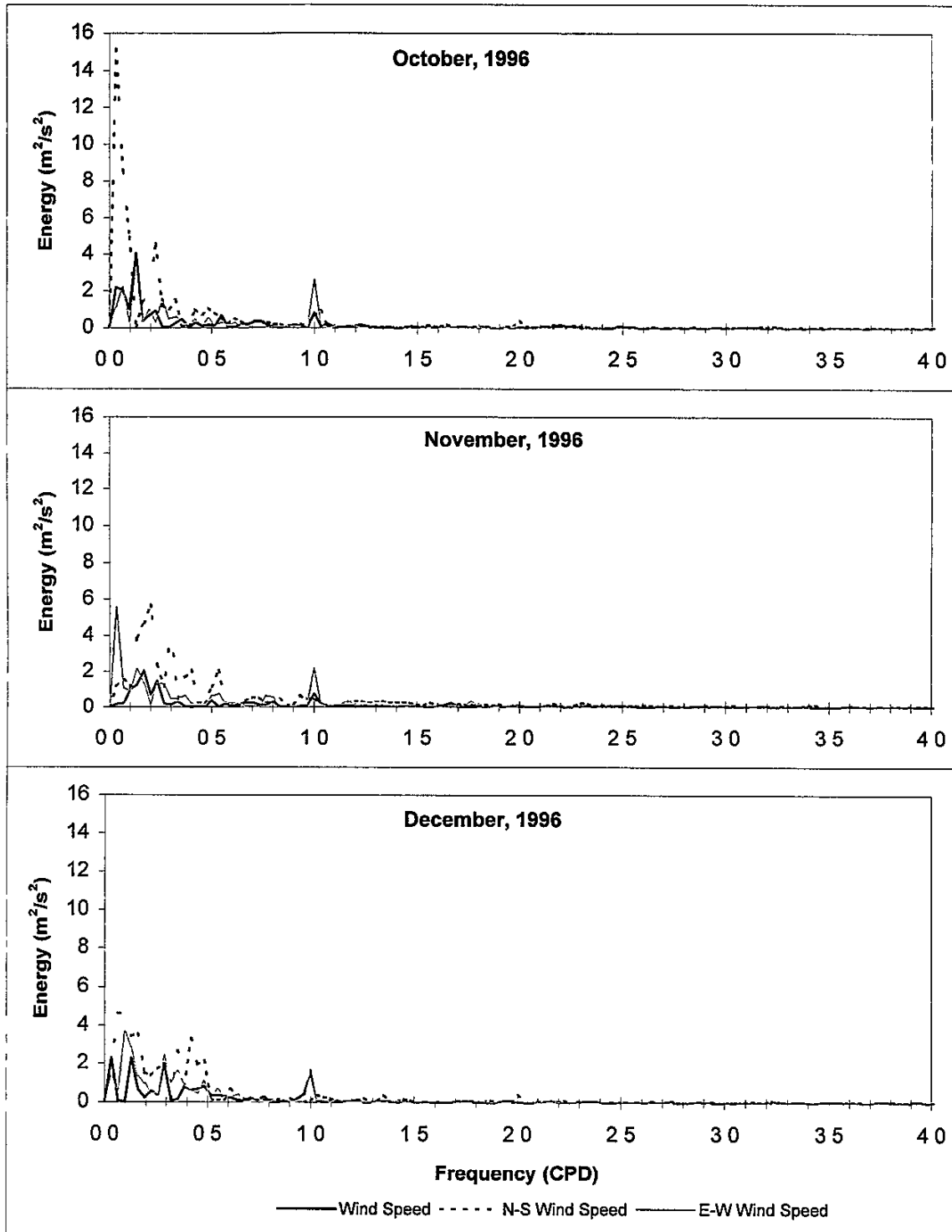


FIGURE 4-15
MONTHLY WIND SPEED SPECTRA AT TCOON STATION
SOUTH BIRD ISLAND

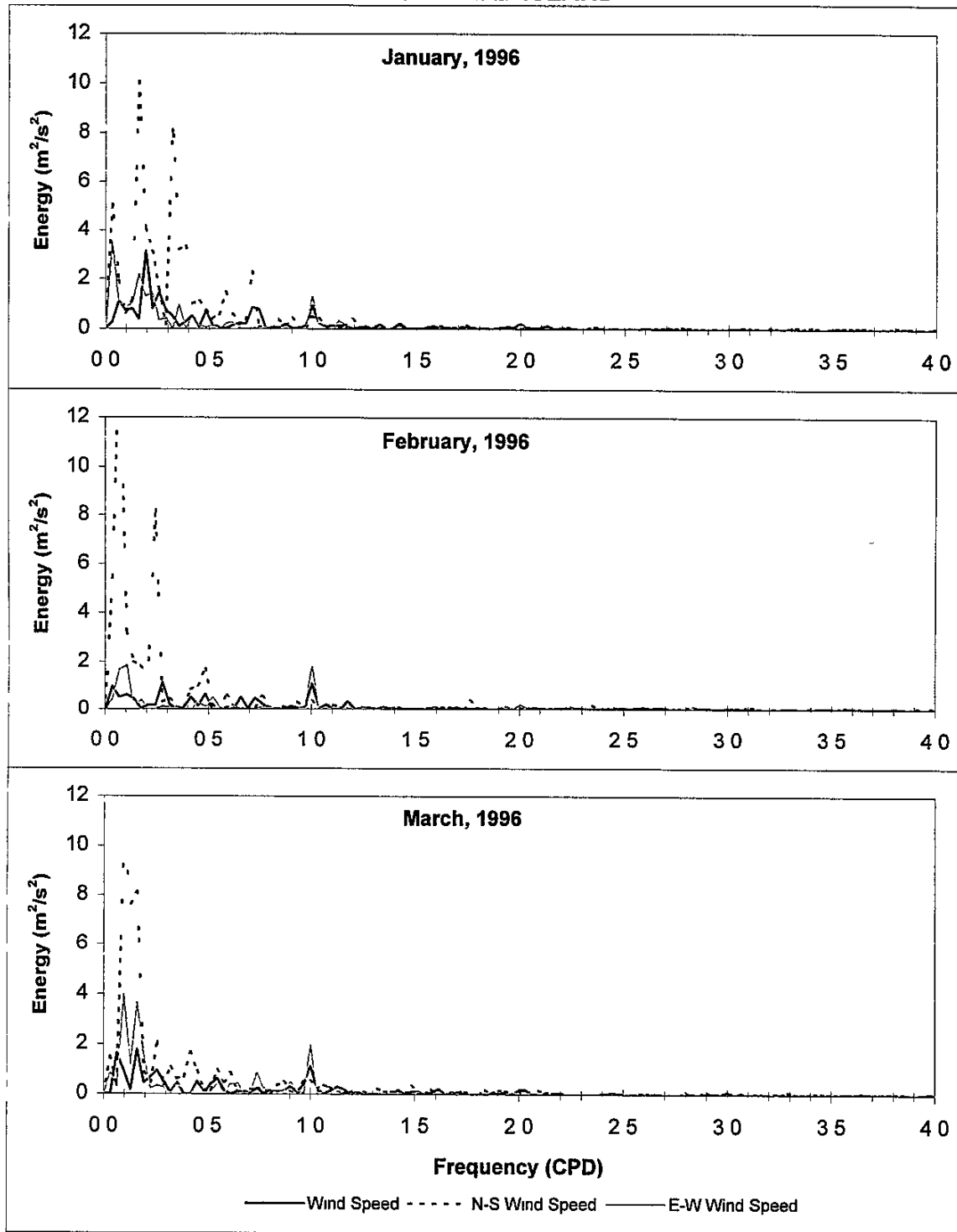


FIGURE 4-16
MONTHLY WIND SPEED SPECTRA AT TCOON STATION
SOUTH BIRD ISLAND

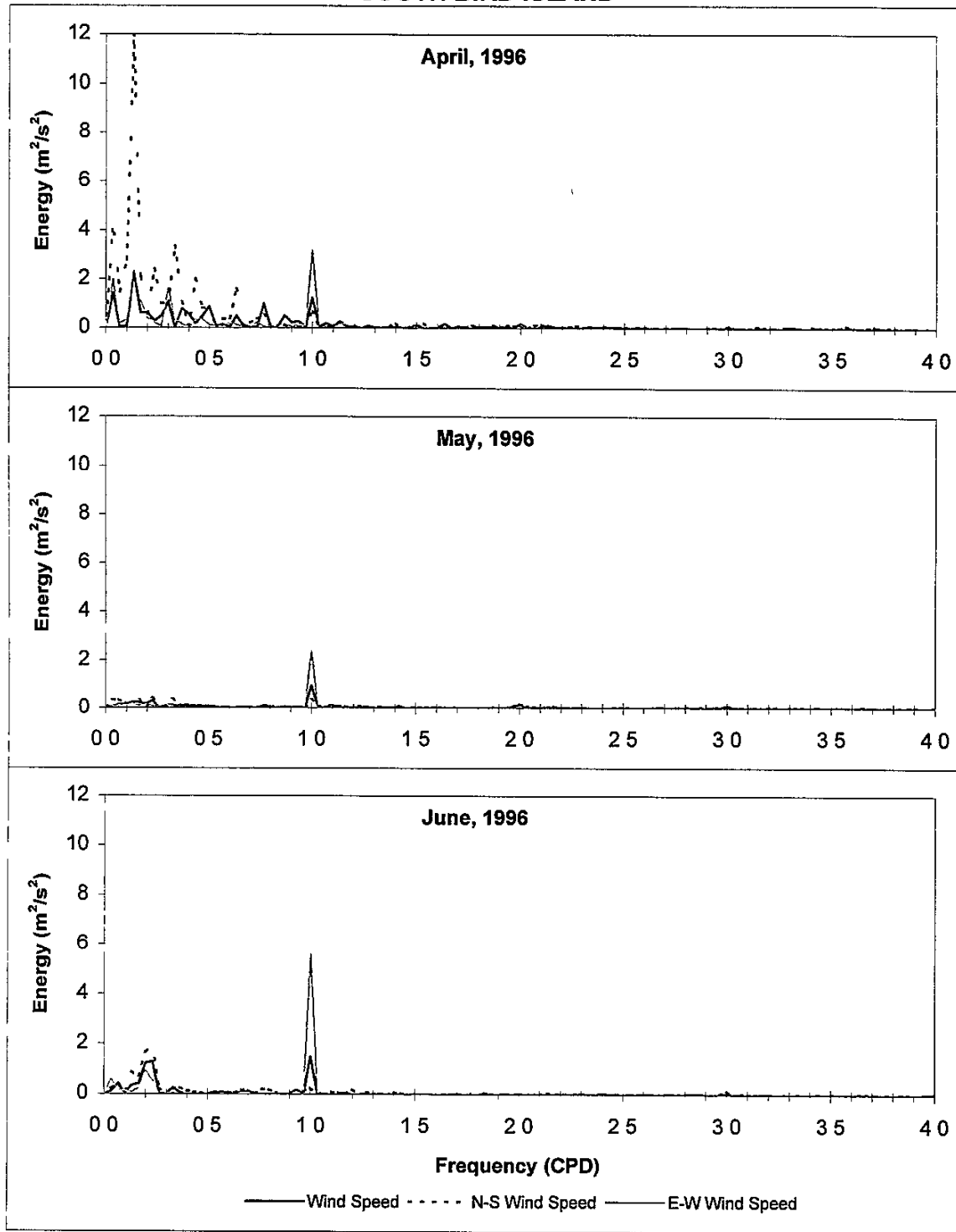


FIGURE 4-17
MONTHLY WIND SPEED SPECTRA AT TCOON STATION
SOUTH BIRD ISLAND

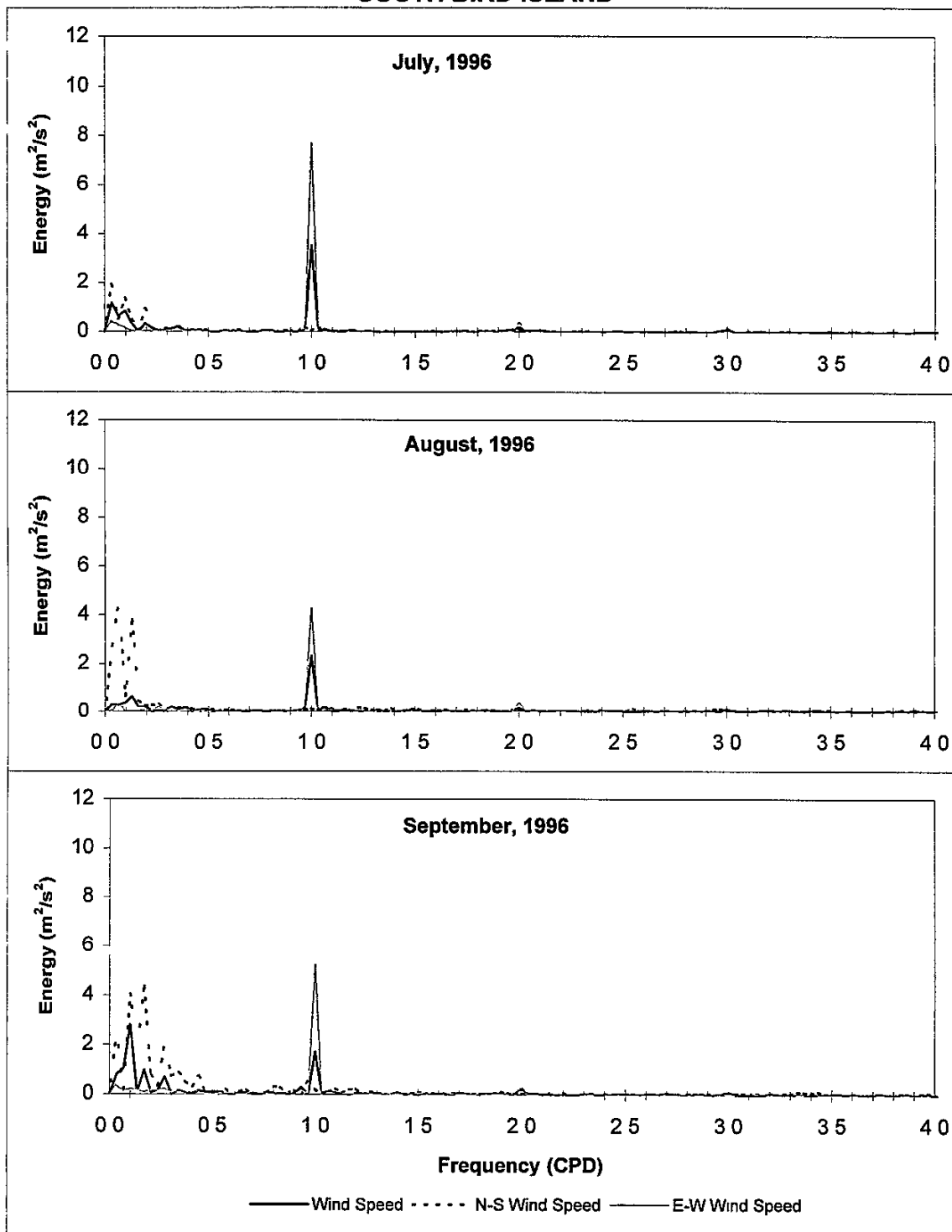


FIGURE 4-18
MONTHLY WIND SPEED SPECTRA AT TCOON STATION
SOUTH BIRD ISLAND

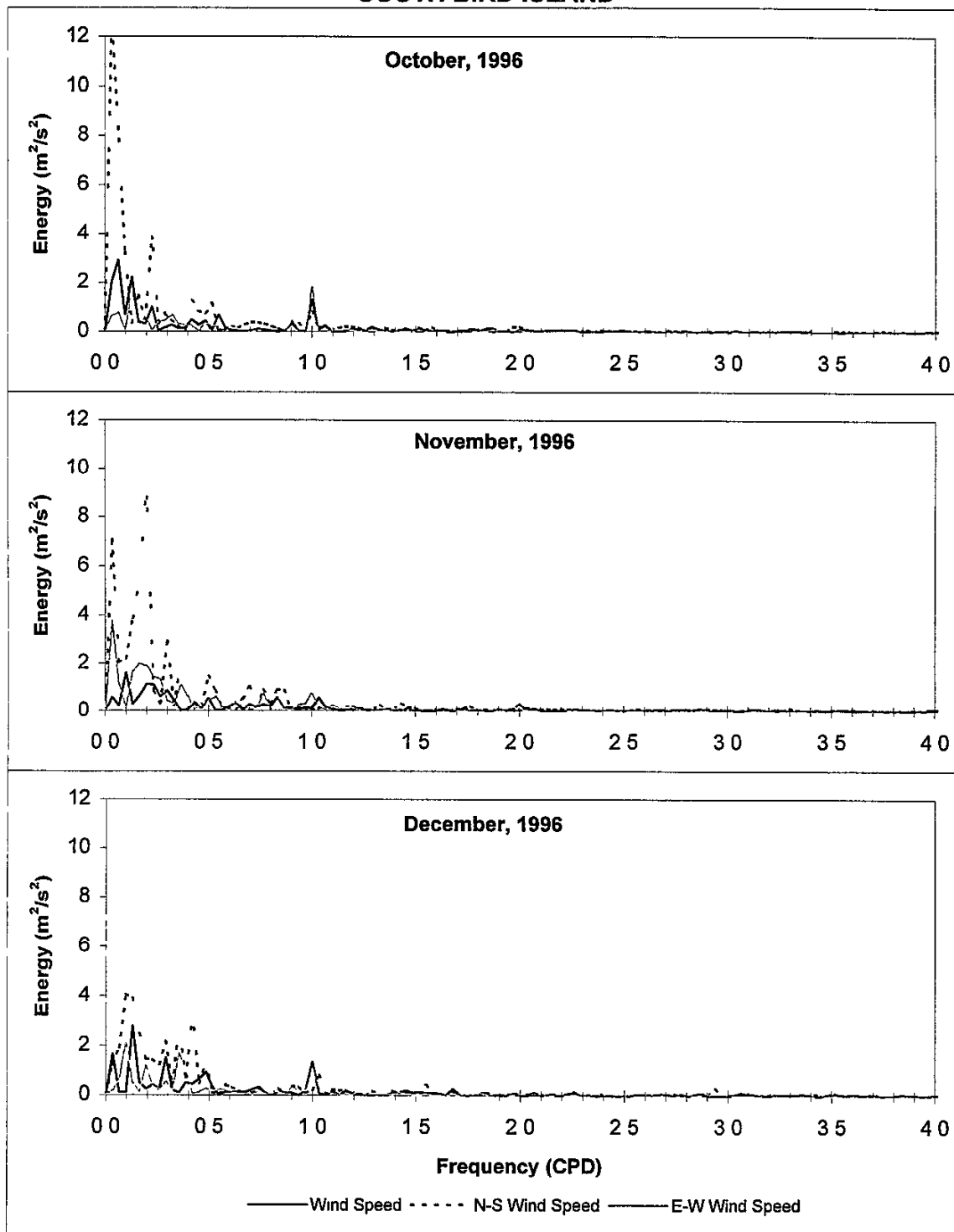


FIGURE 4-19
ANNUAL WATER LEVEL SPECTRA AT TCOON STATION
ARROYO COLORADO

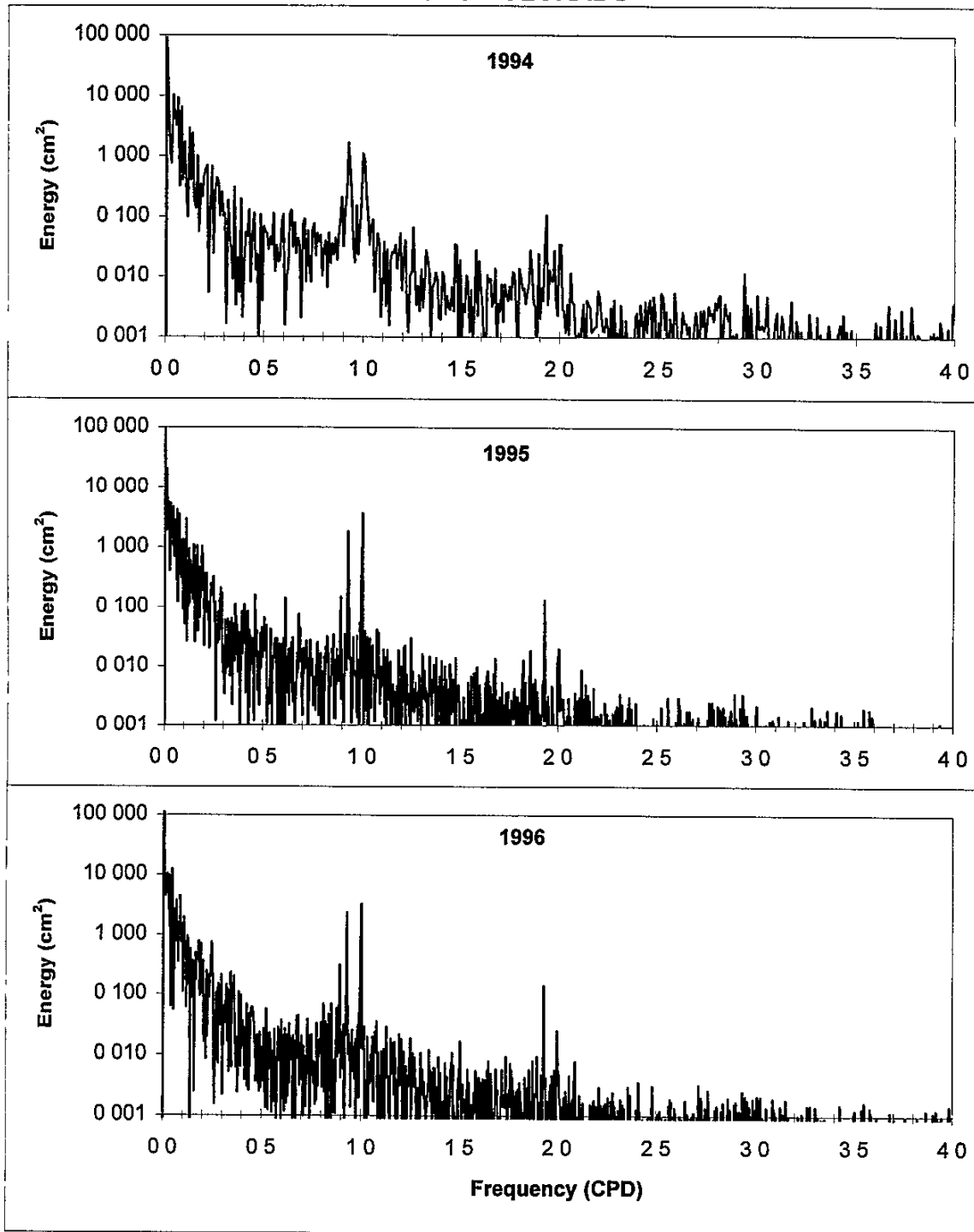


FIGURE 4-19 (Continued)
ANNUAL WATER LEVEL SPECTRA AT TCOON STATION
ARROYO COLORADO

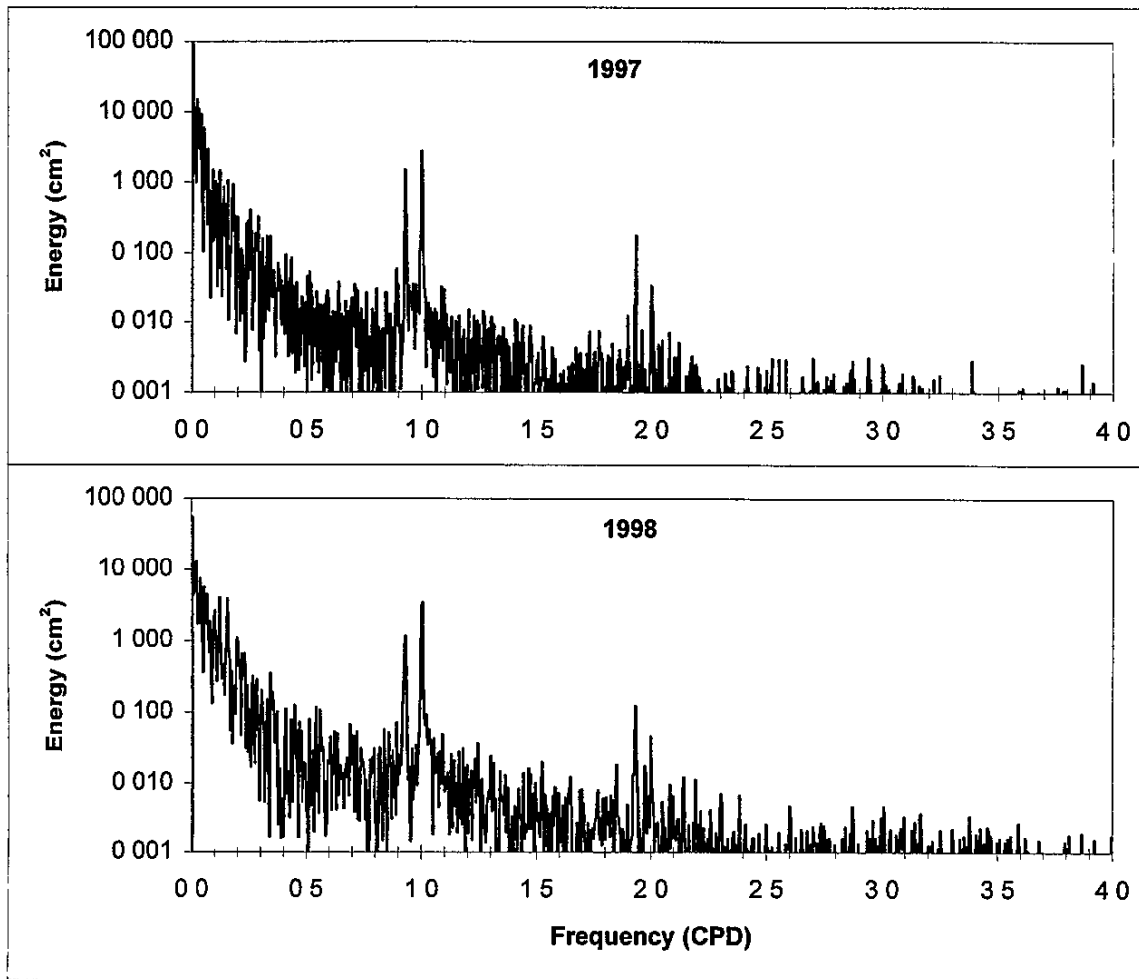


FIGURE 4-20
ANNUAL WATER LEVEL SPECTRA AT TCOON STATION
SOUTH BIRD ISLAND

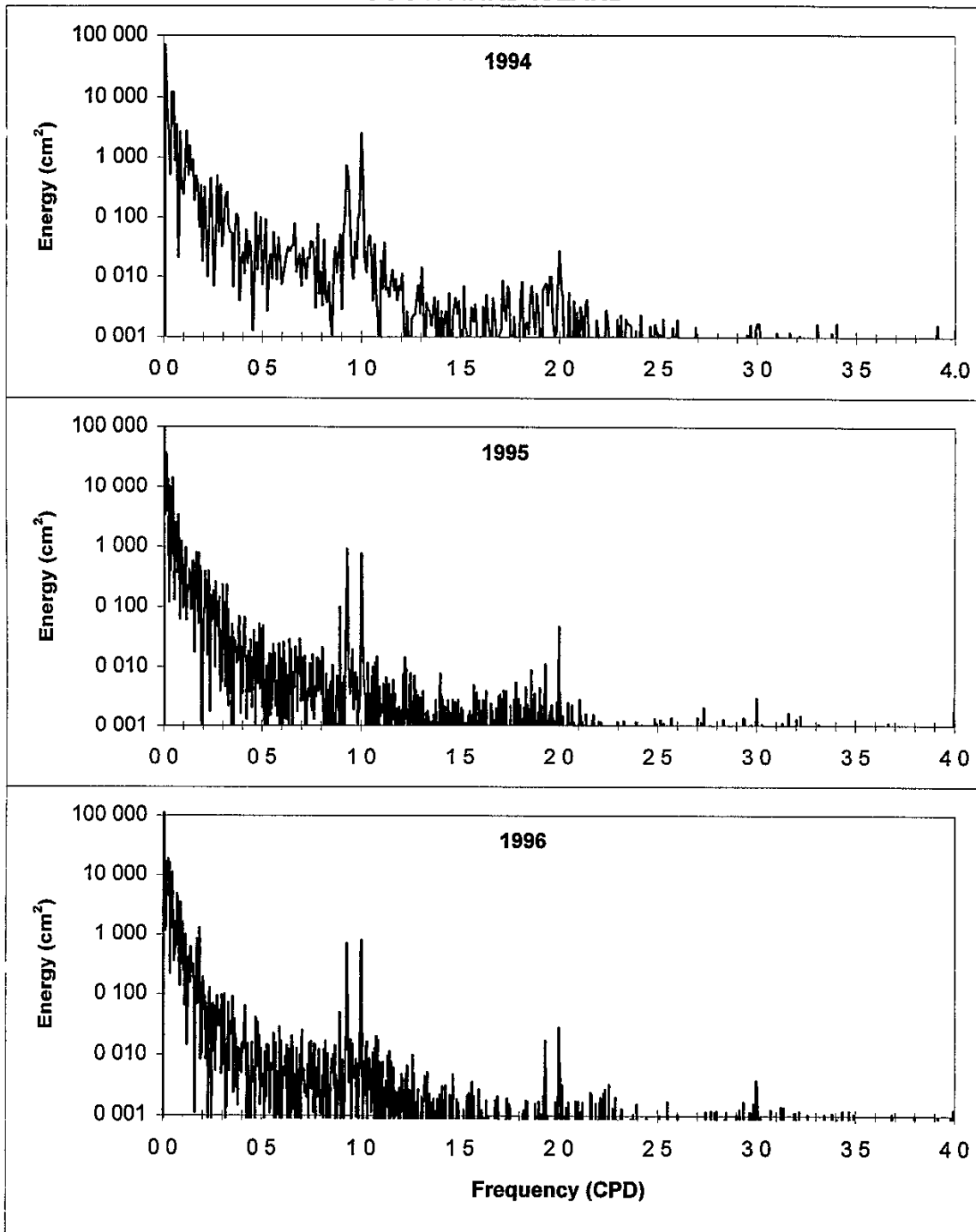


FIGURE 4-20 (Continued)
ANNUAL WATER LEVEL SPECTRA AT TCOON STATION
SOUTH BIRD ISLAND

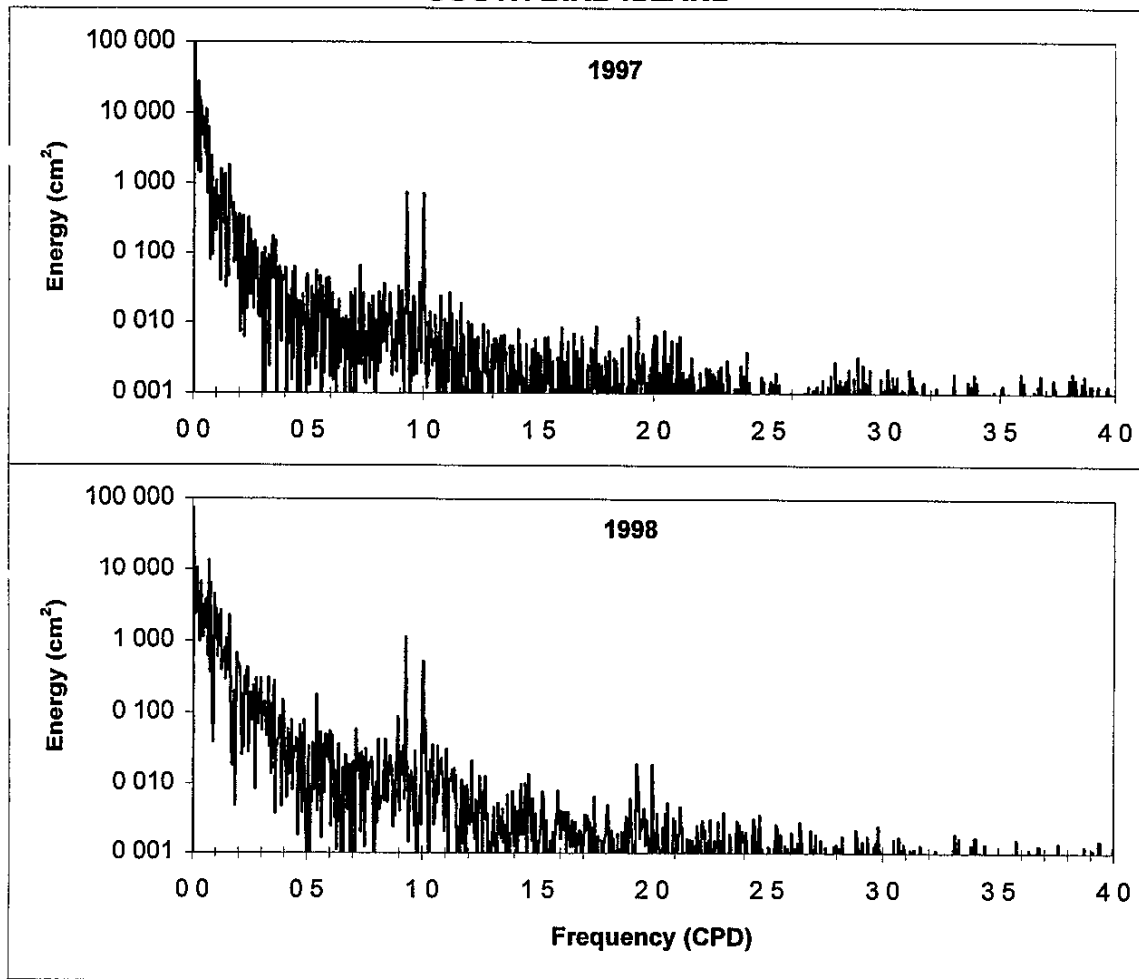


FIGURE 4-21
MONTHLY WATER LEVEL SPECTRA AT TCOON STATION
ARROYO COLORADO

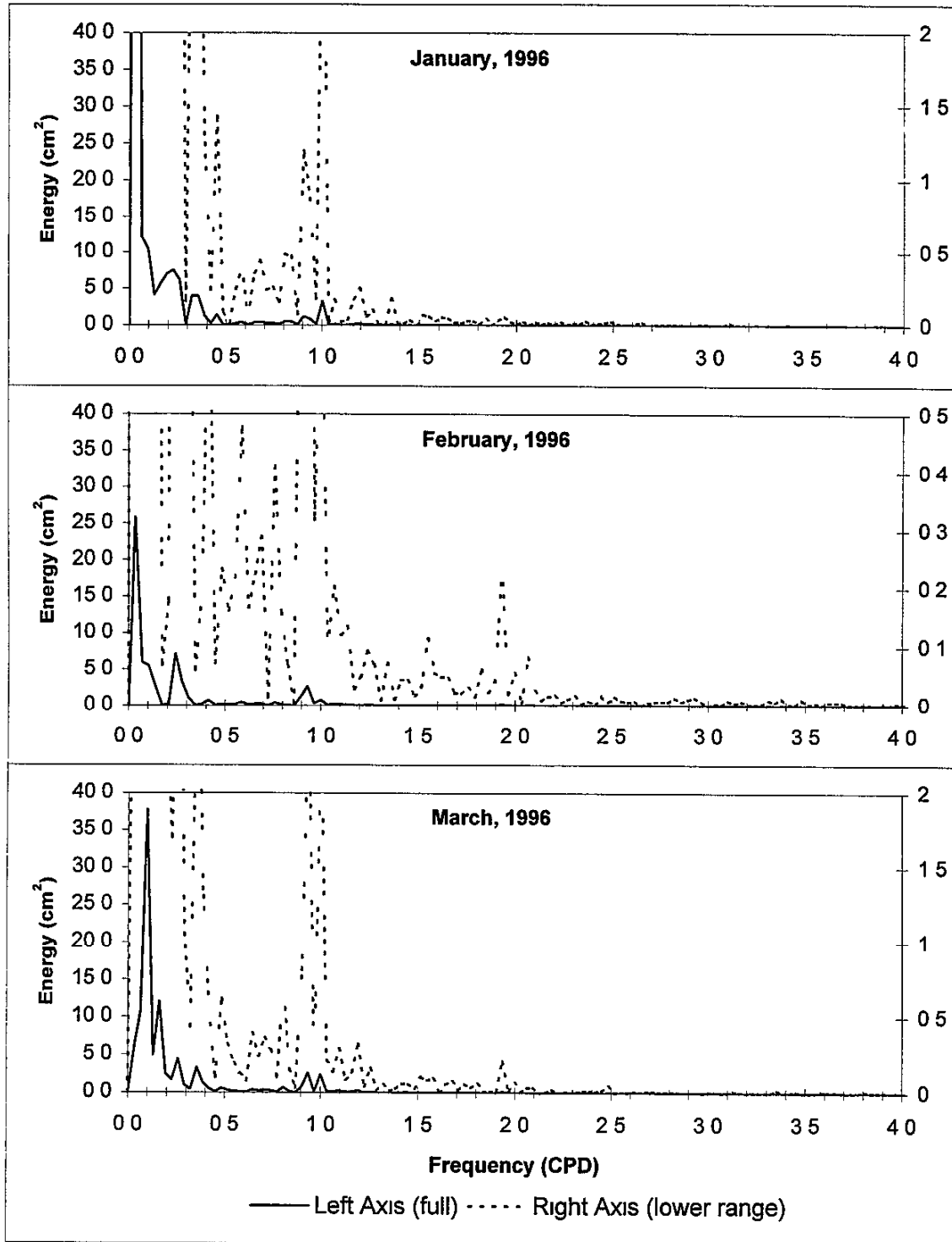


FIGURE 4-22
MONTHLY WATER LEVEL SPECTRA AT TCOON STATION
ARROYO COLORADO

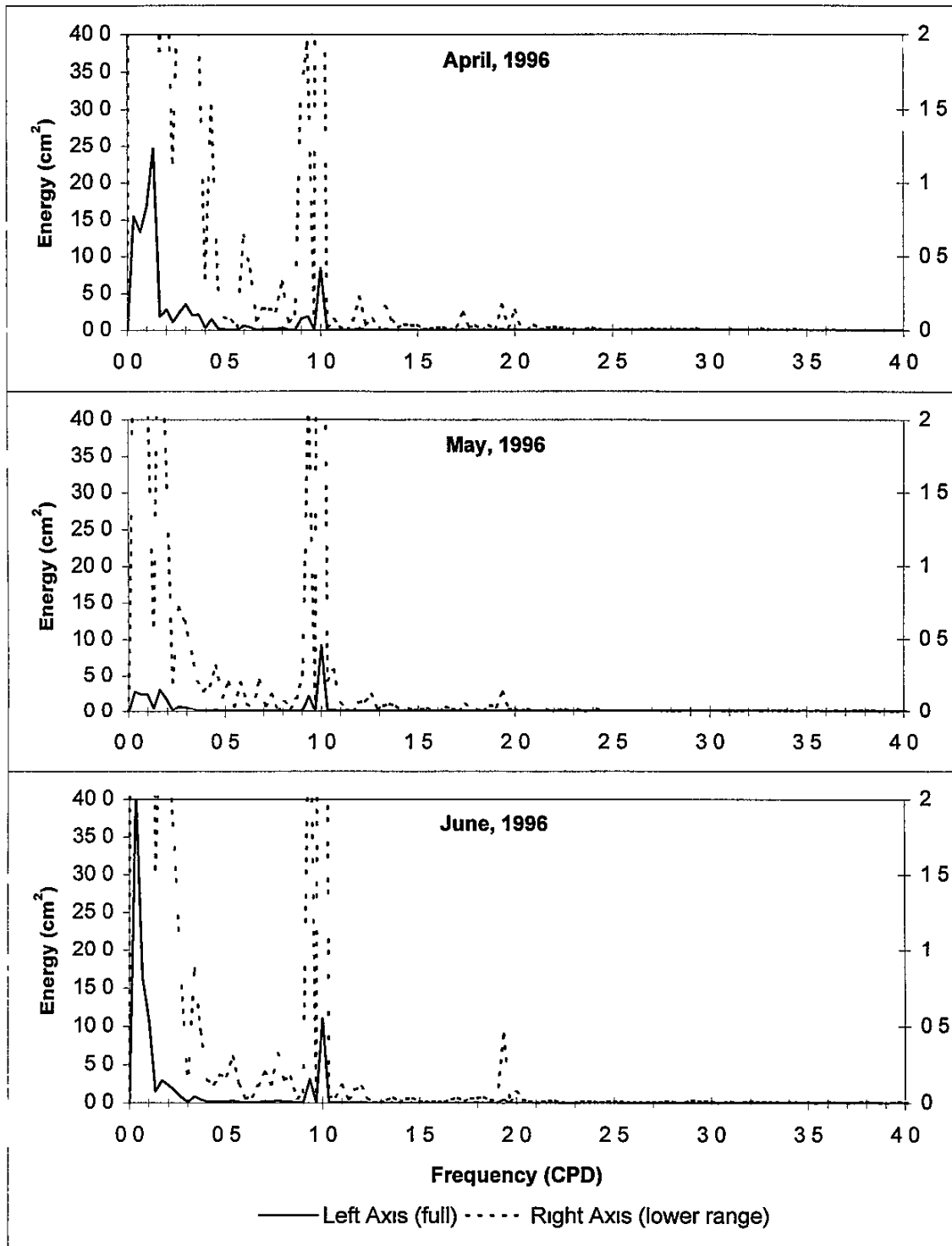


FIGURE 4-23
MONTHLY WATER LEVEL SPECTRA AT TCOON STATION
ARROYO COLORADO

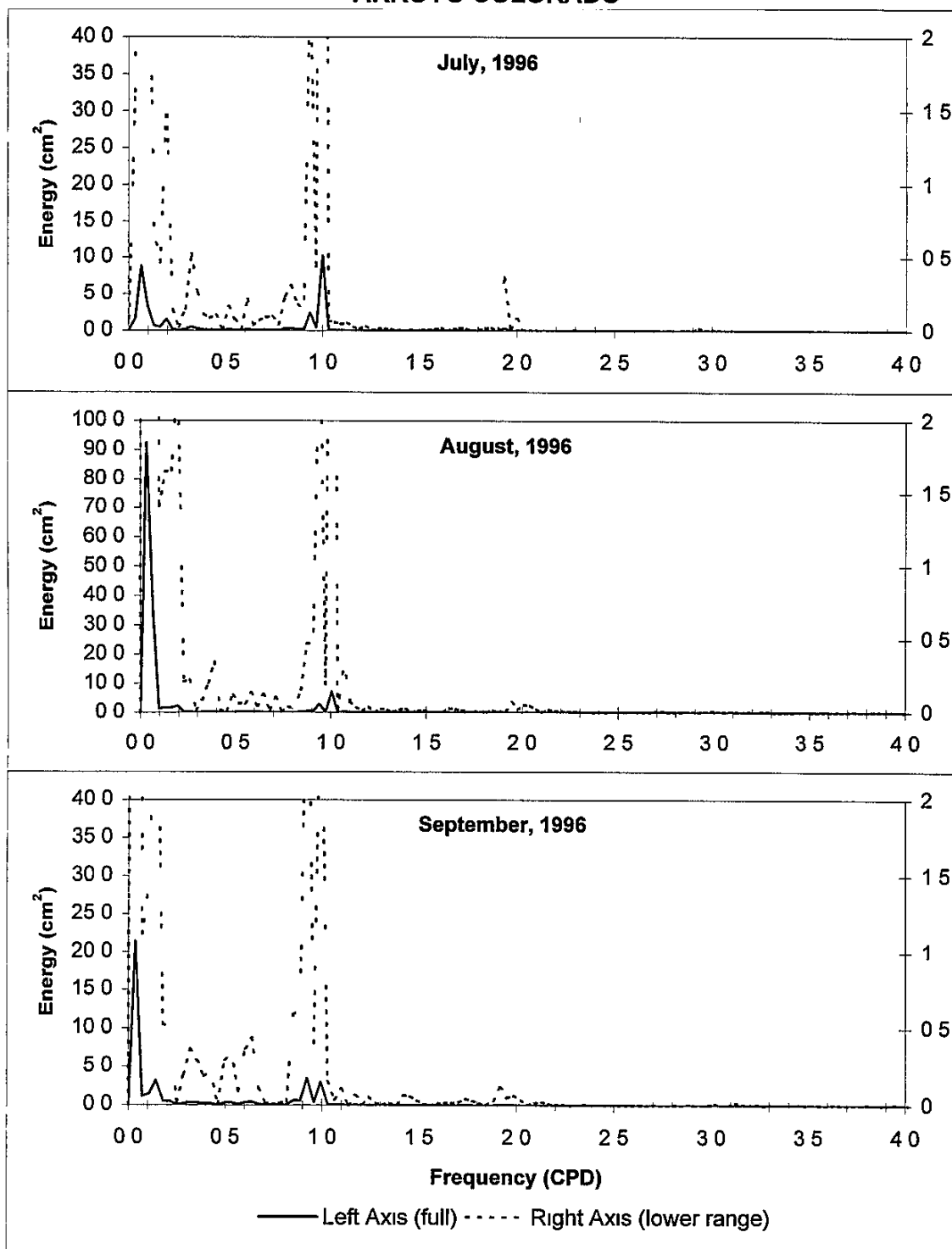


FIGURE 4-24
MONTHLY WATER LEVEL SPECTRA AT TCOON STATION
ARROYO COLORADO

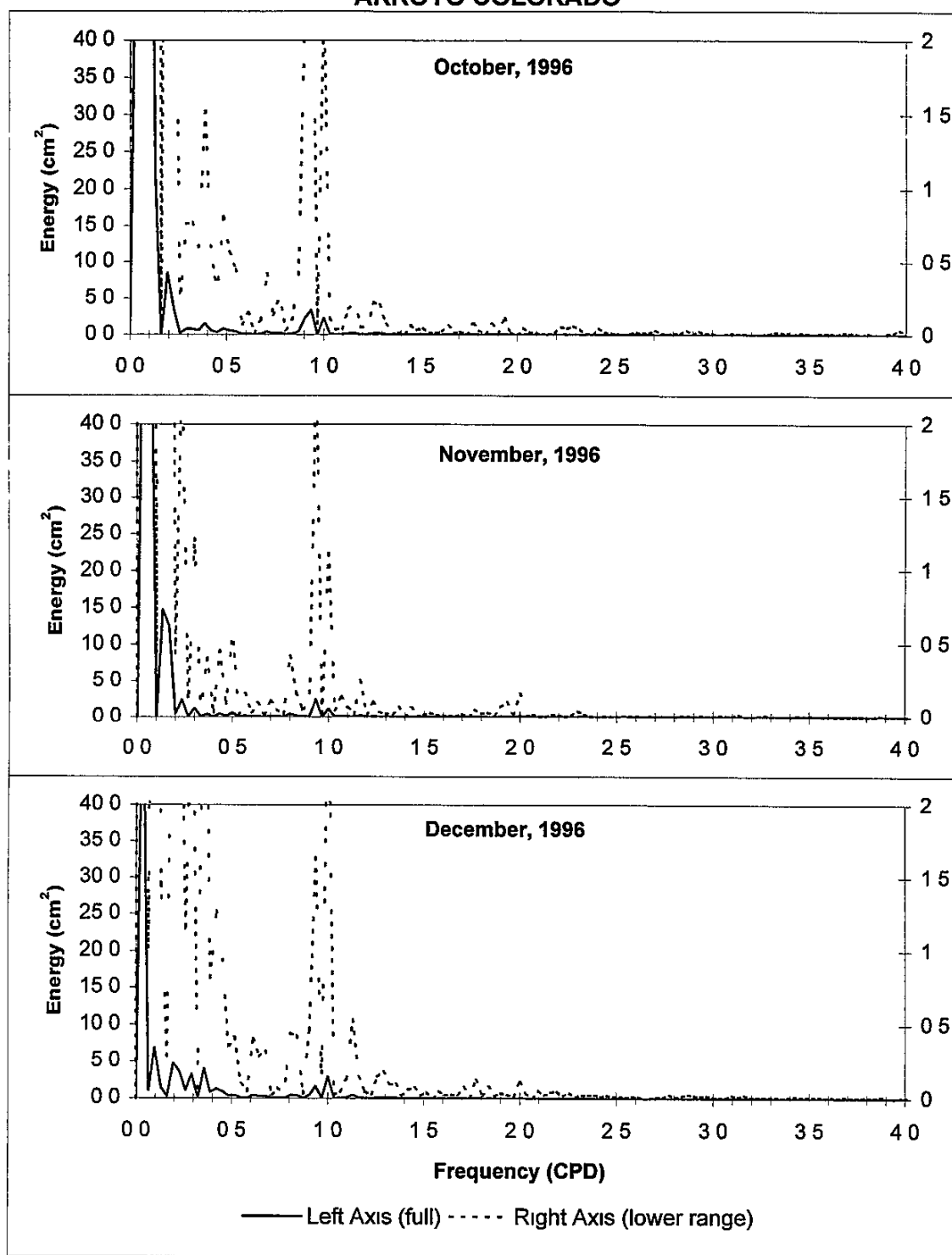


FIGURE 4-25
MONTHLY WATER LEVEL SPECTRA AT TCOON STATION
SOUTH BIRD ISLAND

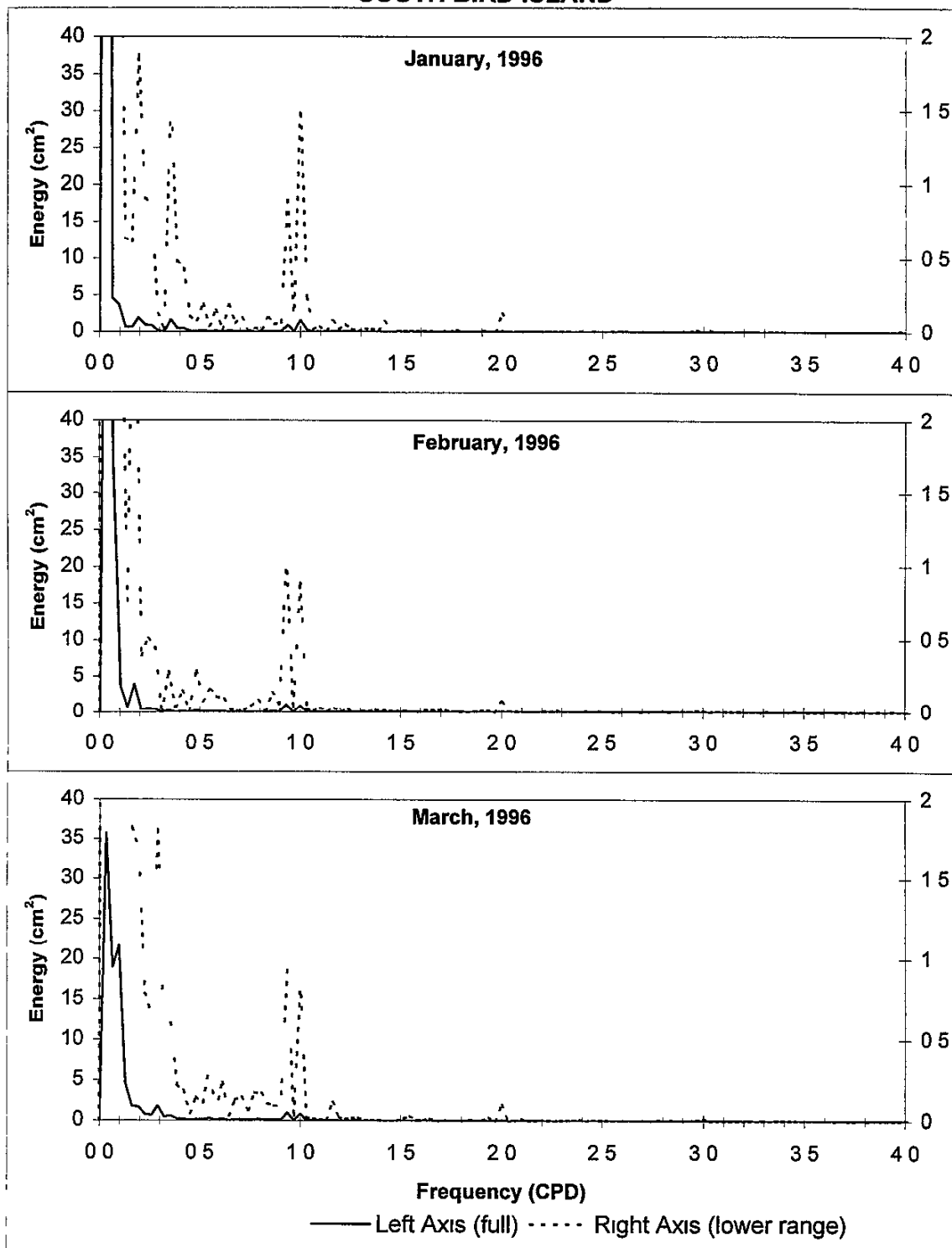


FIGURE 4-26
MONTHLY WATER LEVEL SPECTRA AT TCOON STATION
SOUTH BIRD ISLAND

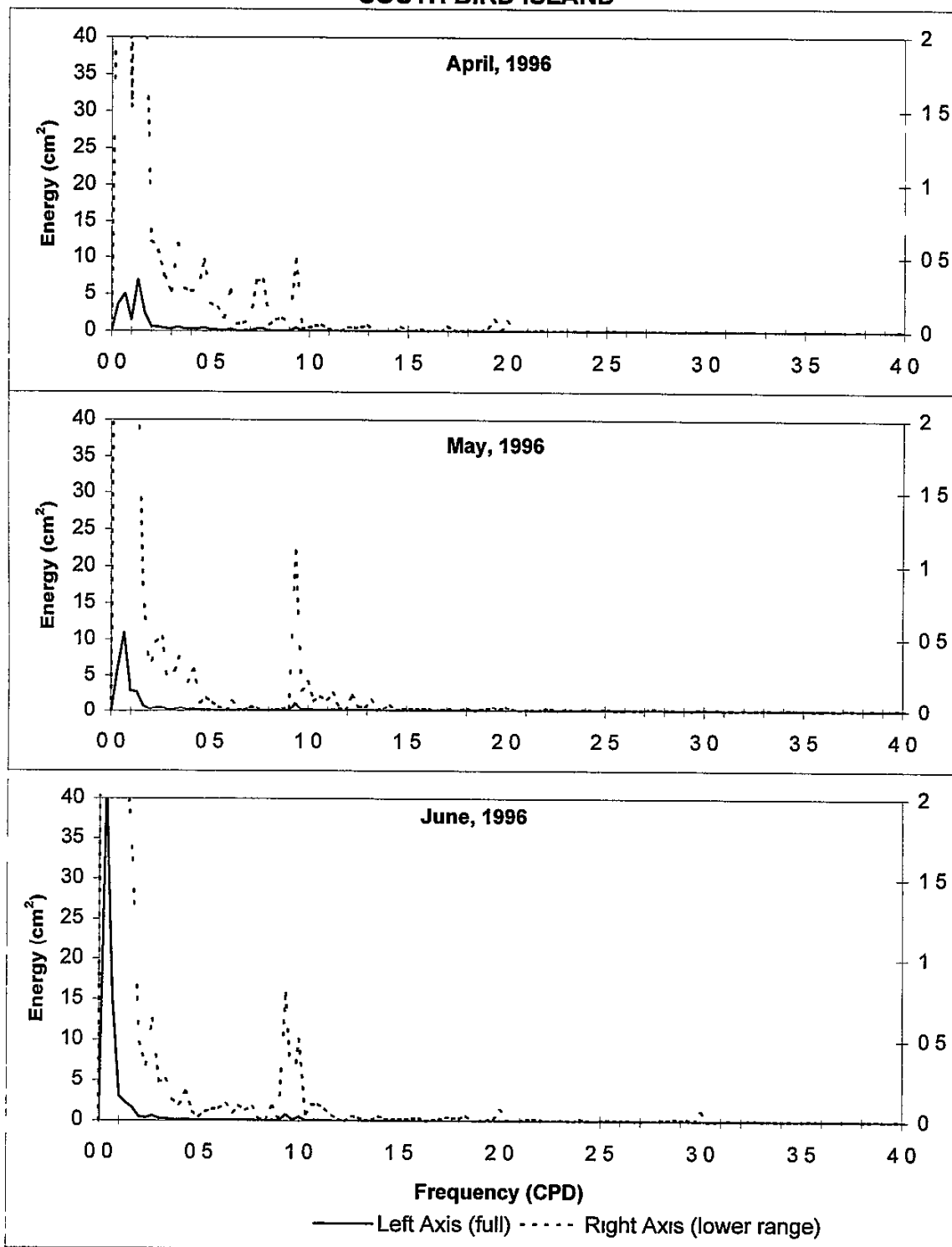


FIGURE 4-27
MONTHLY WATER LEVEL SPECTRA AT TCOON STATION
SOUTH BIRD ISLAND

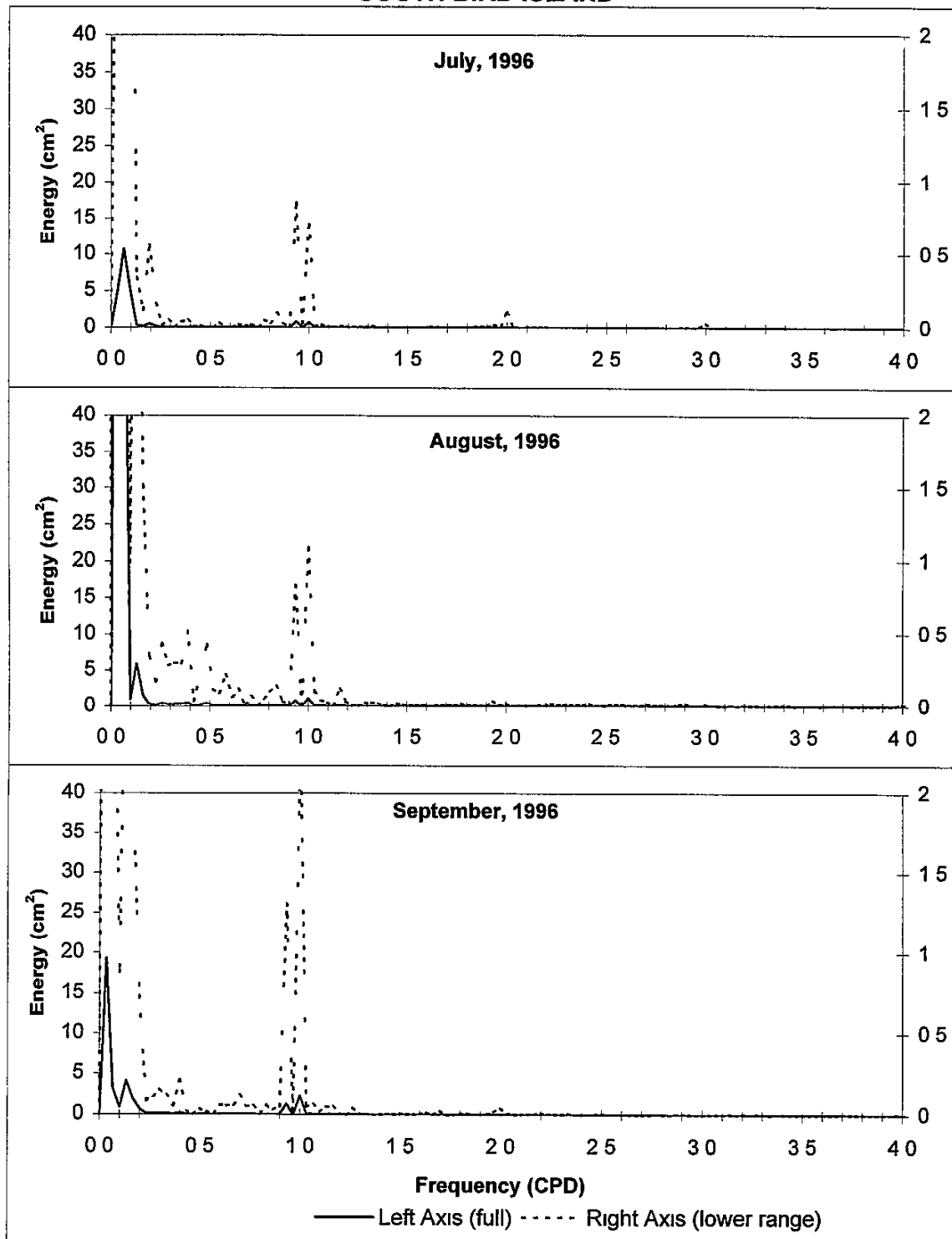
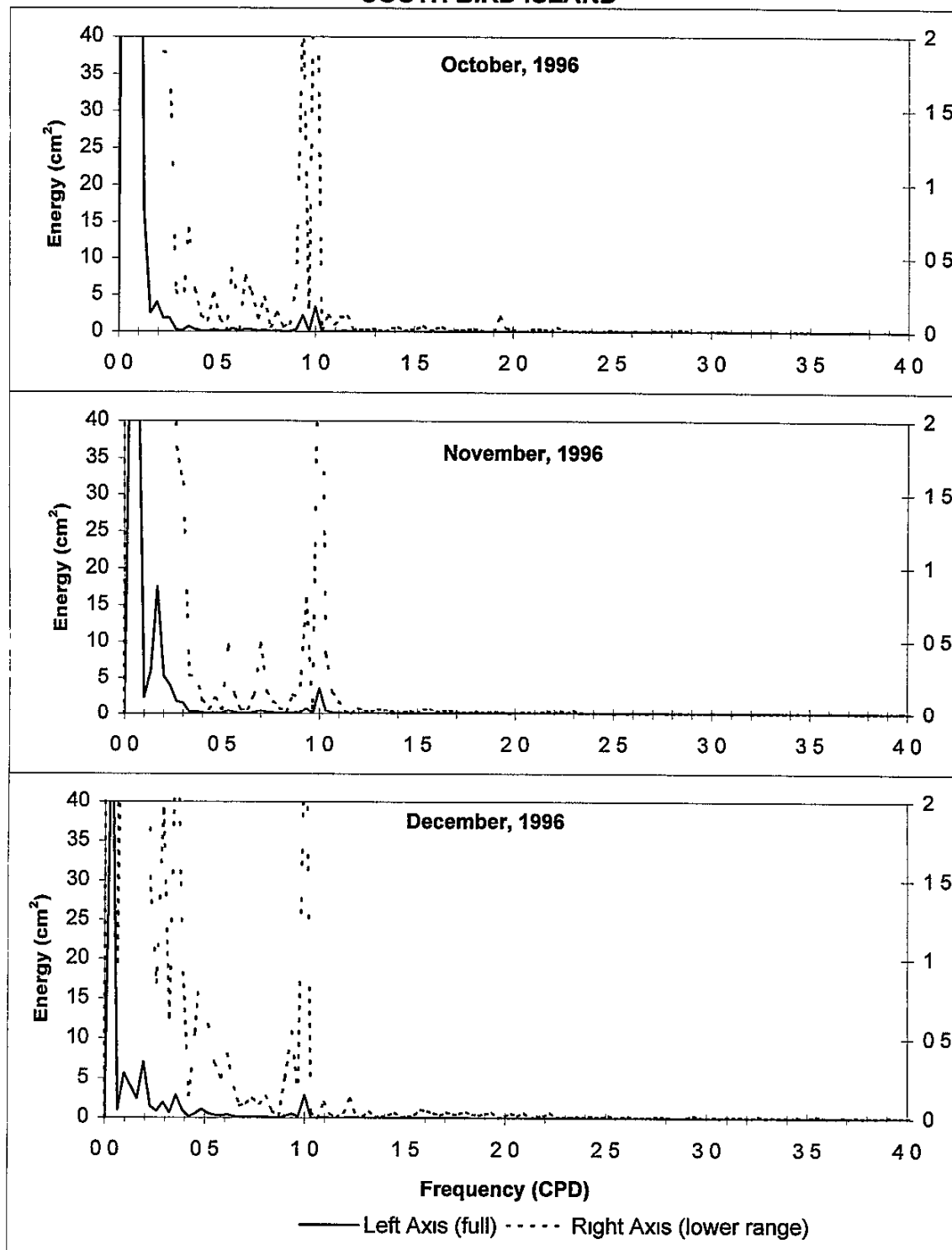


FIGURE 4-28
MONTHLY WATER LEVEL SPECTRA AT TCOON STATION
SOUTH BIRD ISLAND



Coherency is a measure of the correlation (in the statistical sense) for frequencies in the power spectra. Figure 4-29 shows the coherency (squared) for water level signals in the Lower Laguna (Arroyo Colorado) and Upper Laguna (Bird Island) regions. The peaks at 1 cpd (24 hr period) evidence sea-breeze forcing in both regions. The fortnightly signal is not accurately resolved with such a short (1-month) period, but is evident in the high coherency around 0.06 - 0.09 cpd. The source for the coherency around 0.22 - 0.25 cpd (4-5 day periods) is unclear, but is probably frontal passage forcing, being larger and broader in the January data than in the June data.

The obvious conclusion is that wind forcing is responsible for the 24-hr spike in spectral power in water level. This is reinforced by the coherency between wind and water level, examples for summer 1996 at both gauges shown in figures 4-30 and 4-31. Coherency of water level with each of three measures of wind is shown, viz the vector resultant wind, the east-west component and the north-south component. There is a prominent wide-band peak in coherency, very nearly 100%, at 1.0 cpd (24-hr periodicity). This is manifested in both the resultant wind speed and the east-west component, which is very nearly transverse to the coastline.

4.4 TEMPERATURE AND SALINITY

Two additional parameters obtained at some of the CBI stations were temperature and conductivity, from which salinity is determined. These two parameters are of secondary interest in so far as the objectives of this project are concerned but do have two uses. First, together these determine water density, which in turn can be an important hydrodynamic variable, especially if either horizontal or vertical gradients in density occur. Second, and more importantly, both temperature and salinity are, on short time scales, essentially conservative parameters, so when gradients exist, these can serve as water mass tracers. Their vertical homogeneity is an index to the intensity of vertical mixing, and time changes in their values indicate the transport of water masses at the platform location. Of course, when there is little or no gradient, in the horizontal or vertical, as is frequently the case in the Laguna, this utility is minimized.

Tables 4-9 and 4-10 present a summary of monthly descriptive statistics of temperature in the two Laguna Madre segments, and tables 4-11 and 4-12 present the corresponding statistics for salinity. There is little unexpected in the temperature statistics: an annual rise and fall in temperature of about 15°C, maxima on the order of 31°C, minima around 15°C, and a standard deviation that is maximal in the winter months and minimal during the summer. Almost all of the average monthly salinities in the Lower Laguna exceed 30‰ but rarely exceed 36‰ until the first three months of 1998. The uniformly low standard deviations testify to the stability in the salinity structure during the study period. Salinities in the Upper Laguna are somewhat higher, with monthly average values easily exceeding 40‰, especially during summer 1996. The high rainfall and runoff in fall 1998 significantly lowered the salinities, but to a level in the mid-20s, hardly a low salinity by estuarine standards.

FIGURE 4-29
SQUARED COHERENCY BETWEEN SOUTH BIRD ISLAND AND ARROYO COLORADO
WATER LEVELS

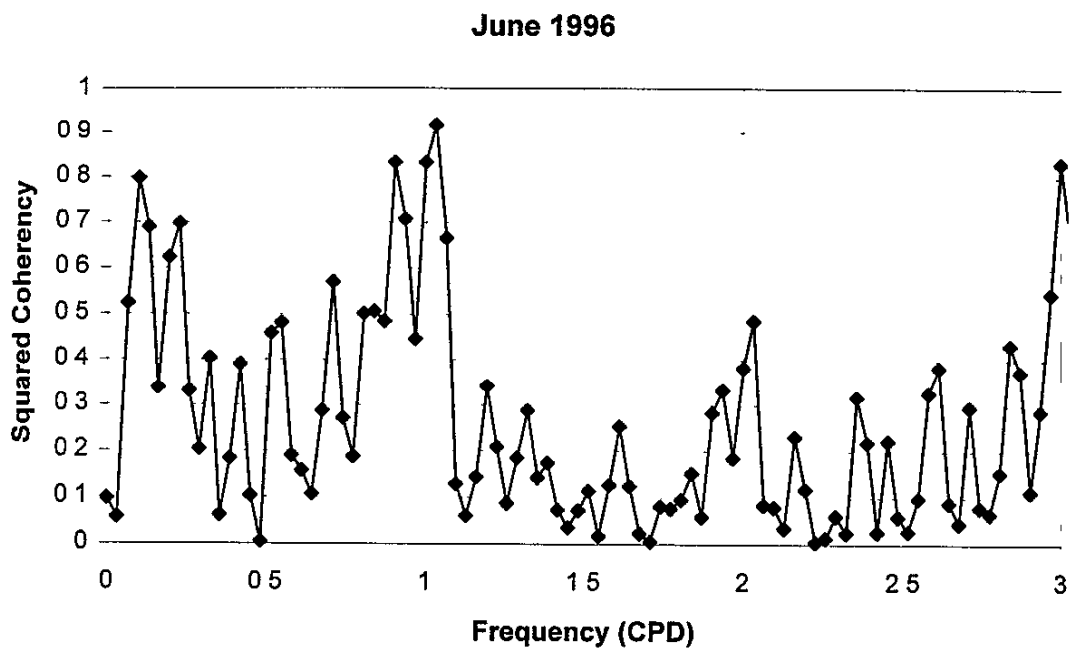
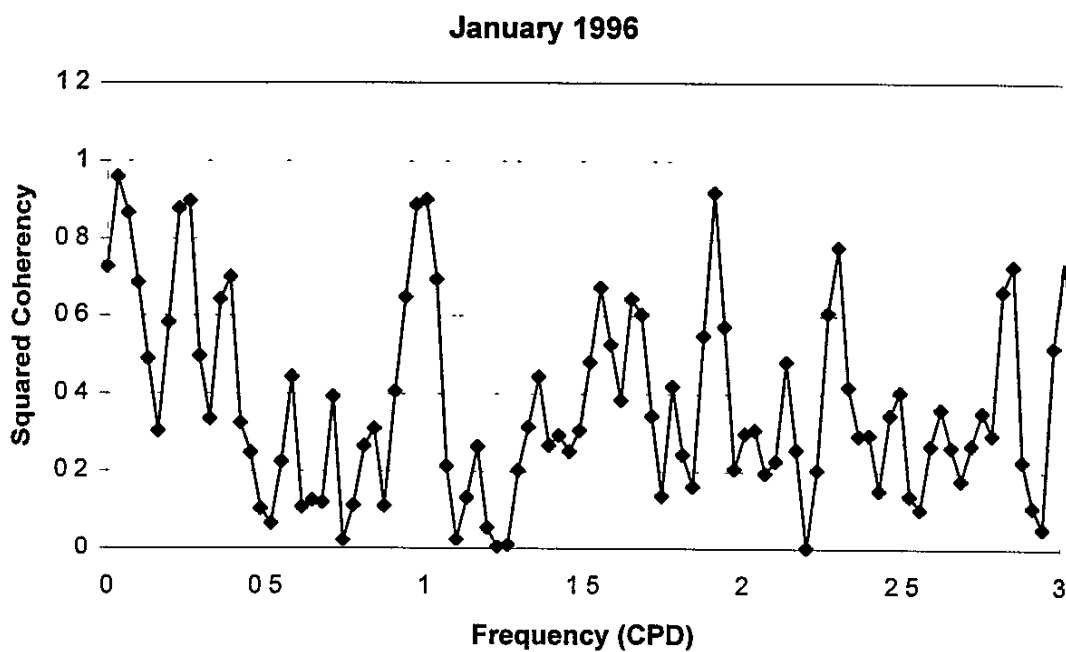


FIGURE 4-30
SQUARED COHERENCY BETWEEN WIND SPEED AND WATER LEVEL
AT ARROYO COLORADO

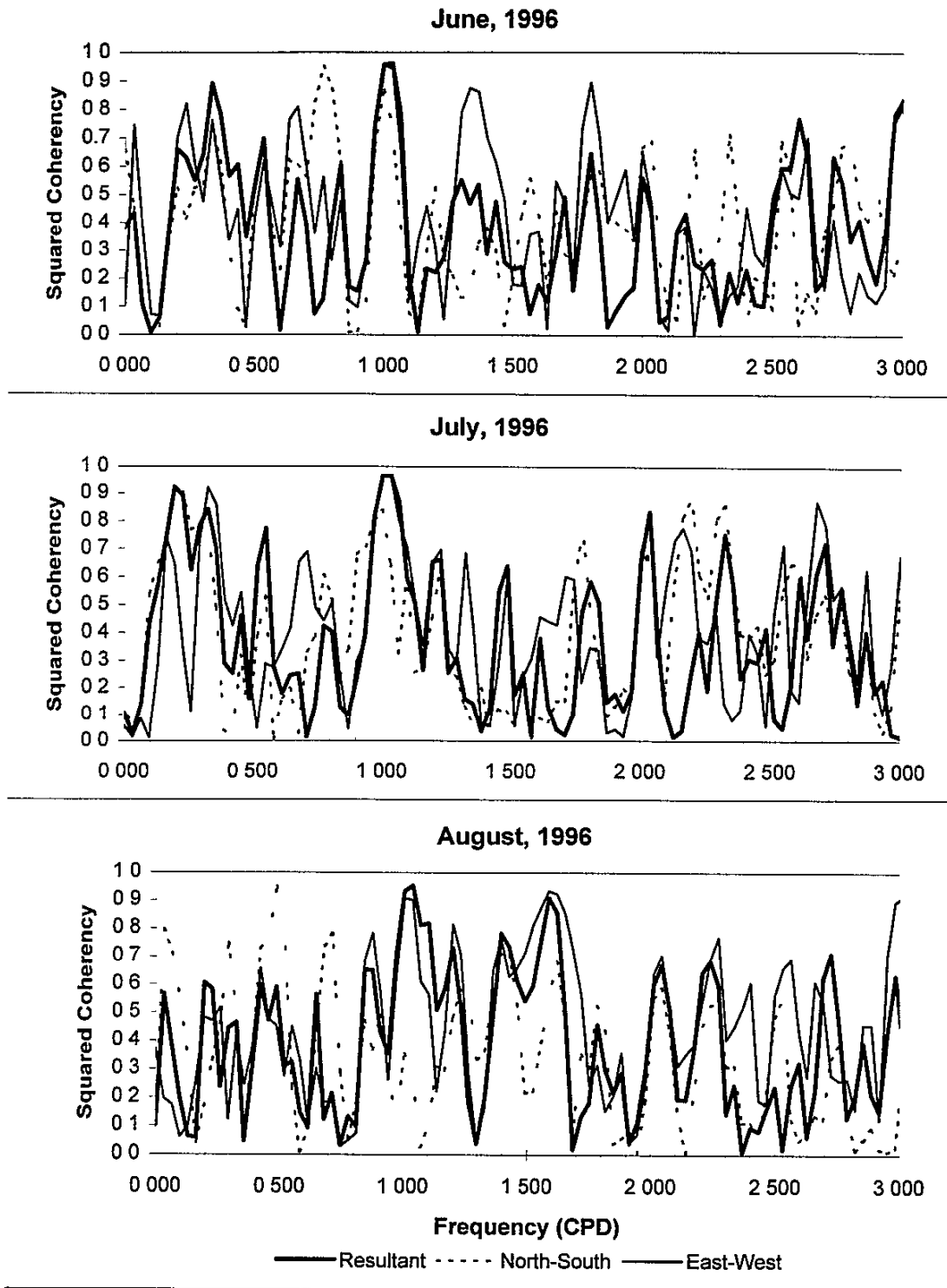
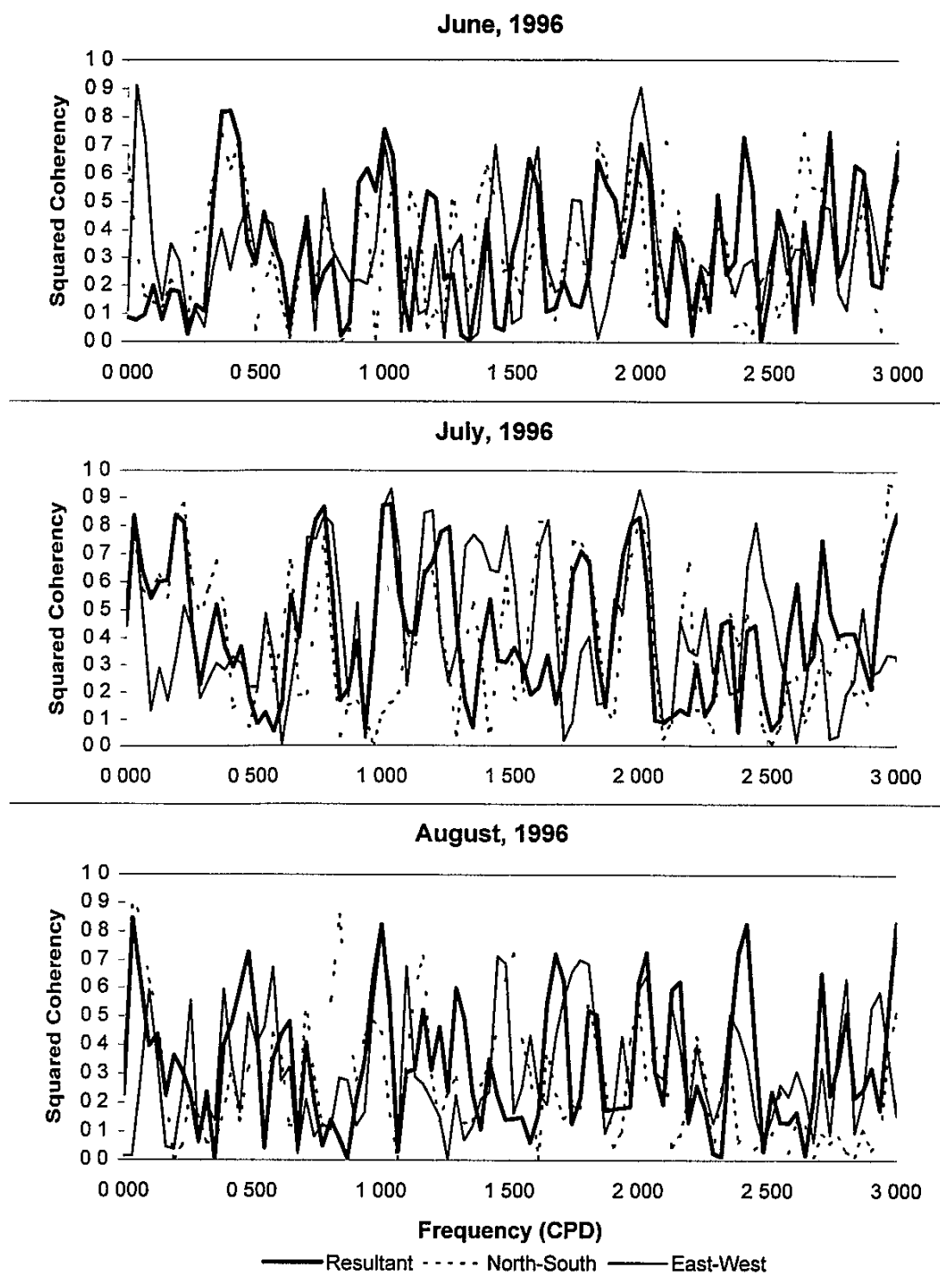


FIGURE 4-31
SQUARED COHERENCY BETWEEN WIND SPEED AND WATER LEVEL
AT SOUTH BIRD ISLAND



**TABLE 4-9
STATISTICS OF TEMPERATURE DATA - LOWER LAGUNA MADRE**

Time	Station LLM1							Station LLM2a/2N							Station LLM3						
	Monthly Average (°C) of Daily				Monthly			Monthly Average (°C) of Daily				Monthly			Monthly Average (°C) of Daily				Monthly		
	Min	Mean	Max	St Dev	Mean	St Dev		Min	Mean	Max	St Dev	Mean	St Dev		Min	Mean	Max	St Dev	Mean	St Dev	
Sep-94	27.4	28.1	29.0	0.5	27.8	1.4															
Oct-94	23.8	25.5	26.4	0.5	25.4	2.4															
Nov-94	22.5	24.0	24.9	0.5	24.3	1.4															
Dec-94	17.8	19.4	20.2	0.4	20.1	3.2															
Jan-95	15.4	16.2	17.2	0.5	16.4	2.7															
Feb-95	17.9	19.1	20.2	0.6	19.2	2.1															
Mar-95	18.4	19.9	20.9	0.6	19.9	3.8															
Apr-95	21.7	23.0	24.0	0.5	22.9	2.3															
May-95	25.9	27.5	28.4	0.5	27.5	1.2															
Jun-95	26.9	28.7	29.8	0.6	28.7	1.2															
Jul-95	28.4	30.1	31.1	0.5	30.2	0.8															
Aug-95	28.5	30.3	31.3	0.5	30.3	1.1															
Sep-95	27.1	29.0	30.1	0.6	29.4	2.1															
Oct-95	23.3	25.1	26.1	0.5	24.9	1.8															
Nov-95	19.0	21.1	22.0	0.5	21.3	2.5															
Dec-95	15.5	17.3	18.4	0.6	17.4	4.9															
Jan-96	14.7	15.7	16.9	0.7	15.5	3.1															
Feb-96	15.3	16.8	18.1	0.7	16.8	5.4															
Mar-96	15.9	17.3	18.9	0.8	17.4	3.4															
Apr-96	20.8	22.3	23.5	0.7	22.3	2.7															
May-96	25.6	27.1	28.0	0.5	27.1	1.9															
Jun-96	27.5	29.4	30.5	0.6	29.4	0.9															
Jul-96	28.3	30.2	31.2	0.6	30.2	0.7															
Aug-96	27.7	29.4	30.4	0.5	29.4	0.8															
Sep-96	27.2	28.8	29.8	0.5	28.8	1.9															
Oct-96	24.0	25.4	26.3	0.5	25.4	1.7															
Nov-96	20.2	21.8	22.5	0.4	21.9	2.7															
Dec-96	15.7	17.0	18.2	0.6	17.0	4.3															
Jan-97	13.1	14.1	15.3	0.7	14.6	5.0															
Feb-97	16.0	17.2	18.2	0.5	17.2	2.2															
Mar-97																					
Apr-97																					
May-97																					
Jun-97																					
Jul-97																					
Aug-97																					
Sep-97																					
Oct-97																					
Nov-97																					
Dec-97	18.1	18.6	19.3	0.4	18.7	1.9	17.4	18.3	19.4	0.7	18.0	2.6	14.9	15.8	17.3	0.8	15.6	3.8			
Jan-98	18.2	19.0	19.8	0.5	18.8	1.2	18.4	19.3	20.5	0.7	19.1	1.4	17.2	18.1	19.3	0.6	18.1	1.4			
Feb-98	17.9	19.4	20.5	0.6	19.4	1.5	19.5	20.1	21.4	0.6	20.1	0.6	17.3	18.9	20.2	0.6	18.9	1.7			
Mar-98	16.2	18.7	19.8	0.6	18.5	2.3	18.8	21.1	22.6	0.8	21.1	2.6	13.2	18.6	19.9	0.6	18.8	0.9			
Apr-98							19.6	22.6	23.7	0.6	22.7	1.0									
May-98																					

TABLE 4-10
STATISTICS OF TEMPERATURE DATA - UPPER LAGUNA MADRE

Time	Station ULM1						Station ULM2						Station ULM3					
	Monthly Average (°C) of Daily				Monthly		Monthly Average (°C) of Daily				Monthly		Monthly Average (°C) of Daily				Monthly	
	Min	Mean	Max	St Dev	Mean	St Dev	Min	Mean	Max	St Dev	Mean	St Dev	Min	Mean	Max	St Dev	Mean	St Dev
Sep-94																		
Oct-94																		
Nov-94	21.0	21.8	22.8	0.5	21.8	0.9												
Dec-94	14.6	15.3	16.2	0.4	15.2	1.2	14.1	15.2	16.2	0.5	15.1	1.0	15.6	16.2	16.8	0.3	16.0	1.2
Jan-95	13.4	14.3	15.8	0.6	14.3	2.2	13.7	14.6	15.9	0.6	14.4	2.8	14.6	15.3	16.2	0.4	15.3	2.9
Feb-95	15.4	17.0	18.7	0.7	17.0	1.6	15.9	17.4	19.1	0.8	17.4	2.0	16.4	17.6	18.7	0.5	17.6	1.8
Mar-95	17.2	18.7	20.2	0.6	19.1	3.1	16.7	18.6	20.2	0.8	18.3	3.5	17.0	17.4	18.7	1.5	12.1	6.2
Apr-95	20.8	22.2	23.3	0.6	22.2	2.1	21.3	23.0	24.4	0.7	23.0	1.9	20.6	22.5	23.3	0.4	22.2	2.8
May-95	24.7	26.3	27.5	0.6	26.3	1.3	25.3	26.9	28.0	0.6	26.8	1.3	25.5	27.0	27.9	0.4	27.1	1.1
Jun-95	26.5	28.5	29.7	0.6	28.4	1.1	26.7	28.8	30.2	0.7	28.8	1.3	27.1	28.8	29.8	0.5	28.8	1.0
Jul-95	27.9	30.1	32.0	0.8	30.1	0.9	28.0	30.3	31.7	0.8	30.3	1.0	28.2	30.0	31.0	0.5	30.0	0.7
Aug-95	28.4	30.4	31.5	0.5	30.3	1.0	28.5	30.4	31.6	0.6	30.4	1.1	28.9	30.5	31.4	0.4	30.5	0.9
Sep-95	27.2	29.1	30.5	0.7	29.1	2.5	26.9	29.1	30.7	0.8	29.3	2.7	27.5	29.2	30.2	0.5	29.0	2.6
Oct-95	22.4	25.2	26.2	0.5	25.2	1.7	22.5	24.6	25.8	0.6	24.6	2.2	23.0	24.7	25.6	0.4	24.8	2.0
Nov-95	18.3	19.5	21.1	0.8	19.2	2.0	17.6	19.5	20.6	0.6	19.5	1.6	18.4	20.2	21.2	0.5	20.1	2.9
Dec-95	13.5	15.2	16.3	0.6	15.0	4.0	15.2	16.7	18.1	0.7	16.9	4.5						
Jan-96	12.1	13.4	15.5	0.9	13.4	2.8	12.9	14.0	15.8	0.8	13.8	3.3	13.6	14.4	15.7	0.6	14.4	3.0
Feb-96	14.7	16.3	18.0	0.7	16.6	3.3	14.2	15.5	17.2	0.7	15.5	5.3	15.0	16.4	17.6	0.6	16.0	4.6
Mar-96	14.8	16.1	17.5	0.7	16.1	2.4	15.0	16.4	18.2	0.8	16.5	3.2	15.8	17.1	18.6	0.7	17.1	3.0
Apr-96	19.6	21.0	22.1	0.6	20.8	2.5	20.1	21.7	23.2	0.8	21.8	2.8	20.8	22.2	23.3	0.5	22.2	2.6
May-96	24.6	26.2	27.1	0.6	26.1	2.4	25.4	26.9	28.0	0.6	26.9	2.0	26.7	27.2	27.8	0.3	27.2	1.6
Jun-96	26.5	28.9	30.0	0.6	28.9	0.9	27.4	29.4	30.7	0.7	29.4	1.0	27.6	29.3	30.1	0.4	29.3	0.8
Jul-96	27.4	30.3	31.7	0.7	30.2	0.8	24.3	29.7	31.8	2.0	29.8	3.5	24.9	29.6	31.1	1.5	29.6	3.2
Aug-96							27.0	29.4	30.6	0.7	29.4	1.2						
Sep-96							26.9	28.9	30.3	0.7	28.9	2.1	27.7	29.2	30.3	0.4	29.2	1.4
Oct-96							23.3	24.8	25.9	0.6	24.8	1.5	23.6	24.9	25.8	0.4	24.9	1.6
Nov-96							19.1	21.0	22.3	0.7	21.0	3.5	21.5	22.0	22.7	0.4	22.1	1.8
Dec-96							14.4	15.7	17.3	0.6	15.6	3.9						
Jan-97	10.5	11.7	13.2	0.8	11.7	4.0	10.4	11.7	13.2	0.8	12.2	4.9	12.1	13.2	14.3	0.5	13.4	4.7
Feb-97	13.1	14.3	15.4	0.5	14.3	1.6	14.4	15.7	17.0	0.6	15.8	2.0	14.4	15.7	17.0	0.6	15.8	2.0
Mar-97																		
Apr-97																		
May-97																		
Jun-97																		
Jul-97																		
Aug-97																		
Sep-97																		
Oct-97																		
Nov-97							15.0	15.6	16.6	0.4	15.6	3.1						
Dec-97	13.5		16.2		14.1	3.0	15.4	18.1	18.9	0.5	18.0	1.1	16.3		17.6		16.9	2.0
Jan-98	16.1		17.5		16.8	1.0	17.2	18.4	19.6	0.8	17.9	3.3	17.2		18.7		17.8	1.3
Feb-98	14.4		17.7		16.6	1.0							17.4		19.6		18.8	1.6
Mar-98	14.6		17.8		16.6	2.2	17.5	19.1	20.4	0.6	19.2	3.1	16.4		20.4		19.2	1.5
Apr-98	21.7		23.5		22.4	1.1	18.5	22.8	23.9	0.6	22.8	0.8						
May-98	20.0		25.6		24.3	1.0												

TABLE 4-11
STATISTICS OF SALINITY DATA - LOWER LAGUNA MADRE

Time	Station LLM1							Station LLM2a/2N							Station LLM3						
	Monthly Average (‰) of Daily				Monthly			Monthly Average (‰) of Daily				Monthly			Monthly Average (‰) of Daily				Monthly		
	Min	Mean	Max	St Dev	Mean	St Dev		Min	Mean	Max	St Dev	Mean	St Dev		Min	Mean	Max	St Dev	Mean	St Dev	
Sep-94	36.4	37.5	38.4	0.6	37.5	0.6															
Oct-94	32.3	34.8	35.7	0.5	34.8	0.5															
Nov-94	32.0	33.8	34.3	0.3	33.8	0.3															
Dec-94	32.3	34.7	35.2	0.3	34.7	0.3															
Jan-95	29.7	30.9	31.8	0.5	30.9	1.2															
Feb-95	30.0	32.3	33.2	0.5	32.4	1.1															
Mar-95	30.0	32.1	32.8	0.4	32.0	1.3															
Apr-95	30.8	32.6	33.1	0.3	32.6	0.8															
May-95	31.0	32.8	33.4	0.4	32.8	1.2															
Jun-95	32.7	34.7	35.3	0.4	34.7	0.9															
Jul-95	33.8	35.5	36.0	0.3	35.6	0.8															
Aug-95	35.8	36.2	36.6	0.2	36.2	0.5															
Sep-95	32.1	35.7	36.2	0.4	35.6	0.6															
Oct-95	31.9	34.3	35.2	0.5	34.2	1.9															
Nov-95	22.4	25.6	26.8	0.8	25.2	3.7															
Dec-95	21.7	24.1	25.6	0.9	24.1	1.8															
Jan-96	26.3	27.4	28.5	0.6	27.3	2.9															
Feb-96	28.2	29.9	30.7	0.4	29.9	1.0															
Mar-96	32.7	34.5	35.3	0.4	34.5	1.3															
Apr-96	33.2	35.2	35.8	0.4	35.2	1.0															
May-96	33.7	35.3	35.7	0.2	35.3	0.6															
Jun-96	34.1	36.1	37.1	0.6	36.1	2.2															
Jul-96	35.3	37.5	38.6	0.6	37.5	1.5															
Aug-96	34.1	36.2	37.0	0.5	36.2	1.4															
Sep-96	33.2	35.1	35.6	0.3	35.1	1.2															
Oct-96	26.5	28.9	29.9	0.5	28.9	3.2															
Nov-96	29.8	31.9	32.7	0.5	31.9	2.5															
Dec-96	31.6	33.7	34.5	0.5	33.7	1.5															
Jan-97	32.2	33.2	34.0	0.5	33.2	1.1															
Feb-97	29.7	31.3	31.7	0.2	31.3	1.8															
Mar-97																					
Apr-97																					
May-97																					
Jun-97																					
Jul-97																					
Aug-97																					
Sep-97																					
Oct-97																					
Nov-97																					
Dec-97	22.8	23.6	24.5	0.6	23.8	0.9	26.4	27.5	28.5	0.7	27.6	1.6	27.7	28.0	28.3	0.2	28.0	0.5			
Jan-98	17.0	17.9	18.5	0.4	17.8	1.3	32.4	32.9	33.4	0.3	33.0	0.7	28.3	28.9	29.3	0.3	28.9	0.8			
Feb-98	35.9	42.0	45.6	3.2	41.7	5.1	32.9	33.5	33.7	0.1	33.5	0.2	23.5	25.4	25.8	0.4	25.4	1.3			
Mar-98	32.3	40.5	43.5	2.2	40.9	3.4	29.8	31.5	31.8	0.2	31.7	1.2	15.1	21.3	21.9	0.4	21.2	0.6			
Apr-98							26.2	30.3	30.6	0.2	30.1	2.2									
May-98																					

TABLE 4-12
STATISTICS OF SALINITY DATA - UPPER LAGUNA MADRE

Time	Station ULM1						Station ULM2						Station ULM3					
	Monthly Average (%) of Daily				Monthly		Monthly Average (%) of Daily				Monthly		Monthly Average (%) of Daily				Monthly	
	Min	Mean	Max	St Dev	Mean	St Dev	Min	Mean	Max	St Dev	Mean	St Dev	Min	Mean	Max	St Dev	Mean	St Dev
Sep-94																		
Oct-94																		
Nov-94	30.4	30.9	32.1	0.4	30.9	0.5												
Dec-94	27.8	28.7	29.4	0.3	28.4	1.8	33.4	38.1	39.6	1.4	37.8	1.9	38.4	38.6	38.8	0.1	38.6	0.5
Jan-95	26.4	26.9	27.5	0.3	26.8	2.7	30.0	34.8	36.8	1.5	34.9	4.1	36.5	37.0	37.7	0.3	37.0	3.3
Feb-95	30.9	33.3	34.0	0.3	33.3	1.3	37.2	42.1	43.2	1.0	42.2	2.0	42.1	44.3	44.8	0.3	44.3	1.7
Mar-95	28.6	30.4	30.9	0.3	30.4	1.0	34.4	37.5	38.6	0.6	37.4	1.6	30.9	39.8	31.7	2.7	26.0	13.7
Apr-95	28.2	30.0	30.5	0.3	30.0	0.8	35.2	37.9	38.7	0.4	37.9	1.8	35.0	38.8	39.2	0.2	38.8	0.7
May-95	28.7	30.3	31.3	0.4	30.3	0.8	37.5	39.5	40.2	0.4	39.5	1.3	35.1	37.4	38.2	0.5	37.3	2.4
Jun-95	31.1	33.0	34.4	0.6	33.0	1.5	33.5	36.1	37.0	0.6	36.2	2.2	32.8	34.3	34.7	0.2	34.3	1.5
Jul-95	31.3	33.8	35.1	0.6	33.7	1.2	32.9	34.8	35.8	0.6	34.8	3.3	30.8	32.6	33.4	0.3	32.6	1.6
Aug-95	33.1	34.8	35.4	0.2	34.8	0.6	35.0	37.3	38.2	0.5	37.3	1.1	32.8	34.8	35.6	0.3	35.0	2.2
Sep-95	33.0	34.5	34.9	0.2	34.5	1.0	35.2	38.6	39.2	0.6	38.5	2.2	34.7	36.3	36.7	0.2	36.0	1.6
Oct-95	29.7	32.4	32.8	0.2	32.4	1.3	35.8	37.9	38.5	0.3	37.8	1.1	36.5	38.2	38.6	0.2	38.1	1.5
Nov-95	29.6	30.7	32.0	0.6	31.1	1.4	35.8	38.6	39.0	0.3	38.6	0.7	36.0	38.2	38.5	0.2	38.1	1.1
Dec-95	29.2	31.4	32.4	0.4	31.4	0.8	36.0	38.0	38.4	0.3	38.0	1.0						
Jan-96	31.7	32.1	32.7	0.2	32.1	0.6	36.9	37.5	38.0	0.3	37.5	0.9	37.7	38.2	38.6	0.2	38.2	0.7
Feb-96	31.0	32.8	33.3	0.2	32.7	0.6	35.0	37.2	37.8	0.1	37.2	0.8	36.1	38.0	38.5	0.3	38.0	1.6
Mar-96	31.9	33.8	34.3	0.3	33.9	0.5	39.1	41.1	41.6	0.3	41.2	1.1	39.0	40.9	41.5	0.3	40.9	1.6
Apr-96	31.7	34.1	35.0	0.5	34.1	1.6	38.3	41.7	42.5	0.6	41.6	1.0	38.8	41.0	41.5	0.3	41.0	2.0
May-96	33.6	35.7	36.4	0.3	35.7	1.4	38.2	40.4	41.5	0.5	40.4	0.8	37.7	38.1	38.4	0.2	38.0	1.1
Jun-96	35.6	38.4	39.5	0.5	38.2	1.7	40.3	42.3	43.0	0.3	42.3	0.7	38.4	40.2	40.5	0.2	40.2	0.6
Jul-96	38.4	41.5	42.7	0.5	41.5	1.1	40.2	44.9	46.6	1.1	44.8	2.8	37.3	42.7	44.0	1.1	42.7	2.6
Aug-96							45.8	48.7	49.4	0.4	48.7	1.3						
Sep-96							43.8	46.6	48.0	0.7	46.6	2.8	39.7	43.0	44.8	0.8	43.0	2.5
Oct-96							42.6	46.4	48.1	1.1	46.4	2.3	40.4	43.2	44.9	0.8	43.2	2.0
Nov-96							43.4	45.8	47.0	0.6	45.8	2.1	39.0	40.5	42.1	0.7	40.4	2.4
Dec-96							46.3	48.6	49.3	0.3	48.7	1.2						
Jan-97	34.4	35.3	36.3	0.5	35.3	1.7	45.1	47.6	49.7	1.3	47.6	2.7	44.2	45.7	47.1	0.8	45.7	4.5
Feb-97	30.5	33.6	34.1	0.4	33.5	1.2	38.7	43.6	45.6	1.2	43.5	3.1	38.7	43.6	45.6	1.2	43.5	3.1
Mar-97																		
Apr-97																		
May-97																		
Jun-97																		
Jul-97																		
Aug-97																		
Sep-97																		
Oct-97																		
Nov-97							22.2	23.3	24.0	0.5	23.2	1.5						
Dec-97	27.0	27.2	27.4	0.1	27.3	0.4	19.2	22.2	22.7	0.4	22.2	0.8	24.3	24.8	25.2	0.2	24.8	1.0
Jan-98	27.3	27.4	27.6	0.1	27.8	0.6	24.6	25.2	25.9	0.4	25.2	0.8	24.8	25.3	25.8	0.3	25.3	1.1
Feb-98	26.0	28.6	29.0	0.2	28.7	2.0							22.0	23.4	23.8	0.2	23.4	0.8
Mar-98	22.0	24.8	25.3	0.3	24.7	1.3	22.3	24.2	25.2	0.6	24.2	1.3	20.4	23.6	24.1	0.2	23.6	0.6
Apr-98	26.1	26.5	27.0	0.3	26.5	2.5	22.8	27.6	27.9	0.2	27.6	0.3						
May-98	21.5	25.8	26.9	0.5	25.5	1.8												

As noted in the previous chapter, current velocity is the primary mechanism operating in the processes of suspension, transport and settling of sediment. Most of the instrumentation and observational effort of this project were directed at quantifying this variable. In this chapter, the features of currents and their variations are examined from several different aspects.

Currents respond to the forcing of wind and water-level variations. As noted earlier, at the smallest space-time scales, the effect of wind is manifested in the production of short period capillary and gravity waves from the wind stress on the surface. Wind waves also have associated currents, which are augmented in shallow waters. With increasing wind speeds, waves overtop and break, creating intense patchy turbulence distributed through the water column. The intense, chaotic currents which result contribute to vertical mixing of waterborne constituents, including suspended sediment. This turbulence also extends to the bottom in shallow systems like the Laguna Madre, directly mobilizing sediment particles from the bed. At larger space-time scales, wind stress forces a direct current resulting in movement of water (and any materials in suspension or solution). A sudden change in wind in either speed or direction (or both) results in a corresponding movement of water and variation in the water level.

Indirect effects on currents and water level in the Laguna Madre can be summarized as the response of the Laguna to direct effects of wind on adjacent waterbodies. The larger the surface area of the waterbody (more specifically, the larger the fetch) and the shallower the depths, the greater the response to wind stress, and therefore the greater the potential for the resultant change in water level to affect the Laguna. The filter through which this effect is passed is the inlet(s) connecting the Laguna and the adjacent waterbody. The Gulf of Mexico is the most important such adjacent waterbody, but Corpus Christi Bay and Baffin Bay can be important in local regions of the Laguna Madre. Ward (1997) and references therein discuss the mechanics of a co-oscillating bay in communication with a larger waterbody through a narrow inlet, and likens the response of the bay to a stilling well, in the way that longer period variations pass through the inlet, but shorter period variations are filtered out.

Water-level forces currents through pressure gradients that accelerate the water. Variation in water level is a direct index, therefore, to currents that mobilize and transport sediment. The nature and sources of water-level variation were addressed in Section 4.2. One of the dominant variations in water level is the semi-annual secular rise and fall of sea level (Ward, 1997). While this is a key process in the large-scale depletion and storage of water in the Laguna, it takes place over such a long time that the direct current resulting is small, and impossible to resolve, even with the precision of modern sensors. What is important

about the semi-annual secular variation is that this is the main contributor to the net annual excursion in water level, and governs the water depths, hence the effect of more dynamic short-term processes.

For shorter-period signals, there is a degree of filtering upon passage of the signal from the Gulf of Mexico through the inlets. Important (astronomical) tidal components include the fortnightly (~ 14 days), the diurnal (24.8 hrs) driven by the lunar day, and the semi-diurnal (12.4 hrs) of the lunar half-day. The 14-day component receives relatively little attenuation, and propagates easily into the Laguna, but like the semi-annual variation, the rise and fall of water is so slow that the resulting current will be manifest, if at all, as a background net flow, upon which more short-term variability is superposed. In Section 4.2, it was inferred that the diurnal and semi-diurnal components of the tide are substantially attenuated within the shallow water of the Laguna. In addition to the astronomical tides, meteorological systems impose additional variation in water level, primarily through the effects of wind stress. Seabreeze circulations contribute a 24-hr component (in addition to the tidal component induced by the sun), and frontal passages, especially during the winter can introduce energy in the 3-7 day components, depending upon the season. In addition, local meteorological forcing results in local set-up and set-down of the water. These responses can have a substantial effect on currents.

Unlike wind, which is a measure of flow in a laterally unbounded system (the atmosphere), current depicts movement in a bounded system. The system is bounded vertically, and the shallow water (and high aspect ratio) of the Laguna confines most of the energy to the horizontal plane. The system is also bounded laterally by shoals and shoreline, which has further confining effects on the directions of current. Also unlike wind, the current velocity sensors are much less rugged and more prone to failure, so the record includes frequent data gaps. For some months, only a few measurements exist, and the corresponding statistical depictions may be significantly distorted.

An inventory and statistics of the current data are presented in tables 5-1 through 5-6, on a monthly basis for the study period, platform by platform. The direction convention on all of these tables and figures is that to which the current flows, which is the usual convention for reporting direction of a current. For purposes of this inventory, the current data is subdivided into several categories:

"Good" - the measurements determined to be physically plausible and therefore included in the final data compilation;

"Outliers" - the measurements whose magnitudes are so large as to be physically implausible, i.e., "freak" values, and are deleted from the compilation;

"Calm" - zero values of both components that occurred under conditions (little wind, steady water levels) making such behavior plausible, and therefore included in the final data compilation,

"Zeros" - zero values that occur in lengthy flatline episodes under conditions unlikely for zero currents to occur, and are therefore deleted from the compilation;

"Missing" - data records containing the CBI character entry for "missing data"

The number of possible measurements in each month, based upon the data reporting interval and the number of days in the month is the value under "Total". The number of "Good" measurements includes the number of "Calm". The data not accounted for by these categories are the records lost to time gaps in the data record, i.e.

$$\text{TIME GAPS} = \text{TOTAL} - (\text{MISSING} + \text{ZEROS} + \text{OUTLIERS})$$

Therefore, the total number of missing records in the data compilation each month is:

$$\text{MISSING} + \text{ZEROS} + \text{OUTLIERS} + \text{TIME GAPS}$$

An important statistic in these tables is the monthly vector mean, given under the heading "Mean Current," as this is a direct measure of any net flow during that month. In contrast, the magnitude of the current vector, given under the heading "Speed" in these tables, is a measure of the mean energy in the current and the variability ("turbulence") of that current is indicated by the standard deviation. It is noteworthy that each station exhibits a propensity for net flow that is fairly consistent from month to month. At both LLM1 and LLM2 there is a northward component in the net flow, the current at the more northerly station (LLM1) setting about 45 degrees more clockwise to E of N. It is interesting to note that the same net northward mean set to the current was detected in the 1980 Intensive Inflow study in this region (Ward, 1981), interpreted as a mean wind-driven circulation entering the Lower Laguna through Brazos Santiago and exiting through Mansfield Pass. In the Upper Laguna, the current at Station ULM2 does not set north-south as one might anticipate from the geometry of the Laguna, and as is exhibited by ULM3 farther south, but has a significant component directed into Baffin Bay. Station ULM1 in Corpus Christi Bay just north of Bulkhead Flats shows predominantly westerly currents, paralleling the trend of the south shoreline and its continuation along the face of the Flats.

TABLE 5-1
STATISTICS OF CURRENT DATA FROM STATION LLM1

Date	Number of Data Points						Speed (cm/s)		Mean Current		North-South Component (cm/s)				West-East Component (cm/s)			
	Total	Good	Missing	Zeros	Outliers	Calm	Mean	St Dev	(cm/s)	(° from N)	Max	Min	Mean	St Dev	Max	Min	Mean	St Dev
09/94	7,200	6,448	4	8	0	7	4.5	2.8	0.2	241.3	7.7	-8.1	3.7	2.5	6.2	-4.8	2.2	1.8
10/94	7,440	4,966	210	196	0	23	6.0	4.1	0.2	170.4	9.1	-9.6	5.3	4.9	5.6	-4.7	2.3	2.7
11/94	7,200	6,324	47	0	0	61	5.3	3.5	0.4	208.7	9.0	-8.3	3.9	5.3	6.6	-6.9	2.9	3.5
12/94	7,440	3,290	32	11	0	13	6.1	3.8	0.1	265.7	8.0	-7.2	4.2	8.1	5.9	-5.7	3.6	5.8
01/95	7,440	5,902	1	31	0	25	8.5	4.7	0.3	333.0	15.0	-12.3	7.3	4.4	8.4	-8.2	3.9	2.7
02/95	6,720	717	5,331	5	0	0	6.1	3.7	1.7	217.1	7.3	-11.1	4.9	12.9	8.6	-5.5	3.4	8.1
03/95	7,440	6,766	1	0	0	4	6.8	3.8	0.4	36.9	11.8	-11.6	5.9	5.6	6.5	-6.5	2.8	3.3
04/95	7,200	4,341	2,213	97	0	7	6.3	3.3	0.8	154.5	10.4	-12.2	5.5	7.7	6.5	-6.3	2.4	4.5
05/95	7,440	2,888	4,110	10	0	19	5.6	3.2	1.0	132.5	11.1	-9.2	5.2	10.0	3.0	-5.1	1.6	5.6
06/95	7,200	6,878	59	0	0	2	6.2	3.5	0.5	84.8	10.9	-9.5	5.8	7.4	3.8	-4.6	1.6	3.8
07/95	7,440	5,672	737	0	0	14	6.1	3.1	1.0	30.9	9.3	-9.0	5.7	8.7	3.3	-3.9	1.6	4.4
08/95	7,440	2,020	3,771	0	0	0	6.0	2.7	0.4	345.9	8.7	-9.3	5.7	14.9	4.1	-2.9	1.5	7.4
09/95	7,200	6,114	2	107	0	25	6.4	3.4	0.5	36.9	11.2	-10.0	6.0	9.2	4.7	-4.3	1.9	4.5
10/95	7,440	3,439	2,059	0	0	24	7.4	4.2	0.2	64.2	12.0	-13.0	7.0	13.0	5.4	-4.6	1.8	6.1
11/95	7,200	3,699	393	0	0	3	8.3	4.8	0.8	189.1	10.2	-9.6	5.9	13.6	9.0	-6.7	4.0	7.0
12/95	7,440	0	5,663	0	0	0												
01/96	7,440	5,637	123	0	0	10	7.6	4.2	0.3	116.9	13.7	-12.8	7.2	4.3	4.5	-4.4	1.7	1.3
02/96	6,960	6,713	0	0	0	4	7.0	3.6	0.5	33.0	12.3	-11.8	6.5	5.4	5.1	-5.1	2.2	1.9
03/96	7,440	7,277	0	0	0	2	6.9	3.8	0.7	31.7	11.6	-11.5	6.5	6.5	4.3	-4.6	1.6	2.2
04/96	7,200	7,165	1	0	0	8	7.0	4.1	1.1	15.8	12.7	-11.2	6.5	7.9	4.5	-5.6	1.7	2.6
05/96	7,440	5,609	1,766	0	0	7	6.0	3.0	1.5	15.3	11.4	-8.8	5.6	9.5	3.3	-5.1	1.3	3.2
06/96	7,200	6,017	857	15	0	3	5.9	2.8	1.1	26.6	10.6	-8.3	5.5	9.6	3.3	-5.0	1.4	3.2
07/96	7,440	7,362	0	0	0	5	6.2	3.1	1.5	15.4	11.3	-9.1	5.8	9.3	3.6	-5.2	1.5	3.1

Tab5-1-6.xls LLM1 9/28/99 9 31 AM YCS

PBS&J

TABLE 5-1 (Concluded)
STATISTICS OF CURRENT DATA FROM STATION LLM1

Date	Number of Data Points						Speed (cm/s)		Mean Current		North-South Component (cm/s)				West-East Component (cm/s)			
	Total	Good	Missing	Zeros	Outliers	Calm	Mean	St Dev	(cm/s)	(° from N)	Max	Min	Mean	St Dev	Max	Min	Mean	St Dev
08/96	7,440	6,665	0	0	0	4	5.8	2.9	1.1	14.0	10.0	-9.6	5.4	10.3	4.1	-5.3	1.6	3.5
09/96	7,200	7,066	3	3	0	2	6.0	3.3	0.4	9.8	10.8	-12.1	5.6	10.5	4.5	-5.2	1.5	3.6
10/96	7,440	7,373	0	0	2	2	7.5	4.4	0.7	20.5	13.3	-13.1	6.9	11.3	4.9	-6.1	2.2	4.0
11/96	7,200	6,825	0	5	0	2	7.3	4.2	0.2	346.3	12.4	-12.5	6.9	12.5	4.5	-4.5	1.8	4.3
12/96	7,440	6,678	66	407	0	34	7.4	4.2	0.2	45.2	12.7	-13.5	7.1	13.3	3.5	-4.1	1.4	4.6
01/97	7,440	6,537	0	868	1	65	6.6	4.0	0.3	6.0	11.6	-12.4	6.4	4.0	3.7	-3.8	1.0	1.2
02/97	6,720	6,708	0	6	2	10	7.5	3.8	1.0	19.3	13.7	-12.7	7.1	5.6	6.0	-4.5	1.7	1.9
03/97	7,440	1	0	0	0	0	12.2		12.2	6.1			19.2				3.0	
04/97																		
05/97																		
06/97																		
07/97																		
08/97																		
09/97																		
10/97																		
11/97																		
12/97	1,488	365	2	0	2	0	8.0	3.5	5.6	344.0	12.7	0.2	5.9	4.5	6.4	-5.1	4.1	2.1
01/98	1,488	870	0	0	0	0	6.5	3.0	3.9	331.7	11.3	-5.5	4.8	3.6	6.8	-4.1	3.2	2.2
02/98	1,344	1,332	0	0	0	0	7.5	2.9	4.8	324.9	12.3	-5.1	4.9	4.5	10.4	-5.6	4.4	3.4
03/98	1,488	566	0	0	0	0	8.6	2.6	6.5	329.9	12.4	-2.5	6.3	7.8	10.1	-4.1	4.4	6.0
04/98																		
05/98																		

TABLE 5-2
STATISTICS OF CURRENT DATA FROM STATION LLM2a/2N

Date	Number of Data Points						Speed (cm/s)		Mean Current		North-South Component (cm/s)				West-East Component (cm/s)			
	Total	Good	Missing	Zeros	Outliers	Calm	Mean	St Dev	(cm/s)	(° from N)	Max	Min	Mean	St Dev	Max	Min	Mean	St Dev
08/96																		
09/96	1,440	1,148	0	0	0	0	3.7	2.3	1.8	331.9	7.8	-4.4	3.1	2.2	4.1	-2.4	1.7	1.1
10/96	1,488	1,277	2	0	0	1	4.0	2.6	1.0	330.6	7.4	-4.8	3.3	3.2	4.5	-2.7	2.0	1.7
11/96	1,440	1,400	0	0	0	0	4.4	2.9	1.7	323.9	8.1	-4.8	3.7	4.0	5.1	-2.3	2.3	2.3
12/96	1,488	1,406	0	23	0	54	2.9	2.8	0.4	268.8	4.8	-5.0	2.4	4.7	3.2	-2.3	1.3	2.7
01/97	1,488	647	6	0	0	16	3.0	3.4	1.3	164.5	3.8	-6.8	2.8	3.3	2.1	-2.3	1.0	1.1
02/97	1,344	945	0	0	0	2	2.7	2.3	1.8	3.3	6.2	-1.8	2.4	3.5	1.7	-2.3	1.0	1.3
03/97																		
04/97																		
05/97																		
06/97																		
07/97																		
08/97																		
09/97																		
10/97																		
11/97																		
12/97	1,488	927	2	0	2	0	4.8	3.5	4.1	327.8	7.1	-0.2	3.6	2.6	6.0	-2.0	2.9	2.6
01/98	1,488	862	0	0	0	1	4.6	3.4	3.8	320.3	6.5	-0.6	3.0	2.2	7.6	-2.3	3.3	2.8
02/98	1,344	49	851	0	851	0	3.1	2.6	2.6	323.2	10.5	-0.4	2.3	9.5	9.4	-1.9	2.1	11.8
03/98	1,488	848	2	0	2	0	6.7	4.2	1.8	315.8	7.0	-8.1	4.7	4.3	6.1	-8.4	4.6	3.8
04/98	1,440	410	5	0	5	0	9.9	3.2	7.8	317.0	10.4	1.4	6.8	6.8	1.2	-11.8	6.5	6.4
05/98																		

TABLE 5-3
STATISTICS OF CURRENT DATA FROM STATION LLM3

Date	Number of Data Points						Speed (cm/s)		Mean Current		North-South Component (cm/s)				West-East Component (cm/s)			
	Total	Good	Missing	Zeros	Outliers	Calm	Mean	St Dev	(cm/s)	(° from N)	Max	Min	Mean	St Dev	Max	Min	Mean	St Dev
08/96																		
09/96																		
10/96																		
11/96																		
12/96																		
01/97																		
02/97																		
03/97																		
04/97																		
05/97																		
06/97																		
07/97																		
08/97																		
09/97																		
10/97																		
11/97																		
12/97	1,488	941	0	0	0	0	3.7	1.4	3.3	256.4	3.2	-1.1	0.8	1.5	-1.8	-5.1	-3.2	1.6
01/98	1,488	822	0	0	0	1	2.0	1.2	0.7	285.5	2.0	-2.3	-0.2	1.3	1.8	-2.7	-0.6	1.8
02/98	1,344	1,333	0	0	0	0	2.4	1.7	0.6	129.1	3.9	-2.9	0.4	1.8	4.0	-2.2	0.5	2.3
03/98	1,488	229	0	0	0	0	3.5	1.1	3.0	93.3	2.8	-1.8	0.2	1.6	4.6	0.3	3.0	1.3
04/98																		
05/98																		

TABLE 5-4
STATISTICS OF CURRENT DATA FROM STATION ULM1

Date	Number of Data Points						Speed (cm/s)		Mean Current		North-South Component (cm/s)				West-East Component (cm/s)			
	Total	Good	Missing	Zeros	Outliers	Calm	Mean	St Dev	(cm/s)	(° from N)	Max	Min	Mean	St Dev	Max	Min	Mean	St Dev
09/94																		
10/94																		
11/94	7,200	0	0	907	0	0												
12/94	7,440	51	0	2,590	0	1	2.6	1.6	2.0	178.5	-0.4	-3.5	0.7	2.6	0.0	-0.1	-1.9	2.0
01/95	7,440	1,400	0	5,462	0	82	1.9	1.7	1.2	178.5	2.7	-3.6	1.9	1.7	0.2	-0.2	0.1	0.1
02/95	6,720	3,389	0	818	0	18	4.9	3.7	1.3	358.5	8.3	-3.8	3.3	3.1	5.3	-6.5	3.0	3.0
03/95	7,440	6,587	0	73	0	9	6.8	4.8	1.1	277.0	7.2	-6.3	4.4	4.0	8.1	-6.7	4.6	4.6
04/95	7,200	6,930	0	30	0	16	5.5	2.6	3.4	315.6	7.4	-3.2	3.8	4.8	8.3	-2.6	3.0	5.0
05/95	7,440	7,438	0	0	0	3	6.2	2.6	4.8	281.4	6.9	-6.0	3.0	5.3	10.2	-0.7	4.9	5.4
06/95	7,200	6,574	0	8	0	5	4.9	2.4	3.6	279.9	5.4	-4.8	2.3	5.9	8.4	-1.6	4.0	6.2
07/95	7,440	6,975	0	6	0	94	5.1	2.6	3.3	307.6	7.9	-4.0	3.1	6.2	8.3	-3.0	3.5	6.6
08/95	7,440	6,658	0	3	0	32	4.8	2.4	2.9	293.9	6.3	-2.9	2.4	6.6	7.1	-2.0	3.6	7.1
09/95	7,200	7,126	0	45	0	8	4.3	2.1	2.2	285.4	6.5	-4.4	2.4	6.7	7.0	-3.2	3.1	7.2
10/95	7,440	7,213	0	27	0	22	6.2	3.6	3.5	267.6	6.4	-6.0	3.6	7.5	9.1	-2.0	4.4	7.7
11/95	7,200	3,819	0	758	0	25	7.0	4.7	1.5	300.6	8.9	-6.2	5.5	11.1	7.1	-4.8	3.5	11.1
12/95	7,440	3,496	0	1,226	0	16	5.9	3.4	2.1	238.8	6.4	-7.4	4.1	12.0	8.2	-4.9	3.6	11.9
01/96	7,440	5,914	0	941	0	2	5.8	3.3	1.5	294.6	8.5	-5.2	4.0	3.3	6.4	-4.8	3.3	2.5
02/96	6,960	5,078	0	237	0	2	6.1	3.3	3.0	320.1	8.5	-3.9	4.6	4.7	7.2	-4.3	3.2	3.8
03/96	7,440	7,159	0	6	0	3	6.4	3.5	3.6	281.3	6.6	-6.1	3.9	5.0	9.9	-2.9	4.4	4.4
04/96	7,200	6,467	0	0	0	46	4.6	3.1	2.8	354.3	8.9	-3.1	4.6	6.1	0.9	-0.3	0.5	4.7
05/96	7,440	7,195	0	0	1	2	8.4	2.2	7.8	305.0	11.0	-0.9	4.6	6.2	11.8	-3.2	6.5	5.2
06/96	7,200	6,816	0	384	0	1	7.2	2.3	6.0	297.9	8.2	-3.3	3.5	6.8	10.8	-0.4	5.6	6.1
07/96	7,440	4,079	0	0	0	7	6.8	2.9	5.3	294.4	8.4	-4.8	3.0	9.0	10.4	-0.7	5.5	8.5

Tab5-1-6.xls ULM1 9/28/99 9 31 AM YCS

PBS&J

TABLE 5-4 (Concluded)
STATISTICS OF CURRENT DATA FROM STATION ULM1

Date	Number of Data Points						Speed (cm/s)		Mean Current		North-South Component (cm/s)				West-East Component (cm/s)			
	Total	Good	Missing	Zeros	Outliers	Calm	Mean	St Dev	(cm/s)	(° from N)	Max	Min	Mean	St Dev	Max	Min	Mean	St Dev
08/96																		
09/96																		
10/96																		
11/96																		
12/96																		
01/97	7,440	7,009	0	426	0	51	6.2	4.0	1.3	298.3	8.1	-6.1	4.3	3.5	8.1	-5.5	4.0	2.9
02/97	6,720	5,717	0	798	0	4	5.9	3.2	3.0	280.6	7.1	-6.0	3.3	4.7	8.8	-3.6	4.3	4.3
03/97																		
04/97																		
05/97																		
06/97																		
07/97																		
08/97																		
09/97																		
10/97																		
11/97																		
12/97	1,488	699	2	0	2	0	8.3	7.0	2.6	270.3	6.0	-6.0	4.7	4.2	10.4	-4.7	6.2	6.2
01/98	1,488	681	0	0	0	0	6.5	4.4	0.4	261.1	4.6	-4.8	3.3	2.9	8.9	-5.0	5.0	4.2
02/98	1,344	481	0	0	0	0	8.8	4.6	6.6	264.9	3.8	-6.9	3.8	4.6	14.5	-1.4	7.2	6.9
03/98	1,488	571	0	0	0	0	8.3	6.9	5.9	290.6	7.3	-4.3	4.2	5.6	12.8	-2.3	6.7	9.1
04/98	1,440	1,399	1	0	1	0	9.5	4.6	7.5	222.9	-0.5	-10.6	6.3	6.5	10.2	-0.6	5.7	6.6
05/98	1,488	347	0	0	0	0	17.4	4.4	16.3	191.3	-9.6	-22.6	16.1	13.8	9.3	-4.5	6.0	13.6

TABLE 5-5
STATISTICS OF CURRENT DATA FROM STATION ULM2

Date	Number of Data Points						Speed (cm/s)		Mean Current		North-South Component (cm/s)				West-East Component (cm/s)			
	Total	Good	Missing	Zeros	Outliers	Calm	Mean	St Dev	(cm/s)	(° from N)	Max	Min	Mean	St Dev	Max	Min	Mean	St Dev
09/94																		
10/94																		
11/94																		
12/94	7,440	0	0	2,316	0	0												
01/95	7,440	1	0	6,433	0	0	3 0		3 0	304 2			1 7				2 5	
02/95	6,720	3	0	6,396	0	0	3 1	1 4	1 9	23 5			3 5	1 4			1 6	1 6
03/95	7,440	3,706	0	2,338	0	68	2 8	2 7	0 7	202 8	4 3	-6 3	1 9	2 0	6 9	-5 9	1 6	2 2
04/95	7,200	4,807	0	1,442	0	247	3 9	2 4	0 3	92 2	7 7	-8 9	2 5	2 6	8 4	-9 2	2 5	2 9
05/95	7,440	4,767	0	2,410	0	206	2 5	2 2	0 1	242 4	6 5	-6 4	1 7	3 2	5 5	-5 1	1 4	3 3
06/95	7,200	5,892	0	550	0	44	2 6	1 8	1 0	222 8	3 6	-5 1	1 8	3 2	4 9	-3 0	1 6	3 3
07/95	7,440	7,440	0	0	0	5	2 2	1 3	0 1	90 1	3 4	-4 4	1 7	3 1	3 3	-2 8	1 2	3 1
08/95	7,440	7,375	0	0	0	4	2 3	1 5	0 8	253 5	3 2	-3 6	1 4	3 3	5 2	-3 1	1 7	3 4
09/95	7,200	6,609	0	99	0	101	2 0	1 5	0 9	239 3	2 5	-4 1	1 3	3 6	5 2	-2 9	1 4	3 8
10/95	7,440	5,678	0	310	0	27	2 6	1 9	1 3	229 9	2 0	-4 1	1 9	4 2	5 2	-2 2	1 6	4 3
11/95	7,200	4,800	0	0	0	5	2 1	1 5	0 4	243 9	3 1	-3 4	1 6	4 7	4 0	-2 6	1 3	4 8
12/95	7,440	6,440	0	269	0	8	2 0	1 2	0 4	242 9	2 5	-3 2	1 4	4 1	3 5	-2 4	1 2	4 3
01/96	7,440	6,078	0	110	0	221	2 1	1 8	0 7	233 8	2 9	-4 0	1 6	1 5	3 7	-2 5	1 1	1 3
02/96	6,960	6,223	0	0	0	4	2 6	1 9	0 7	270 8	4 1	-4 3	2 1	2 2	4 8	-2 4	1 3	1 8
03/96	7,440	7,187	0	3	0	3	3 0	1 9	1 2	229 8	3 1	-5 1	2 2	2 7	4 9	-2 7	1 7	2 2
04/96	7,200	7,049	0	0	0	3	3 0	1 8	0 5	276 0	4 8	-4 5	2 4	3 2	4 9	-3 3	1 5	2 5
05/96	7,440	7,440	0	0	0	4	2 7	1 4	0 1	153 6	4 7	-4 5	2 1	3 3	3 9	-3 8	1 4	2 7
06/96	7,200	7,200	0	0	0	10	2 4	1 3	0 3	170 1	3 8	-4 9	1 9	3 6	3 2	-3 5	1 2	2 9
07/96	7,440	7,438	0	0	0	8	2 5	1 3	0 2	151 3	4 1	-5 5	2 1	3 7	2 9	-3 3	1 0	3 0

Tab5-1-6.xls ULM2 9/28/99 9 31 AM YCS

PBS&J

TABLE 5-5 (Concluded)
STATISTICS OF CURRENT DATA FROM STATION ULM2

Date	Number of Data Points						Speed (cm/s)		Mean Current		North-South Component (cm/s)				West-East Component (cm/s)			
	Total	Good	Missing	Zeros	Outliers	Calm	Mean	St Dev	(cm/s)	(° from N)	Max	Min	Mean	St Dev	Max	Min	Mean	St Dev
08/96	7,440	7,440	0	0	0	7	2.3	1.4	0.5	202.8	3.7	-4.9	1.9	3.9	3.5	-3.5	1.2	3.2
09/96	7,200	7,197	0	0	0	9	2.5	1.5	0.3	16.3	4.8	-4.9	2.0	4.2	4.2	-3.5	1.3	3.4
10/96	7,440	7,440	0	0	0	13	3.1	2.1	0.5	257.5	4.1	-4.3	2.1	4.5	5.3	-3.9	2.0	3.7
11/96	7,200	7,180	0	0	0	3	3.0	1.7	0.6	224.3	4.1	-4.7	2.2	4.9	4.8	-3.7	1.7	4.0
12/96	7,440	6,233	0	450	0	20	2.6	1.7	0.6	229.8	4.1	-4.2	1.9	5.4	4.8	-3.4	1.4	4.5
01/97	7,440	7,403	0	37	0	24	3.5	2.6	1.3	222.0	4.6	-7.0	2.8	2.2	6.2	-3.8	1.8	1.7
02/97	6,720	6,668	0	52	0	24	3.7	2.4	2.0	225.9	3.3	-6.3	2.5	3.0	6.8	-3.9	2.4	2.7
03/97																		
04/97																		
05/97																		
06/97																		
07/97																		
08/97																		
09/97																		
10/97																		
11/97	1,440	816	2	0	2	0	3.2	2.1	1.4	281.6	2.7	-2.1	0.9	0.9	5.9	-3.1	2.8	2.2
12/97	1,488	405	0	0	0	0	3.3	1.7	1.3	275.3	2.2	-2.5	0.8	1.4	5.5	-3.1	3.0	3.6
01/98	1,488	514	6	0	1	0	6.3	9.7	3.8	162.9	-1.7	-9.3	4.9	9.3	1.8	-5.7	3.2	3.6
02/98																		
03/98	1,488	1,055	0	0	0	0	4.7	2.4	2.9	87.0	5.4	-5.7	2.9	3.6	7.0	-0.4	3.0	6.8
04/98	1,440	320	0	0	0	0	3.5	1.3	2.6	70.2	1.9	-4.5	1.7	6.7	5.1	-0.8	2.6	12.3
05/98																		

TABLE 5-6
STATISTICS OF CURRENT DATA FROM STATION ULM3

Date	Number of Data Points						Speed (cm/s)		Mean Current		North-South Component (cm/s)				West-East Component (cm/s)			
	Total	Good	Missing	Zeros	Outliers	Calm	Mean	St Dev	(cm/s)	(° from N)	Max	Min	Mean	St Dev	Max	Min	Mean	St Dev
09/94																		
10/94																		
11/94																		
12/94	7,440	5	0	2,673	0	0	10	07	04	112.8	-0.4	-0.8	0.9	0.5	-0.1	-0.3	0.4	0.4
01/95	7,440	5	0	7,431	0	0	13.0	17.3	9.7	236.8	-5.6	-6.6	7.4	6.5	-0.9	-2.4	9.8	16.8
02/95	6,720	4,140	2,564	16	0	70	0.5	0.5	0.1	354.8	0.9	-1.2	0.3	0.4	2.5	-1.0	0.3	0.7
03/95	7,440	4,089	9	0	13	1	5.1	5.2	1.2	228.4	9.2	-13.5	3.7	3.7	18.3	-9.2	2.6	4.4
04/95	7,200	777	0	1,239	0	46	1.1	2.1	0.2	321.1	1.7	-3.9	0.8	8.6	3.2	-1.5	0.6	10.1
05/95	7,440	6,497	246	0	0	4	4.8	3.4	1.9	28.0	10.3	-6.1	4.2	4.6	3.5	-5.7	1.8	3.8
06/95	7,200	7,124	4	0	0	3	4.0	2.7	2.3	15.5	9.3	-3.5	3.5	5.2	2.6	-4.0	1.2	3.7
07/95	7,440	7,051	0	30	0	6	4.7	3.2	2.6	29.9	9.5	-4.7	4.0	6.3	2.6	-6.1	1.7	4.0
08/95	7,440	7,376	3	0	2	4	4.0	3.3	2.3	16.3	11.6	-4.6	3.5	7.0	3.0	-5.1	1.2	4.1
09/95	7,200	6,338	185	23	0	50	3.4	2.3	1.6	9.5	8.0	-5.2	3.1	7.9	3.8	-3.4	1.0	4.5
10/95	7,440	6,087	0	16	0	58	3.6	2.5	1.4	27.1	8.2	-5.6	3.1	8.5	2.3	-4.2	1.2	4.7
11/95	7,200	7,197	1	0	0	2	3.9	2.8	1.4	3.9	9.4	-5.9	3.5	8.3	3.4	-4.3	1.3	4.5
12/95																		
01/96	7,440	7,356	0	75	0	18	3.6	2.8	0.1	92.3	7.4	-7.2	3.2	2.8	3.4	-4.1	1.3	1.1
02/96	6,960	6,286	0	0	0	2	4.0	2.7	0.9	9.1	8.6	-6.2	3.5	4.1	3.5	-4.5	1.3	1.7
03/96	7,440	7,343	0	0	0	2	4.5	3.1	1.3	23.9	10.2	-6.4	4.0	5.0	3.5	-5.6	1.4	2.0
04/96	7,200	7,032	0	0	0	12	4.6	3.0	1.7	28.7	10.6	-7.1	3.9	5.9	5.2	-5.5	1.7	2.5
05/96	7,440	6,953	1	0	0	1	3.6	2.4	1.4	54.0	8.8	-5.8	2.9	6.5	2.7	-5.5	1.6	2.7
06/96	7,200	6,856	0	0	0	1	3.8	2.3	0.8	64.9	8.1	-7.0	3.3	7.0	2.9	-5.0	1.4	3.0
07/96	7,440	7,427	0	0	0	10	3.7	2.3	1.4	40.4	8.8	-5.2	3.1	7.1	2.9	-5.0	1.5	3.0

Tab5-1-6.xls ULM3 9/28/99 9 31 AM YCS

PBS&J

TABLE 5-6 (Concluded)
STATISTICS OF CURRENT DATA FROM STATION ULM3

Date	Number of Data Points						Speed (cm/s)		Mean Current		North-South Component (cm/s)				West-East Component (cm/s)			
	Total	Good	Missing	Zeros	Outliers	Calm	Mean	St Dev	(cm/s)	(° from N)	Max	Min	Mean	St Dev.	Max	Min	Mean	St Dev.
08/96	7,440	1	0	0	0	0	1.8		1.8	59.0			4.0				3.0	
09/96	7,200	6,839	13	0	0	0	6.9	4.2	5.5	11.8	15.2	-4.5	6.5	8.6	4.5	-5.8	1.8	3.5
10/96	7,440	6,502	0	934	0	14	6.1	4.4	4.6	14.0	13.2	-4.5	5.6	9.8	2.8	-6.0	1.9	4.0
11/96	7,200	3,434	2	0	0	0	5.8	3.5	3.4	20.2	10.9	-4.9	5.2	14.1	3.0	-4.5	1.7	5.7
12/96	7,440	1,769	0	3	0	7	4.9	3.4	2.8	19.3	7.4	-5.0	4.4	19.9	2.1	-3.5	1.5	8.0
01/97	7,440	7,393	0	3	0	3	5.8	4.7	3.3	18.6	12.3	-6.7	5.1	4.8	3.7	-5.7	2.1	1.7
02/97	6,720	6,668	0	52	0	24	3.7	2.4	2.0	225.9	3.3	-6.3	2.5	5.3	6.8	-3.9	2.4	2.7
03/97																		
04/97																		
05/97																		
06/97																		
07/97																		
08/97																		
09/97																		
10/97																		
11/97																		
12/97	1,488	594	2	0	2	0	5.0	1.9	3.7	88.4	4.4	-4.9	2.7	2.4	6.2	1.1	3.7	1.3
01/98	1,488	1,178	0	0	0	0	4.7	2.5	3.0	87.9	7.4	-5.0	3.0	2.8	6.1	0.4	3.1	1.5
02/98	1,344	1,104	2	0	2	0	6.2	3.1	4.7	114.7	9.7	-3.7	3.8	4.4	7.8	1.2	4.3	2.5
03/98	1,488	425	0	0	0	0	5.9	2.7	4.2	108.0	8.5	-5.2	3.6	7.8	7.0	0.8	4.0	4.4
04/98																		
05/98																		

The current is a three-dimensional vector quantity, and is measured by separate determinations of the component currents along three mutually perpendicular axes, north-south, west-east and vertical. The vertical component, if averaged sufficiently to remove the instantaneous effects of waves, is generally very small compared to the horizontal components, and difficult to measure accurately. The instrument packages which re-equipped the platforms during the Data Set IV period excluded direct measurement of vertical component, but substituted the measurement of pressure (which can be converted into water level, a variable that was not included in the instrument package for Data Sets I - III).

The vertical components for Data Sets I-III, as measured by these current meter arrays, proved to be on the same order of magnitude as the horizontal currents. Moreover, when averaged over an extended length of time (several hours or more), the mean of the vertical component was found to differ substantially from zero. These two facts raise much suspicion in our mind as to the validity of the vertical component measurement. For this reason, little analysis was carried out of this component, and none is presented here. Instead, we focus on the more important components, the horizontal.

The raw current meter measurements are displayed graphically in two ways, as time plots and as vector scatter plots, and statistics of currents are displayed as roses and, in the following section, as spectra. The time plots of component currents are the most complete display format, but also the most difficult to interpret. Plots of the north-south (u) and west-east (v) components of current are presented in Appendix TP, with positive values indicating flow towards the north and west, respectively. The reader is cautioned that this convention is a departure from the normal convention of designating u as positive east and v as positive north. This convention was initiated by the Year-1 work (Brown and Kraus, 1997, Militello and Kraus, 1994) preserving the measurement convention employed for the platforms, and we have elected not to change it. (This convention is also observed in the component statistics of tables 5-1 *et seq*.)

As noted above, the individual components do not communicate the vector character of the current (hence examples are not shown in this report but are relegated to Appendix TP). Current roses and monthly scatter plots better display the vector character of current behavior. Current roses attempt to display the statistical distributions of current vector by speed and direction on some sort of north-oriented polar diagram. There are numerous formats in the oceanographic literature for current roses, none of which is completely satisfactory (which is why there are so many). The current roses constructed for this study are based on sorting the data into 45° bins centered on the principal compass directions, and 3 cm/s bins by speed, then displaying the relative proportion (as a percent) by colored isopleths on a polar plot, analogous in appearance to the wind roses of figures 4-1 through 4-4.

Current roses for all of the available data collected by years are displayed, station by station, in figures 5-1 through 5-6. These are referred to as "annual" current roses for brevity, but for most years at most stations the extant data do not uniformly represent the indicated year. In inspecting these graphs, the reader should look for several features. First, the degree of rotational symmetry should be assessed. Some stations show a prominence of one or more directions. Station LLM1, for example, exhibits a generally bi-directional current, primarily along a N-S axis, with some year-to-year variation. A similar bi-directionality is evidenced for LLM2a/2N (Figure 5-2), see 1996. In contrast, Station ULM1 shows a preferential direction to the west, see 1995 (Figure 5-4), with little compensating flow to the east. This is diagnostic of a significant average net current to the west. Second, the distribution of color is a direct indicator of typical current speeds. Those roses with a prevalence of yellows and oranges indicate generally higher current speeds than those with a prevalence of blues. Compare, for example, the 1996 current rose at LLM1 (Figure 5-1) with its yellow and orange coloration, with the 1995 and 1996 roses at ULM2 (Figure 5-5) dominated by blues. One would infer more higher speed currents at the former than at the latter. Third, the symmetry of coloration in these roses is important as well. The 1996 rose at LLM1 (Figure 5-1) is symmetric with respect to coloration in both directions, while the same rose at LLM2a (Figure 5-2) shows more yellow and orange to the N and more blue to the S. Thus, at the latter there is an asymmetry in speed, with currents to the north generally being higher than those to the south. Fourth, some current roses indicate more than one favorable axis of current movement, such as 1998 LLM2N (Figure 5-2), a feature that will prove to be even more important when examined on a monthly basis.

Monthly scatter plots are constructed by plotting data points representing the head of the horizontal current vector. (There is little point in producing a display like this on an annual basis, since there would be over 50,000 data points on a single graph.) This type of display indicates the range in speeds, and the prevalence of direction. But the reader is cautioned that interpretation of such a display is biased toward the higher magnitude measurements in the data record. The lower speed measurements cluster around the origin of the display, and are densely overplotted, so it is impossible to infer any sense of relative frequency from such a diagram (at least, when the high frequency measurement scheme of Data Sets I - III is involved). A selection of example scatterplots are shown as figures 5-7 through 5-17. Here the dashed line indicates the orientation of the GIWW near the platform location. (Of course, some of the platforms, such as LLM2a, are located a considerable distance from the GIWW.) The complete set of scatterplots of the current at all stations for individual months are presented in Appendix CS. The corresponding current roses (i.e., for the same selection of stations and months) are shown in figures 5-18 through 5-28. Current roses by month for all stations for the entire study period September 1994 through June 1998 are provided in Appendix CR.

**FIGURE 5-1
ANNUAL CURRENT ROSE AT LLM1 STATION**

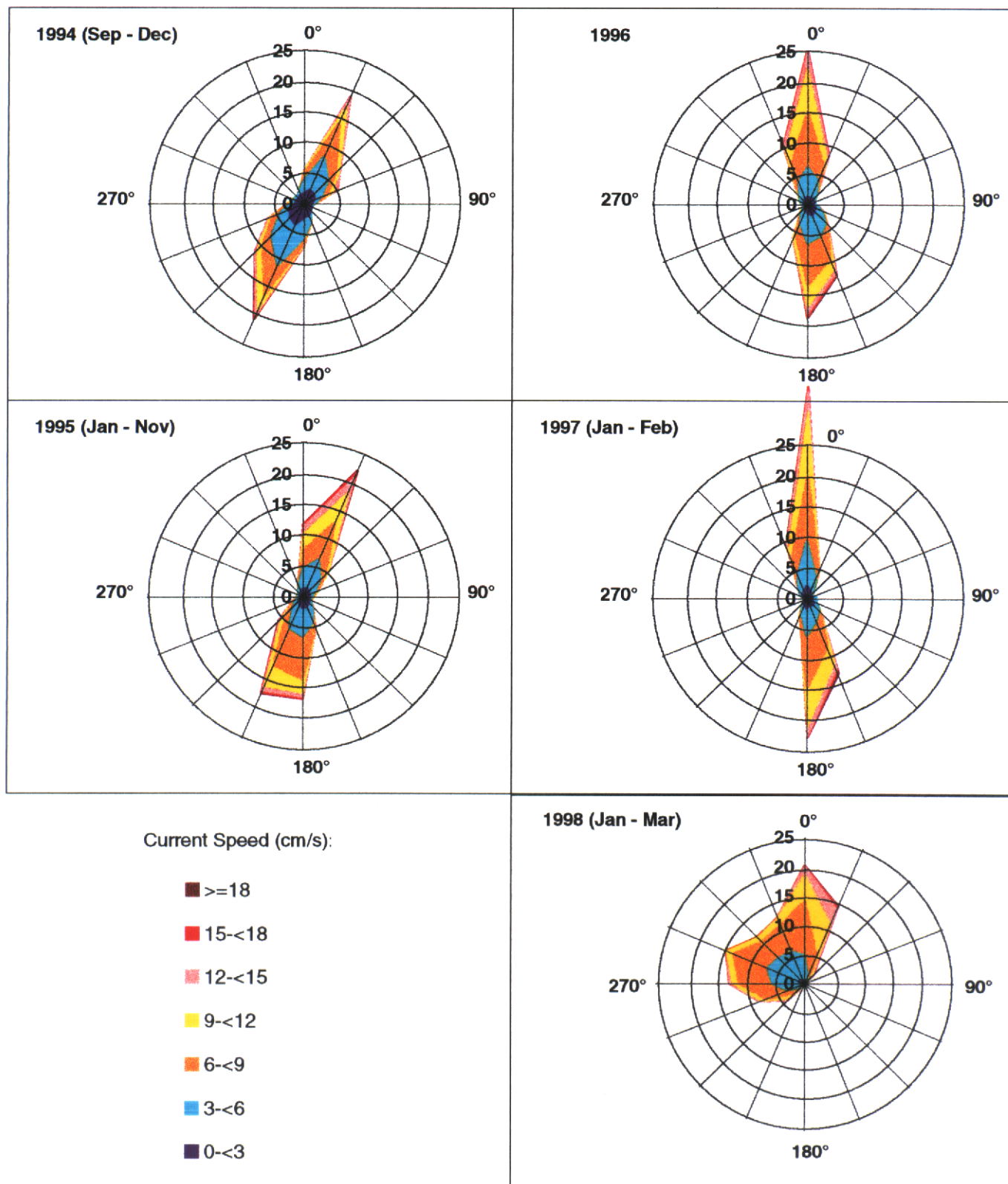


**FIGURE 5-2
ANNUAL CURRENT ROSE AT LLM2a/N STATION**

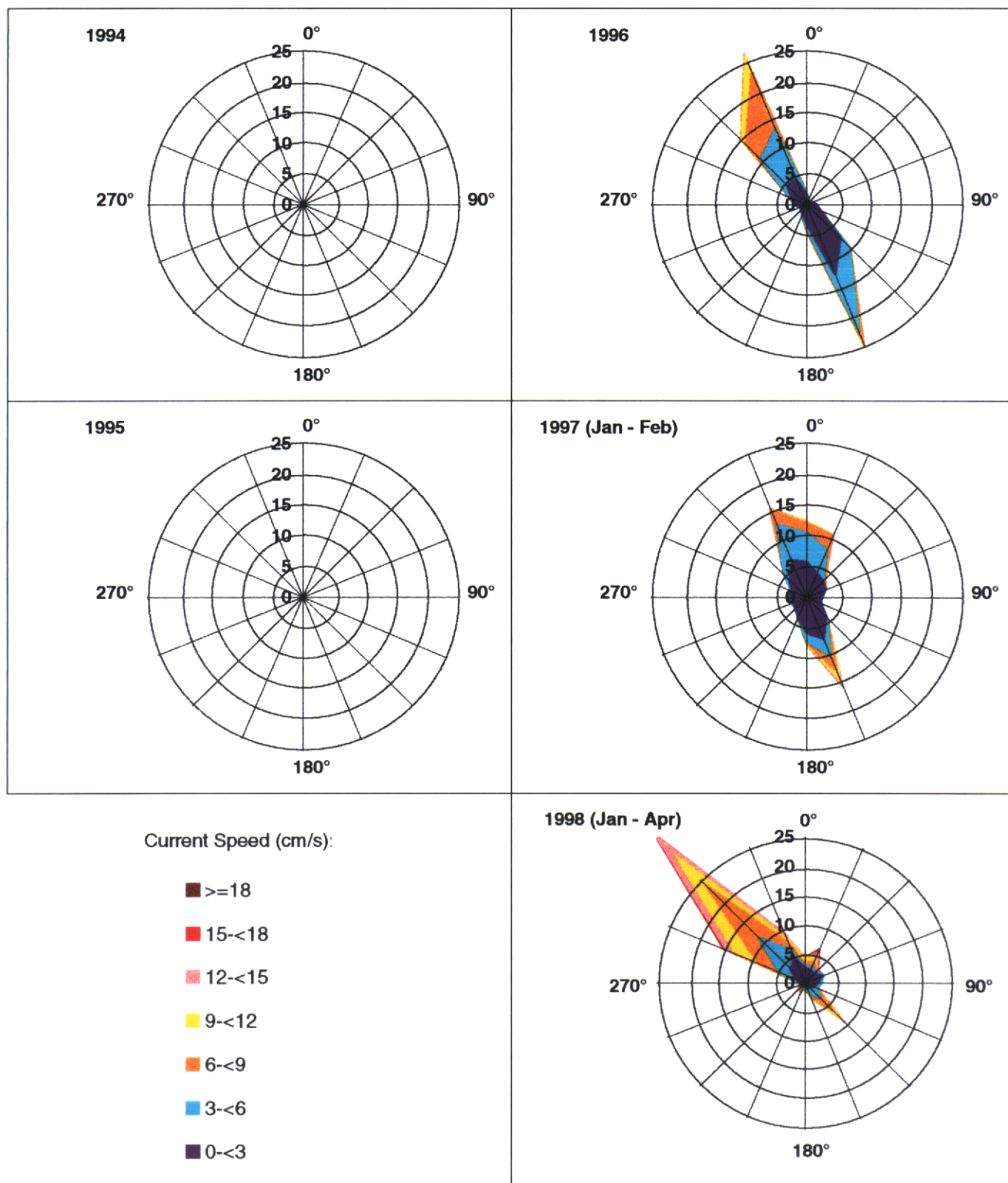


**FIGURE 5-3
ANNUAL CURRENT ROSE AT LLM3N STATION**

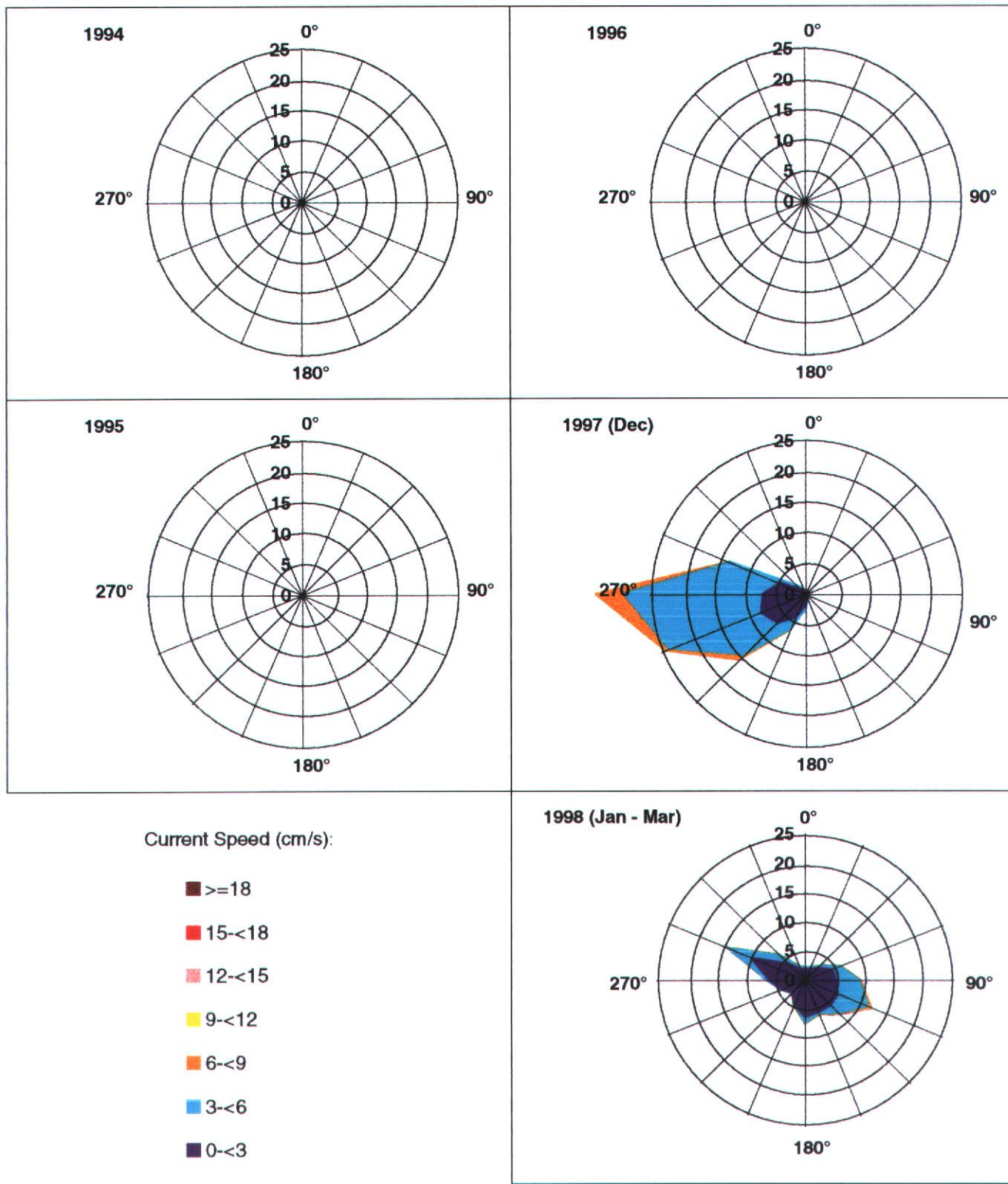


**FIGURE 5-4
ANNUAL CURRENT ROSE AT ULM1 STATION**

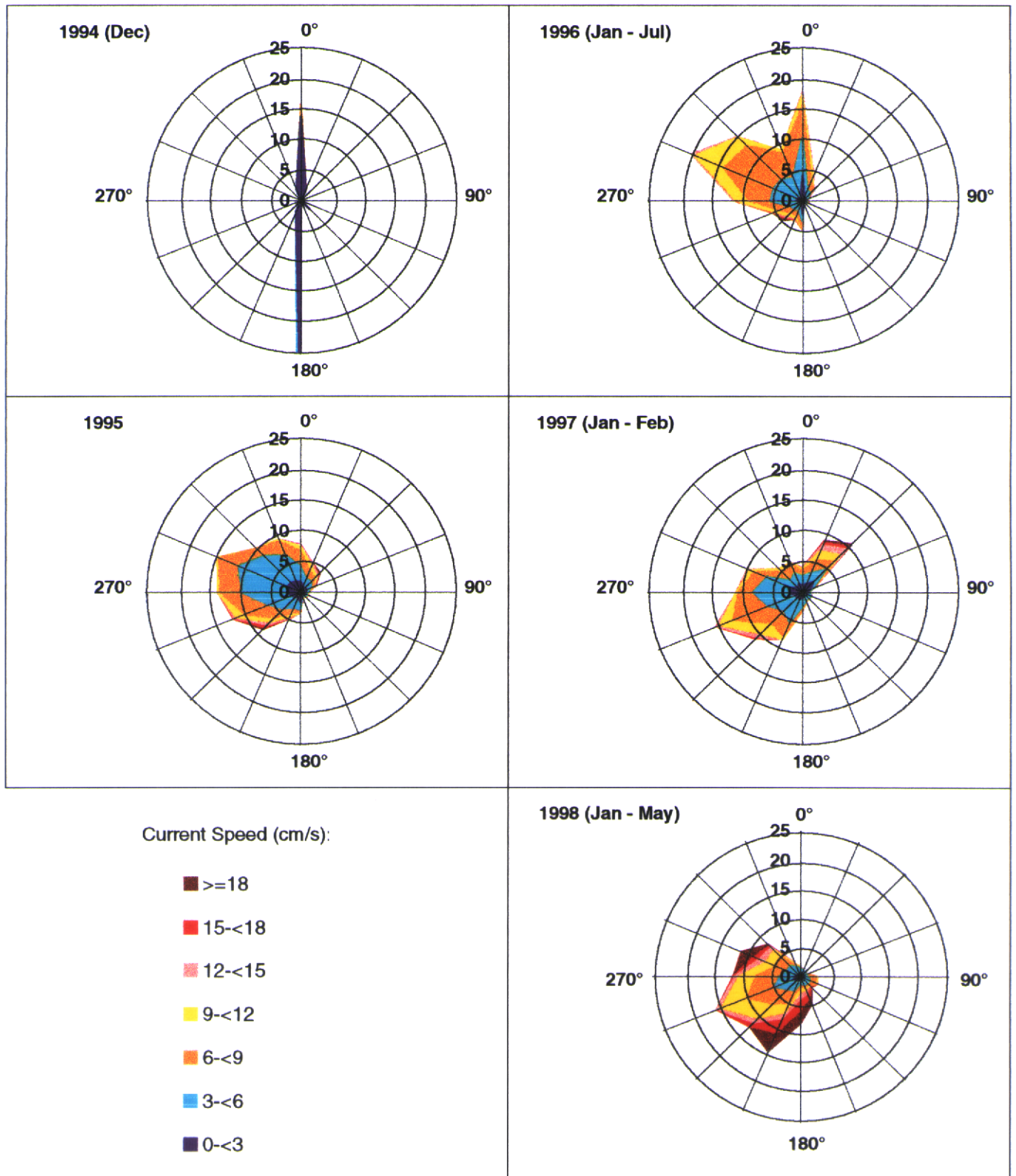


**FIGURE 5-5
ANNUAL CURRENT ROSE AT ULM2 STATION**

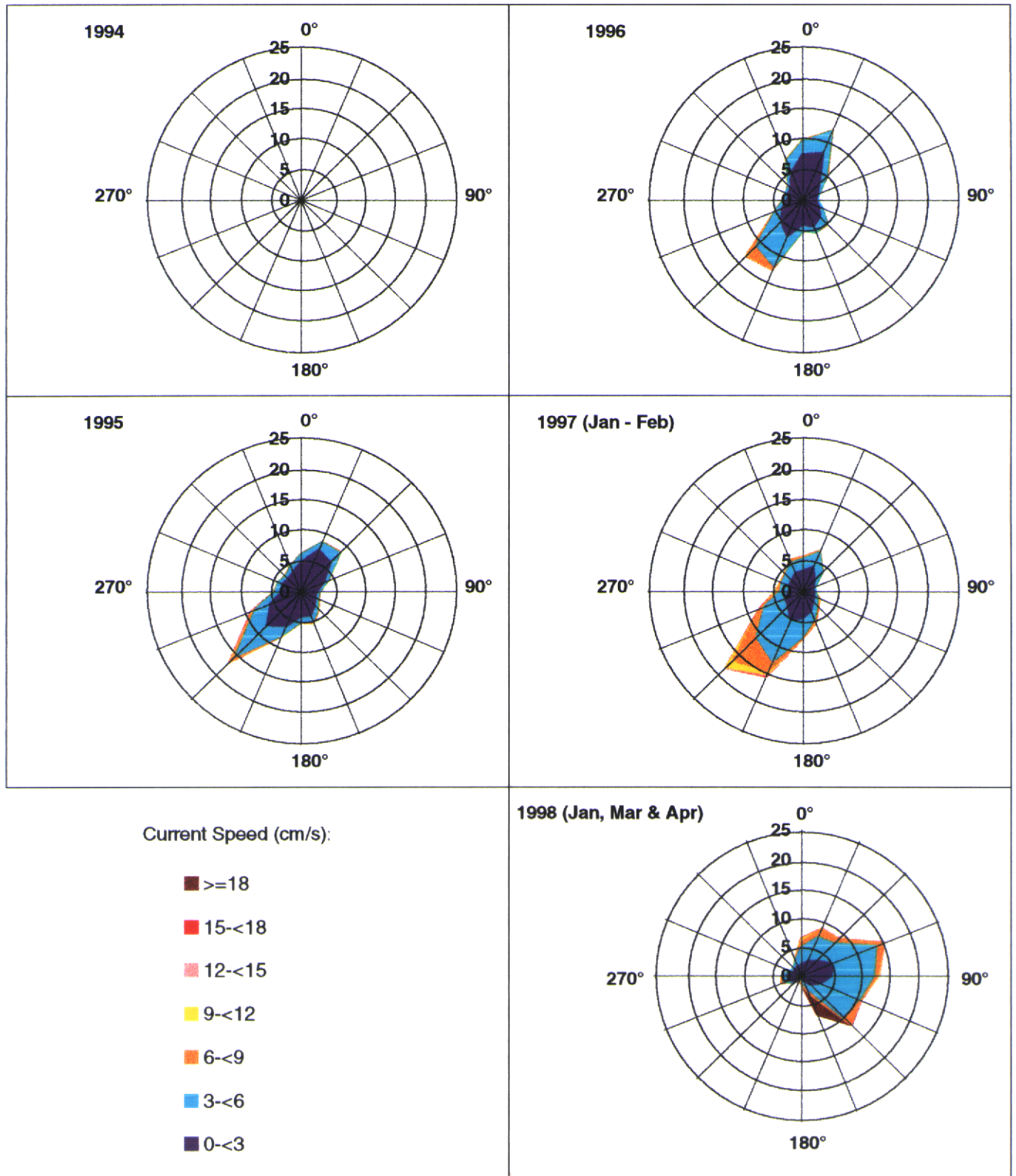


**FIGURE 5-6
ANNUAL CURRENT ROSE AT ULM3 STATION**

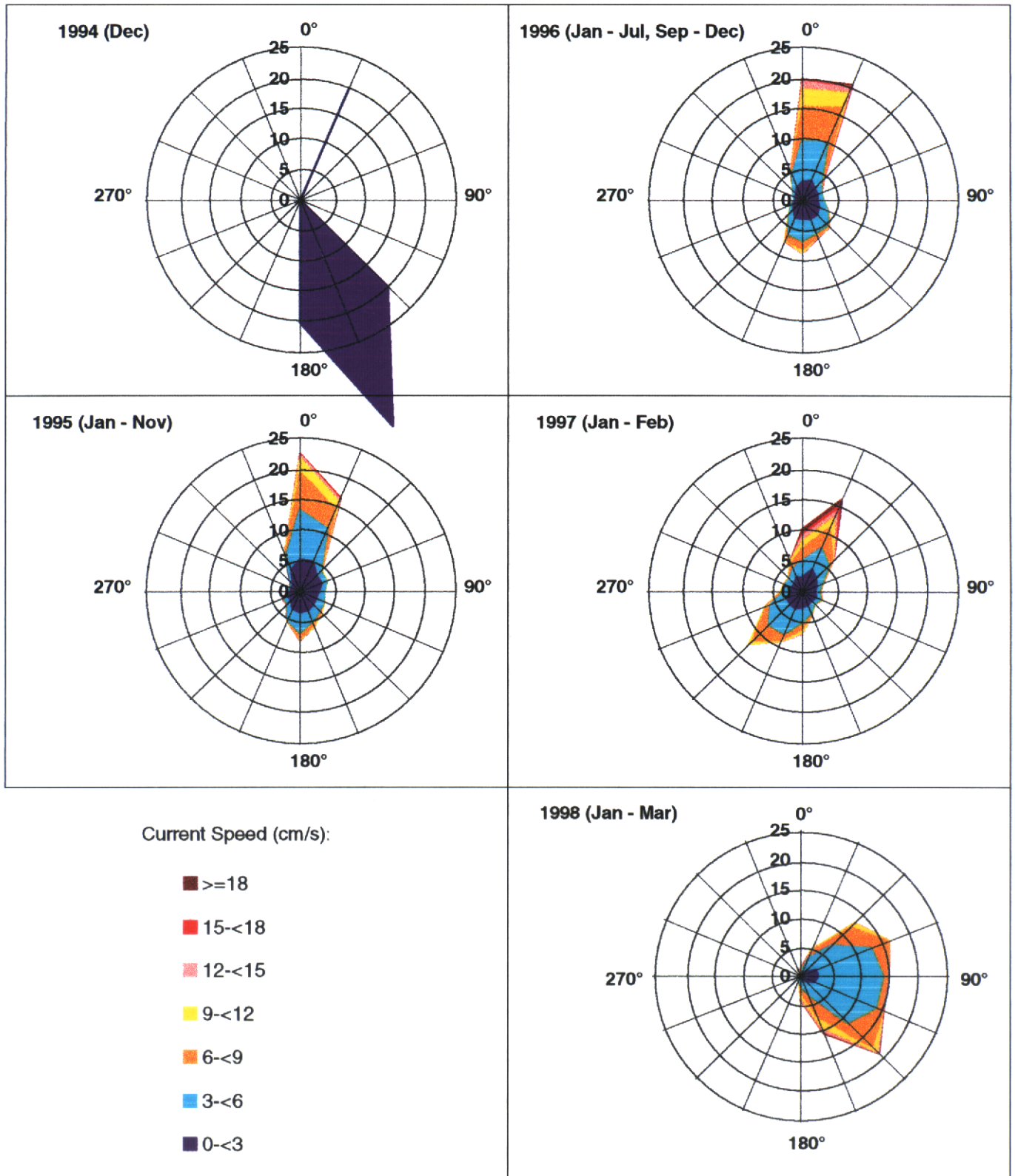


FIGURE 5-7
SCATTER PLOTS OF CURRENTS AT STATION LLM1

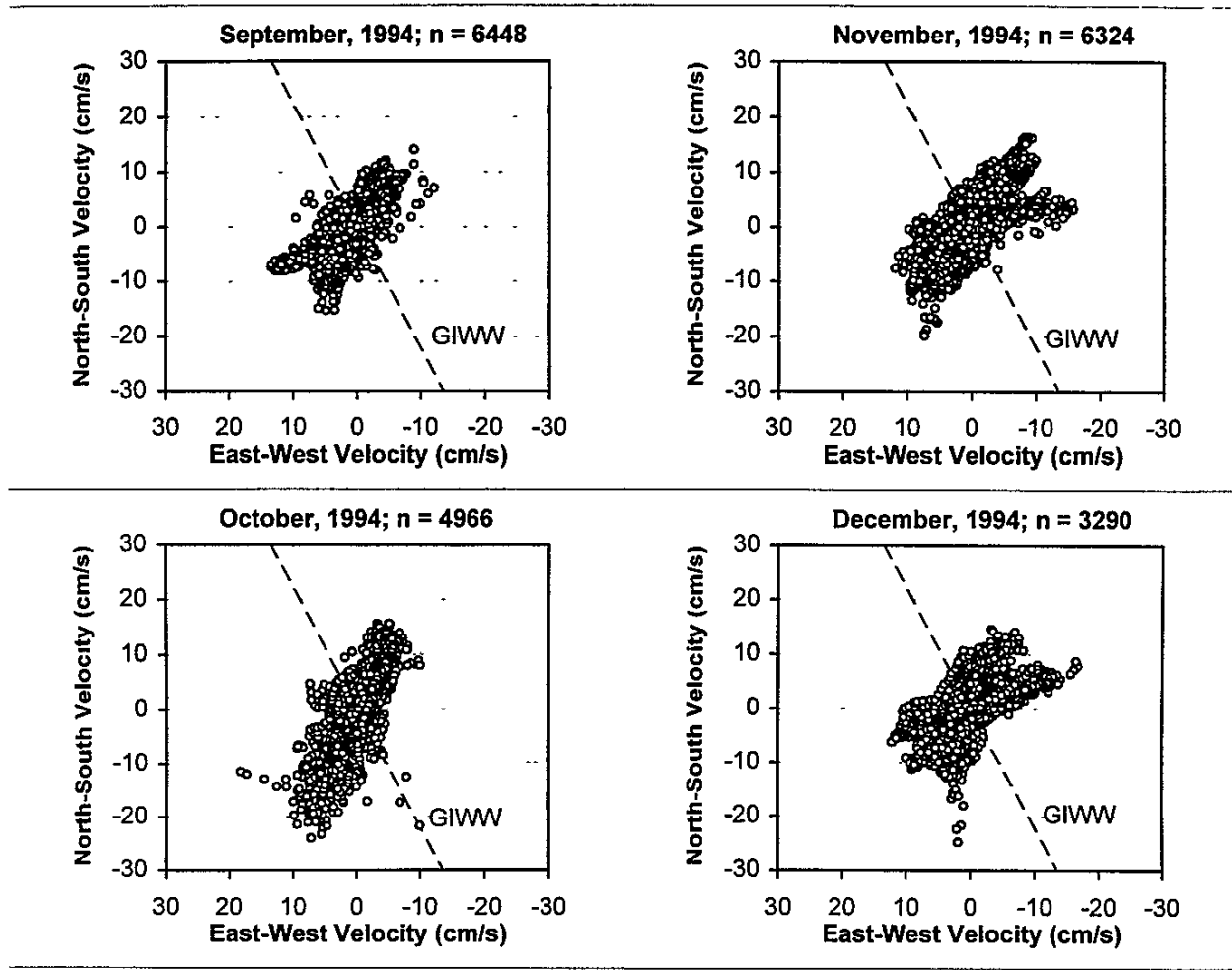


FIGURE 5-8
SCATTER PLOTS OF CURRENTS AT STATION LLM1

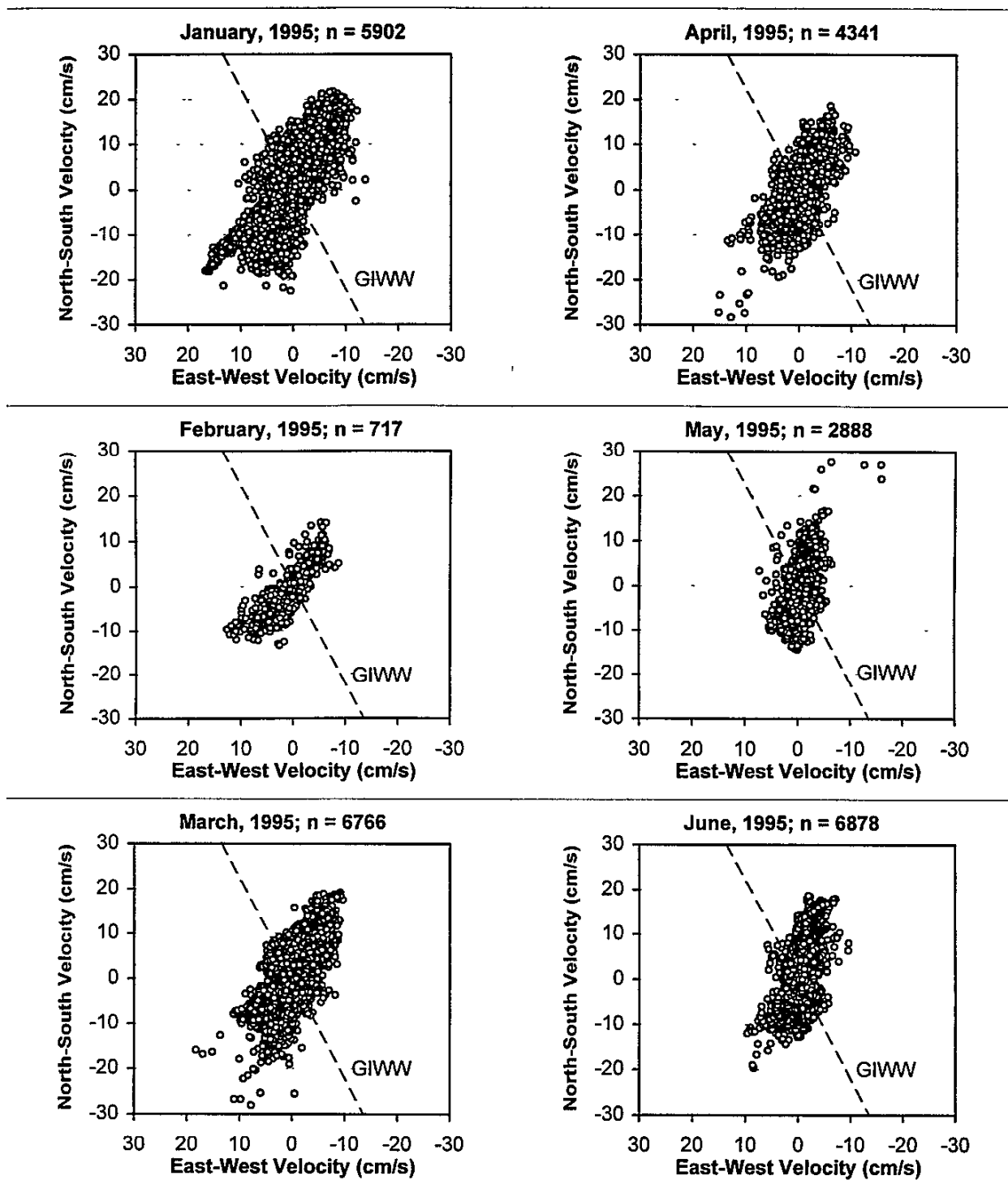


FIGURE 5-9
SCATTER PLOTS OF CURRENTS AT STATION LLM1

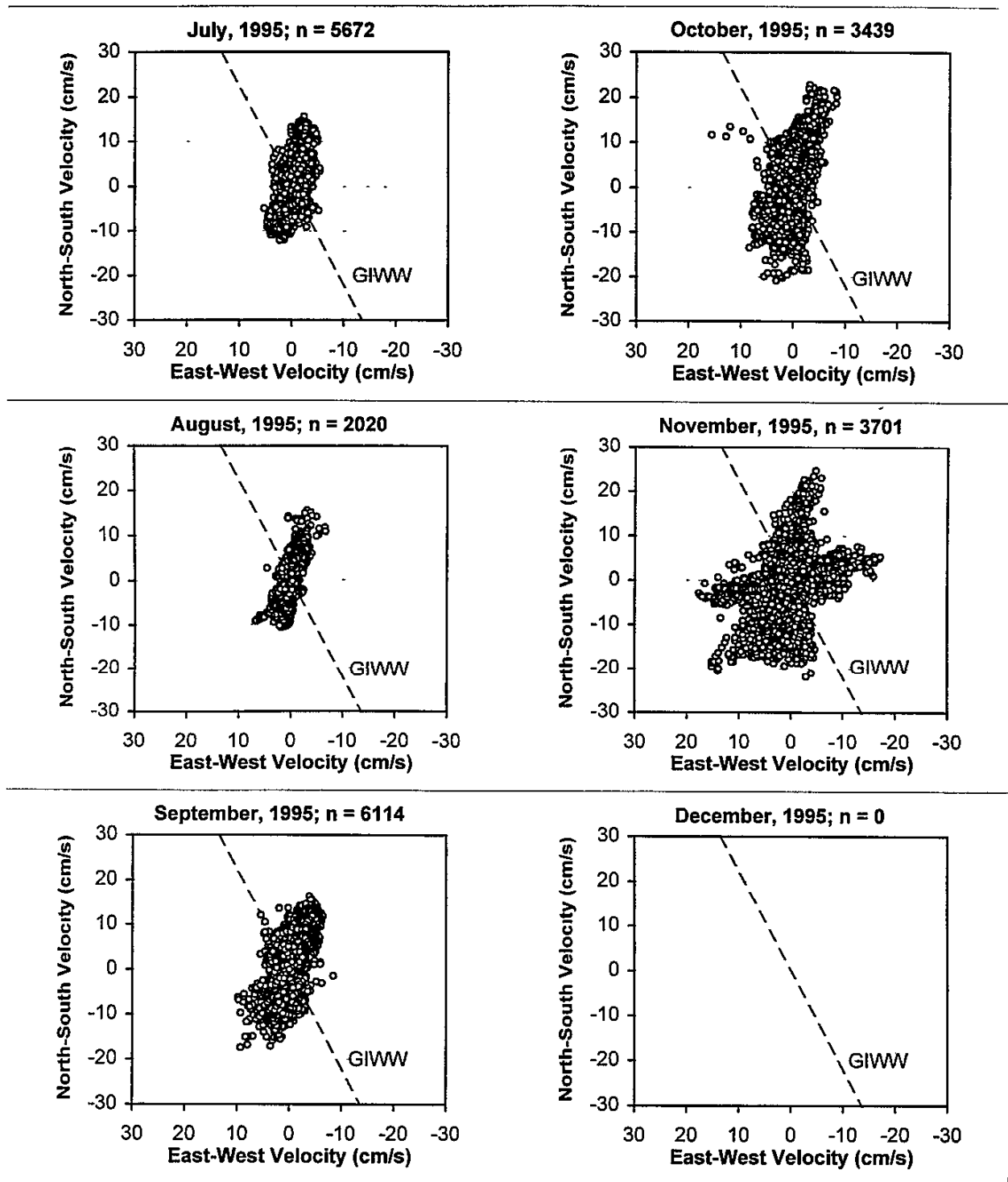


FIGURE 5-10
SCATTER PLOTS OF CURRENTS AT STATION LLM1

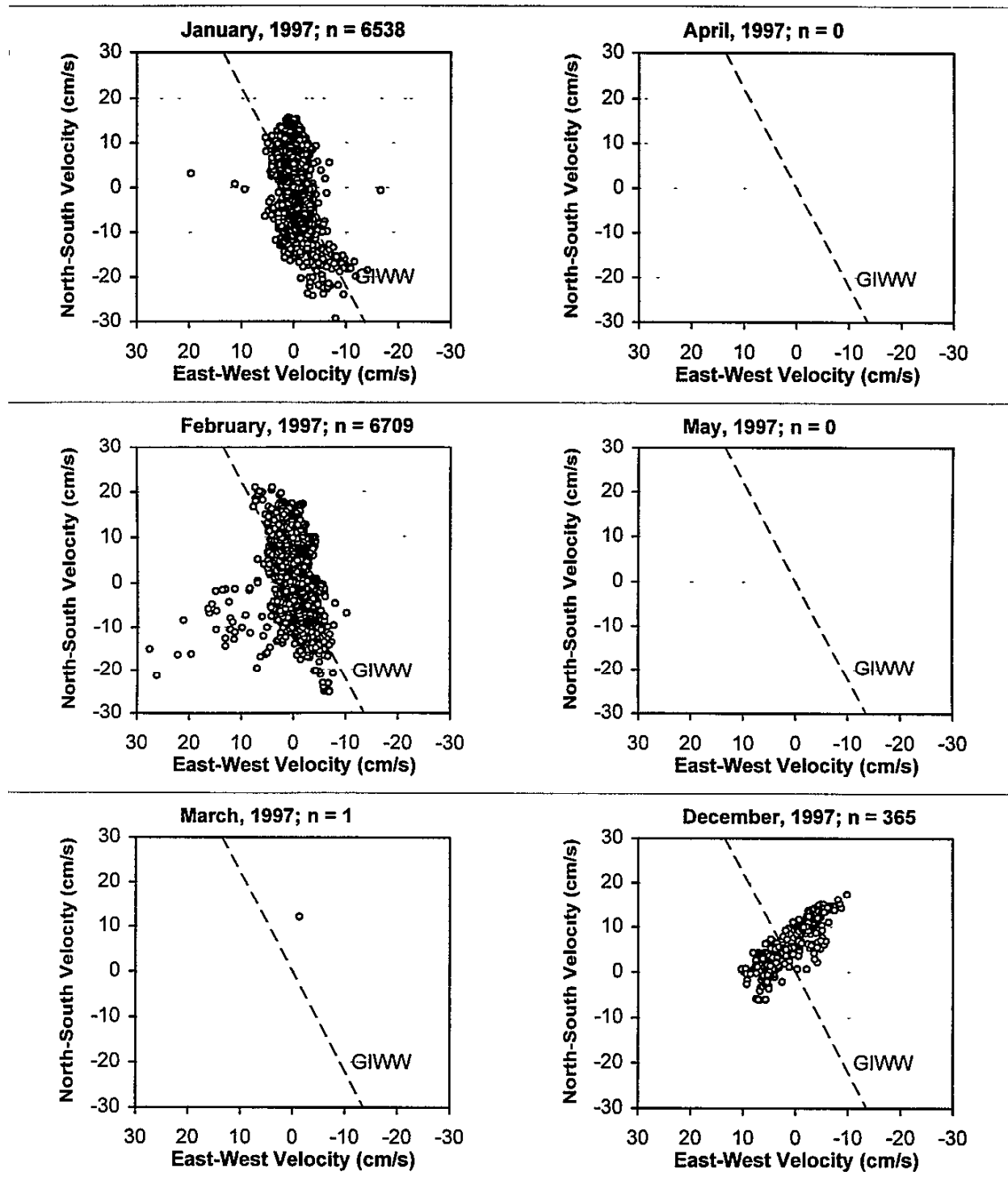


FIGURE 5-11
SCATTER PLOTS OF CURRENTS AT STATION LLM2a/N

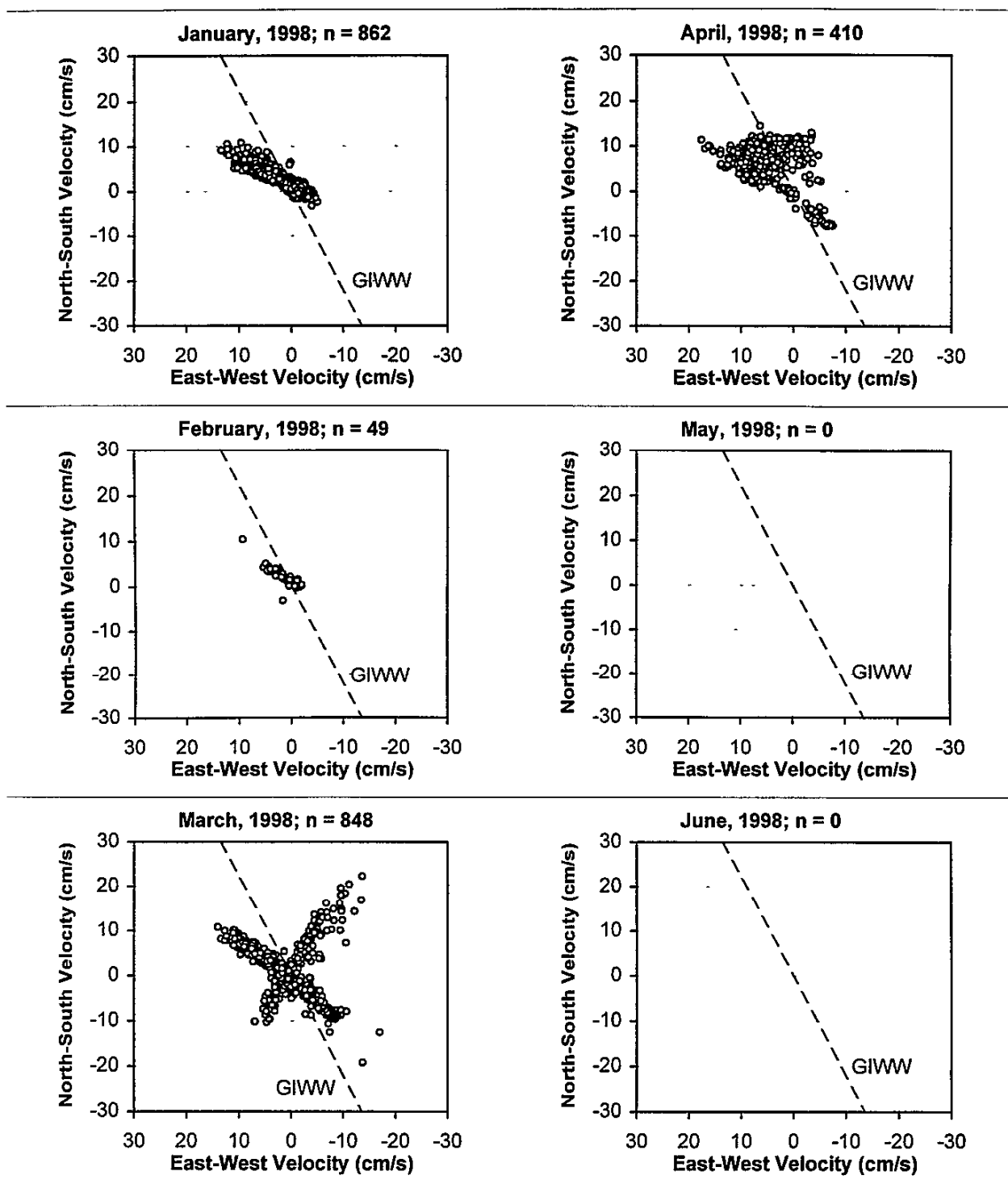


FIGURE 5-12
SCATTER PLOTS OF CURRENTS AT STATION ULM1

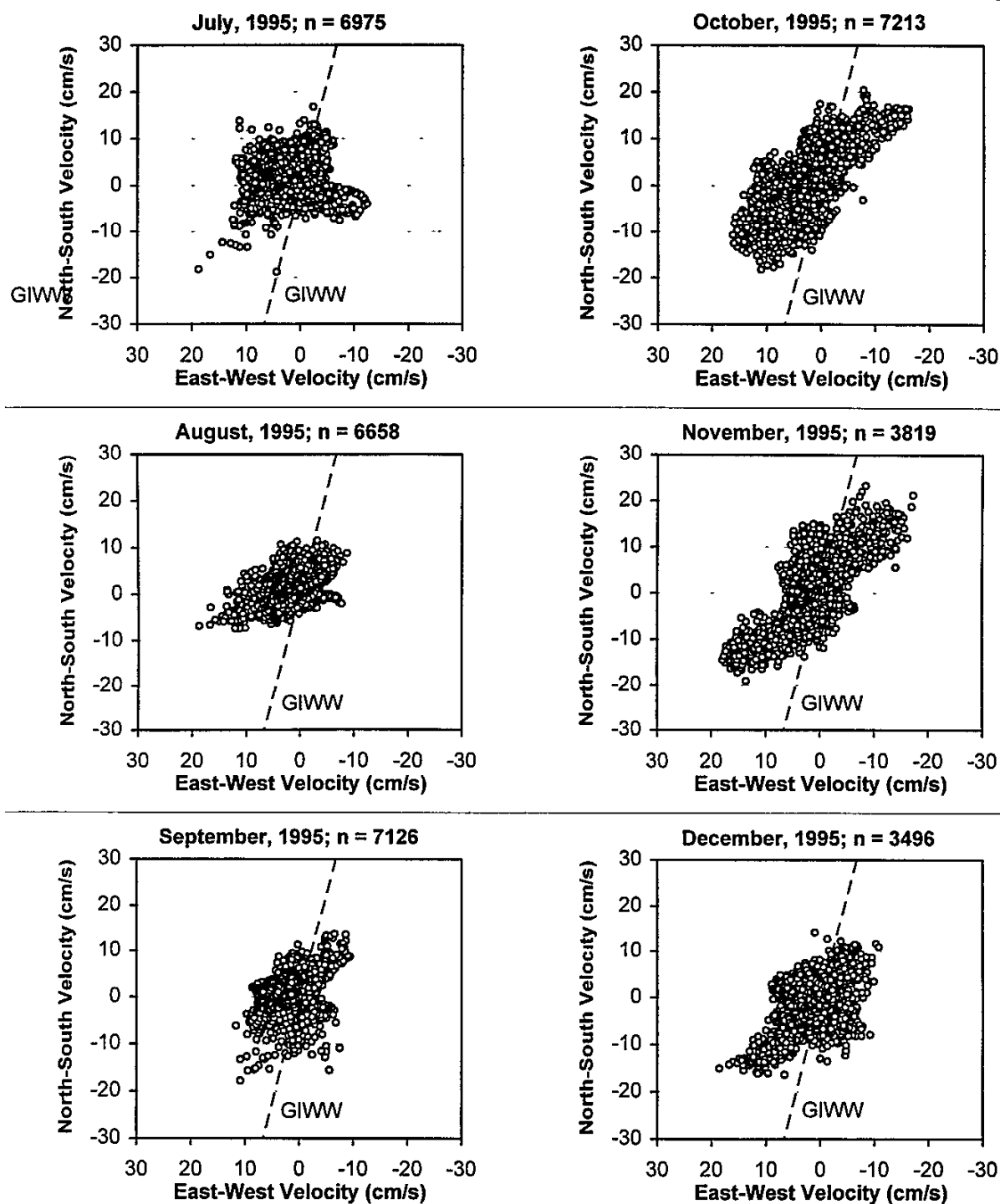


FIGURE 5-13
SCATTER PLOTS OF CURRENTS AT STATION ULM1

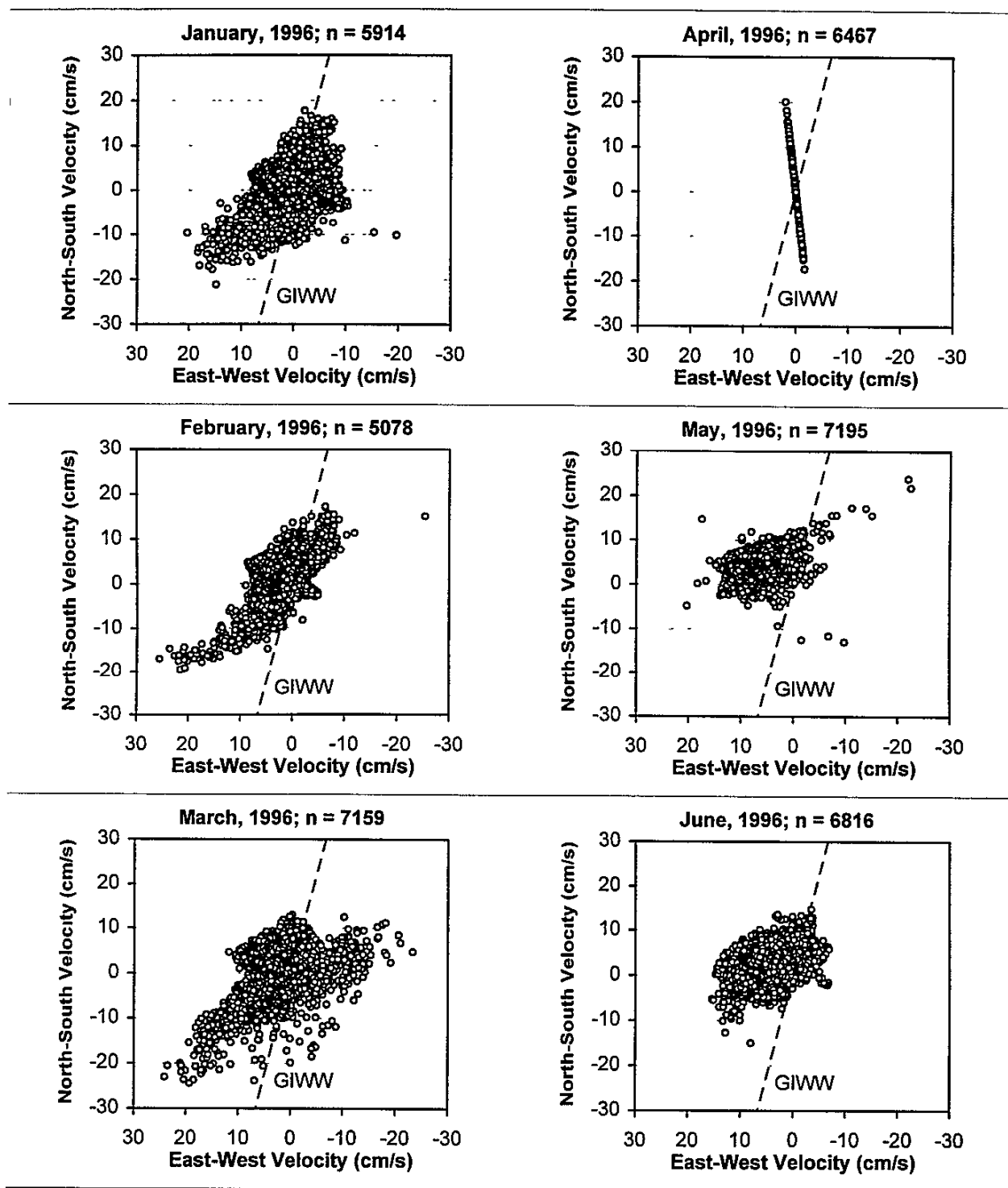


FIGURE 5-14
SCATTER PLOTS OF CURRENTS AT STATION ULM1

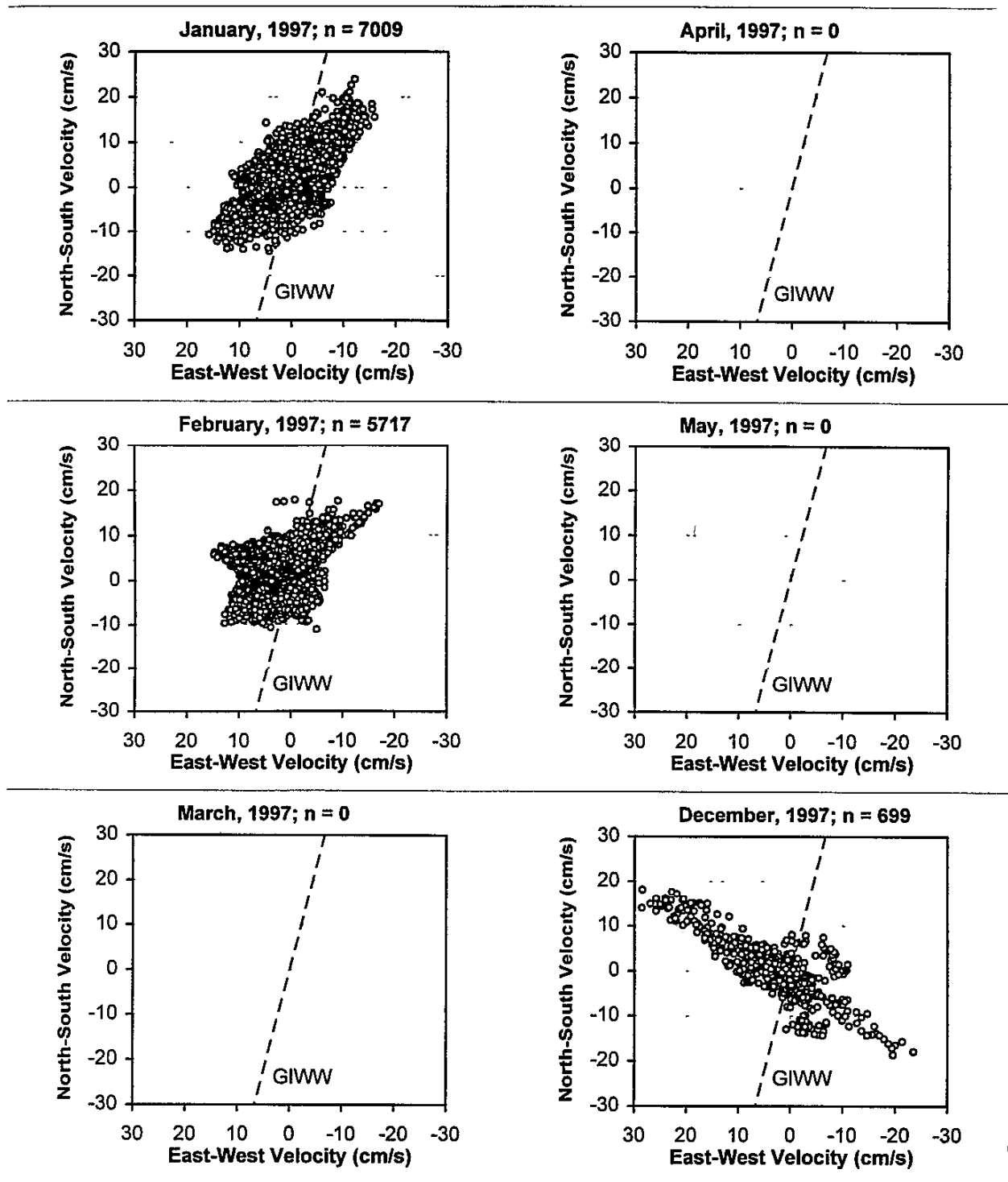


FIGURE 5-15
SCATTER PLOTS OF CURRENTS AT STATION ULM2

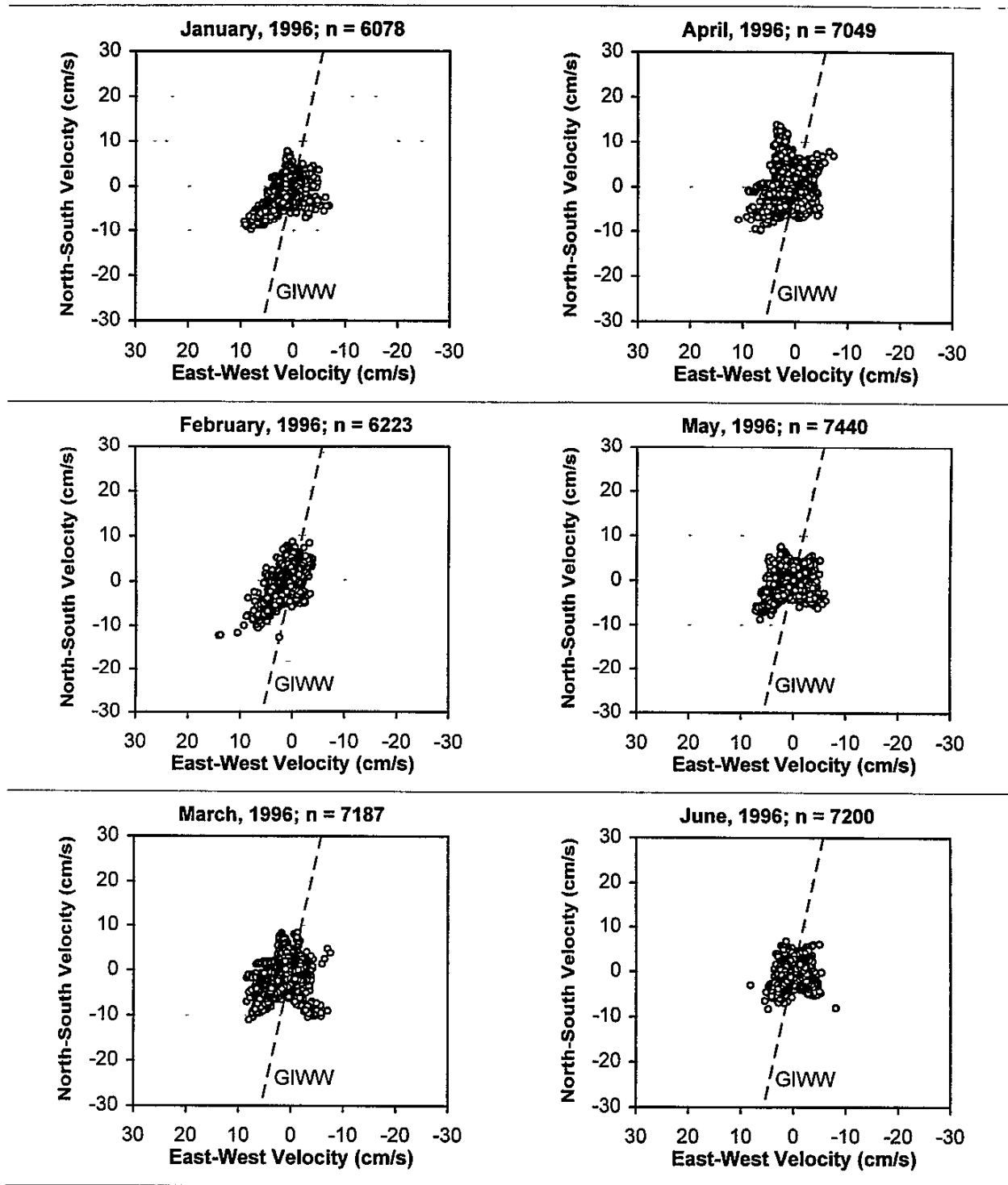


FIGURE 5-16
SCATTER PLOTS OF CURRENTS AT STATION ULM3

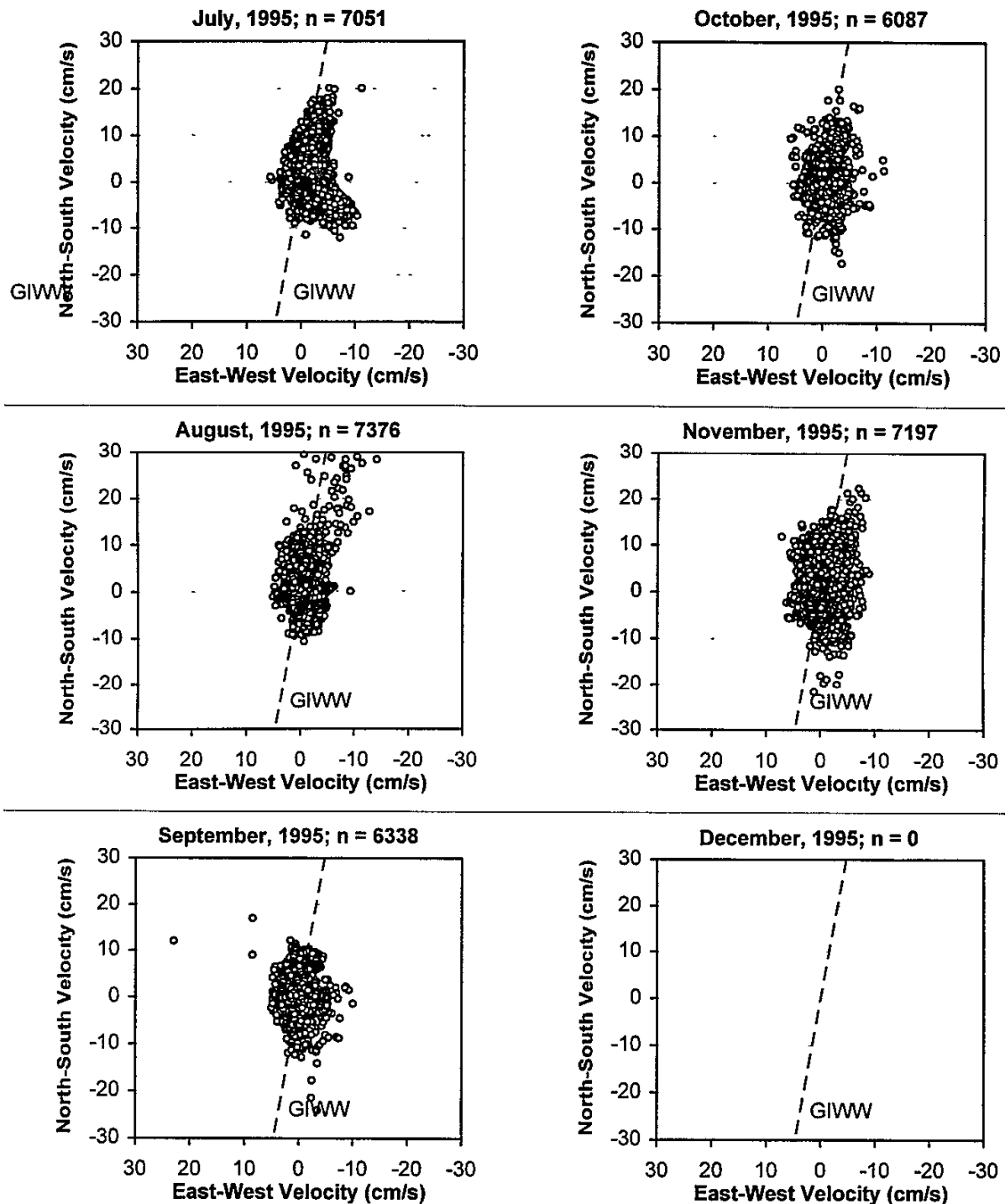
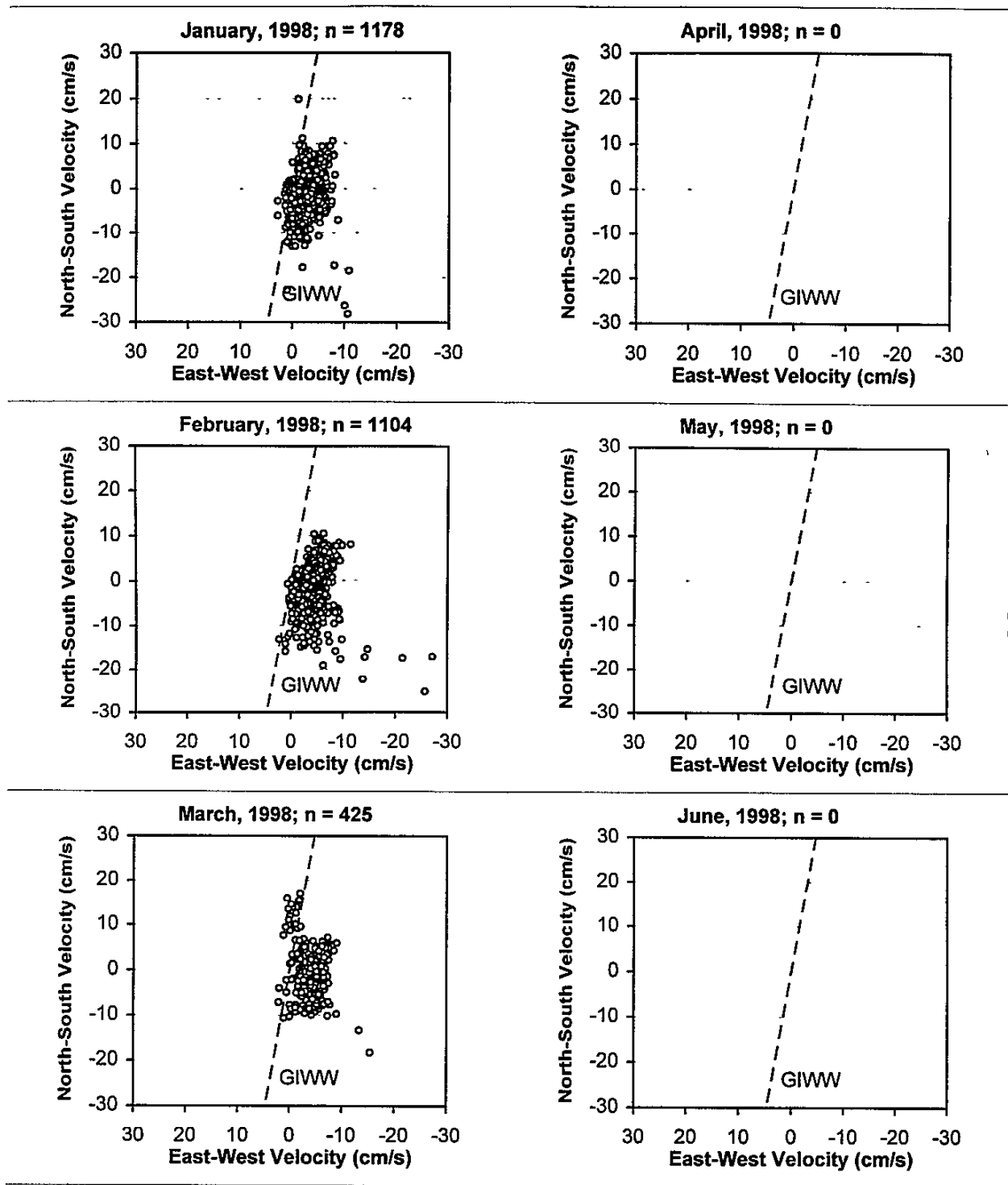
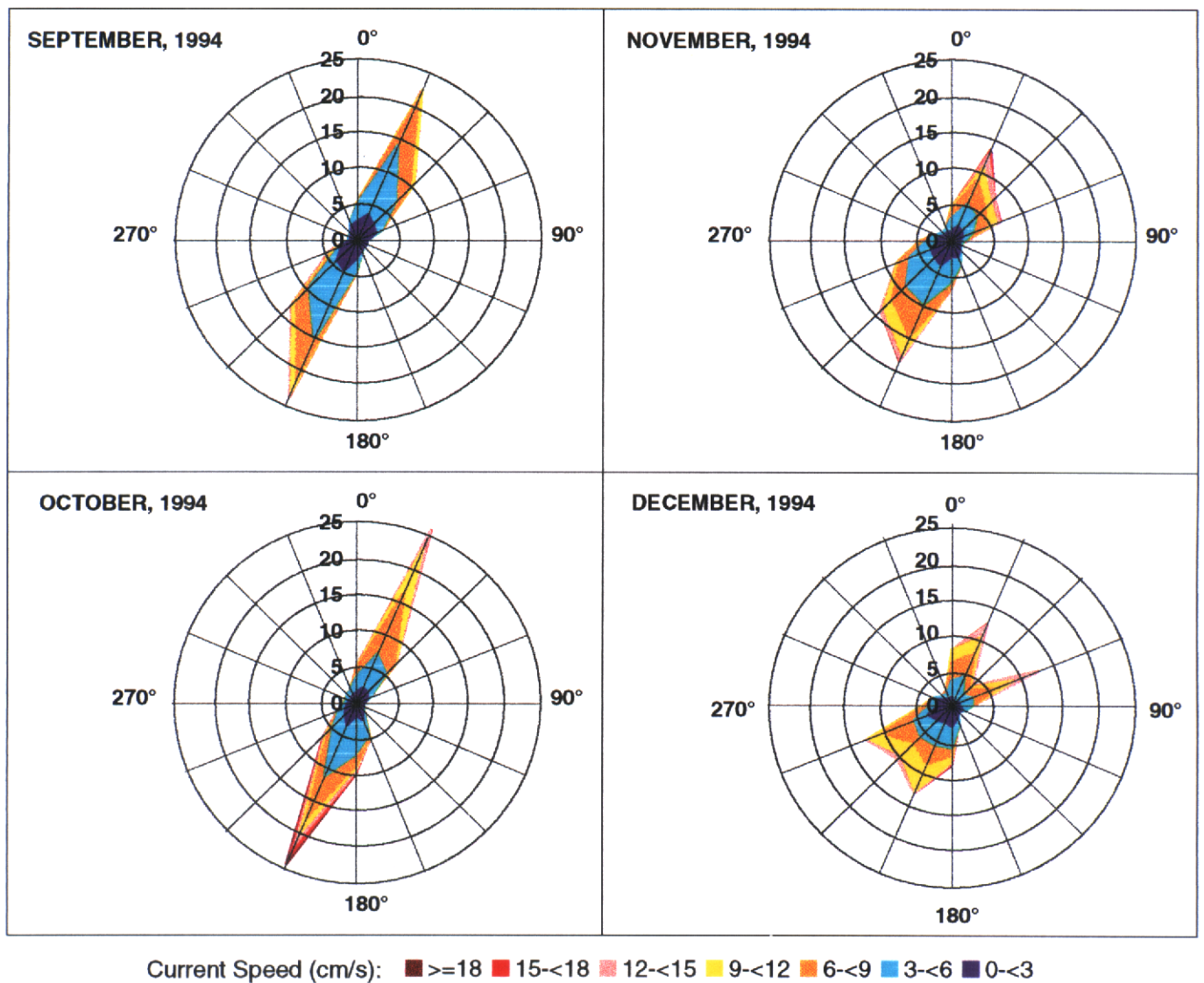


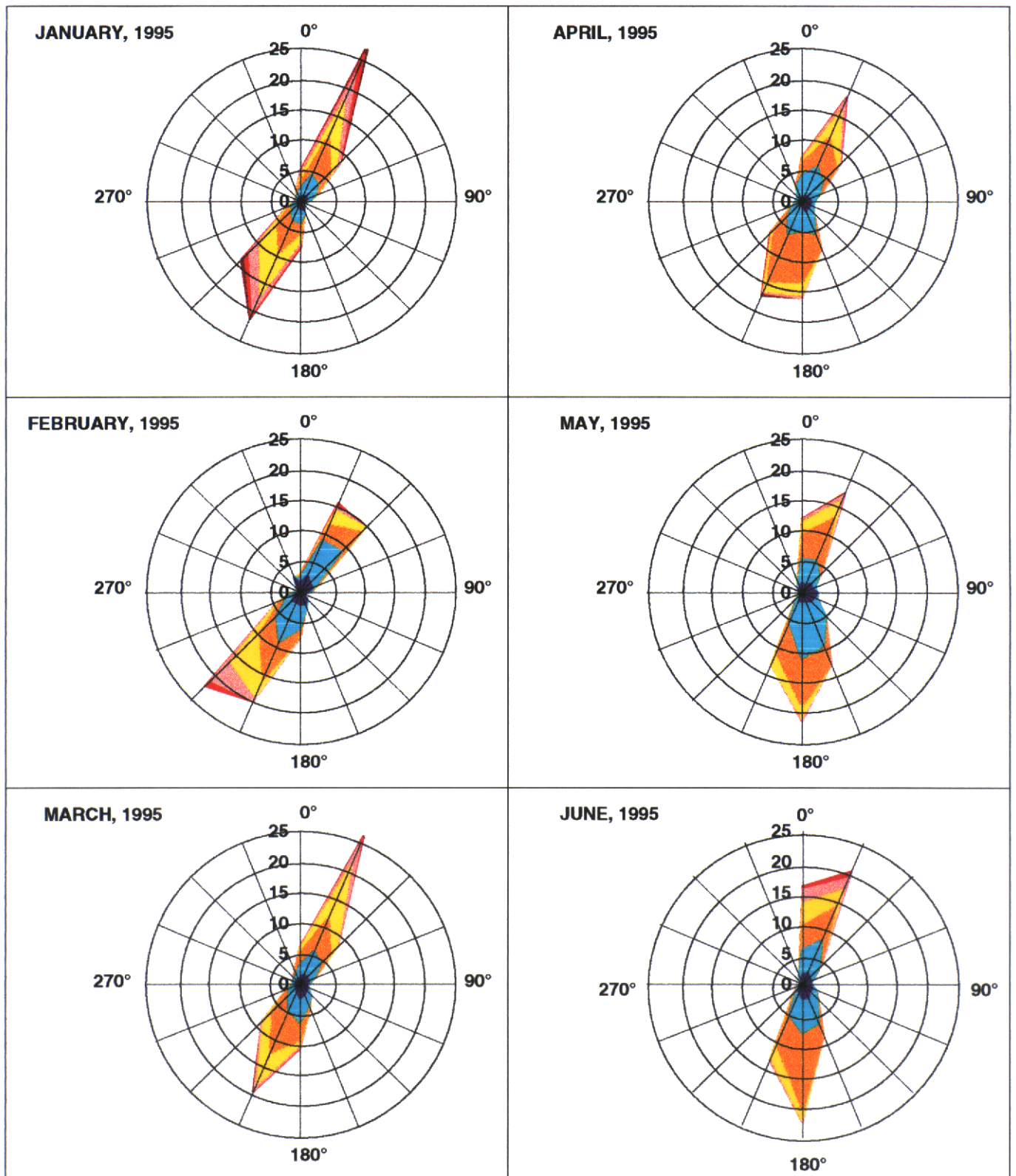
FIGURE 5-17
SCATTER PLOTS OF CURRENTS AT STATION ULM3



**FIGURE 5-18
MONTHLY CURRENT ROSE AT LLM1 STATION**

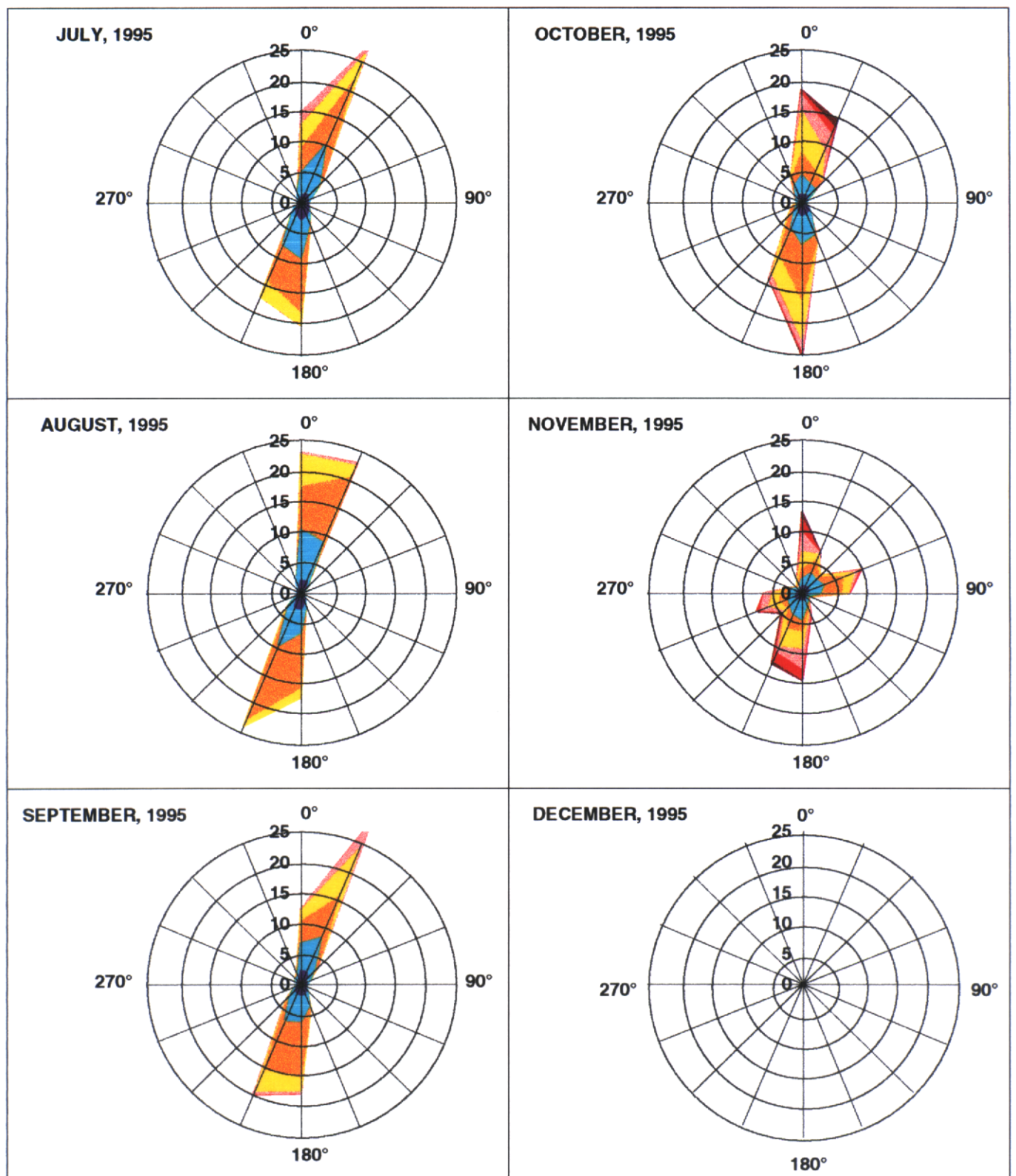


**FIGURE 5-19
MONTHLY CURRENT ROSE AT LLM1 STATION**



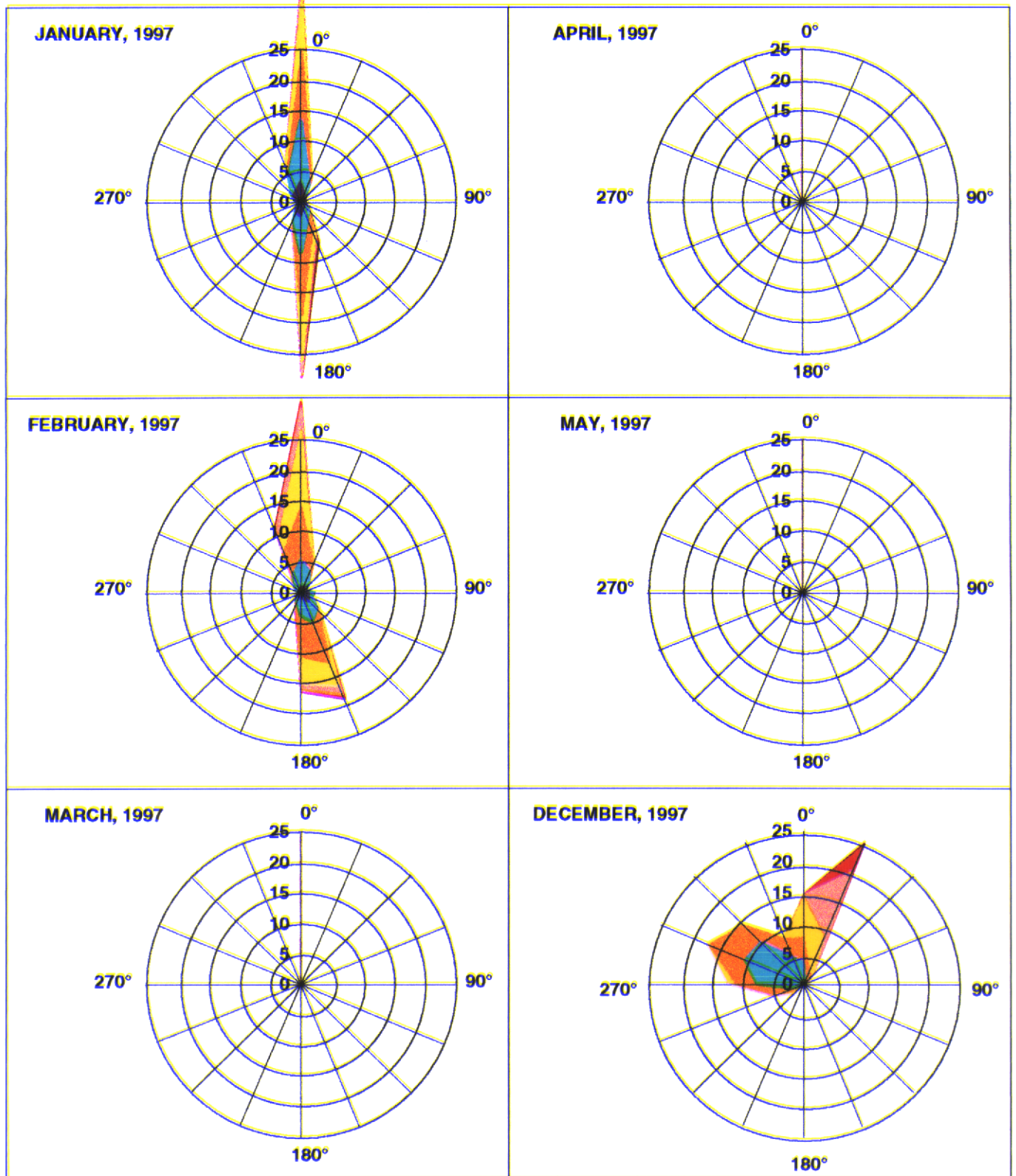
Current Speed (cm/s): ■ ≥18 ■ 15-18 ■ 12-15 ■ 9-12 ■ 6-9 ■ 3-6 ■ 0-3

**FIGURE 5-20
MONTHLY CURRENT ROSE AT LLM1 STATION**



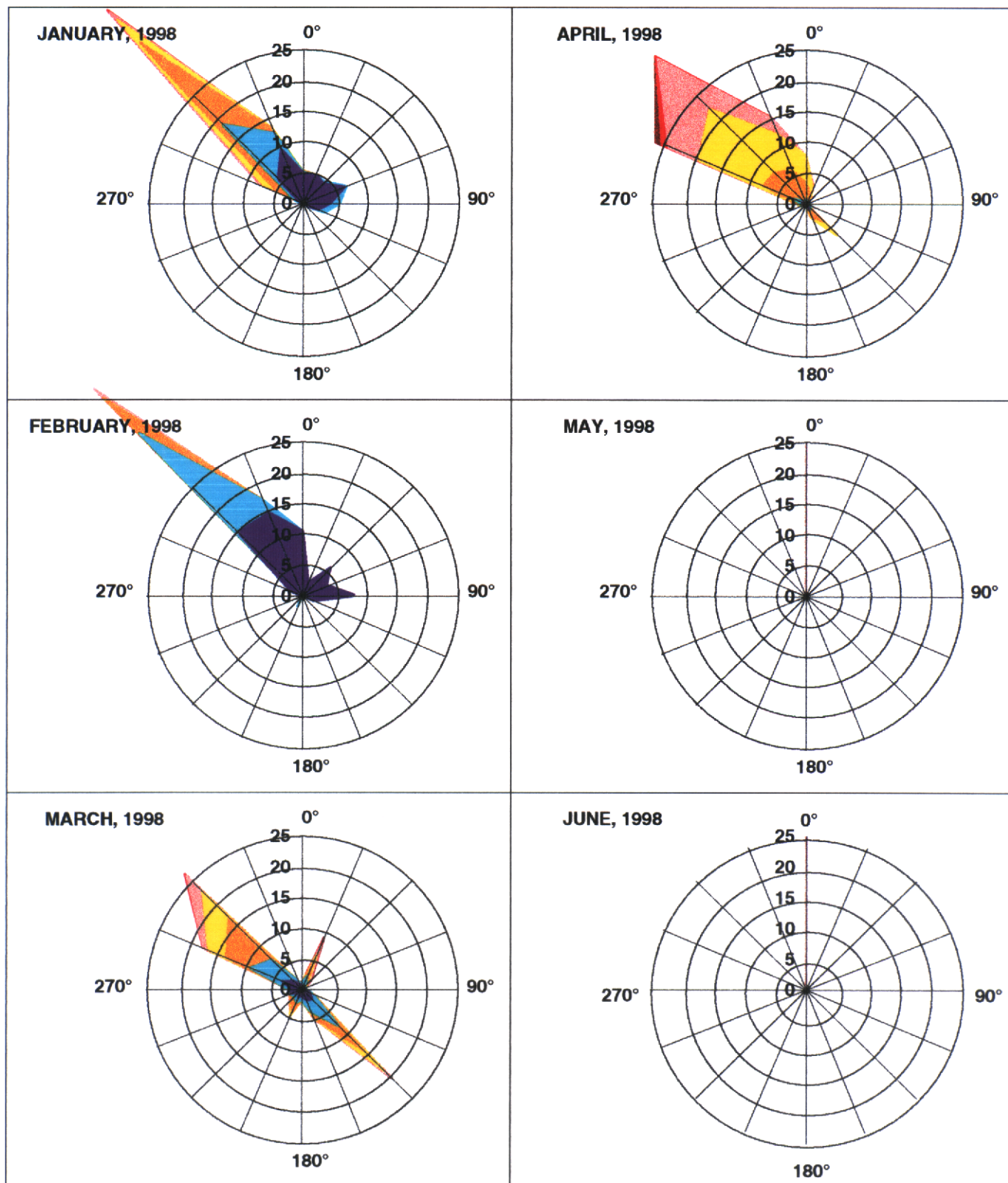
Current Speed (cm/s): ■ >=18 ■ 15-<18 ■ 12-<15 ■ 9-<12 ■ 6-<9 ■ 3-<6 ■ 0-<3

**FIGURE 5-21
MONTHLY CURRENT ROSE AT LLM1 STATION**



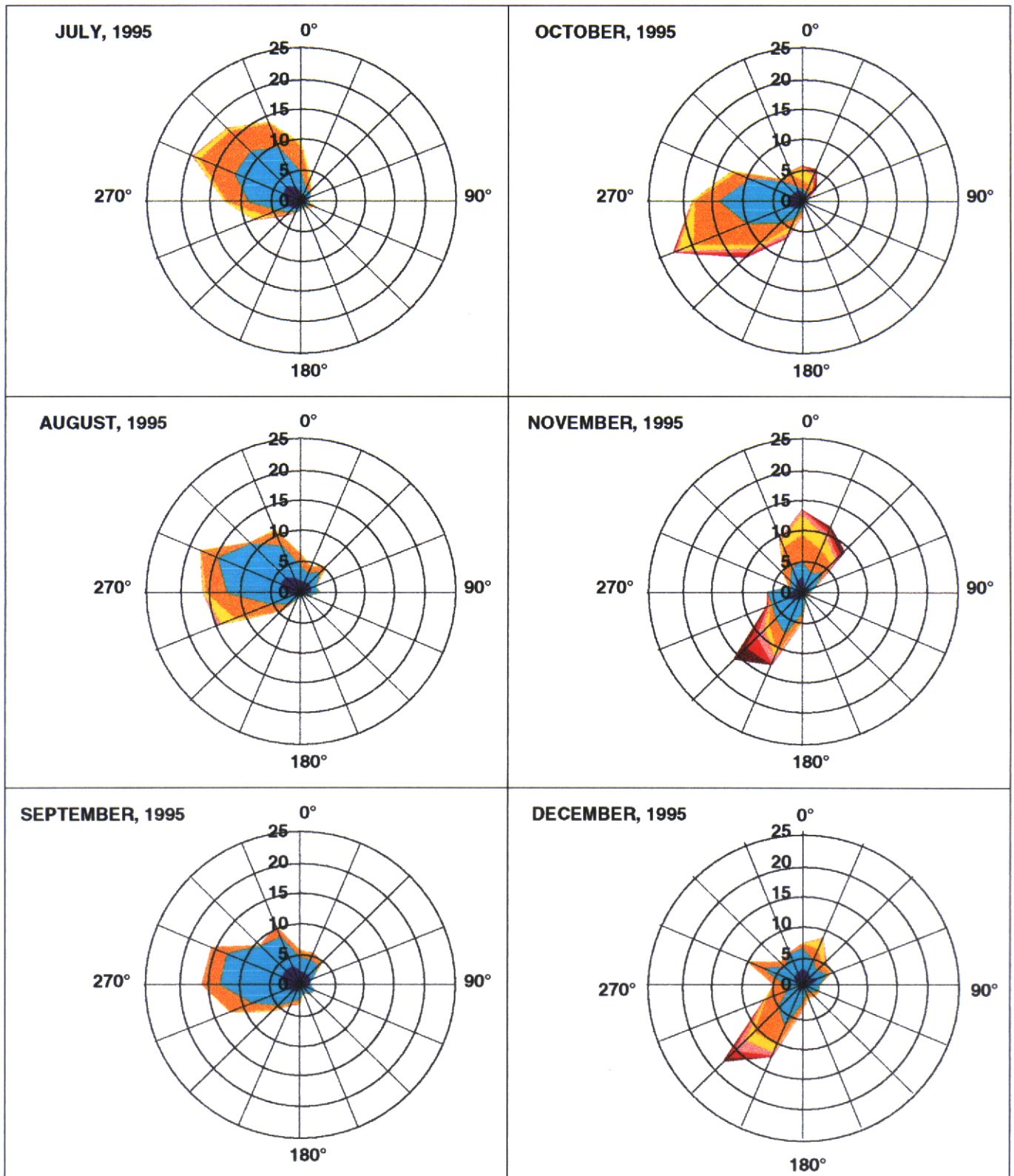
Current Speed (cm/s): ■ ≥ 18 ■ 15-18 ■ 12-15 ■ 9-12 ■ 6-9 ■ 3-6 ■ 0-3

**FIGURE 5-22
MONTHLY CURRENT ROSE AT LLM2a/N STATION**



Current Speed (cm/s): ■ ≥ 18 ■ 15-18 ■ 12-15 ■ 9-12 ■ 6-9 ■ 3-6 ■ 0-3

**FIGURE 5-23
MONTHLY CURRENT ROSE AT ULM1 STATION**



Current Speed (cm/s): ■ ≥ 18 ■ 15-18 ■ 12-15 ■ 9-12 ■ 6-9 ■ 3-6 ■ 0-3

**FIGURE 5-24
MONTHLY CURRENT ROSE AT ULM1 STATION**

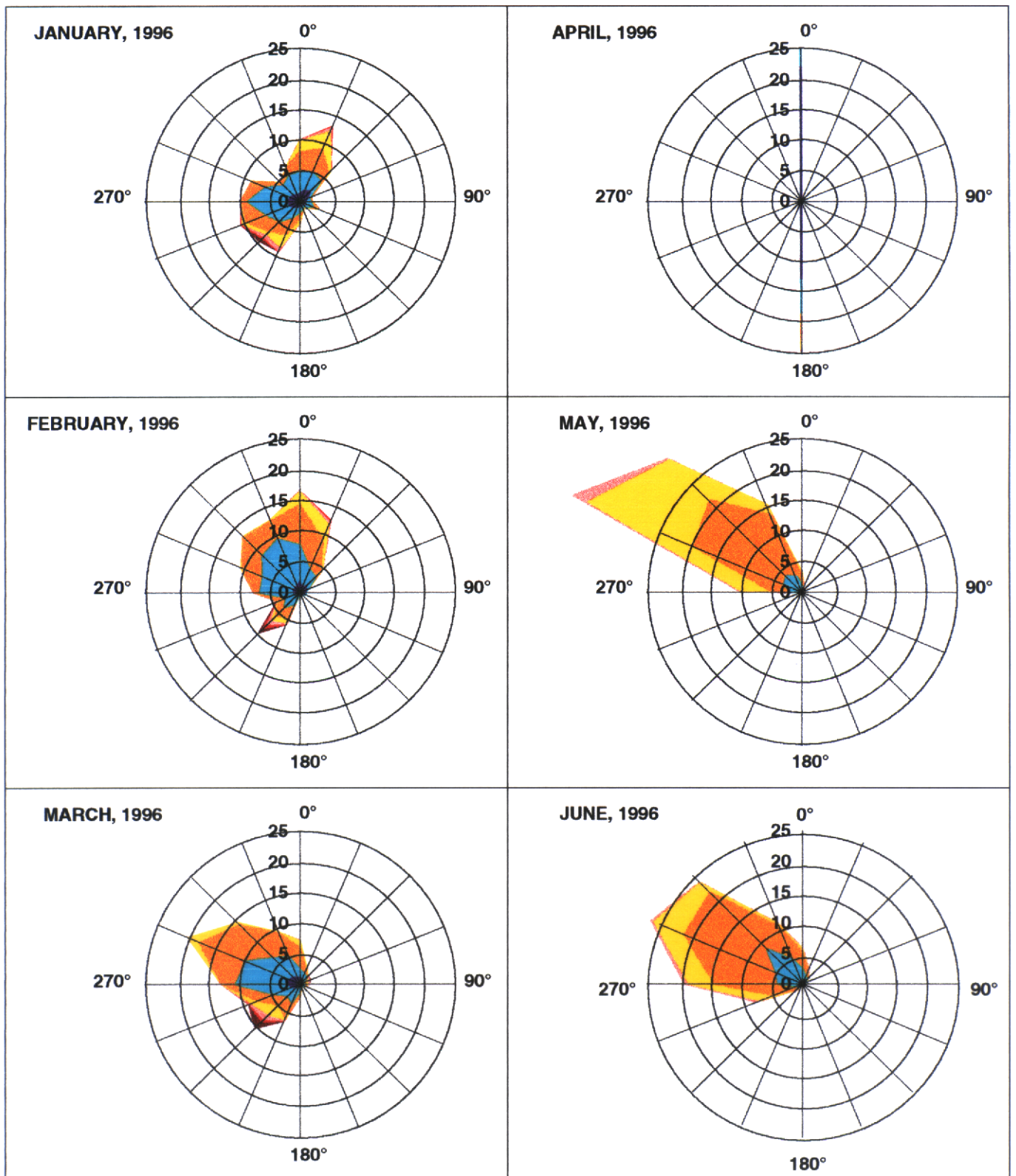


**FIGURE 5-25
MONTHLY CURRENT ROSE AT ULM1 STATION**

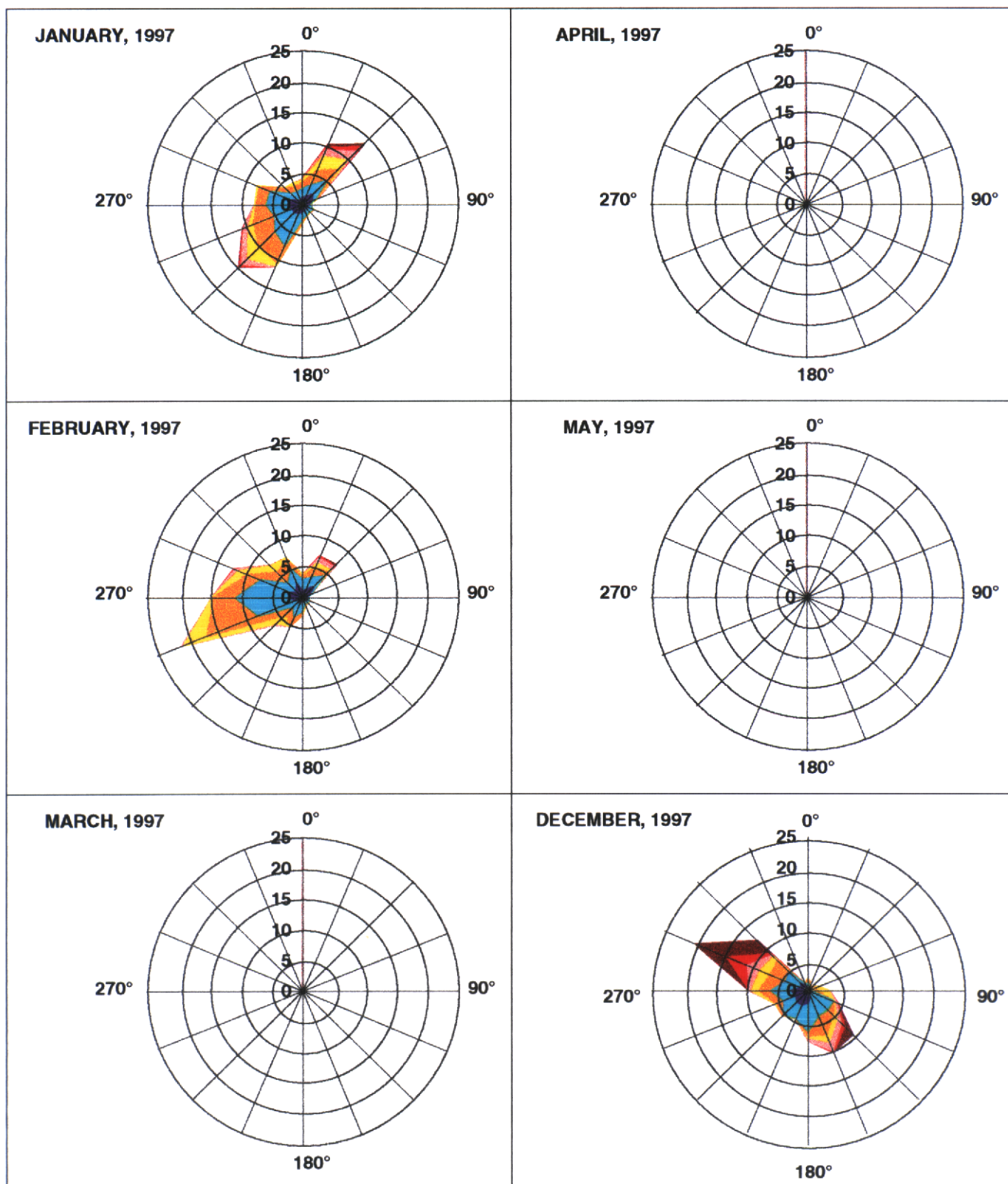
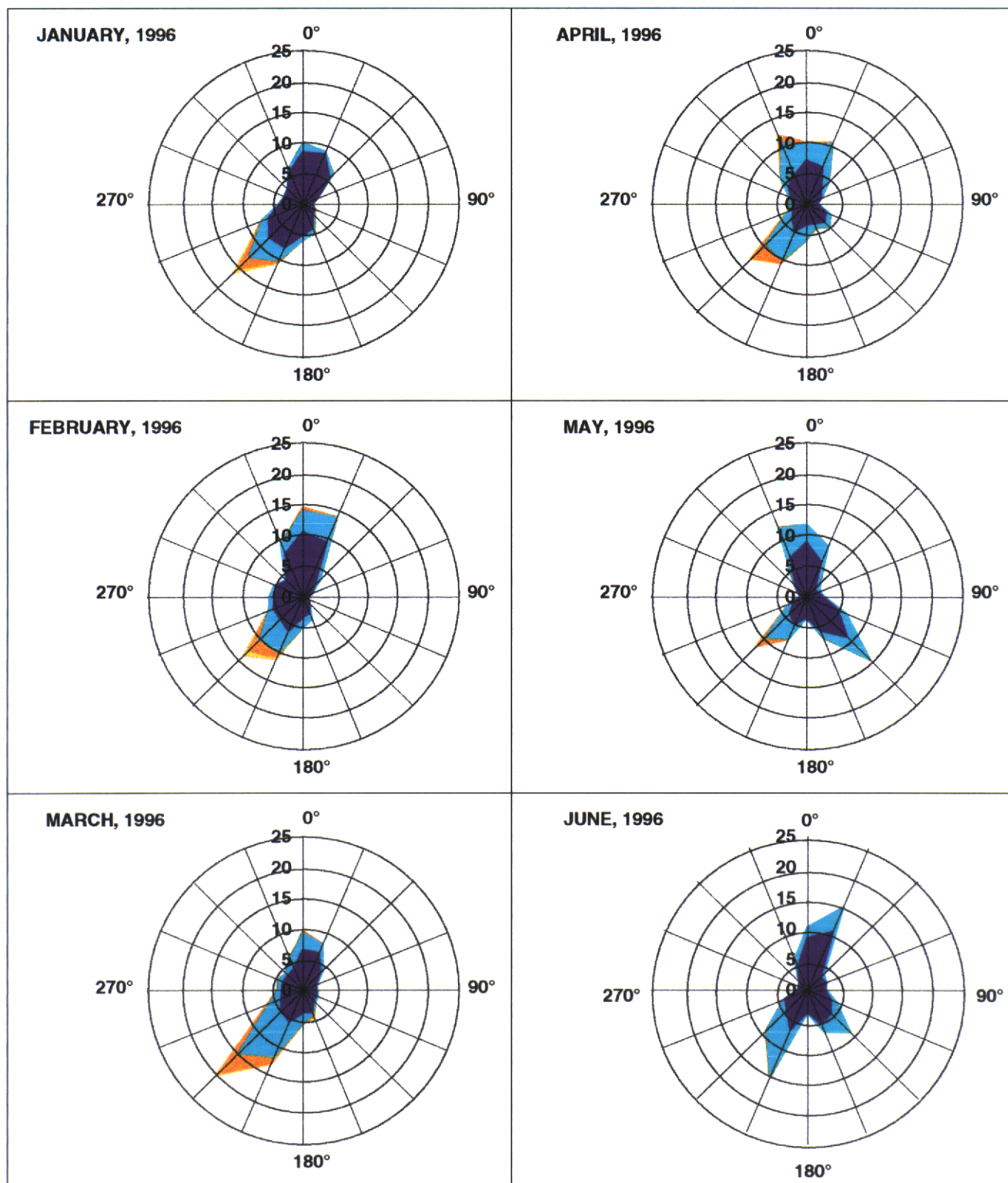
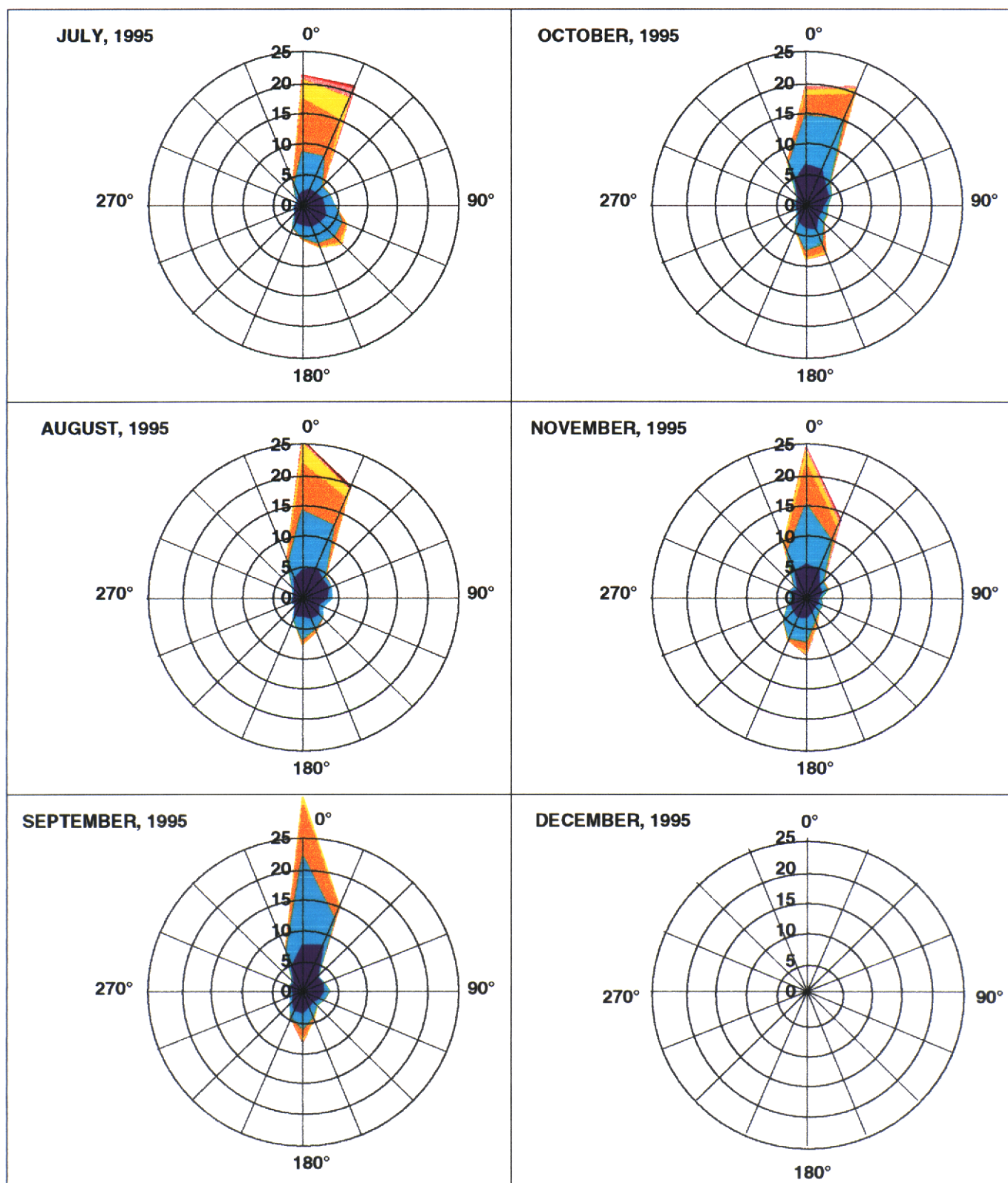


**FIGURE 5-26
MONTHLY CURRENT ROSE AT ULM2 STATION**



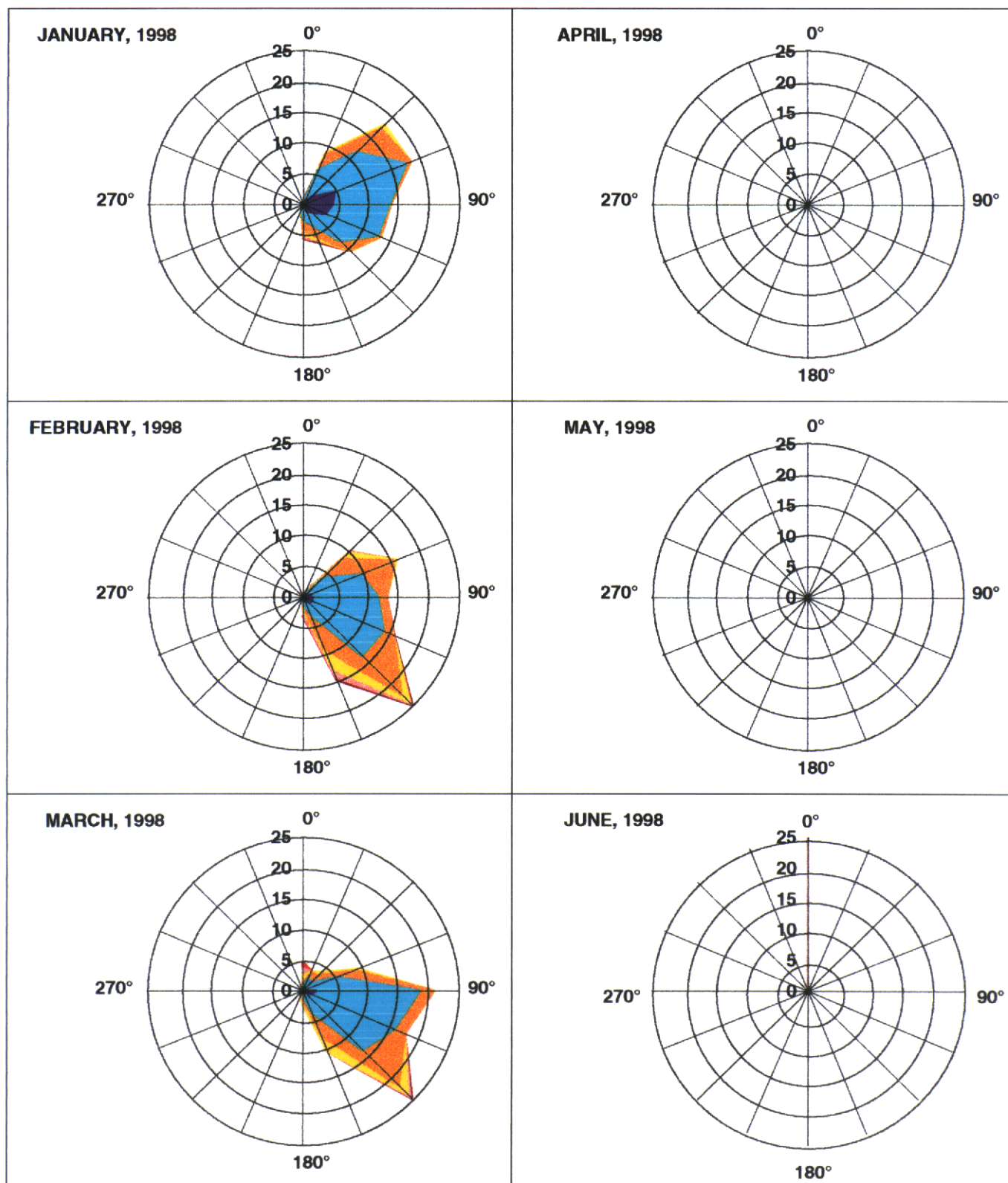
Current Speed (cm/s): ■ ≥ 18 ■ 15-18 ■ 12-15 ■ 9-12 ■ 6-9 ■ 3-6 ■ 0-3

**FIGURE 5-27
MONTHLY CURRENT ROSE AT ULM3 STATION**



Current Speed (cm/s): ■ ≥18 ■ 15-18 ■ 12-15 ■ 9-12 ■ 6-9 ■ 3-6 ■ 0-3

**FIGURE 5-28
MONTHLY CURRENT ROSE AT ULM3 STATION**



Current Speed (cm/s): ■ ≥18 ■ 15-18 ■ 12-15 ■ 9-12 ■ 6-9 ■ 3-6 ■ 0-3

The current roses and the current vector scatterplots are complementary plots. Both attempt to graphically communicate the general behavior of the horizontal current vector. The scatterplots preserve all of the vector information of the individual measurements, in that each represents the exact direction and speed of that measurement. To some extent, the distribution of the data points can give a visual impression of the speed/ direction variation of the data. But, as noted above, the density of data and consequent overplotting can obscure this display, biasing the display toward the extreme values. This can be an advantage in situations when a process is dominated by the higher speed currents, sediment mobilization and transport being one such process. The current rose on the other hand is a statistical summary in graphical format, so all measurements, both low speed and high speed, are represented in the display. Directional resolution is reduced, because the current directions are sorted into 45° bins centered on the principal compass directions, and speed resolution is similarly compromised because the data are sorted into 3 cm/s bins. But the display is more democratic than the elitist scatterplot.

With these differences in mind, the reader should examine the two displays as companions for each month/ platform in the record. Current data from the fall months of 1994 at LLM1 are shown as scatterplots in Figure 5-7 and as roses in Figure 5-18. There is a superficial similarity to these displays in the prominent direction of current, and its bi-directionality. There are also differences. The scatterplots of November and December, Figure 5-7, are almost identical. However, the corresponding current roses of Figure 5-18 are different, in that the December rose displays two favored directional axes, to the ENE and to the NNE, in agreement with both of the scatterplots, while the November rose shows only one favored axis, to the NNE. The second favored axis disappears from the rose display in November because of the predominance of smaller current speeds in the NNE direction (which are obscured in the scatterplot format). All of the displays agree, however, in the important fact that the predominant direction of flow is at a substantial crossing angle to that of the GIWW.

The scatterplots of Figure 5-8 and 5-9, and the companion roses of figures 5-19 and 5-20, agree in the bi-directionality of the current at LLM1 aligning generally NNE-SSW. From early 1995 (figures 5-8 and 5-19) to late 1995 (figures 5-9 and 5-20) the direction of this favored axis of motion shifts more to a N-S line, a shift that is better captured by the roses of Figure 5-20 than the scatterplots of Figure 5-9. Early 1997 data, figures 5-10 and 5-21, indicate a continuing slight counterclockwise turn from the NNE axis of 1995, some of the scatterplot data indicating current even to the west of north, aligning closely with the GIWW. Then after the gap in data (at the end of Data Set III), the December 1997 scatterplot shows a direction perpendicular to the GIWW. The lower current speeds, obscured in the scatterplot, in fact set to the northwest, a fact which emerges from the current rose, Figure 5-21. If one only looked at the scatterplot data of Figure 5-10, without the companion roses or without the earlier data, one might conclude that the current measurement sensors of Data Set IV were on the fritz, giving currents at right angles to the "correct" direction. However, an inspection of the previous months' data, e.g.,

figures 5-7 through 5-9, reveals that the crossing angle to the GIWW is in fact rather variable, and the axis followed by the December 1997 currents has been manifested in the past in the data from the original sensors. Notably, the data from November 1995 display *both* axes rather prominently, in the scatterplot (Figure 5-9) and the current rose (Figure 5-20). The scatterplots of January and February 1995 also show the WSW-ENE axis in the patterns of scatter of the higher speeds. Though the rose displays do not exhibit it so obviously because the lower speed data align more along the N-S axis, once one has realized WSW-ENE is a favored direction (perhaps after looking at the scatterplot), then its signature in the rose display is apparent as well. (The style of current rose display used in the Year-1 report, unfortunately, does not so readily reveal such favored axes, cf. figures 4-13 and 4-14 of Brown and Kraus, 1997)

Data from 1998 (Data Set IV) at Station LLM2N are shown as scatterplots in Figure 5-11 and roses in Figure 5-22. The displays for March 1998 are particularly significant. This bizarre appearing scatterplot, which is reinforced—but less obviously—by the rose diagram of Figure 5-22, was strongly suggestive of a measurement artifact, and triggered our close investigation of this data, discussed further in Chapter 7 below. It is, in fact, not the result of an instrumentation error but evidence of a very real aspect of the current behavior shifting from one favored axis to another. Some evidence of these same axes can be discerned in the other panels, especially of the scatterplots (Figure 5-11)

The remainder of the examples of these displays are taken from the data for the Upper Laguna monitoring program. Station ULM1 is located in Corpus Christi Bay near the GIWW (about 400 m to the east) and just north of the shoals of Bulkhead Flats. The bayward boundary of Bulkhead Flats is well defined, trending WNW-ESE along a line that one would construct extending the south shoreline of Corpus Christi Bay and curving up to the northeast to merge with the bayshore of Mustang Island. Currents following the arc of shoreline might trend WNW-ESE if running longshore from the west, or SW-NE if following the curve of shoreline from Mustang Island from the east. Both of these axes are evidenced in the data. The scatterplot for July 1995, Figure 5-12, is suggestive of the latter. The companion rose diagram, Figure 5-23 also displays a prominent direction to the WNW, but a substantial asymmetry, obscured in the scatterplot, with most of the current trending to the west. This same westward net current is seen through October 1995, Figure 5-23. By fall, an increasing southward component is evident in the rose display. In the November data, both the scatterplot and the rose indicate bi-directional currents, but not exactly reversing. Rather the northward currents trend more due north, while the southward currents are predominantly to the southwest. The December 1995 rose, Figure 5-23, indicates presence of both directions in the data, viz. WNW and SW. This is even more evident in the plots of figures 5-13 and 5-24, with a continued net movement to the west. It is instructive to compare the displays of March 1996, in the different renderings of the scatterplot and the rose diagram. As with Figure 5-10, one seeing Figure 5-14 without the preceding figures or the companion current roses of Figure 5-25 might be tempted to conclude from the very different prominent directions of January-February 1997 (Data Set III with the original sensor

technology) and of December 1997 (Data Set IV with re-equipped platforms) that an error had been made in installing or processing the new currents. In fact, even in the data of February 1997 there is evidence of both of these axes of favored motion in the scatterplot (but not in the rose). These data demonstrate a very different mode of circulation in this region of Corpus Christi Bay in winter 1997 than exhibited previously in the same year or in earlier years.

The current speeds in the Upper Laguna at both Stations ULM2 and ULM3 are lower in general than at the other platforms, not surprisingly given the isolated, protected nature of the Upper Laguna. The lower speeds are evident in the compressed clustering of the scatterplots, Figure 5-15, and the blue-predominance of the roses, Figure 5-26. Particularly interesting is the propensity for flow along any of three favored axes, N-S (aligning with the main axis of the Laguna), SW-NE and NW-SE. This is particularly evident in the scatterplot of March 1996, Figure 5-15, and the roses of May and June 1996, Figure 5-26. The fact that ULM2 was located out from the mouth of Baffin Bay and was therefore potentially subject to flows across the main axis of the Upper Laguna is doubtless part of the reason for this. But Station ULM3, located farther south, shows flows along the N-S axis of the Laguna in summer and fall 1995, figures 5-16 and 5-26, but in 1998 there was considerable E-W currents transverse to the main axis of the Laguna, figures 5-17 and 5-28. In all of these displays from ULM3, there is a net northward transport evidenced by the current roses that is obscured in the scatter plots.

In summary, important attributes of the current data shown by the displays include:

- (1) extent of bi-directionality
- (2) prevalence of noncompensating directions, indicating a net nonzero flow component
- (3) asymmetry in current speeds
- (4) prevalence of favorable axes, versus more omnidirectional distributions
- (5) alignment with physiographic axes and/or shoreline

Attribute (3) is important from the standpoint of inferences about sediment transport. Any asymmetry in current speeds translates to a greater capacity for mobilizing and transporting sediment by the higher speeds. Attribute (4) deserves special note. Some of these plots indicate favorable axes of motion along which the current vectors cluster or as revealed by the directional statistics of the current rose. This is an unexpected and important behavior relevant to the circulation of the Upper and Lower Laguna that is given more analysis and discussion in Chapter 7.

To identify the periodic components of variations in current, as was done for water level and wind in Chapter 4, spectral analyses were performed for subsets of the complete time series. These were computed on a monthly basis for the u and v components separately and for the speed of the current. The reader is reminded that the component convention used for these data is unusual, being rotated clockwise 90° from the usual configuration, so that u denotes positive north and v denotes positive west. The complete set of monthly spectra are presented in Appendix CF. Within this report, example spectra for all stations, primarily for 1996, are shown. Figures 5-29 and 5-30 display spectra for the Lower Laguna for September 1994 and June 1995, for the north-south component of the current, water level (at the Arroyo Colorado TCOON gauge) and east-west component wind speed. These correspond to, and agree exactly with, the graphs given in figures 4.20 and 4.23 of the Year-1 report (Brown and Kraus, 1997). These are, however, amplitude spectra. For the purposes of this project, we consider the power (or "energy") spectrum to be the more useful analysis (see Priestley, 1981), which are the spectra presented in Appendix CF and in the remainder of this chapter. Another difference between these analyses and those of Brown and Kraus (1997) is that they computed a sort of directional spectrum by determining the linear regression passing through the scatterplot, finding the component along this regression, and computing its spectrum. (No results were presented in their report from this analysis, however.) We have not performed this computation because it turns out that there is no single linear regression through the scatterplot, as noted in Section 5.2 and further discussed below in Chapter 7.

A selection of such spectra for various months is shown for the Lower Laguna in figures 5-31 through 5-35, and for the Upper Laguna in figures 5-36 through 5-45. In these figures, separate spectra have been computed and are presented for the individual u- and v-component currents, and for the magnitude of the resultant, i.e. the speed of the horizontal current. Inspection of the complete set of spectra in figures 5-31 through 5-45 leads to the following observations:

- (1) There is a consistent prominent spike at 1.0 cpd, and at some of stations additional spikes at approximately 0.93 and 1.92 cpd, with an occasional weak signal at 2.0 cpd.
- (2) The energy in the current spectrum is greatest in the Lower Laguna at LLM1 and lowest in the Upper Laguna, especially ULM2.
- (3) There is considerable month-to-month variation in spectra at some of these stations, as well as year-to-year variation.

FIGURE 5-29
AMPLITUDE SPECTRUM PLOTS
LOWER LAGUNA MADRE, SEPTEMBER 1994

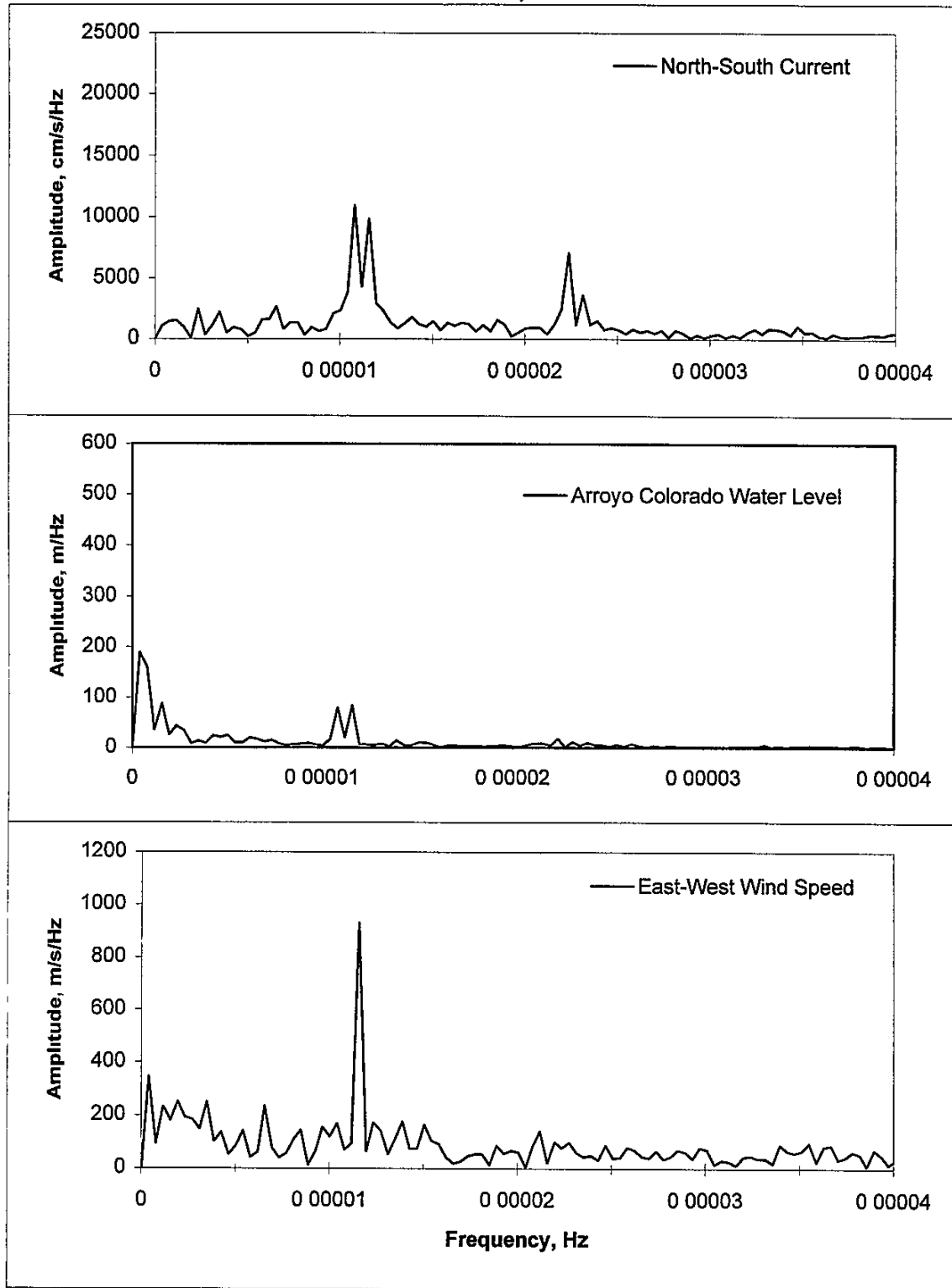


FIGURE 5-30
AMPLITUDE SPECTRUM PLOTS
LOWER LAGUNA MADRE, JUNE 1995

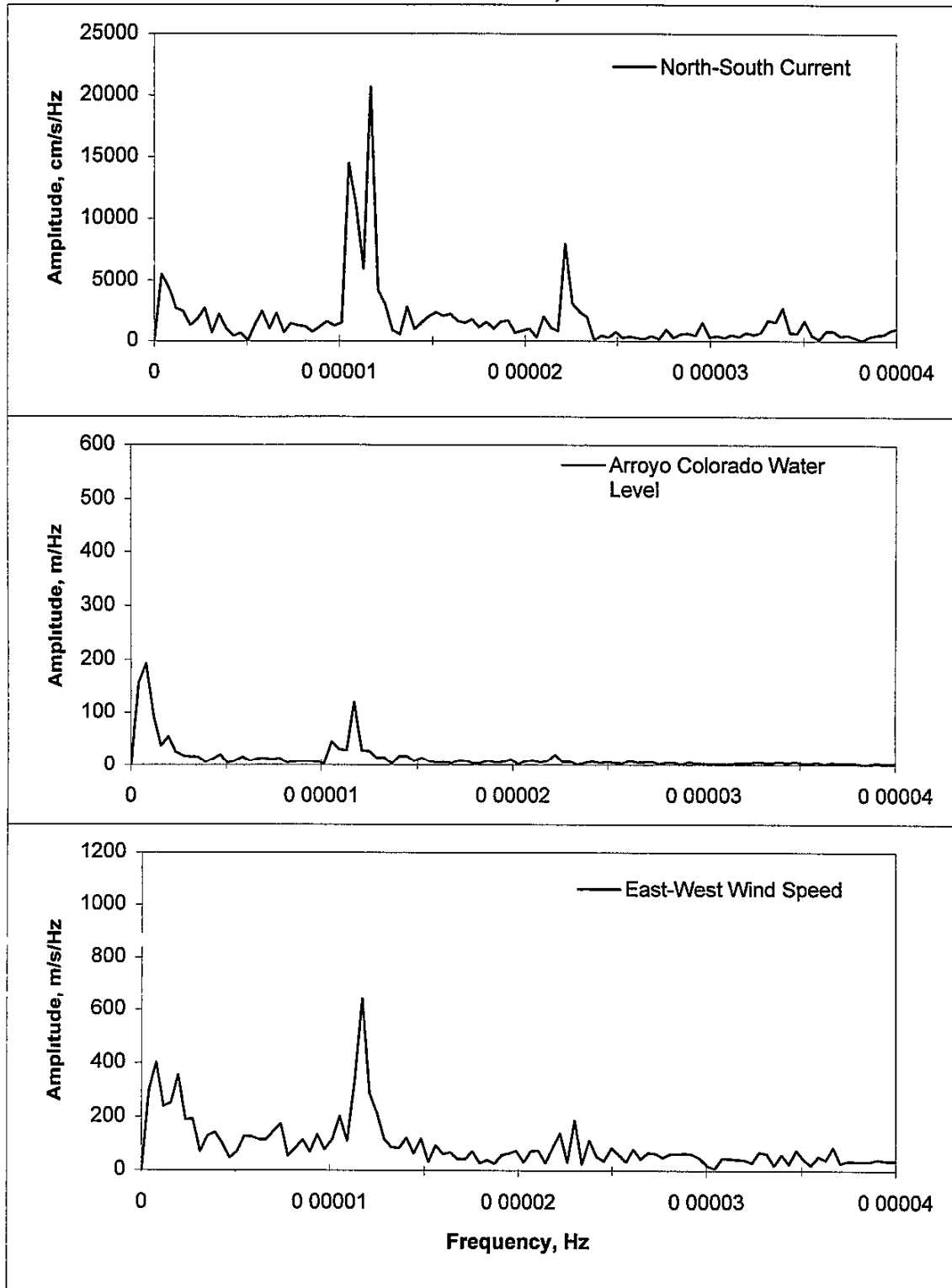


FIGURE 5-31
MONTHLY CURRENT SPEED SPECTRA AT LOWER LAGUNA MADRE
STATION 1

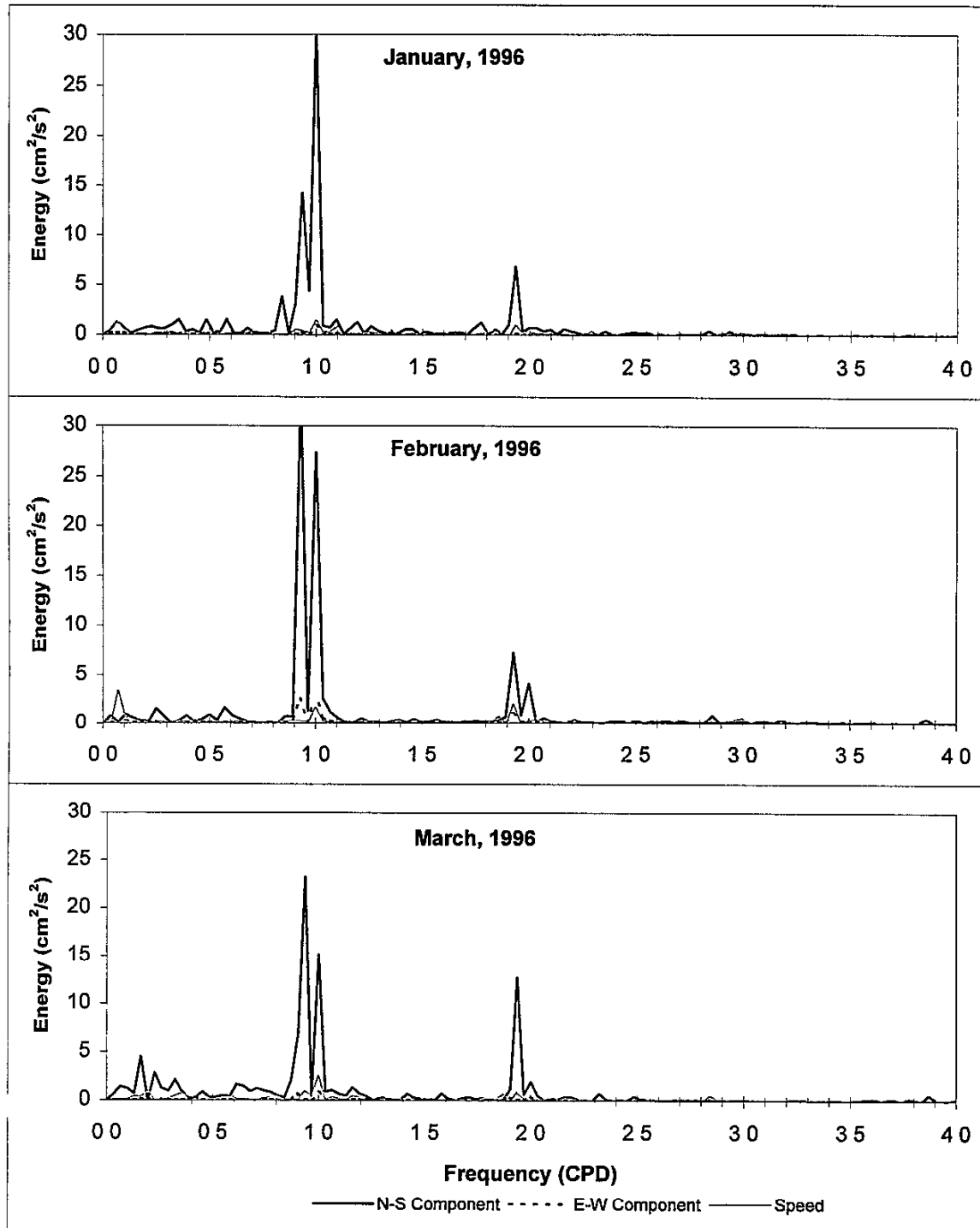


FIGURE 5-32
MONTHLY CURRENT SPEED SPECTRA AT LOWER LAGUNA MADRE
STATION 1

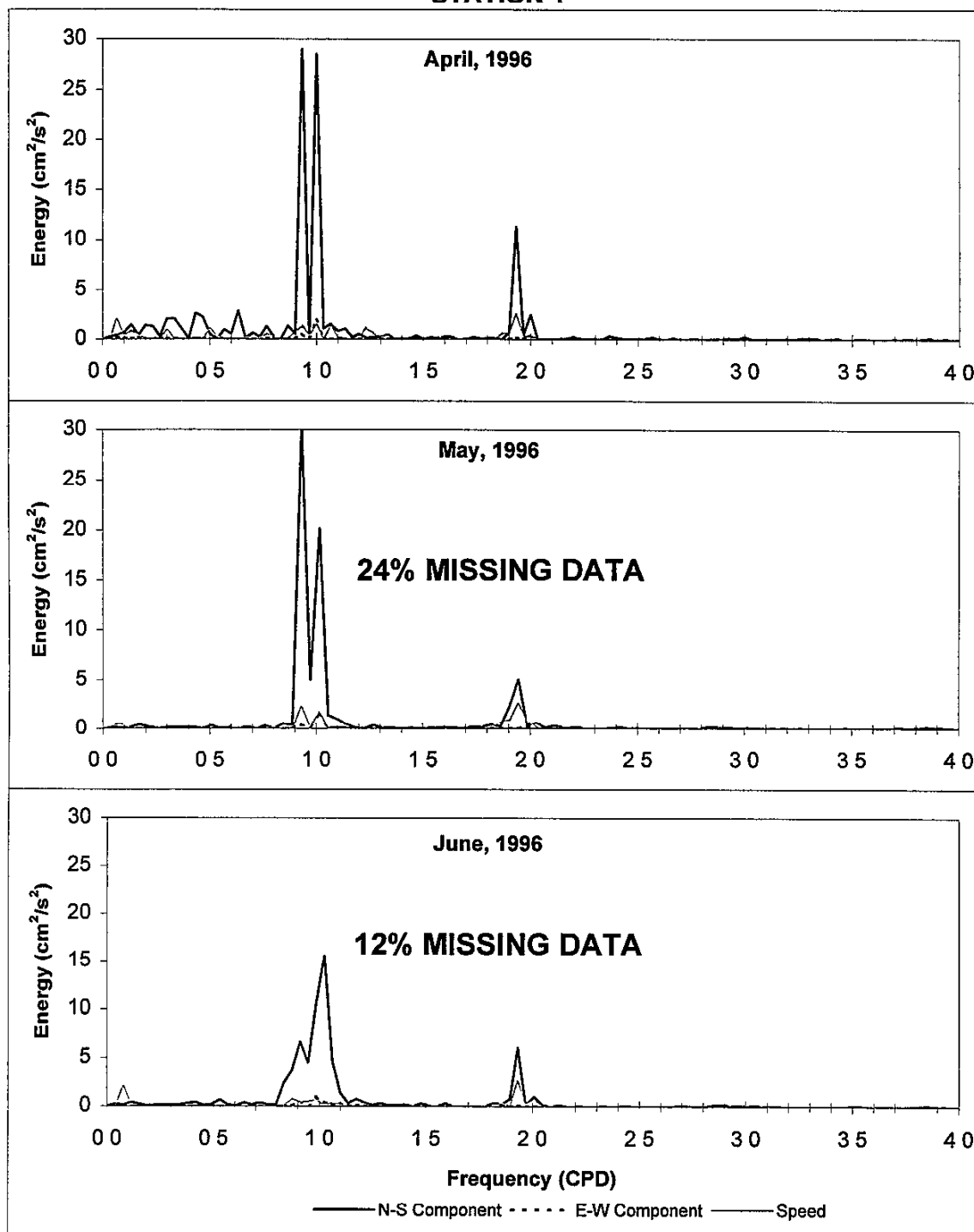


FIGURE 5-33
MONTHLY CURRENT SPEED SPECTRA AT LOWER LAGUNA MADRE
STATION 1

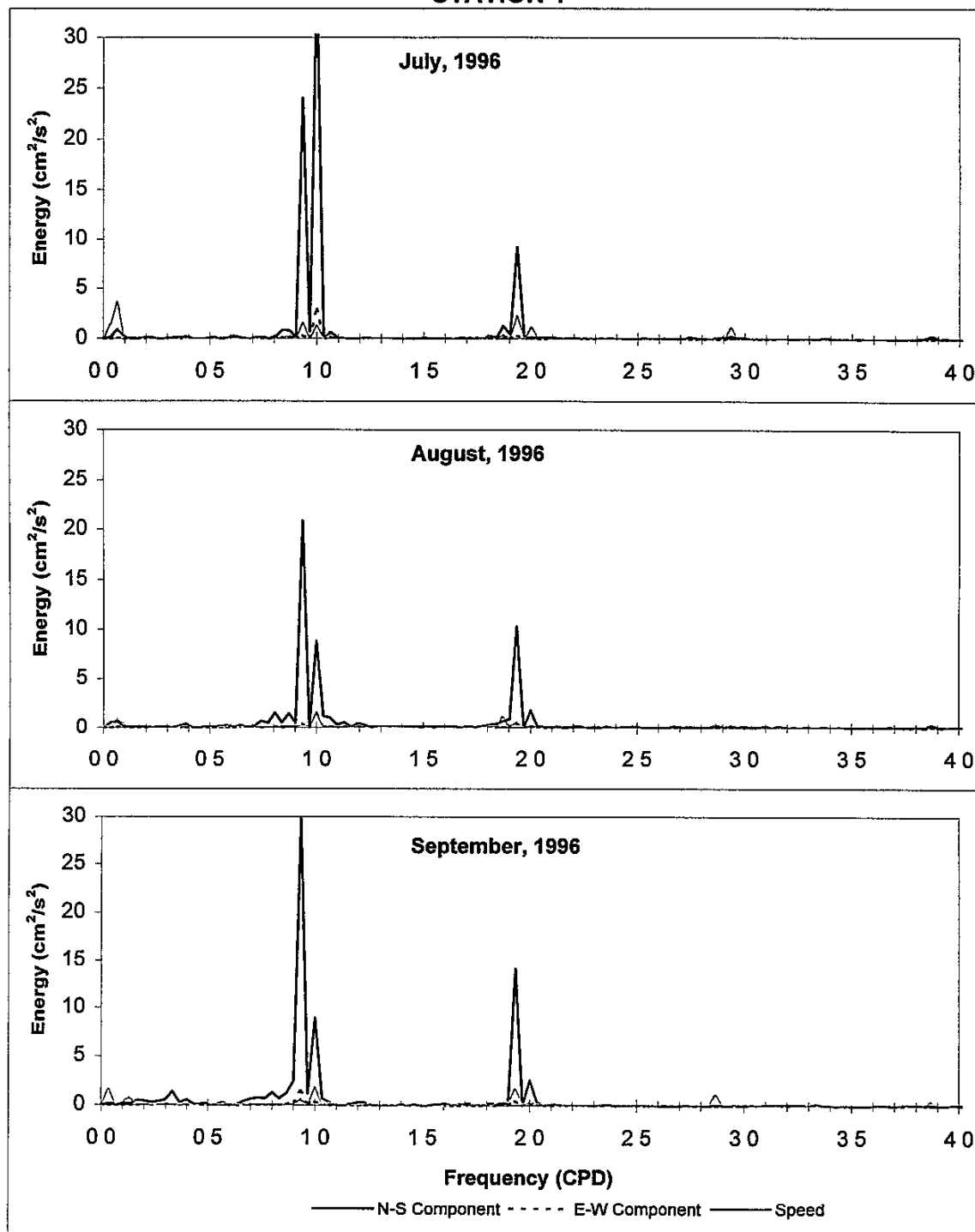


FIGURE 5-34
MONTHLY CURRENT SPEED SPECTRA AT LOWER LAGUNA MADRE
STATION 1

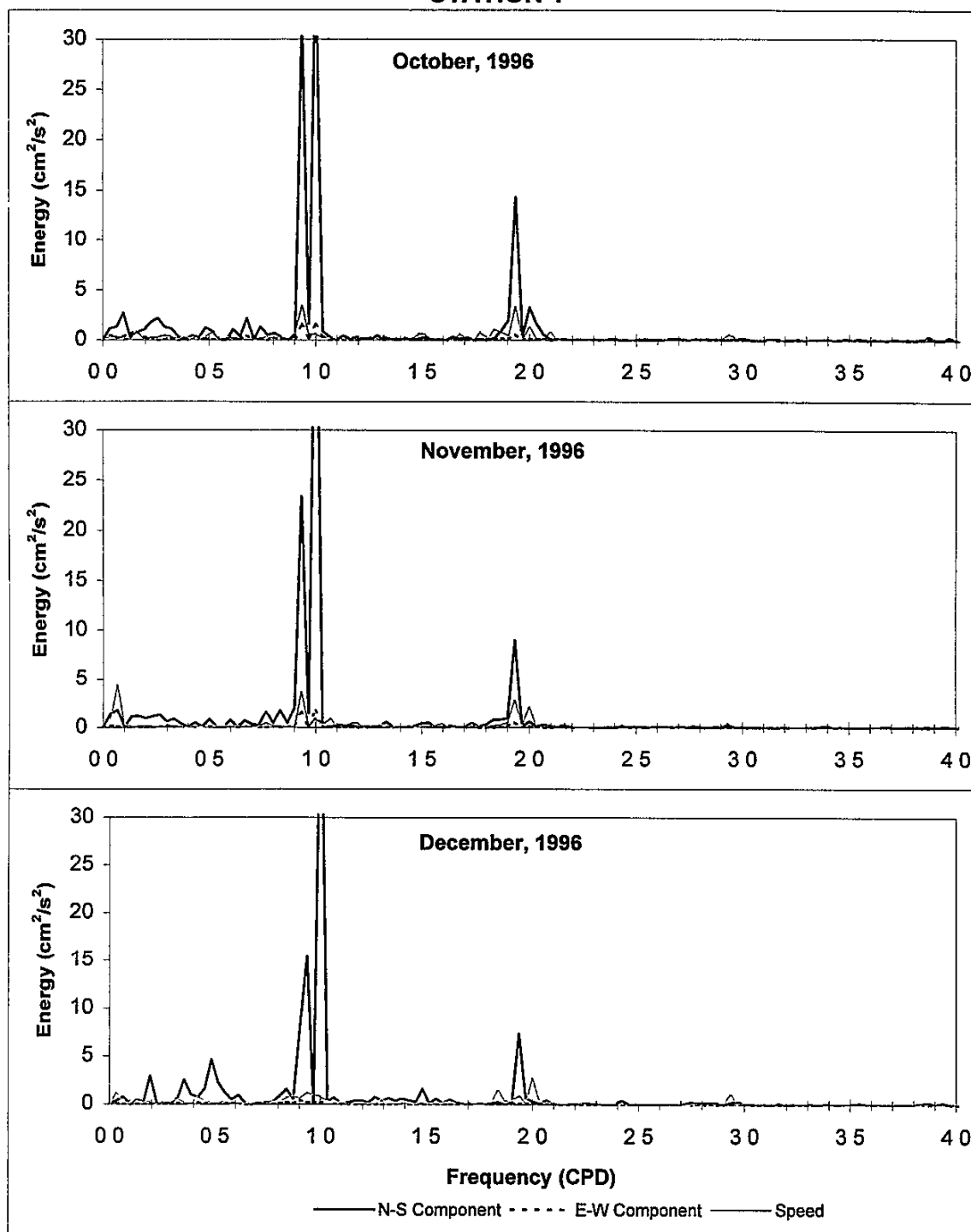


FIGURE 5-35
MONTHLY CURRENT SPEED SPECTRA AT LOWER LAGUNA MADRE
STATION 2A

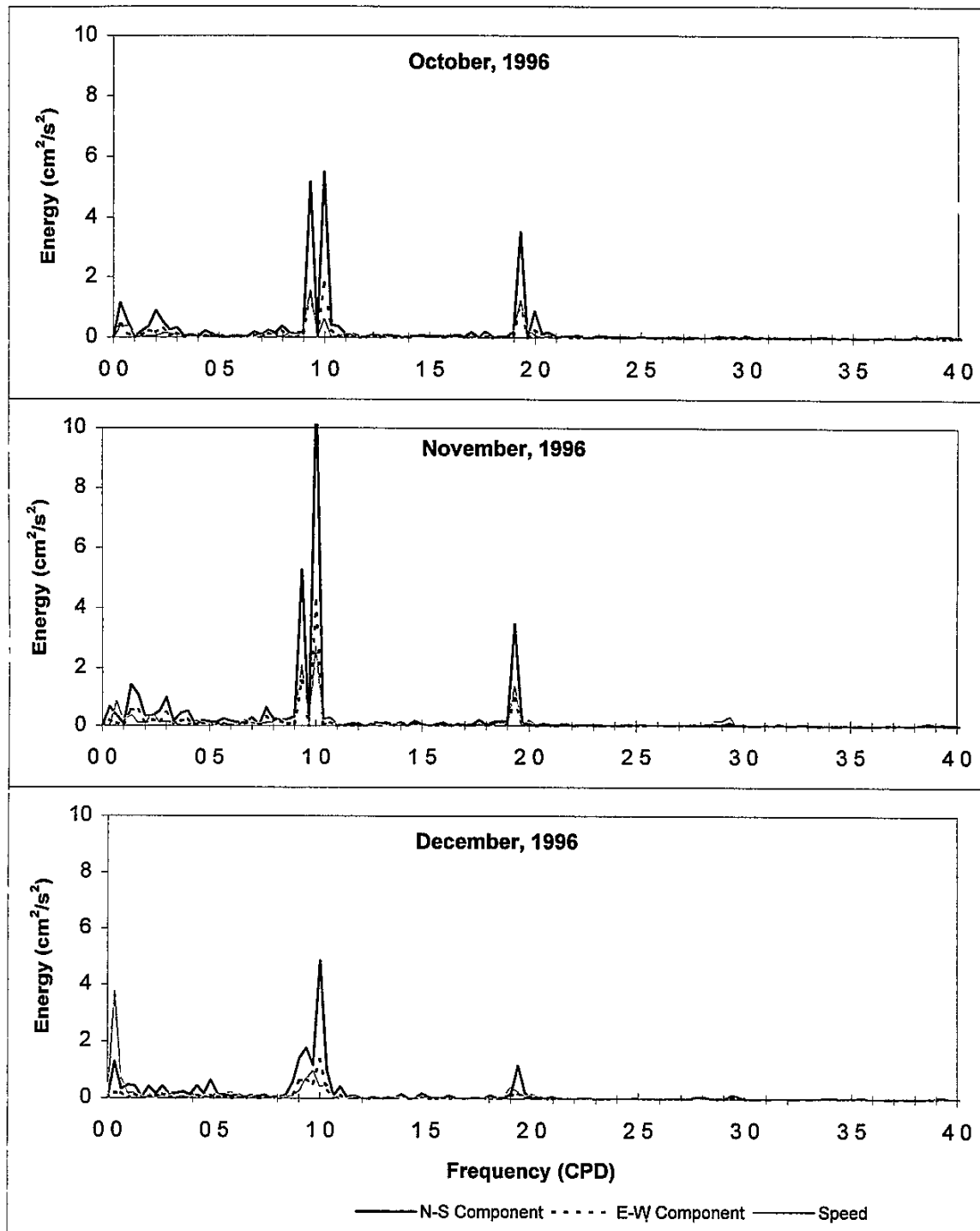


FIGURE 5-36
MONTHLY CURRENT SPEED SPECTRA AT UPPER LAGUNA MADRE
STATION 1

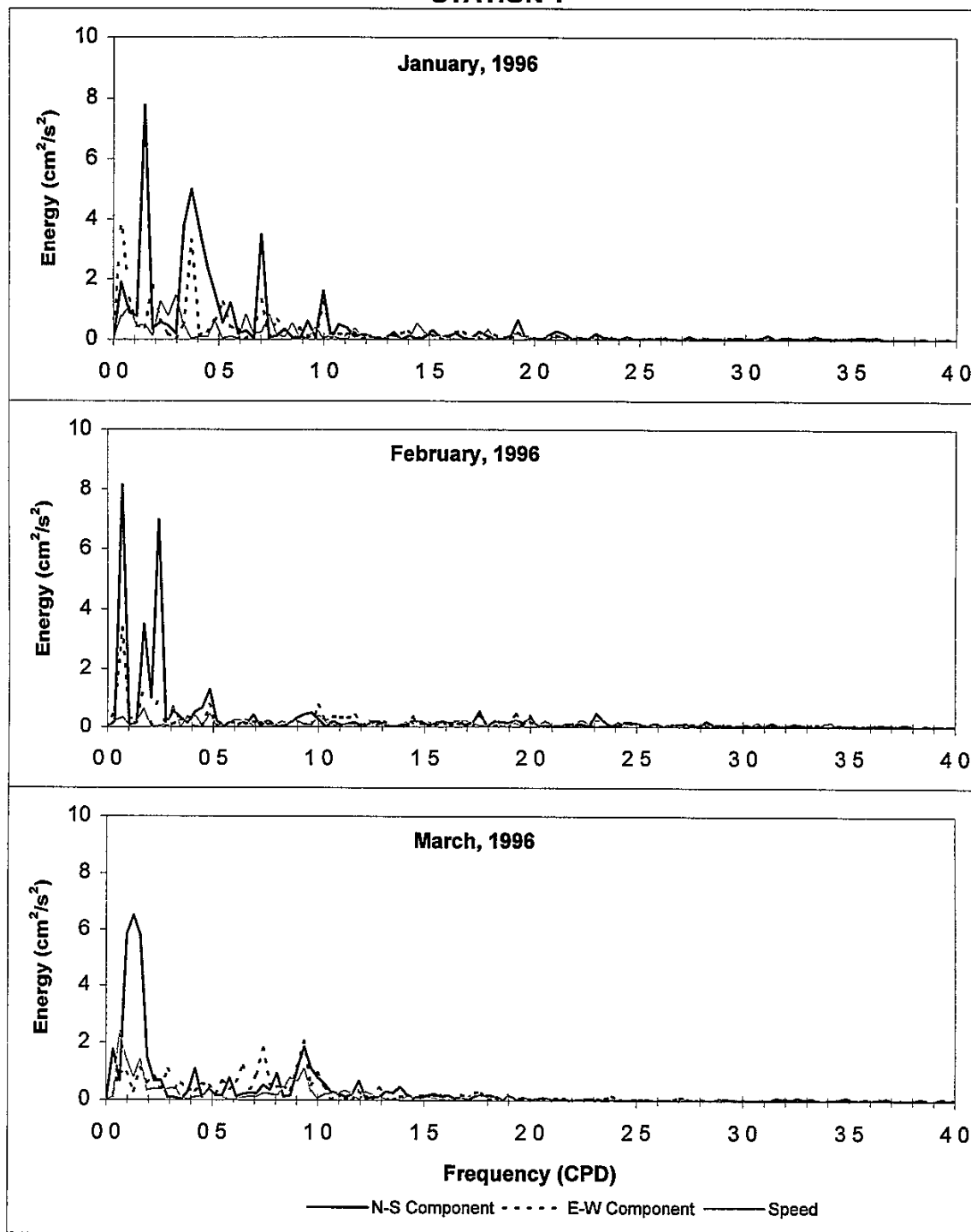


FIGURE 5-37
MONTHLY CURRENT SPEED SPECTRA AT UPPER LAGUNA MADRE
STATION 1

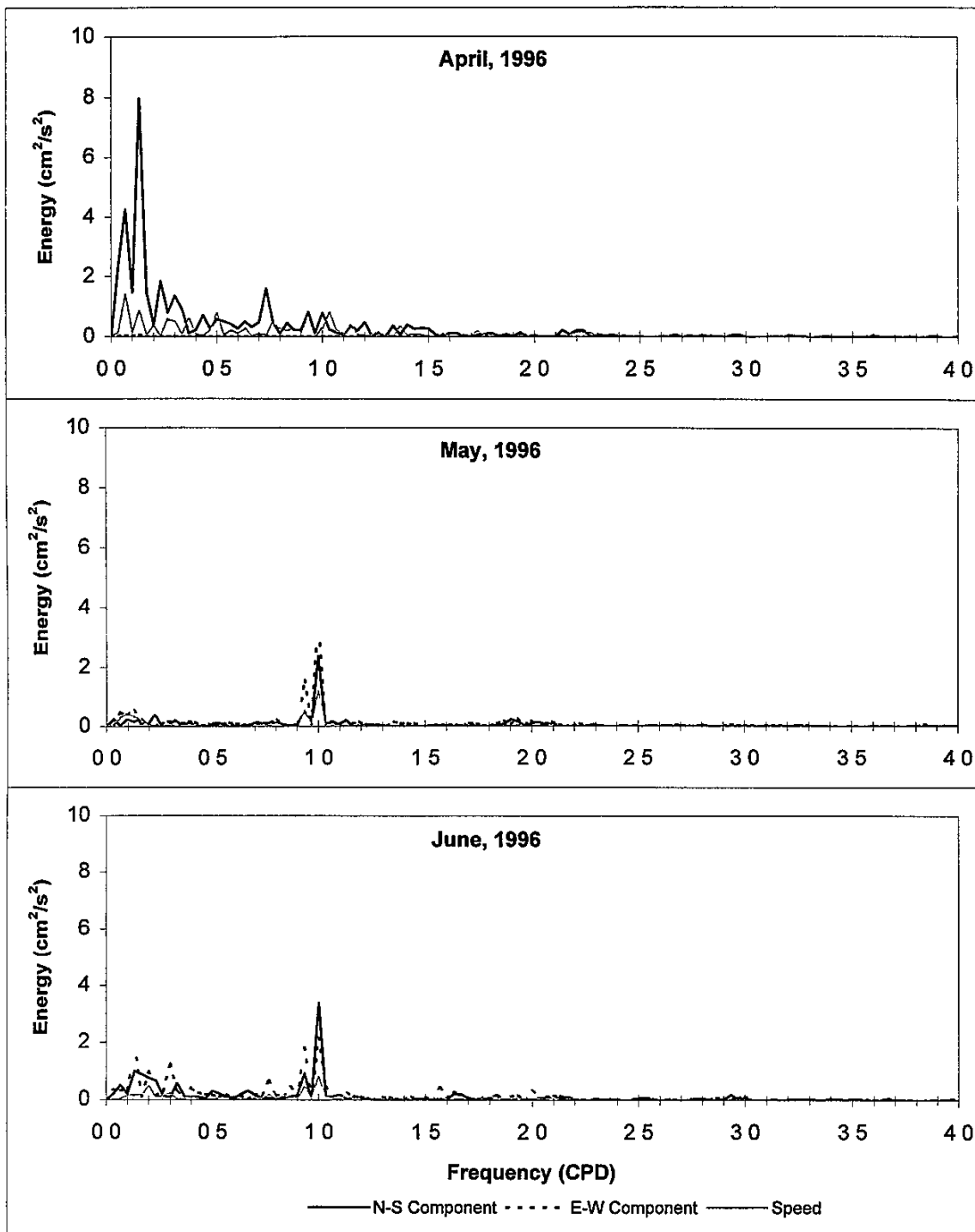


FIGURE 5-38
MONTHLY CURRENT SPEED SPECTRA AT UPPER LAGUNA MADRE
STATION 1

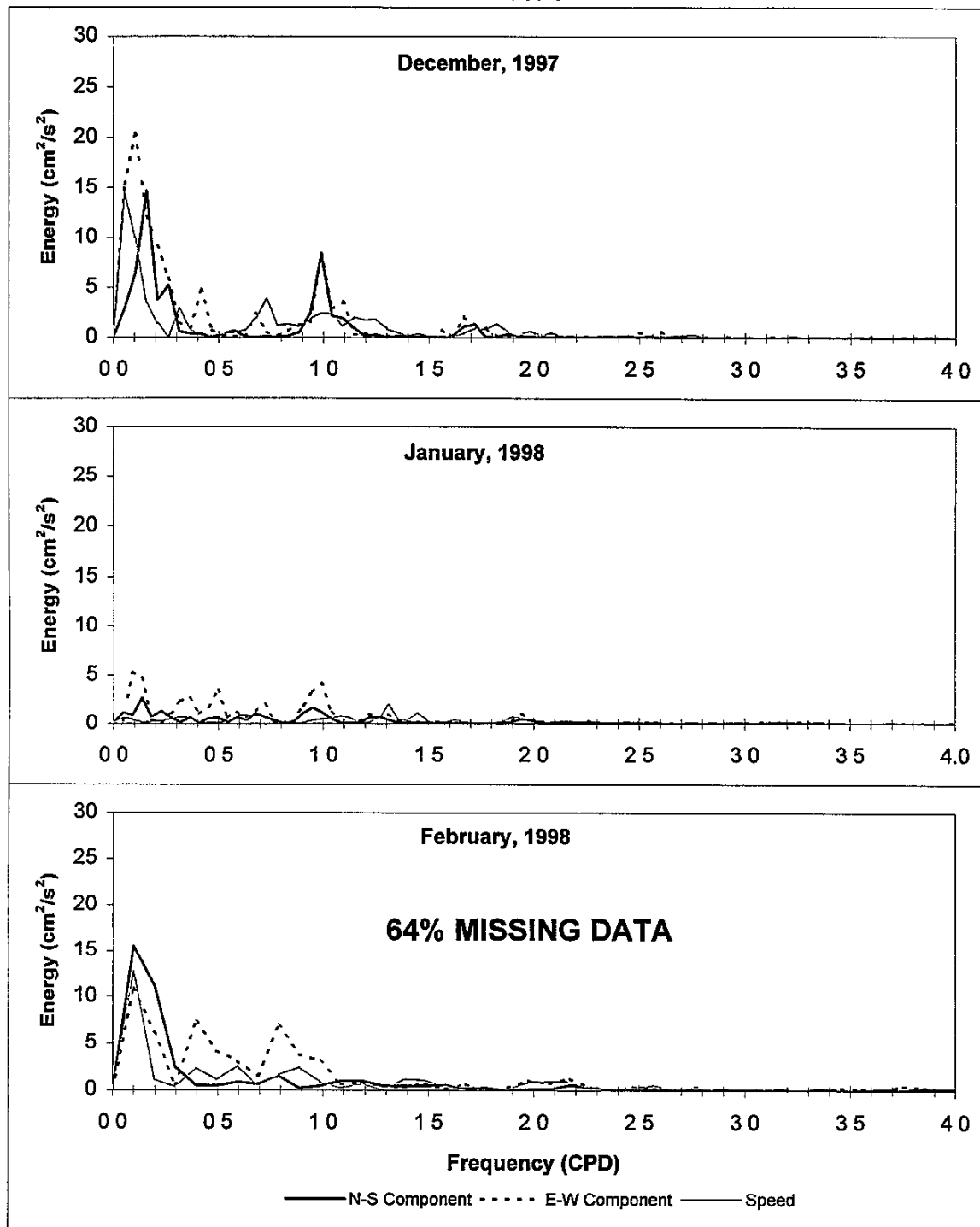


FIGURE 5-39
MONTHLY CURRENT SPEED SPECTRA AT UPPER LAGUNA MADRE
STATION 2

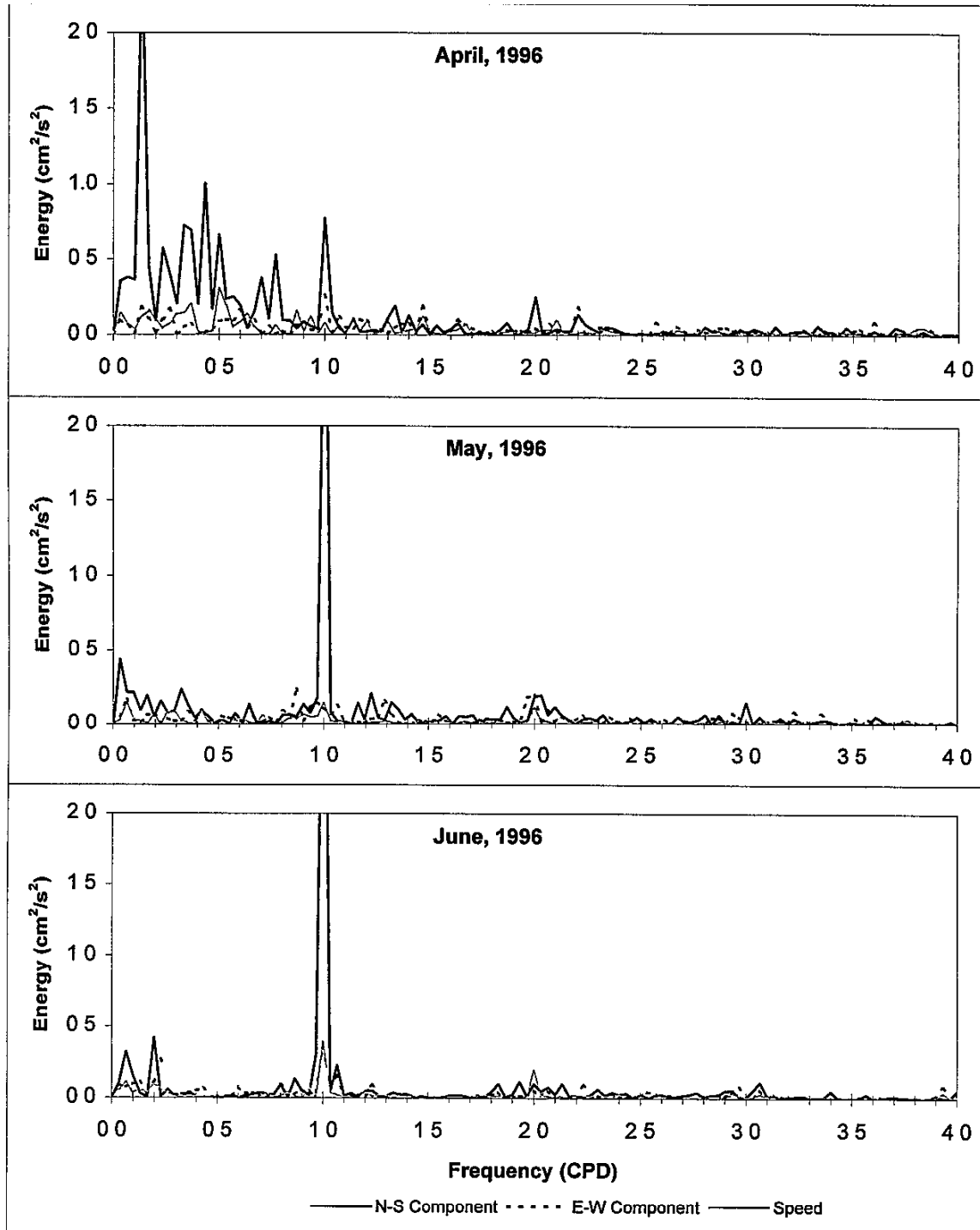


FIGURE 5-40
MONTHLY CURRENT SPEED SPECTRA AT UPPER LAGUNA MADRE
STATION 2

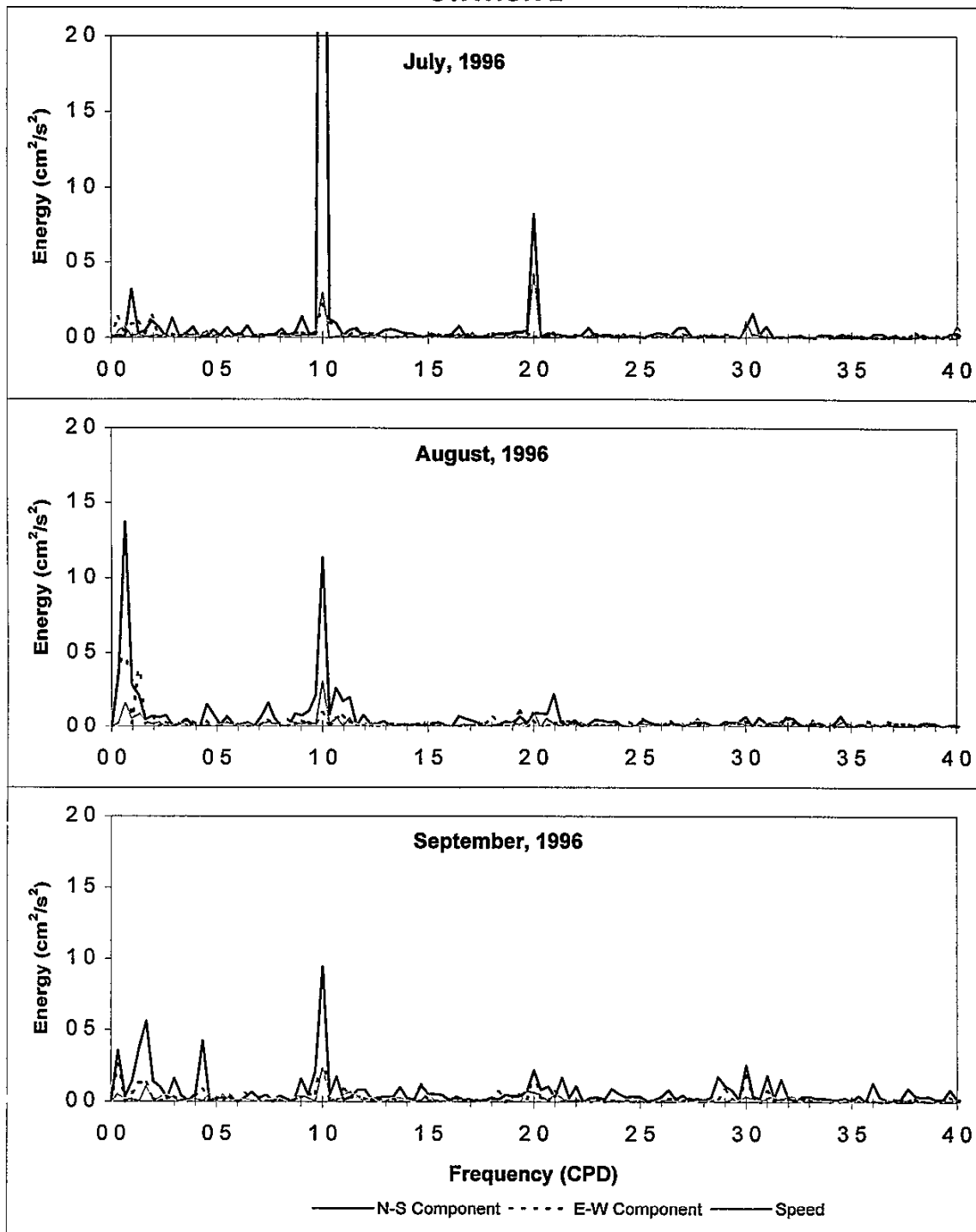


FIGURE 5-41
MONTHLY CURRENT SPEED SPECTRA AT UPPER LAGUNA MADRE
STATION 2

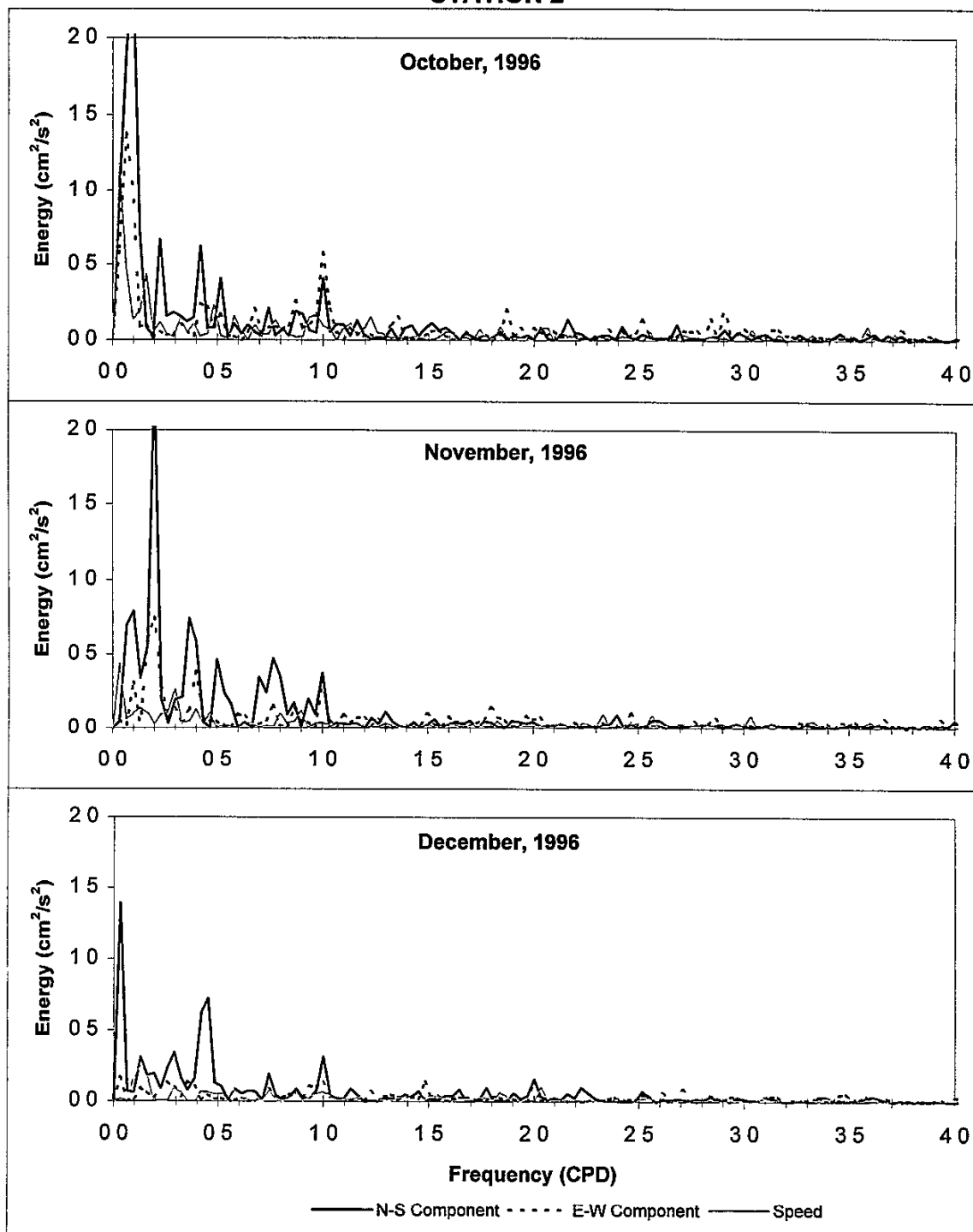


FIGURE 5-42
MONTHLY CURRENT SPEED SPECTRA AT UPPER LAGUNA MADRE
STATION 3

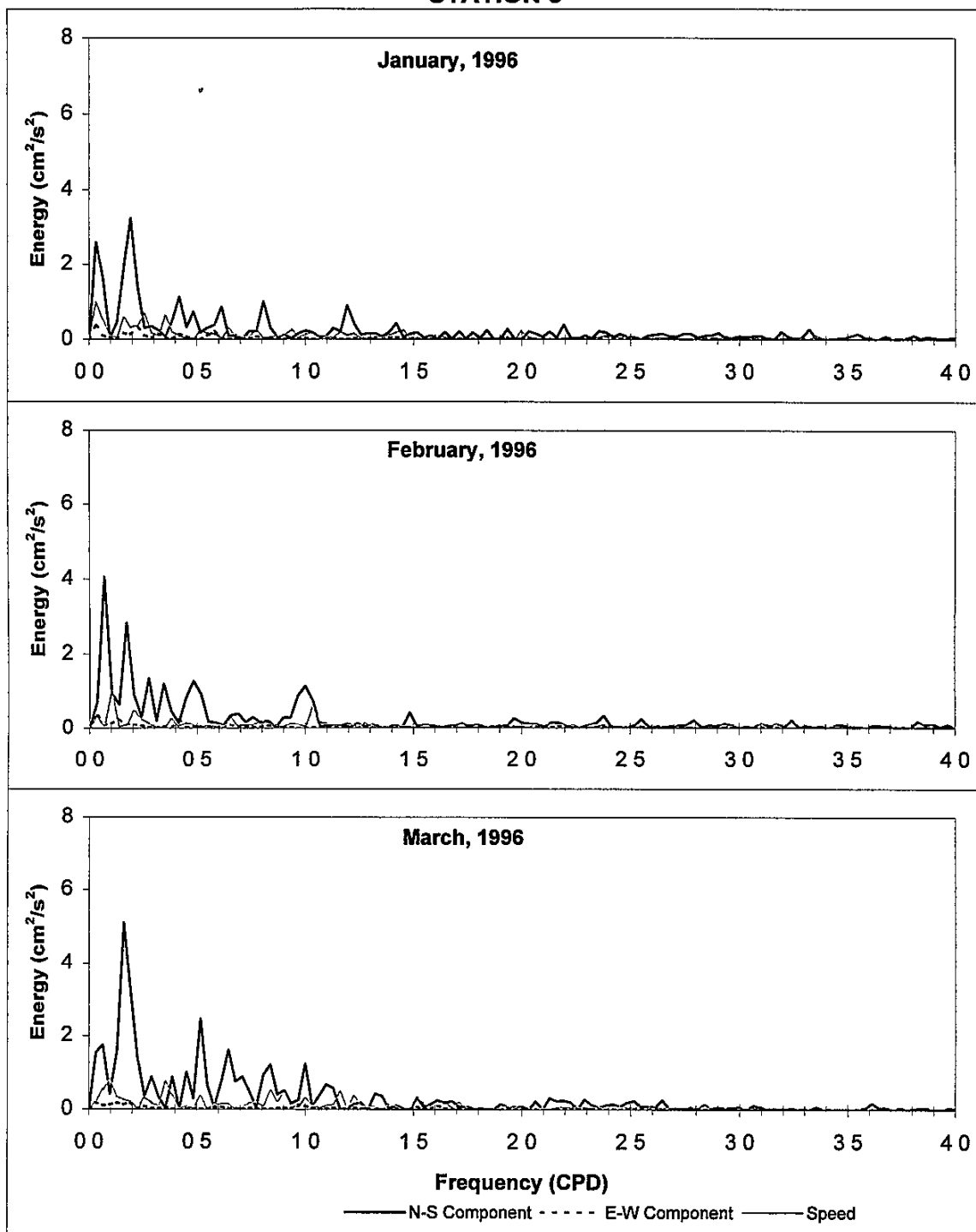


FIGURE 5-43
MONTHLY CURRENT SPEED SPECTRA AT UPPER LAGUNA MADRE
STATION 3

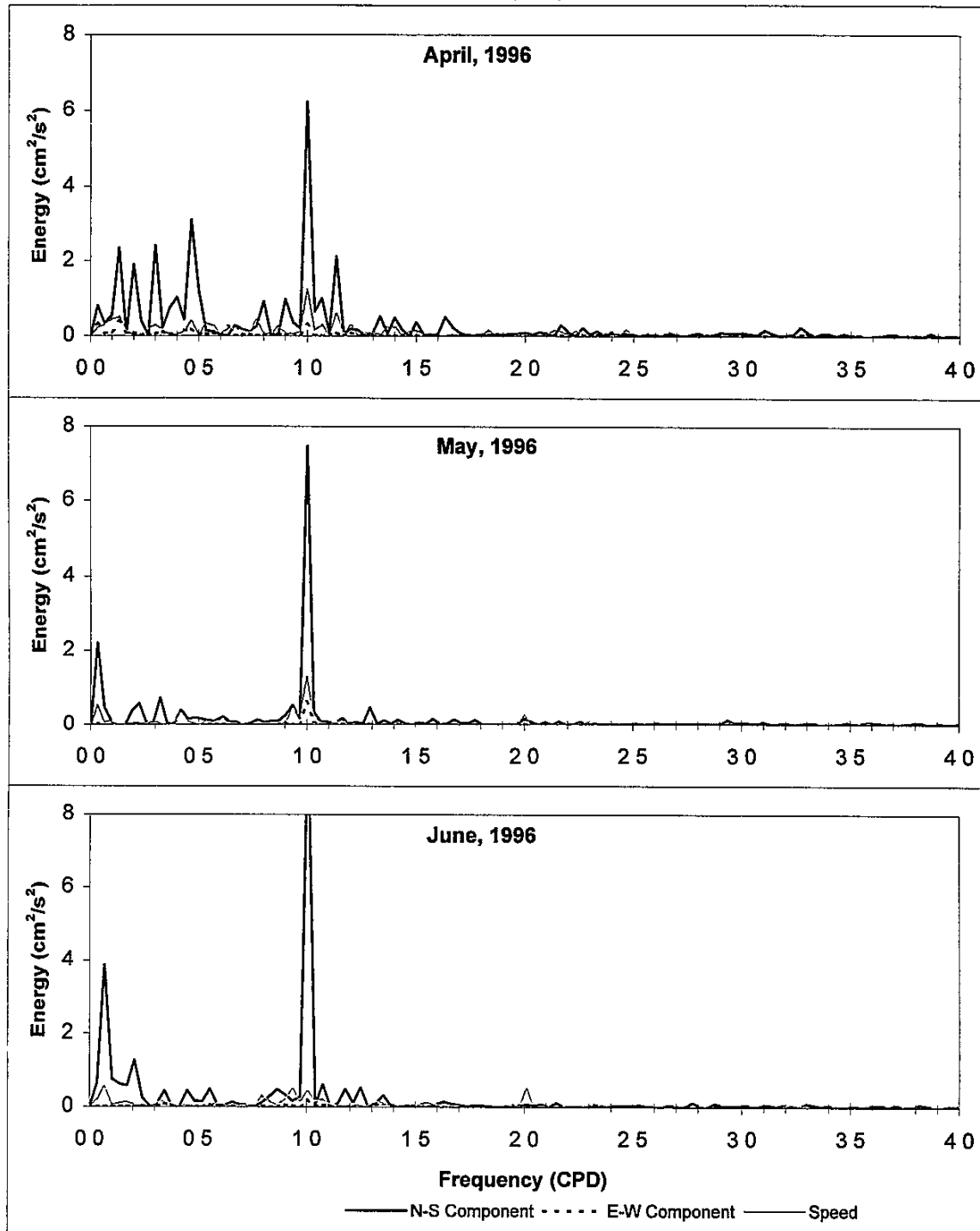


FIGURE 5-44
MONTHLY CURRENT SPEED SPECTRA AT UPPER LAGUNA MADRE
STATION 3

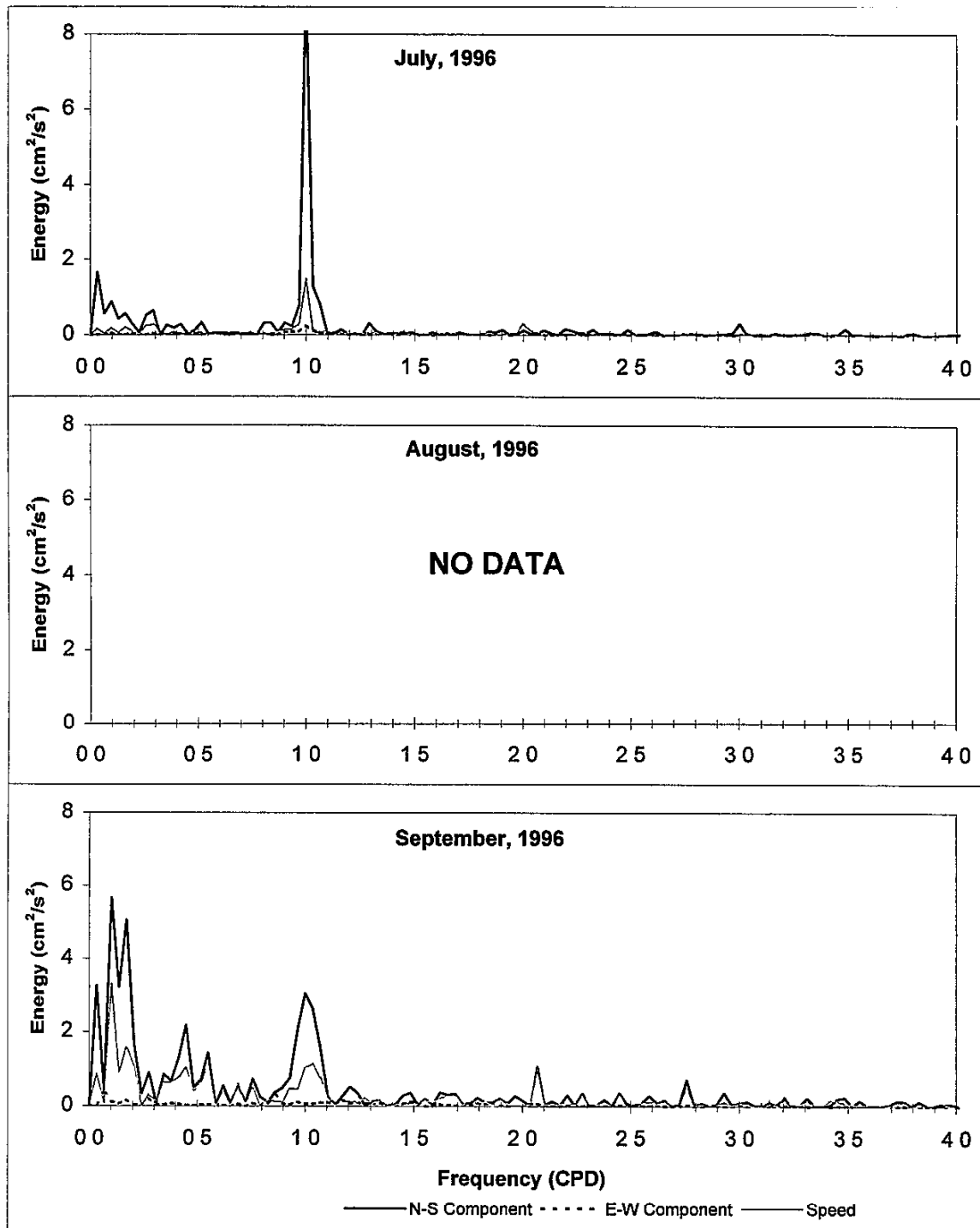
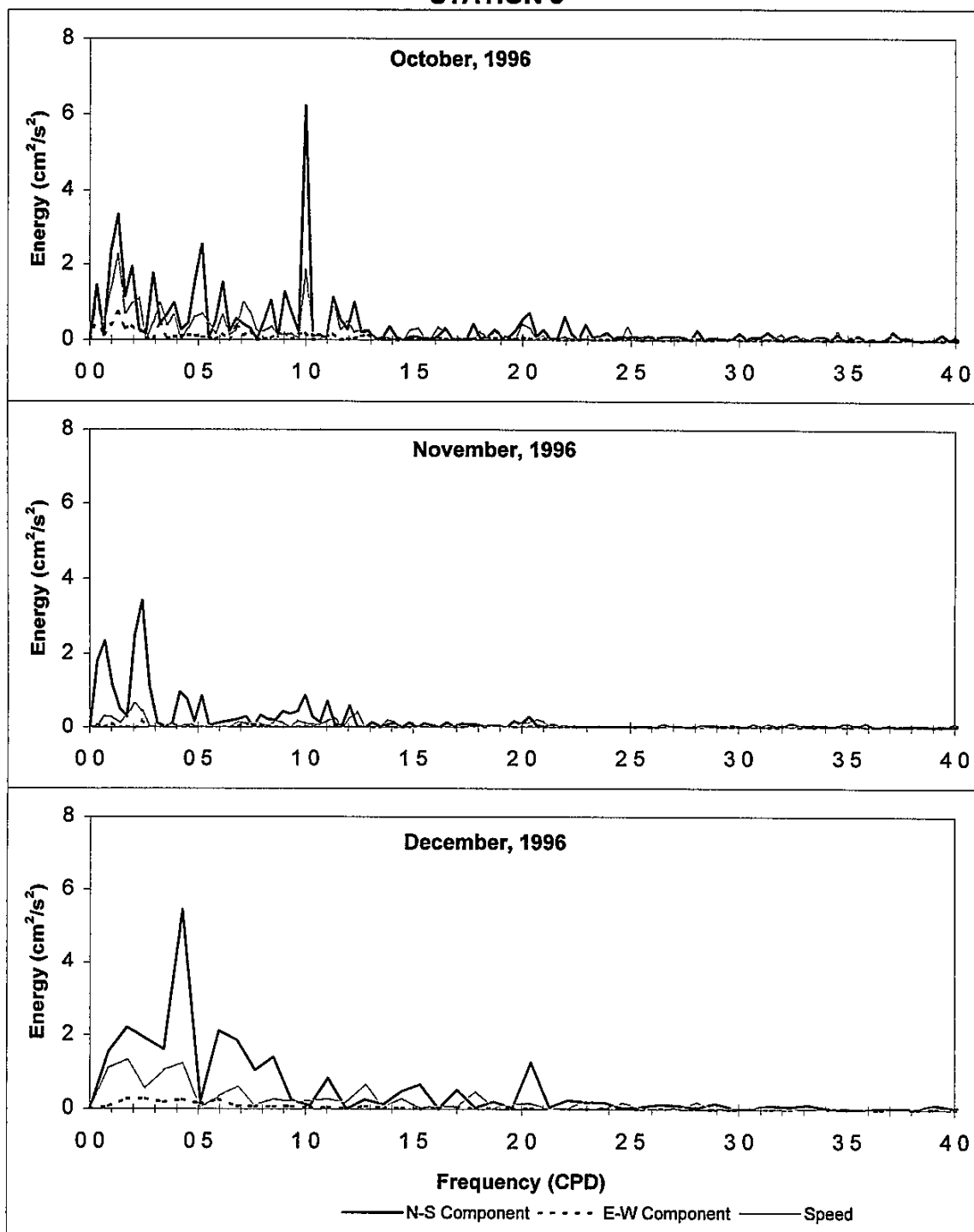


FIGURE 5-45
MONTHLY CURRENT SPEED SPECTRA AT UPPER LAGUNA MADRE
STATION 3



- (4) Energy in the lower frequency (longer period) portion of the spectrum is more prominent during the winter months than in the summer, and is more prominent in the Upper Laguna than in the Lower.

The most prominent peaks in the power spectra are at solar diurnal, and lunar diurnal and semidiurnal periods. These correspond to the seabreeze and the principal diurnal and semidiurnal tides, respectively. The solar diurnal is a pure periodicity of 24 hours. A spectrum does not discriminate the sources of a given periodicity. There are components in the *astronomical* tide of 24-hr periodicity, and, of course, the seabreeze is a 24-hr period signal. Both of these contribute to the spike at this period in the spectra, but it is impossible to separate their effects from a spectral analysis alone. The lunar tidal components are more complex. The standard elementary dynamics indicate periodicities of 24.8 hrs and 12.4 hrs, and if the moon revolved in a perfect circle about the earth, these would indeed result. But the effect of an elliptical orbit whose plane crosses both those of the earth's rotation and the solar ecliptic, combined with various additional astronomical perturbations is to replace the simple periodicities of 24.8 and 12.4 hours with line spectra. These are further filtered or amplified by the propagation of the tide wave itself interacting with the boundaries of the basin (in the present case, the Gulf of Mexico), see Pugh (1987). On the Texas coast, the principal lunar component of period 1.076 solar days makes up the majority of the energy in the lunar diurnal component. Thus in Figure 5-31 *et seq*, the lunar diurnal component appears closer to 0.93 cpd than the simple 24.8-hr frequency of 0.98 cpd. Lee (1997) in a careful spectral analysis of observed tides in Galveston Bay found the predominant energy to be in 12.420, 23.934 and 25.819 hr components. The results of Figure 5-31 *et seq*. are consistent with this.

Station LLM1 is located in the center of the Lower Laguna near the GIWW, and presumably on or near the principal tidal trajectory. Both the 24-hr and diurnal tidal component are most prominent at this station. Station LLM2a/N, on the other hand, is in a relatively sheltered region of the Laguna. This difference in location has a direct effect on the energy in the spectrum, there being much greater energy at LLM1, Figure 5-34, than at LLM2, Figure 5-35. (The difference is even more exaggerated than these plots would suggest, because they are plotted at different scales.) No data were taken at Station LLM3.

Station ULM1, which is in fact in Corpus Christi Bay north of Bulkhead Flats, exhibits substantial seasonal variation in the spectra, with low-frequency components (0.2 - 0.5 cpd) appearing in winter in association with frontal passages, and the 24-hr signal (1.0 cpd) becoming increasingly prominent in the summer and early fall, figures 5-36 through 5-38. The spectra from Data Set IV, the re-equipped program, Figure 5-38, are broader and "noisier" than those of Data Sets I-III, this is primarily due to the resolution of the data, being 30 mins for the former and 6 mins for the latter. In ULM2, in the Upper Laguna in the mouth of Baffin Bay, the tidal components are missing, the 24-hr signal from the seabreeze

builds steadily through the spring, Figure 5-39, to a maximum in July then subsides in the autumn, Figure 5-40.

The lower frequency signals are apparent from fall through early spring, figures 5-40 and 5-41. ULM3 exhibits basically the same behavior as ULM2, except that more of the component energy is in the north-south (u) component, which agrees with the geometry of the Laguna at this station location.

This chapter presents the suspended sediment and related data collected in this study. The inferred mechanisms of resuspension are introduced and summarized, but this subject is given more detailed treatment in the following chapter in the context of interactions among hydrographic variables. Suspended sediments, *a.k.a.*, suspended solids, are measured by filtration as the total suspended solids (TSS), a laboratory procedure that is relatively unaffected by sample handling, is inexpensive and straightforward. Probably the most important aspect of sediment in the present context is its texture, *viz.* the distribution of grain sizes.

Sediments in shallow-water environments are mobilized by currents, in turn generated by various hydrographic or meteorological processes that include tidal currents, wind-driven currents, responses of water movement to larger scale forcing by meteorology or tides, and windwave-induced currents. Resuspension of sediment is site specific and dependent upon numerous factors including water depth, bottom type (e.g., presence or absence of vegetation, sediment grain size, sediment cohesion and bottom configuration), and proximity to sediment sources, as well as fetch (the distance that the wind blows over water). In shallow-water systems with fine-grained sediments, such as the Laguna Madre, wind-generated waves are often the dominant mechanism for sediment resuspension (Ward, *et al* 1984, Shideler 1984, Pejrup 1986, Schoellhammer 1995). There are numerous practical implications of increased sediment resuspension, which are relevant to the present project, including increased sediment transport resulting in shoaling of maintained channels, and increased light attenuation that may reduce available seagrass habitat and/or production.

With respect to the latter, the presence of suspended matter in the water column interferes with the passage of light, thereby increasing the turbidity of the water. This provides an alternative means of measuring suspending particulates, *viz.* some parameter related to water turbidity. As noted in Chapter 2, the platform equipment for the present project included an OBS-turbidimeter, to provide a virtually instantaneous measure of turbidity. The potential of the high time resolution afforded by an automatic electrometric measurement compared to the labor-intensive process of collecting a water sample for laboratory analysis, warranted an experiment in operating the OBS. Another parameter is the attenuation coefficient of light, the rate constant in the exponential decline of light intensity with depth in the water column. In the Year-1 report, Kaldy and Dunton (1996) analyze the relations between suspended solids, photosynthetically available radiation, and light attenuation coefficient.

In general, estuarine sediments derive from three basic waterborne sources, fluvial, littoral and internal re-working (Ward and Montague, 1996). In addition, there is an airborne source of sediment, referred to as aeolian, that can be important in regions with strong winds and easily mobilized surface

sediments. Fluvial describes those sediments carried into the estuary by flowing water from the land surface, especially streams and rivers. Littoral applies to those sediments entering the estuary from the sea, primarily from the littoral zone of the nearshore, which in turn may originate from the Inner Continental Shelf, from the surf zone or the beach (including barrier islands). Internal reworking refers to the erosion of the boundary and bed of the estuary, mobilizing sediments laid down in earlier time periods. Sediments in Laguna Madre are derived from all of these sources, most important being sands and finer particulates from the barrier island, deflation of mudflats, erosion of prehistoric sand bars, and silts and clays from mainland drainage such as the Arroyo Colorado. Shepard and Rusnak (1957) found that the surficial sediment distribution of the study area consists of primarily sand on the eastern side of the laguna, most probably transported from the barrier island by wind action, with the sand content (relative to silts and clays) decreasing with distance from the barrier island. In the deeper portions of the study area and near the mouth of the Arroyo Colorado, the silts and clays begin to dominate the surficial sediment distribution. (Of course, silts and clays also originating from the barrier island environment will be carried farther inland than sands, so this distribution of finer inland does not unequivocally imply a fluvial source.)

Breuer (1962) observed that the turbidity in lower Laguna Madre was highly variable, an observation with which most workers will readily agree. However, he posited that the most important factor influencing the distribution of turbidity was the presence or absence of vegetation. Breuer also found that the turbidity was less over a sandy bottom, such as along the bay side of South Padre Island, and greater over a silt or clay bottom, such as in the deeper portion of the study area. These observations accord generally with the expected effect of clays and silts on light penetration together with their propensity for being easily resuspended in the water column.

Once mobilized, sediments are readily transported by currents, and the effect of suspended sediments on light penetration produces dramatic patterns of water appearance in high-altitude imagery. Under the right conditions, the patterns of transported sediment can be used as an indicator of current patterns. Ward (1993) presented a dramatic example of turbidity-delineated streak lines in Galveston Bay. In the study area, James, *et al* (1977) inferred circulation and sediment transport patterns from satellite imagery of suspended sediment. One of their images, showing a turbid plume to cross the GIWW in the south area of the Lower Laguna Madre, was reprinted by Brown and Kraus (1997), who pointed out that the location of this plume was in the general area of a high maintenance-dredging reach and aligned with a cross-channel component of current indicated by the current measurements from Data Set I. This is discussed further in Chapter 7.

One special process of sediment mobilization is that of dredging. The disruption of bed sediment by the cutter head, and the locally intense currents associated with dredge operation, as well as fugitive injection of sediment into the water column when these sediments are deposited in a placement area,

all can result in substantially higher suspended sediments in the vicinity of such dredging operations. Unfortunately, there is very little data applicable to the Lower Laguna to quantify the importance of such anthropogenic sediment resuspension, compared to natural processes.

In the Year-1 report, Brown and Kraus examined the 16-month period September 1994 - December 1995, the period of data then available to them. The first half of this period, through April 1995, was characterized by higher suspended solids. Dredging was known to have begun in the Lower Laguna reach of the GIWW in late-September 1994 and to have been completed in late autumn. Brown and Kraus (1997) subdivided this period into "pre-dredging" (31 August - 25 September), "dredging" (26 September - 29 October), and "post-dredging" (31 August - 25 September 1995), and found significantly higher concentrations in the "dredging" period compared to either "pre-dredging" or "post-dredging". They note that in the "pre-dredging" period, the concentration of suspended solids was typically less than approximately 200 mg/L. "During dredging", the variation in TSS increased and frequently exceeded 400 mg/L. In the "post dredging" period, TSS returned to levels similar to those observed in "pre-dredging". With the larger data base available to us, after nearly two additional years of TSS data collection, we present the TSS variation over the study period and revisit its association with dredging.

Figures 6-1 and 6-2 show the concentrations of total suspended solids in the Lower and Upper Laguna Madre, respectively. (The complete time plots of TSS are given in Appendix TS) The contract periods of dredging are also shown on these same plots, based upon records of Galveston District Corps. Several qualifications need to be registered about this information. These are the *contract* periods. There is no information as to when dredging started, when it ended, which end of the dredged reach the dredge began at, or where the dredge was in the contracted reach at any point during the contract period. In the Lower Laguna, the same dependency observed by Brown and Kraus (1997) is evident in Figure 6-1, with higher TSS magnitudes during the dredging periods than prior to the contract or (one year) after the contract terminated. While dredging would appear to be a factor, there are clearly other processes operating, because the TSS magnitudes are nearly as large in spring of 1996 when no dredging was underway. Brown and Kraus (1997) noted that "a portion of the increase in concentration of suspended solids immediately subsequent to dredging may be attributable to changes in the meteorological conditions and the increased frequency of passage of fronts."

In the Upper Laguna, Figure 6-2, the data is equivocal, partly due to the fact that the contract dredging period was not well sampled. There does seem to be a propensity for extremes in TSS to occur in January in the Upper Laguna reach, including ULM1 in Corpus Christi Bay. But there is no clear difference between "dredging" and "post-dredging" periods.

FIGURE 6-1
TOTAL SUSPENDED SOLIDS LEVELS AT LLM STATIONS

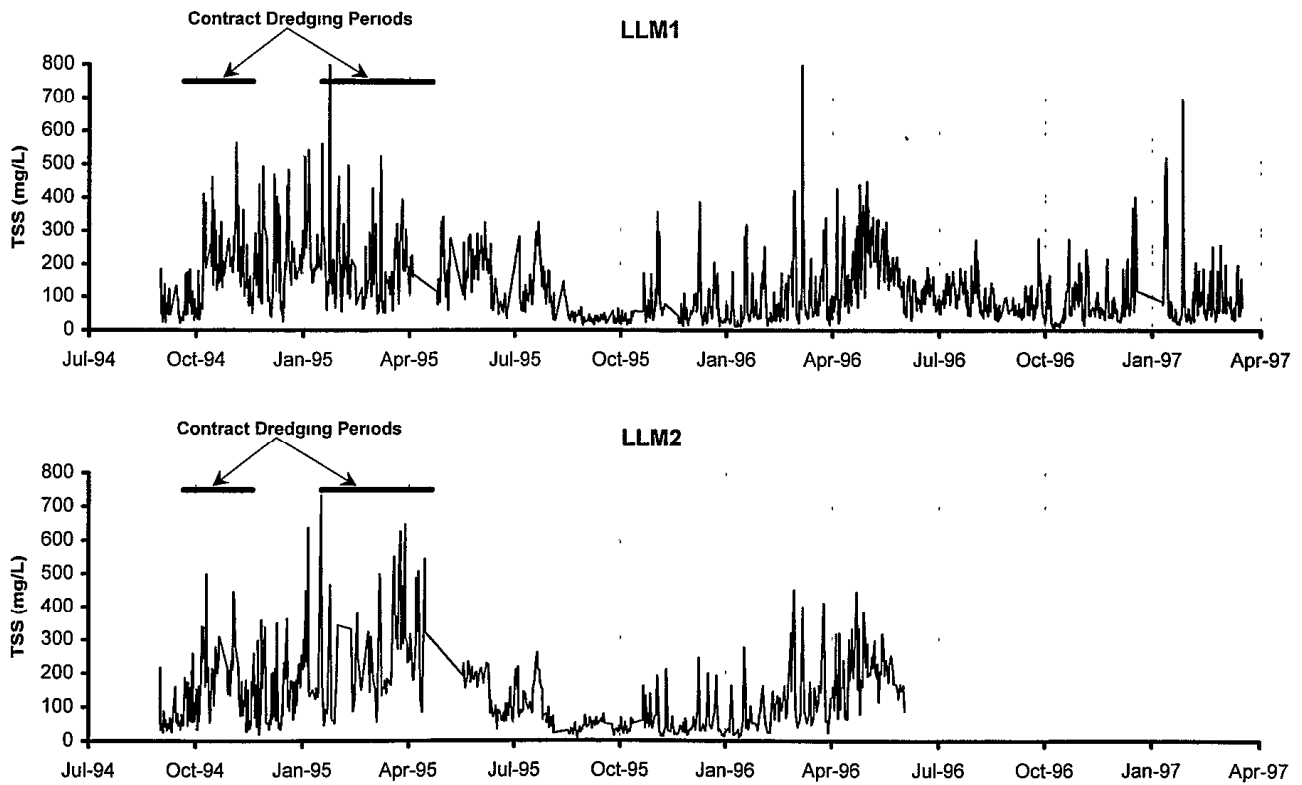


FIGURE 6-1 (Concluded)
TOTAL SUSPENDED SOLIDS LEVELS AT LLM STATIONS

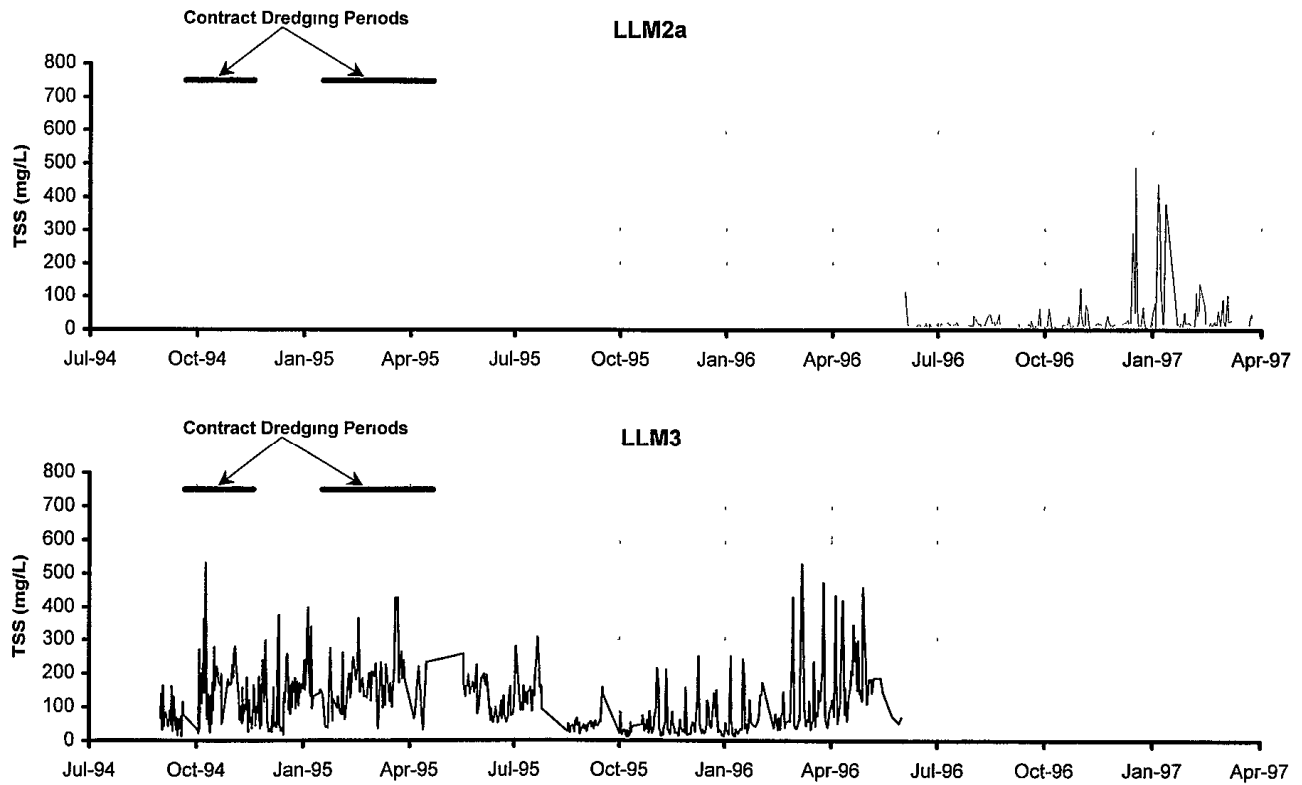
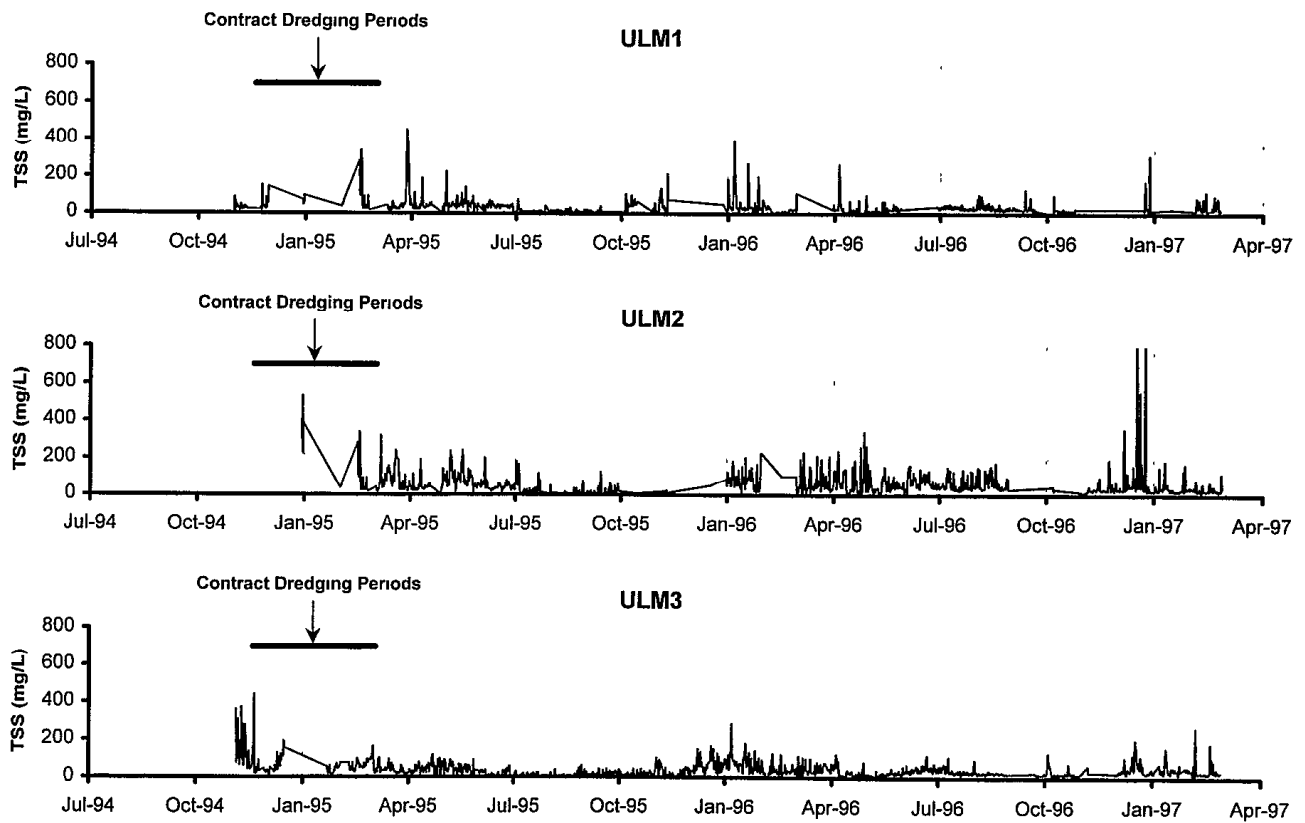


FIGURE 6-2
TOTAL SUSPENDED SOLIDS LEVELS AT ULM STATIONS



**TABLE 6-1
SUMMARY OF STATISTICS FOR TOTAL SUSPENDED SOLIDS**

LLM Station	No Dredging (pre-09/21/94)					Dredging (09/21/94-11/19/94)					No Dredging (11/20/94-01/16/95)				
	Data Range		No of Samples	TSS (mg/L)		Data Range		No of Samples	TSS (mg/L)		Data Range		No of Samples	TSS (mg/L)	
	Begin	End		Mean	St Dev	Begin	End		Mean	St Dev	Begin	End		Mean	St Dev
LLM1	08/31/94	09/20/94	28	71.4	42.2	09/21/94	11/19/94	101	180.7	106.5	11/20/94	01/16/95	103	214.6	110.9
LLM2	08/31/94	09/20/94	37	61.4	38.0	09/21/94	11/19/94	86	161.1	95.6	11/20/94	01/16/95	100	172.2	118.5
LLM2a															
LLM3	08/31/94	09/20/94	25	70.7	42.4	10/02/94	11/19/94	71	136.8	87.3	11/20/94	01/15/95	92	135.4	84.0

LLM Station	Dredging (01/17/95-04/22/95)					No Dredging (Post-04/22/95)				
	Data Range		No of Samples	TSS (mg/L)		Data Range		No of Samples	TSS (mg/L)	
	Begin	End		Mean	St Dev	Begin	End		Mean	St Dev
LLM1	01/17/95	04/05/95	130	191.1	173.1	04/26/95	03/19/97	1,214	105.7	89.6
LLM2	01/17/95	04/16/95	70	255.9	150.9	05/19/95	06/04/96	374	106.1	86.8
LLM2a						06/04/96	03/26/97	255	31.6	57.7
LLM3	01/17/95	04/16/95	74	163.1	84.7	05/19/95	06/02/96	317	98.5	88.3

ULM Station	No Dredging (pre-11/19/94)					Dredging (11/19/94-03/04/95)					No Dredging (Post-03/04/95)				
	Data Range		No of Samples	TSS (mg/L)		Data Range		No of Samples	TSS (mg/L)		Data Range		No of Samples	TSS (mg/L)	
	Begin	End		Mean	St Dev	Begin	End		Mean	St Dev	Begin	End		Mean	St Dev
ULM1	11/01/94	11/12/94	24	32.4	18.0	11/23/94	02/25/95	42	72.0	72.2	03/12/95	02/27/97	857	35.9	40.0
ULM2						12/30/94	03/04/95	29	117.1	136.3	03/05/95	02/28/97	1,040	58.6	64.5
ULM3	11/05/94	11/18/94	28	144.7	99.2	11/19/94	03/04/95	114	63.7	50.3	03/05/95	02/28/97	1,261	36.0	30.2

The previous chapters have presented the bare facts of data, using various statistics and tabular and graphical displays to communicate the information in the measurements. The present chapter assumes a more interpretive stance, exploring the apparent interactions among hydrographic variables, and identifying potential cause-and-effect relationships. The ultimate goal is to interpret the behavior of suspended sediment in the Laguna Madre, but the behavior of waves and currents are important intermediaries in pursuing this goal. The earlier interpretations of Militello and Kraus (1994) and Brown and Kraus (1997), based upon preliminary data holdings from this program, provide important precedents that in some cases are further reinforced by the newer data, and in some cases must be revised.

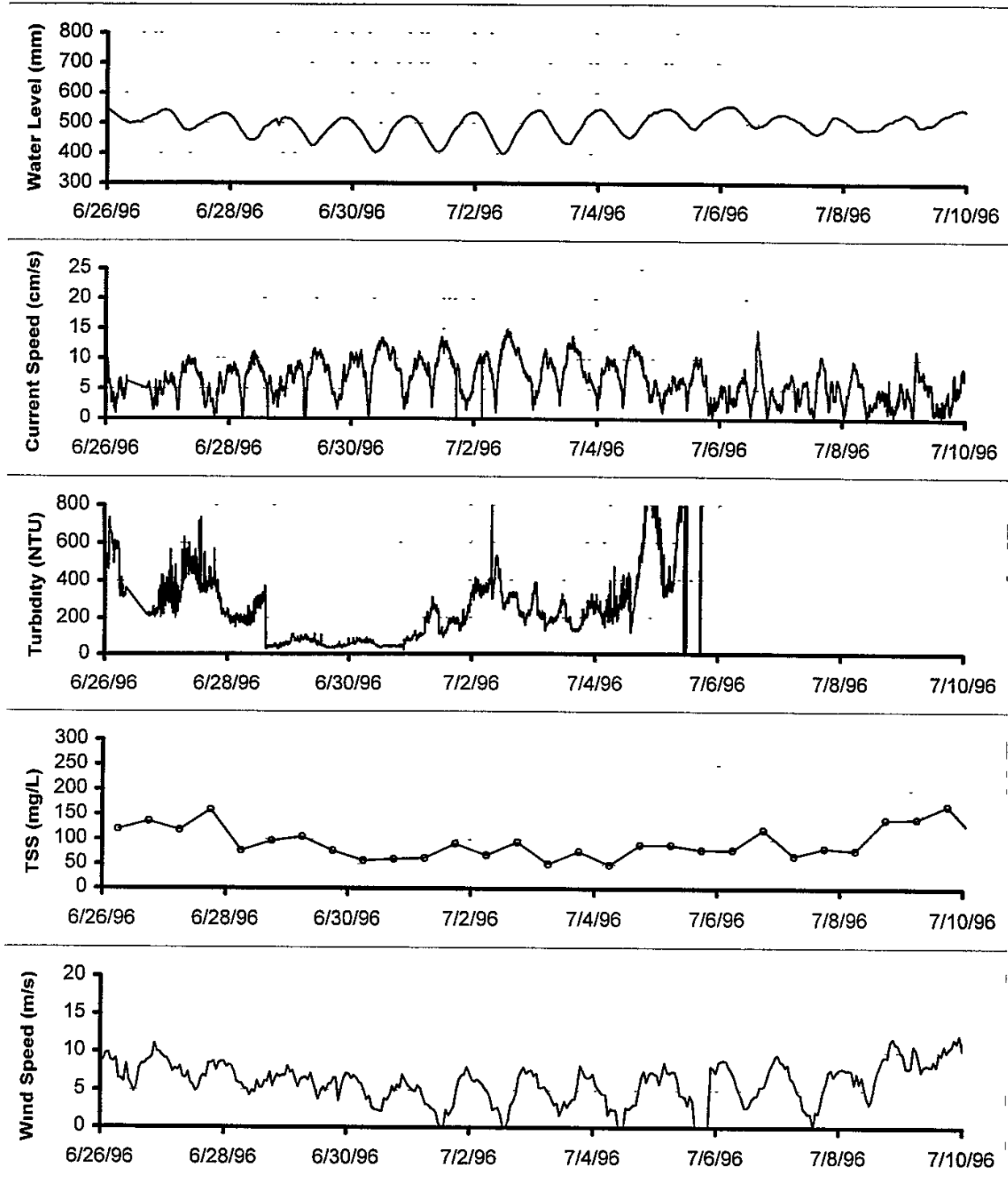
HYDROGRAPHIC INTERACTIONS AND SUSPENDED SEDIMENTSummer Conditions

The closest approach to quiescent conditions in the study area occurs in the summer, when the Laguna Madre region is relatively free of disturbances in the westerlies and the associated meteorological perturbations. Under these conditions, the Laguna is dominated by the seabreeze. As an example of the behavior of the hydrographic factors and the resulting turbidity, Figure 7-1 displays time series from late June and early July 1996, for the Lower Laguna areas. On the same plot are shown time series for water level, current speed, OBS turbidity, suspended sediment as measured by TSS, and wind speed.

It will be recalled (Chapter 5) that this region is affected by the diurnal lunar tide in addition to the seabreeze. A quasi-diurnal variation is evident in both the water level and the current speed. Because there are two components of nearly equal periodicity, viz 24-hr and 25-hr periods, it is difficult to differentiate these by eye (which is why one performs a spectral analysis). Nevertheless, the essentially diurnal variation in these parameters is apparent. (At first glance, the current speed appears to have a strong semidiurnal component, but this is an illusion. Because the current speed oscillates through zero—as the current reverses—the time plot of its magnitude, viz speed, is rectified.) The variation introduced by the seabreeze is evident in the time plot for wind speed.

This graph also illustrates why the OBS turbidimeter data is not used in these analyses. The signal is clearly corrupted, as matters turned out due to biofouling of the sensor. However, short segments of the record do yield some useful insight. For example, in Figure 7-1 from about noon on 2 July through 5 July, a clear semidiurnal signal in OBS turbidity emerges. This is coherent with the variation of current speed, and is clearly due to resuspension of sediment at the race of the current. Overall, the elevated TSS on 26-27 June and on 8-9 July appear to be most correlated with the wind, which has higher speeds and no

FIGURE 7-1
LLM1 WATER LEVEL, CURRENT, TURBIDITY, TSS AND WIND SPEED
DURING TIDALLY-DOMINATED FLOW



overnight calm during these periods. If the mechanism is wind waves, their effects on currents are not clear, unless it may be the increasing noise in the current record toward the end of the period shown

Figure 7-2 shows similar plots for ULM1 in lower Corpus Christi Bay. (The water level record shown is that of the TCOON Packery Channel gauge, not S Bird Island) Even though the same wind behavior is manifested here, there is no corresponding response in the TSS values. Instead these remain more or less 50 mg/L throughout the displayed period. The current speeds here are noisier than at LLM1, without as clear a diurnal signal. There is a slight increase in current speeds in the last 2 days of the record (correlating with the increase in sustained wind speeds) but no corresponding effect on TSS.

Figures 7-3 and 7-4 display the same variables and period for the Upper Laguna stations at Baffin Bay and the mudflats. Water level variation displays a slight diurnal component, considered (from the spectral analyses of Chapter 5) to be primarily the seabreeze effect. Current speeds are small and variable. The OBS turbidity is evidently buggy throughout this period, while the TSS values vacillate around 50 mg/L. At ULM2, in the mouth of Baffin Bay, there is an increase in TSS associated with the increasing windspeeds in the last 2 days of the record.

During the plotted period of figures 7-1 through 7-4, the tidal variation in the LLM slowly varies from a small declination to great declination, back to small declination over the 14 days plotted, as illustrated by the range, but no correlation is evident with TSS. During this data collection period, the moon's maximal declination was near its minimal epochal value, on 30 June, $18^{\circ} 35.4'$, passing through zero on 23 June (3 days before the plotted period of Figure 7-1) and 7 July. During the Data Set I period treated by Brown and Kraus (1997), the maximal lunar declination was still low, around 20° .

Brown and Kraus (1997) argue that in order for bed sediments to move, the current velocity at the bottom must exceed a certain threshold value, which they suggest should be, for a uniform current and 0.15-mm sand, in the range of 10 to 20 cm/sec. Such current speeds are barely attained in the 14-day periods of Figure 7-1, and this during the period of maximal declination, 28 June - 4 July, say. The turbidity and suspended solids during this period were at minimal levels showing no response at all. In fact, in the later period plotted of 8-9 July in which the observed TSS in fact increases, the currents subside to below this threshold. There are at least two reasons why TSS would seem to defy the specified threshold. First, the resuspensions may be due to wind wave action, perhaps some distance from the platform, and the suspended sediments are simply migrating into the platform area. Second, the turbidity is probably more influenced by silt and clay sediments rather than sands.

Based upon their analysis of Data Set I, Brown and Kraus (1997) note that tidal influence on sediment resuspension is "minimal," and observe that turbidity data (meaning TSS) indicate that the

FIGURE 7-2
ULM1 WATER LEVEL, CURRENT, TURBIDITY, TSS AND WIND SPEED
DURING TIDALLY-DOMINATED FLOW

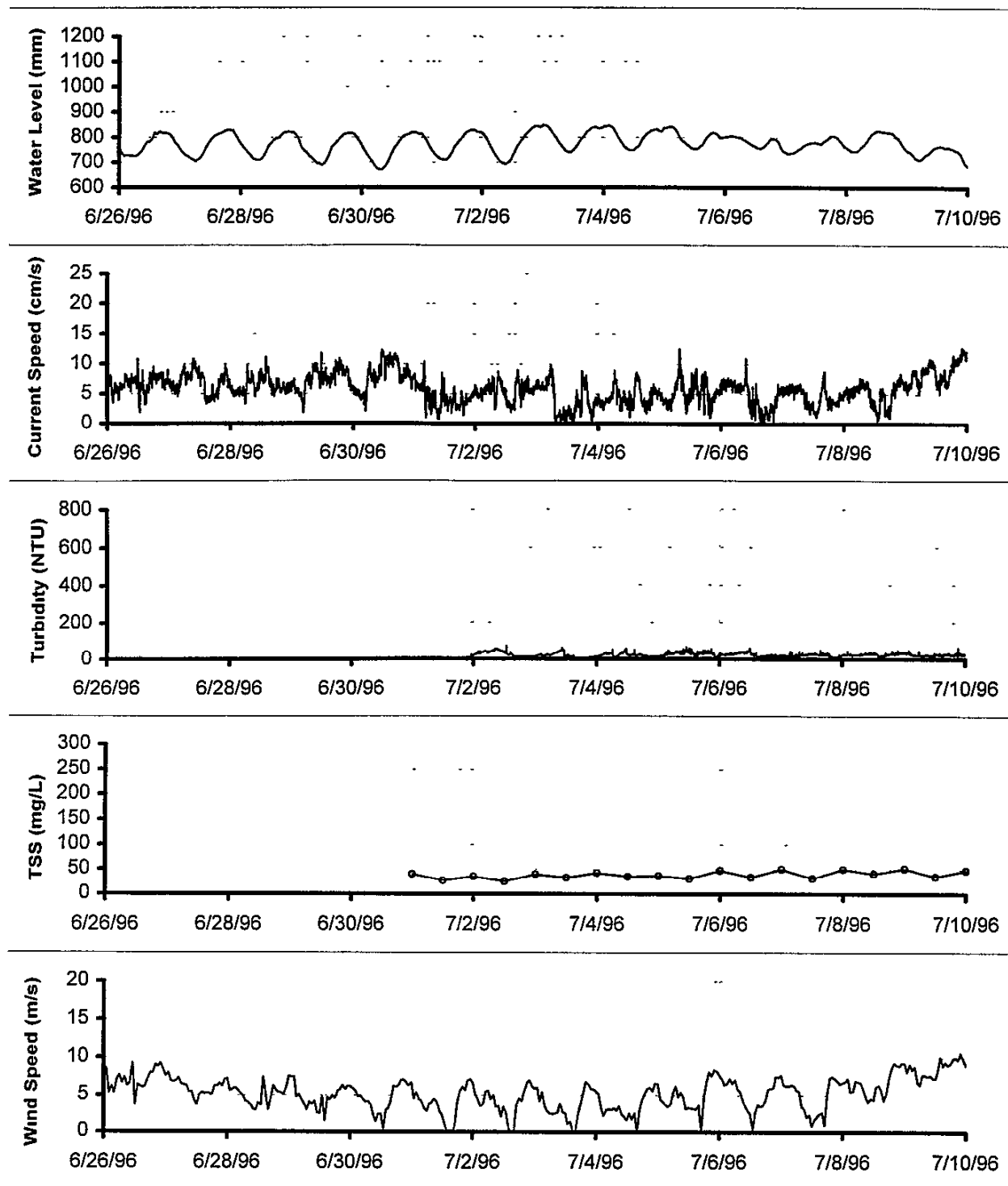


FIGURE 7-3
ULM2 WATER LEVEL, CURRENT, TURBIDITY, TSS AND WIND SPEED
DURING TIDALLY-DOMINATED FLOW

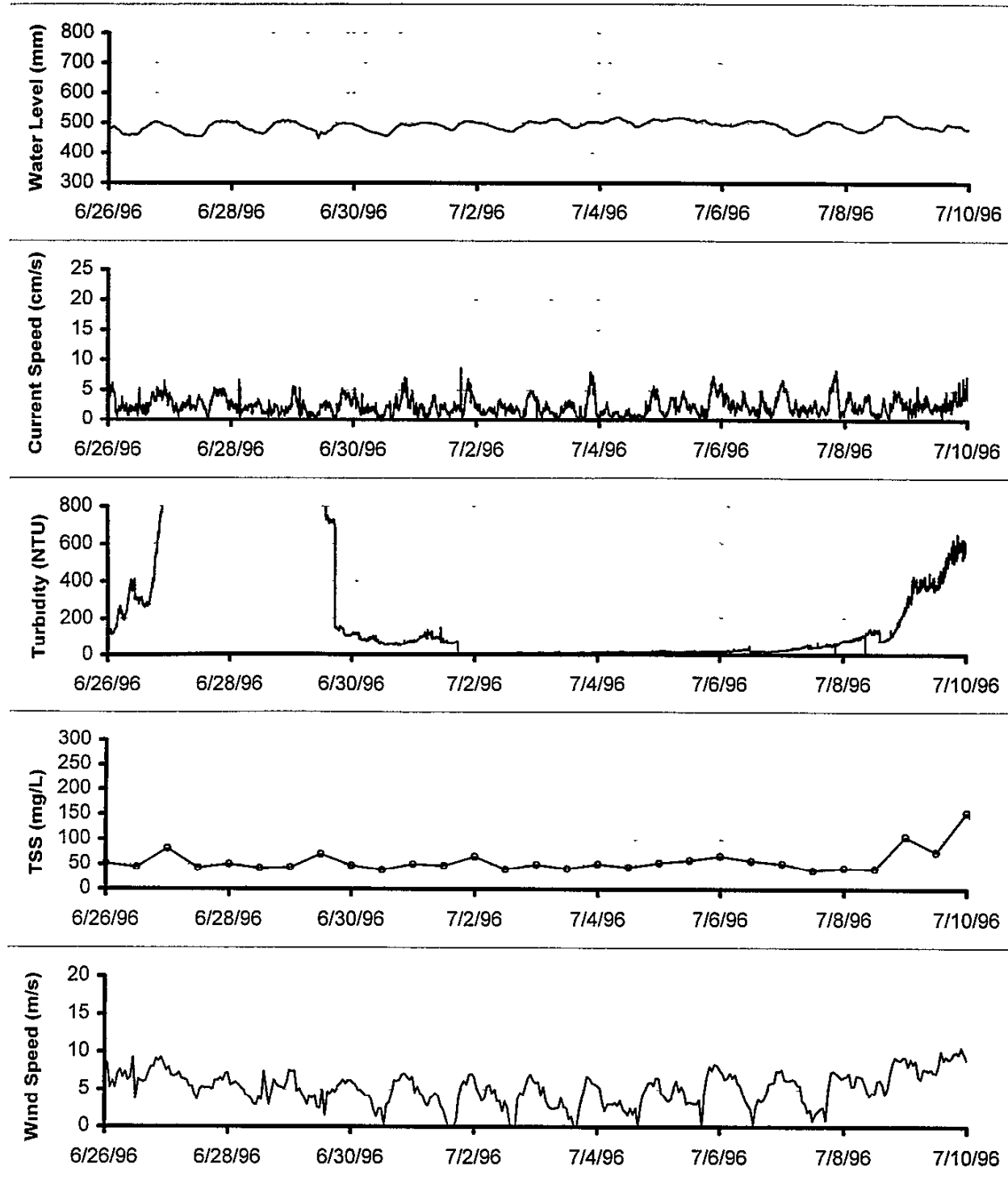
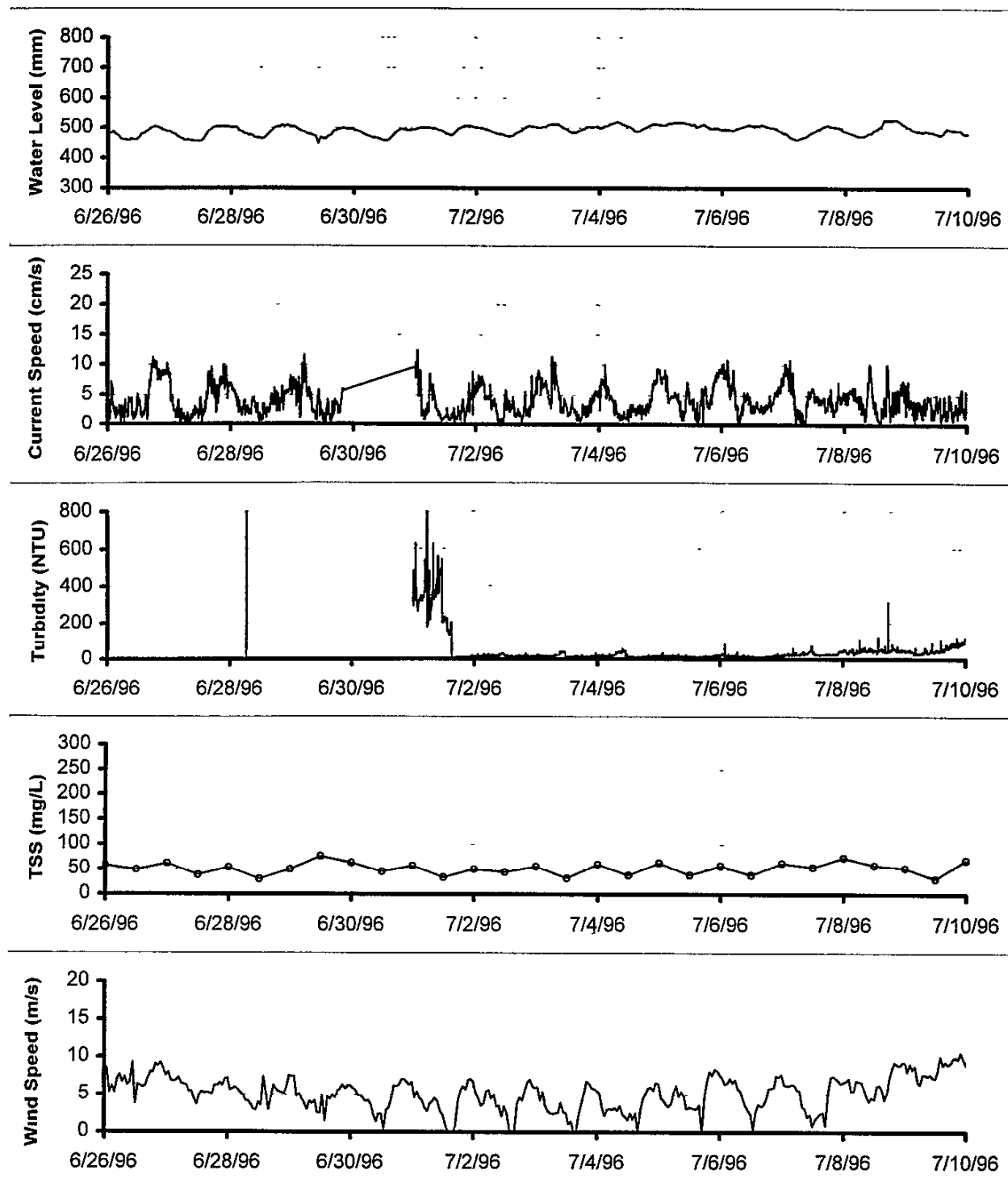


FIGURE 7-4
ULM3 WATER LEVEL, CURRENT, TURBIDITY, TSS AND WIND SPEED
DURING TIDALLY-DOMINATED FLOW



astronomical tidal current in the study area is not of sufficient magnitude to resuspend sediment for normal conditions. While one could bicker with the estimation of threshold of motion, this conclusion of Brown and Kraus (1997) is certainly illustrated by the time series of figures 7-1 through 7-4. On these and subsequent time plots, the tick marked with a date corresponds to 00 CST on that date. As noted above, all of this data was taken under low lunar declination conditions, in that even when lunar declination was maximal, it was still 20° or less (considerably less than the maximum possible value of $28^\circ 40'$). We may speculate that the currents in the study area might exceed the necessary resuspension threshold levels during peak ebb or flood tide when the moon is at larger declinations. Although the tidal current may not be effective in resuspending sediment, the current is a mechanism for transporting sediment once it is resuspended by some other mechanism.

7 1 2 Winter Frontal Conditions

Higher currents can also be produced by meteorological responses, so it is useful to examine a period in which such forcing was known to be operating. This is illustrated by figures 7-5 through 7-8, showing similar plots as above but for the periods 27 January - 9 February 1996 for figures 7-5 and 2-16 February 1996 for figures 7-6 through 7-8. (Again, in Figure 7-6, the water-level record is from TCOON Packery Channel, not S Bird Island.) In the plotted period of Figure 7-5, a frontal passage occurs mid-morning on 31 January, after which winds are from the northern quadrant for the next 5 days, veering and diminishing in speed in the last 3 days plotted. This is clearly an outbreak front (in the terminology of Ward, 1997), and during the next several days after the frontal passage, water levels decline monotonically in the Lower Laguna, as shown by the upper panel. The current variations are much more extreme than the summer case of Figure 7-1, but throughout the setdown period (1-5 February), lunar declination is falling to zero, so that tidal effects are insignificant. Winds are sustained at around 10 m/s. The reasons for the strong oscillations in current speed are not clear, their period is irregular from 8 to 12 hours, and there is no associated water level oscillation (which eliminates seiche as an explanation). The TSS response is dramatic, a prominent rise from the time of frontal passage to a maximum around 250 mg/L, then declining as winds start to subside on 5 February.

In figures 7-6 through 7-8, winds from the north prevail during the first several days of the plotted period (due to the same 31 January front). A second, less-intense reinforcing frontal passage occurs on 11 February. In Corpus Christi Bay, at ULM1, the currents are neither as high as at ULM1 nor are the oscillations as prominent. There is no TSS response, the values starting out at a low of 50 mg/L and becoming even smaller over the plotted 14-day period. In the Upper Laguna Madre at Baffin Bay, Figure 7-7, the currents are smaller yet. It should be noted that the water levels plotted, from the Bird Island gauge, are in fact in the upper reach of the Laguna Madre. It is well known that frontal passages initially move the water southward in the Upper Laguna, in response to north winds, then if the Gulf of

FIGURE 7-5
LLM1 WATER LEVEL, CURRENT, TURBIDITY, TSS AND WIND SPEED
DURING FRONTAL PASSAGE

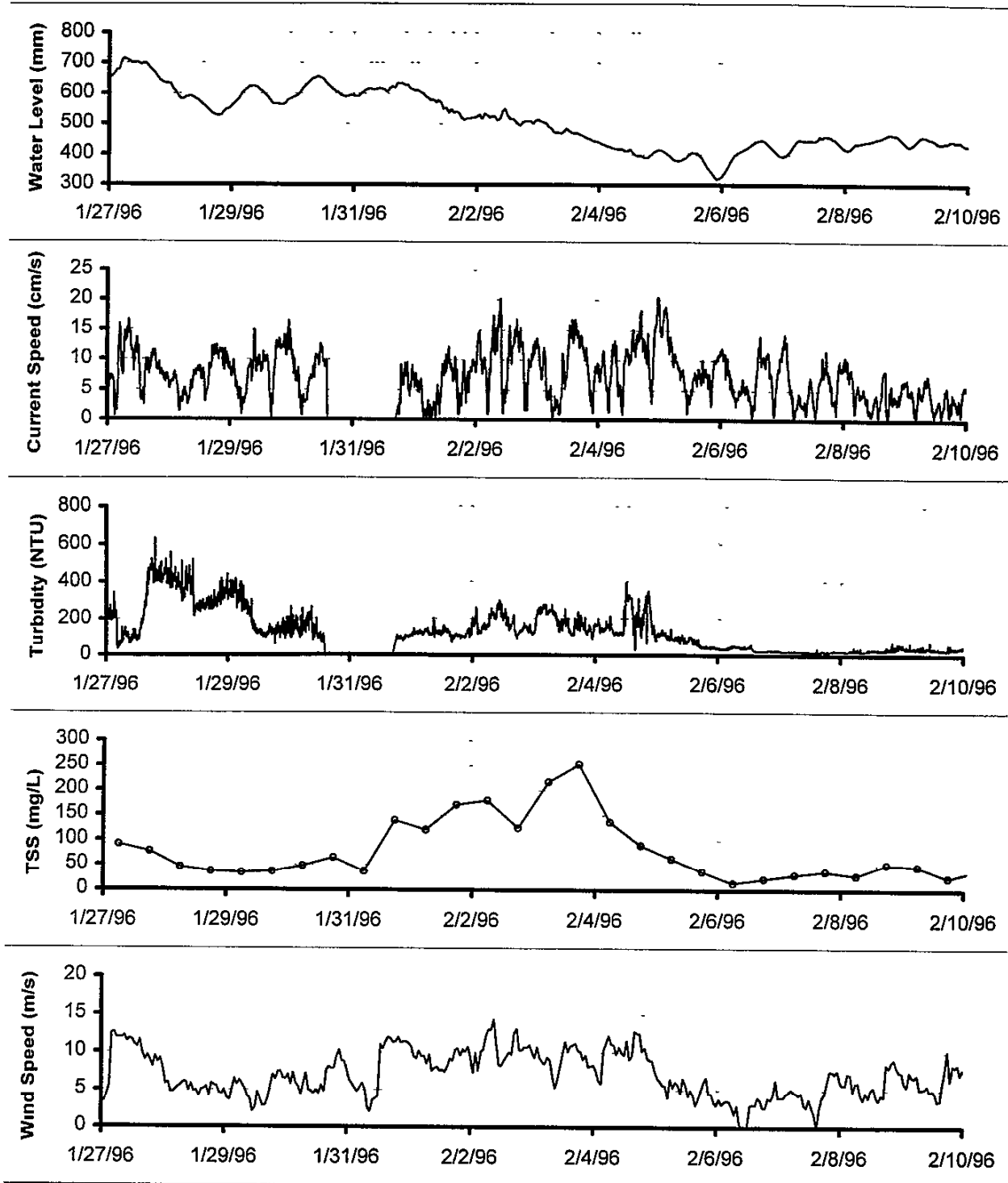


FIGURE 7-6
ULM1 WATER LEVEL, CURRENT, TURBIDITY, TSS AND WIND SPEED
DURING FRONTAL PASSAGE

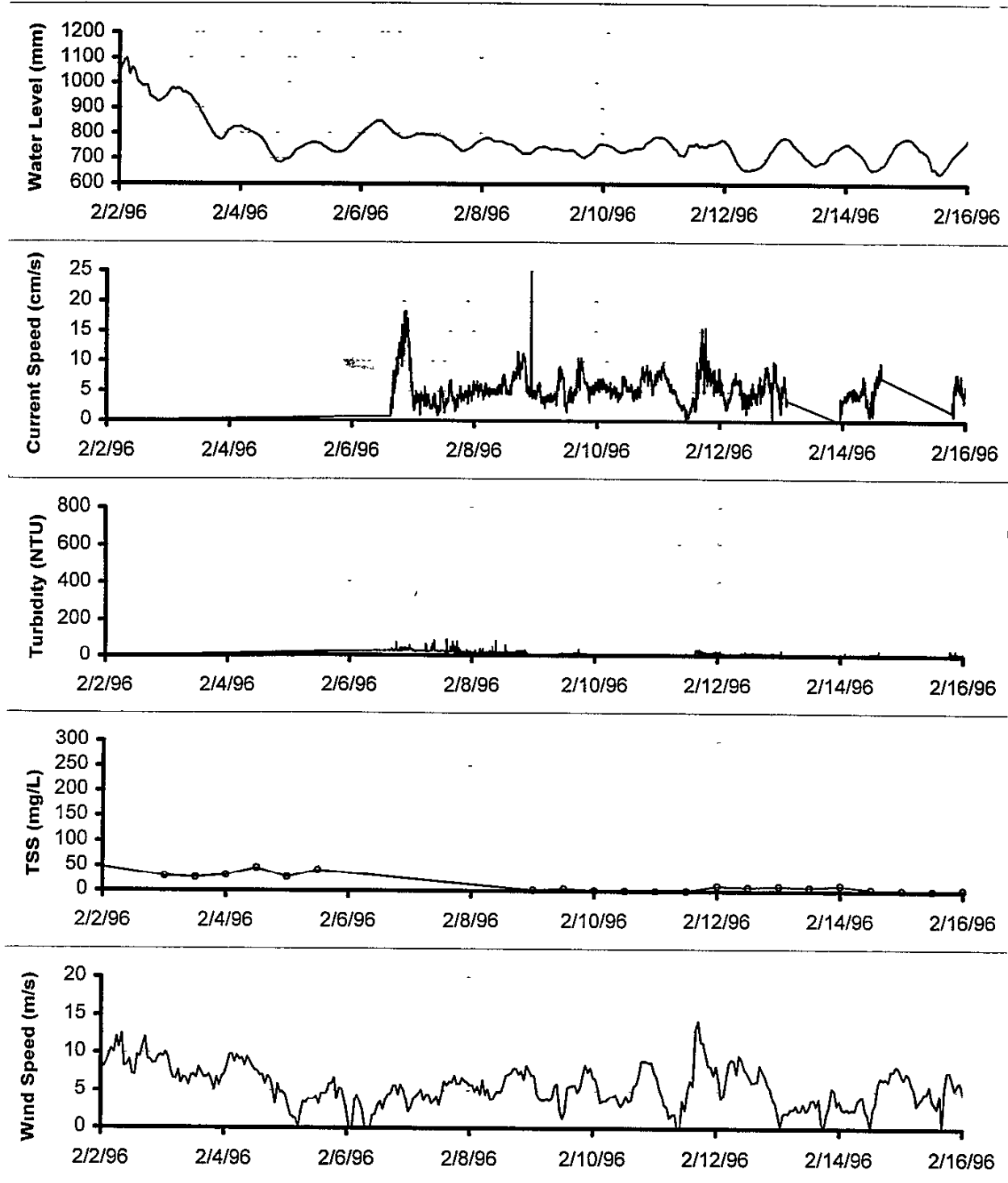


FIGURE 7-7
ULM2 WATER LEVEL, CURRENT, TURBIDITY, TSS AND WIND SPEED
DURING FRONTAL PASSAGE

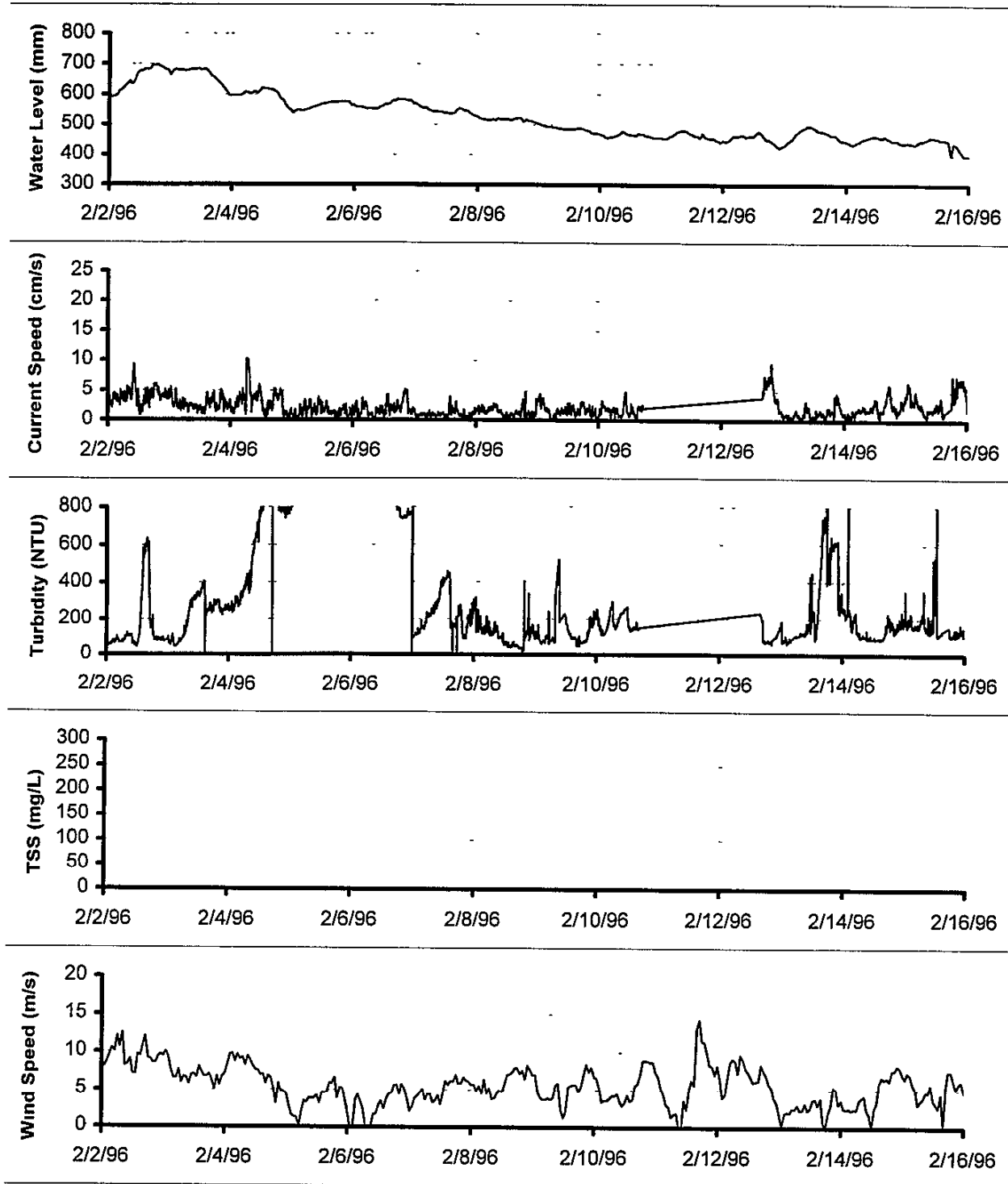
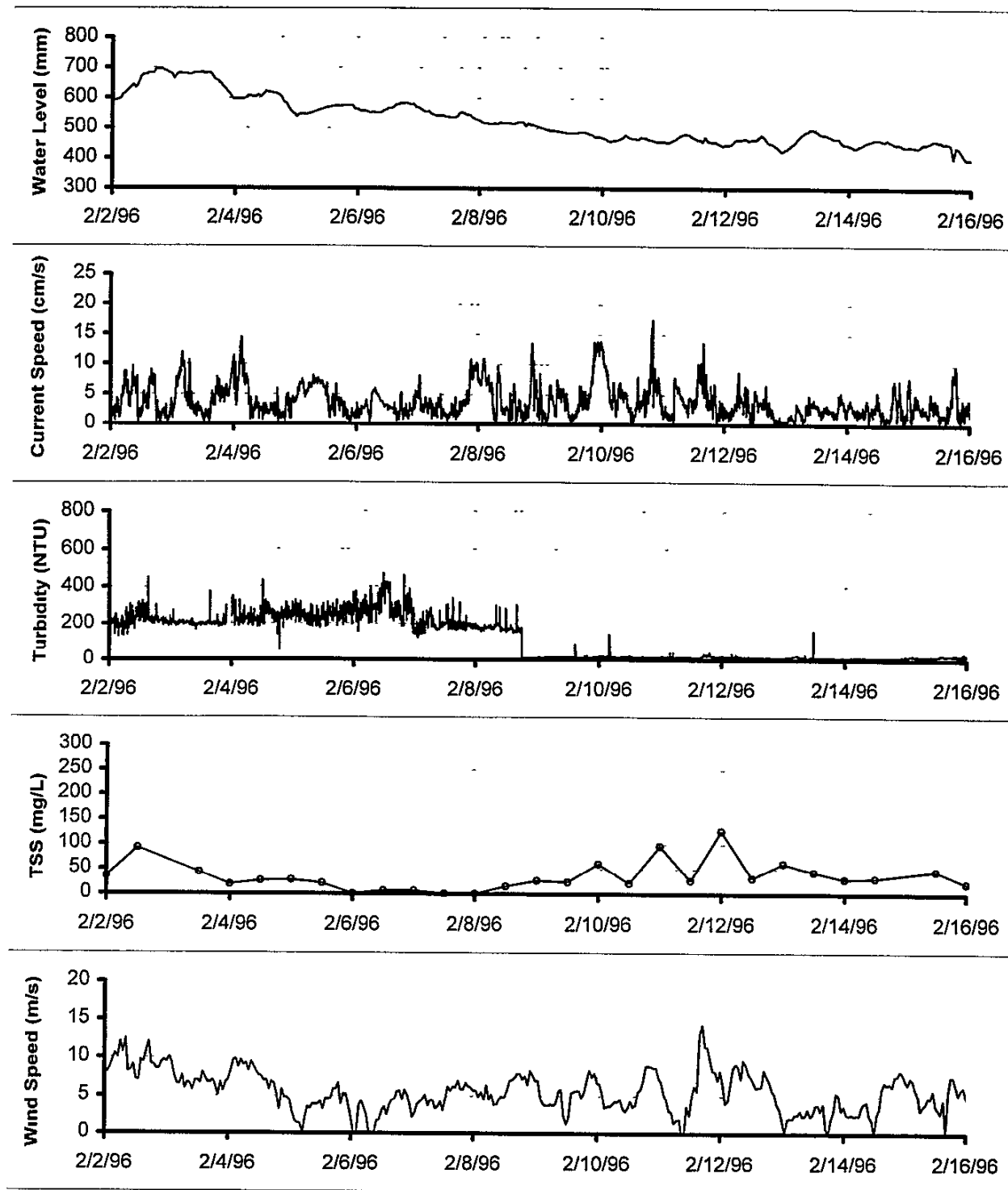


FIGURE 7-8
ULM3 WATER LEVEL, CURRENT, TURBIDITY, TSS AND WIND SPEED
DURING FRONTAL PASSAGE



Mexico is set down (as is the case for "outbreak fronts"), the water depth throughout the Upper Laguna (and the entire Corpus Christi system) lowers in response, see Ward (1997). Unfortunately, there is no TSS from the ULM2 platform for this period.

The water level record plotted therefore is probably not strictly applicable at the current-meter platform. In the ULM3 platform farther south near the middle ground, the currents are substantially larger and there is a TSS response, albeit modest, peaking at only 100 mg/L. The fact that this peak does not correlate with the maximum currents, which occurred about 48-hrs earlier, suggests that it is due to sediment being carried into the platform region from the northern end of the Upper Laguna, rather than being sediments that are locally resuspended. It is noteworthy that this peak in TSS does correlate almost exactly with a period of increased sustained wind speeds.

7.1.3 TSS and Currents

Brown and Kraus (1997) note the apparent increase in turbidity when the wind speed exceeds approximately 10 m/s, and argue that this is consistent with other studies conducted in shallow wind-driven environments with fine-grain bed sediments, citing Chesapeake Bay (Ward *et al.*, 1984) as an example. The apparent influence of such a threshold in wind speed is also evident in the data of figures 7-1 through 7-8. The explanation that immediately comes to mind, and is offered by Brown and Kraus (1997), is that the higher current speeds created by wind, either through frontal response or increased windwave action, are responsible for mobilizing and resuspending the sediments. There is not, however, an apparent correlation with current speeds in the plots of figures 7-1 *et seq*.

This is explored in the time series of figures 7-9 through 7-12. These show, on a much more compressed time axis, the component currents and accompanying TSS measurements for an entire year of data. A cursory inspection of these time series reveals no clear association between current velocity and the surges of TSS. In the spring 1996 period, there are spikes of current in the southward direction, corresponding to frontal events, and for many of these there is a corresponding surge and recession in TSS, but the time phasing is variable, and there are surges in TSS without accompanying irregularities in current.

In the Lower Laguna, the April-May 1996 period shows a 60-day rise and fall in TSS with no associated change in current magnitude. There is, however, a more pronounced northward net component to the current that is discernible by careful inspection of Figure 7-9, also evident in the current roses for these months (Appendix CR). At ULM1, in Corpus Christi Bay, Figure 7-10, the TSS values are generally much lower than those in the Lower Laguna (Figure 7-9), and in the time series, there are a number of quick spikes and recessions in TSS. These seem to be generally correlated with southward excursions in current speed, indicating an association with frontal passages. But the magnitudes of the TSS

FIGURE 7-9
TIME SERIES OF TSS AND CURRENT COMPONENTS AT LLM1

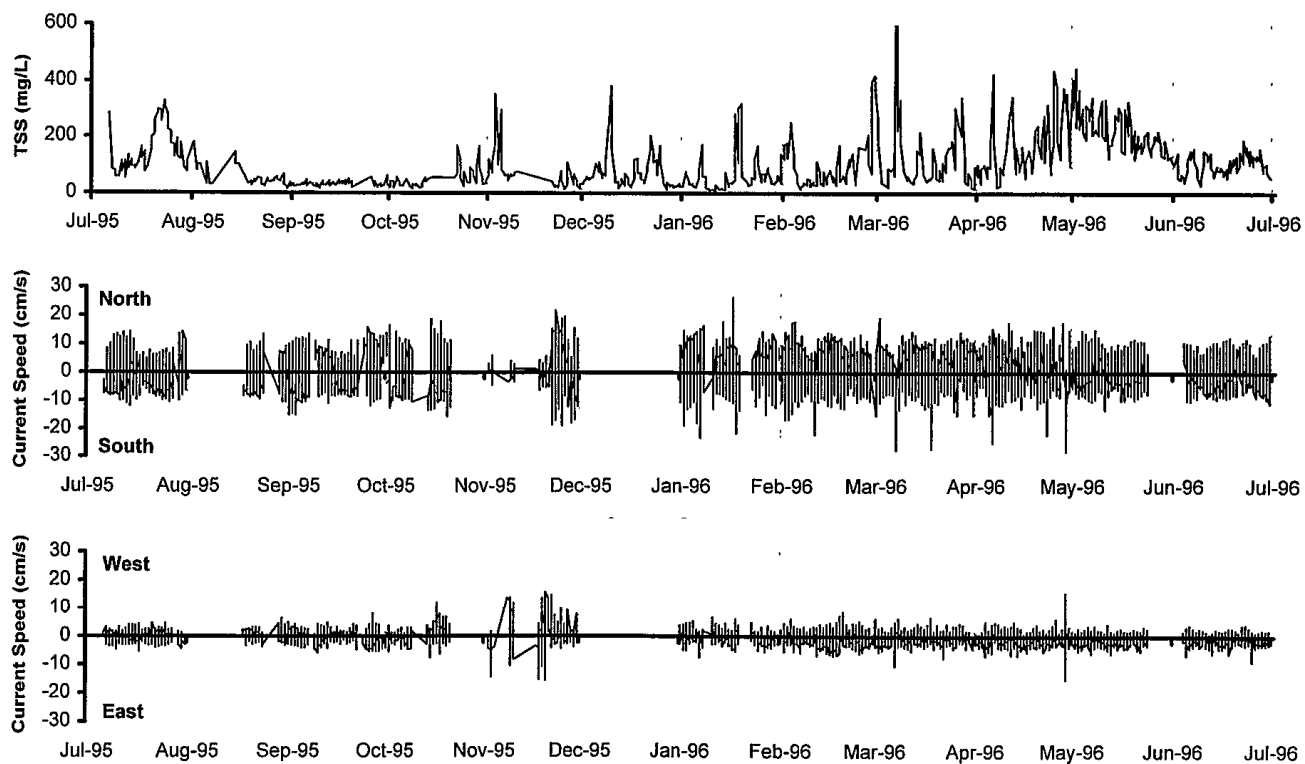
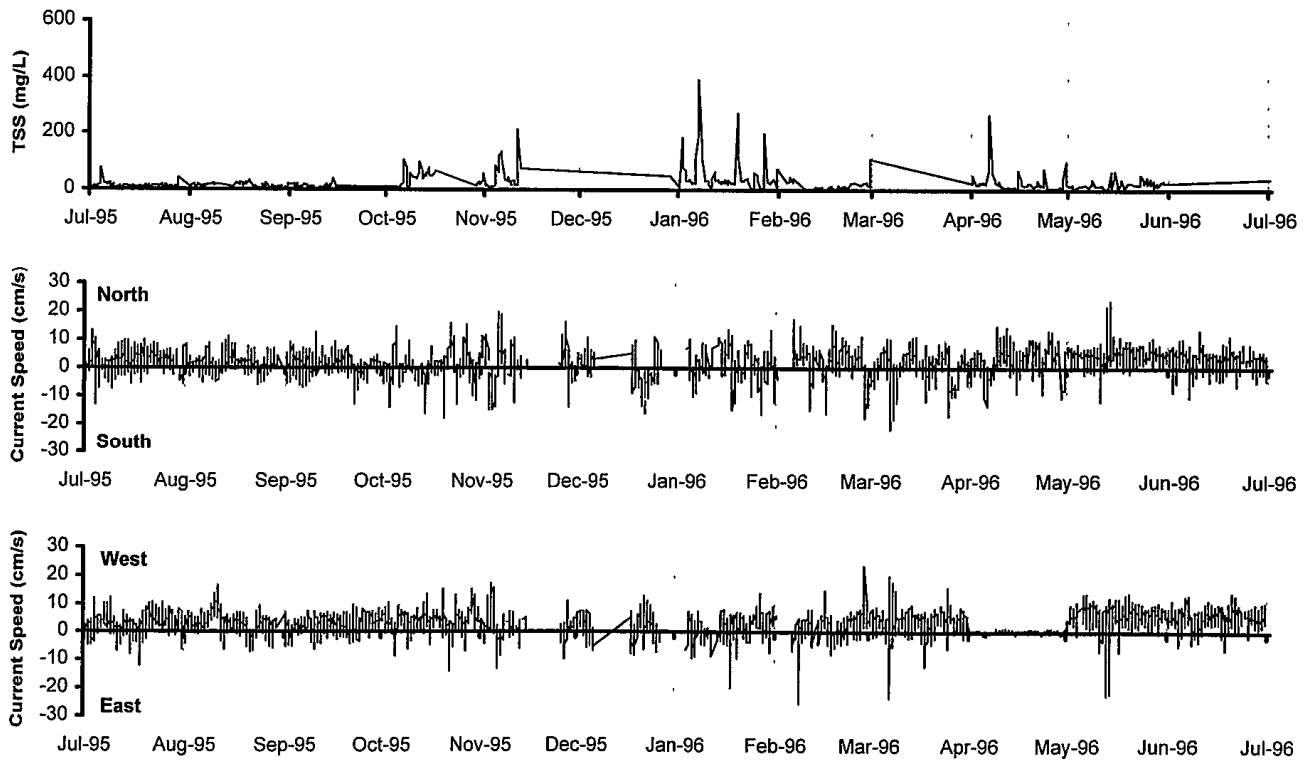


FIGURE 7-10
TIME SERIES OF TSS AND CURRENT COMPONENTS AT ULM1



7-14

FIGURE 7-11
TIME SERIES OF TSS AND CURRENT COMPONENTS AT ULM2

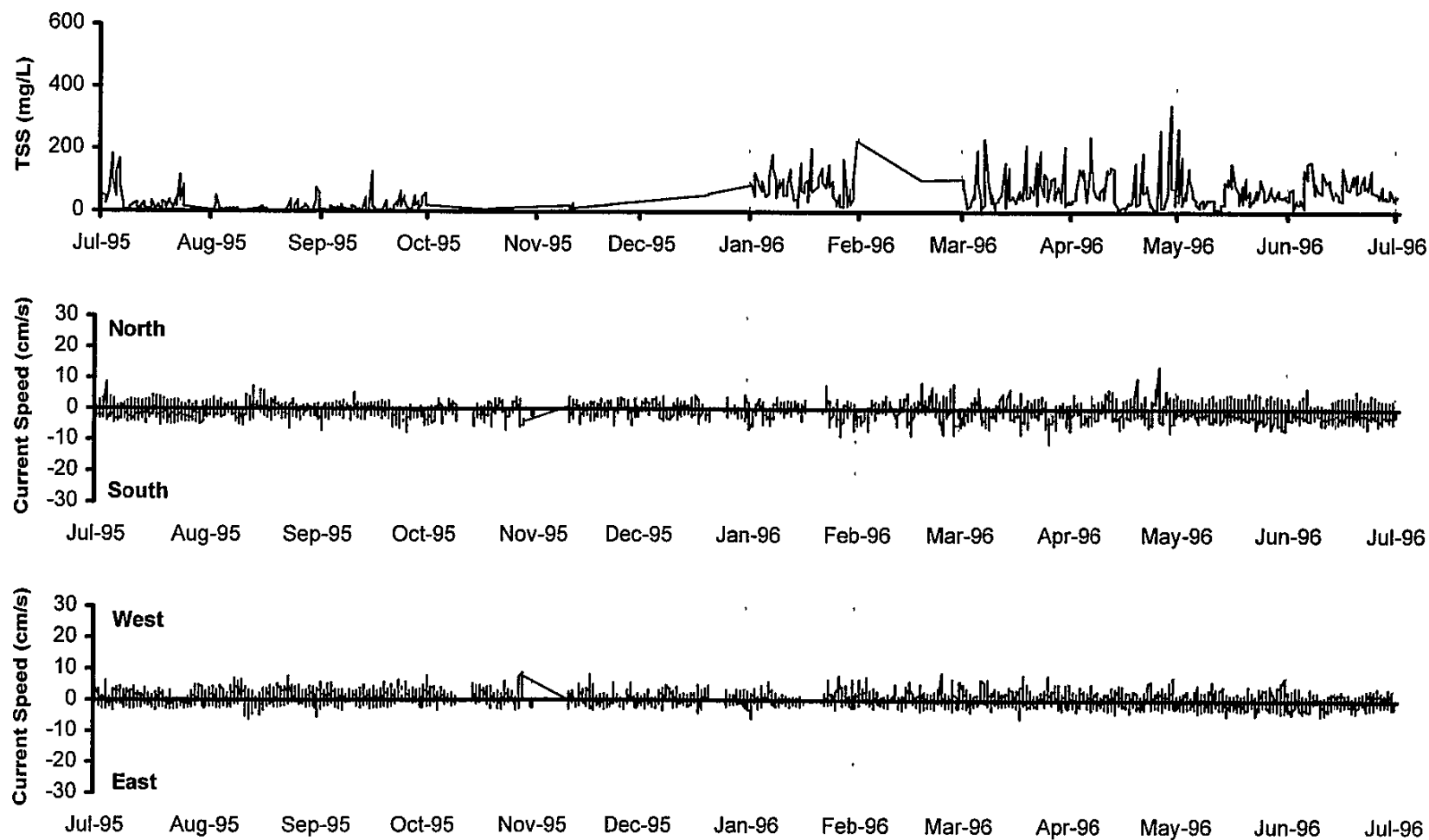
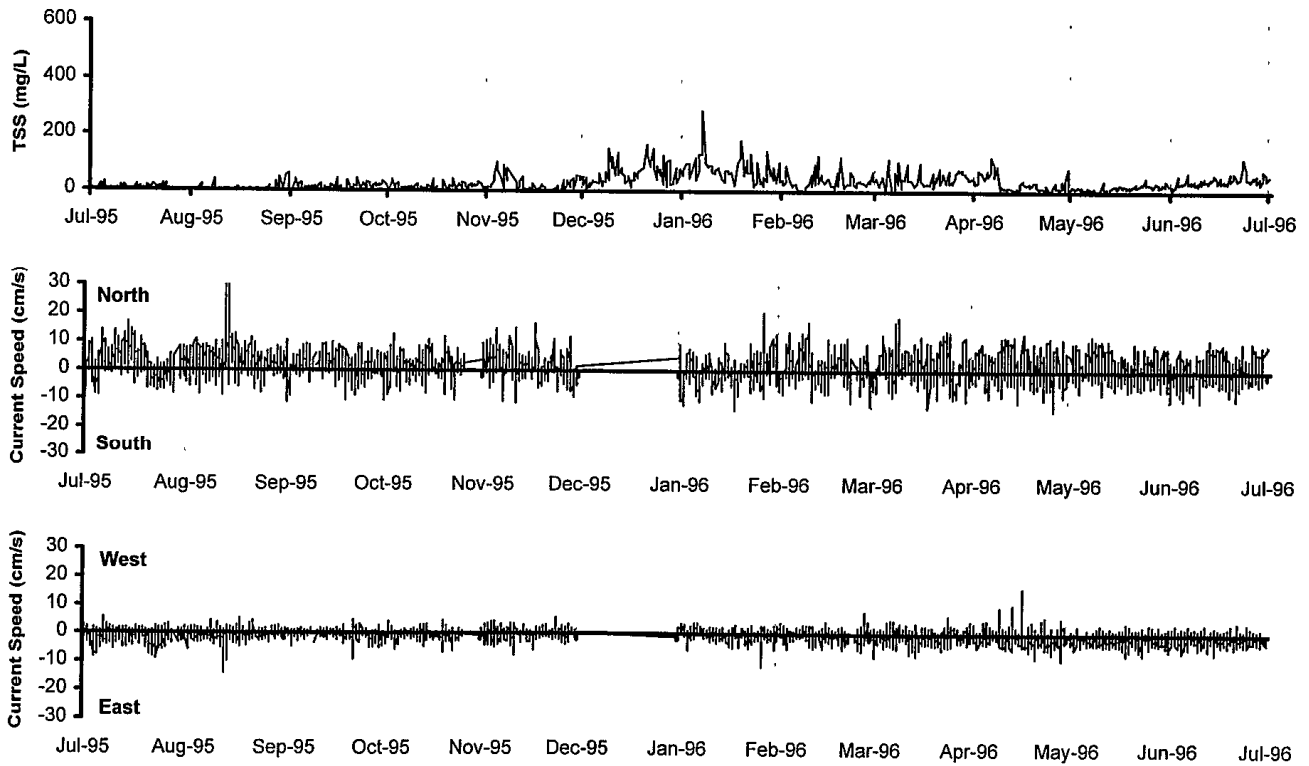


FIGURE 7-12
TIME SERIES OF TSS AND CURRENT COMPONENTS AT ULM3



excursions do not correlate well with the magnitudes of the southward current excursions, and there are southward current excursions for which a corresponding TSS surge does not occur.

In the Upper Laguna, where current speeds are generally lower, there is even less correlation. In the mouth of Baffin Bay, Figure 7-11, most of the exceptional excursions in current speed seem to be in the north-south component, but the association with TSS is not apparent. Compare, for example, the currents for the month of July 1995 and for June 1996, which appear almost identical, yet the TSS values for the former are substantially lower than those for the latter. As was the case in the Lower Laguna, LLM1, the period March-May of 1996 is one of relatively high TSS at ULM2, and some of the peaks in TSS correspond to high currents, but others do not. At the northern limit of the middle ground, ULM3, this same period of March-May is not exceptional in TSS, see Figure 7-12, but rather it is the period December 1995 - January 1996 in which the largest TSS values of the period were registered. The most prominent feature of the currents for this period is the higher southward components, but again this is not a strong association.

The association between TSS and wind speed for the same time periods are shown in figures 7-13 through 7-16. In the Lower Laguna, LLM1, Figure 7-13, there is immediately evident an association between wind speeds and TSS, viz. elevated TSS values during periods of sustained higher winds, notably July and August 1995, and April and May 1996. There are also clear correspondences between surges ("spikes") of TSS and spikes in wind speed, the clearest being for those wind spikes exceeding 12 m/s. In Corpus Christi Bay, ULM, Figure 7-14, the same general association is apparent, though the values of TSS are lower than was the case in the Lower Laguna. At this station, the clearest association is for wind speed spikes exceeding 14 m/s.

In the interior of the Upper Laguna, as well as in Corpus Christi Bay at ULM1, the TSS values are generally higher in the late spring and summer of 1996, compared to the summer of 1995. The wind speeds were also higher in the later period than in the earlier. The wind and TSS time series are both spikey at ULM2, Figure 7-15, and if one hunts for correlated spikes, one can find them, but one can also find numerous noncorrelated spikes. Clearly, the association between wind and TSS surges is complex and murkier at this station. If there is a causal connection, it would be expected to be complex at ULM2, because this station is influenced by north-south excursions of wind and currents along the axis of the Laguna, and east-west exchanges through the mouth of Baffin Bay. Farther south, at ULM3, the TSS is somewhat more elevated and less spikey, but the association with wind is not at all apparent. The high TSS period of December 1995 - January 1996 is not associated with any remarkable difference in wind speed variation.

FIGURE 7-13
TIME SERIES OF TSS AT LLM1 AND WIND SPEED AT ARROYO COLORADO

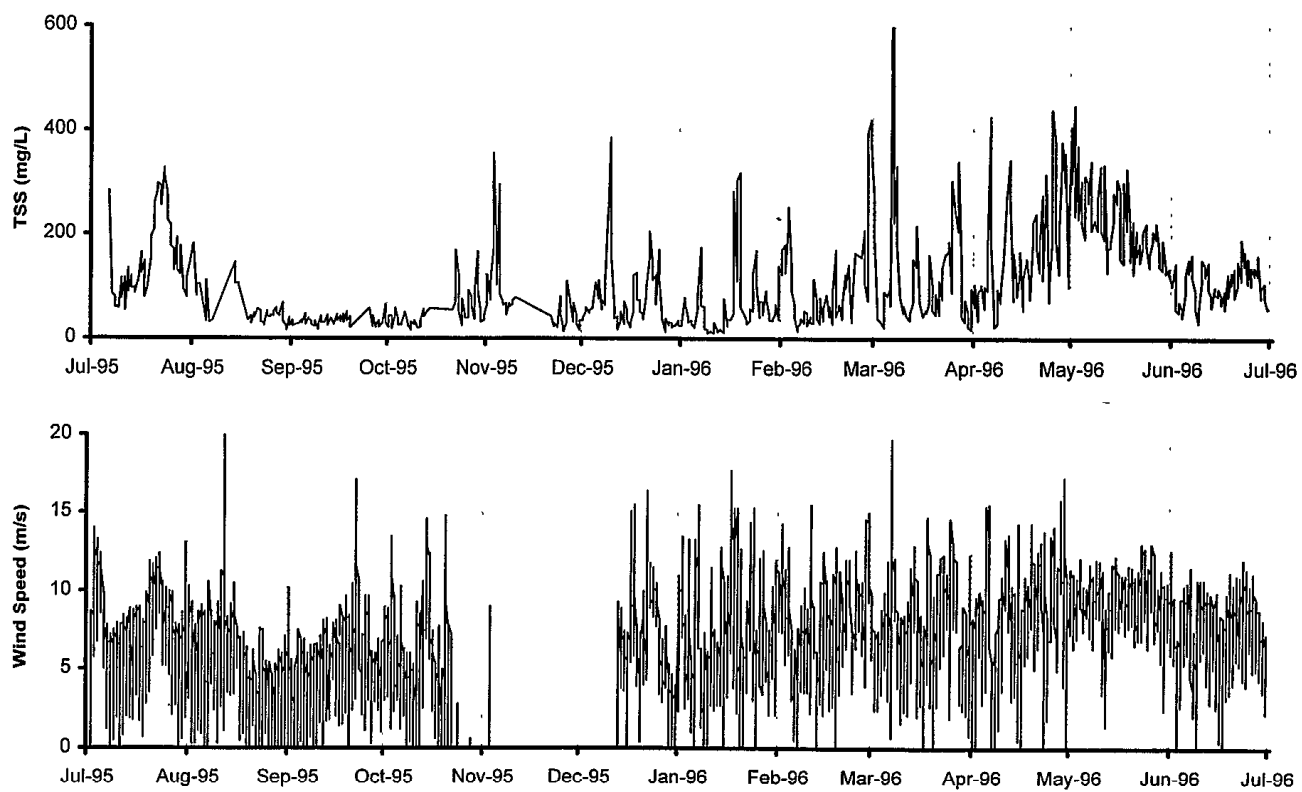


FIGURE 7-14
TIME SERIES OF TSS AT ULM1 AND WIND SPEED AT S. BIRD ISLAND

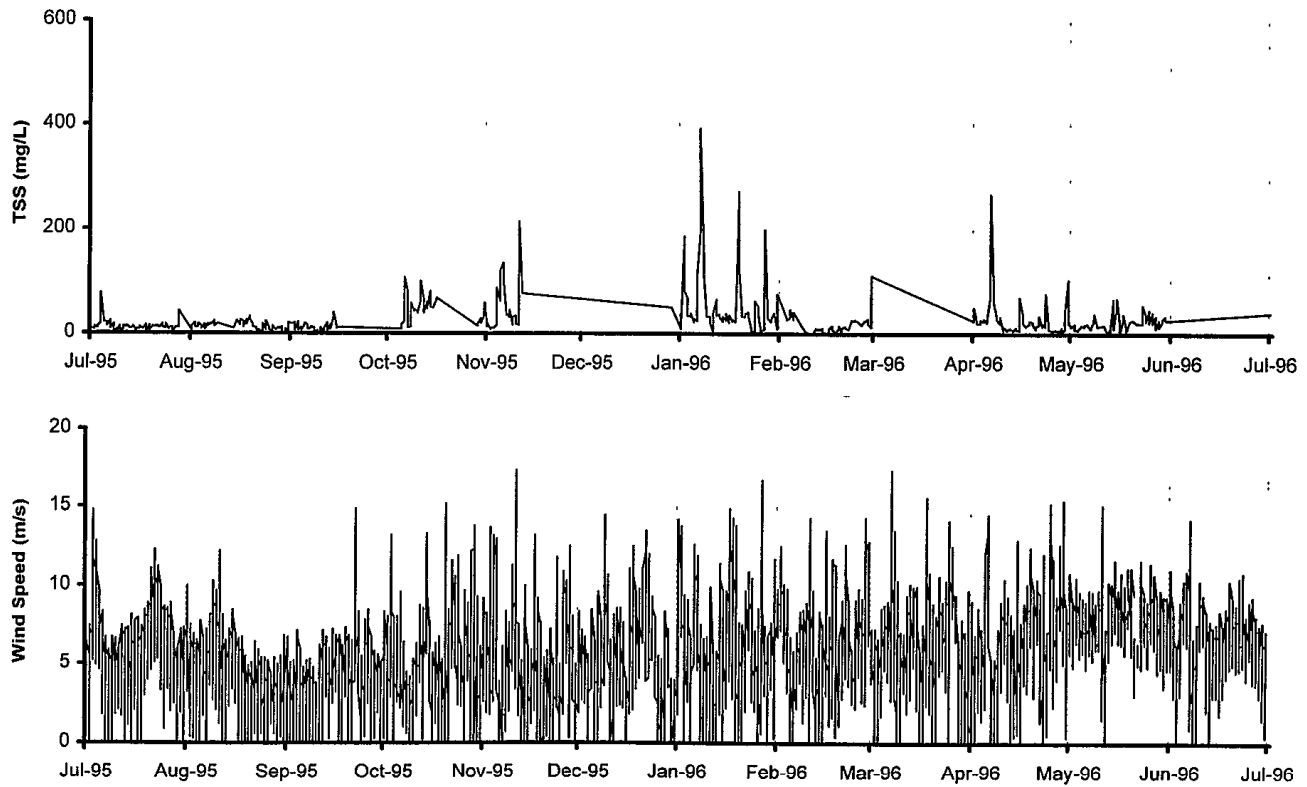


FIGURE 7-15
TIME SERIES OF TSS AT ULM2 AND WIND SPEED AT S. BIRD ISLAND

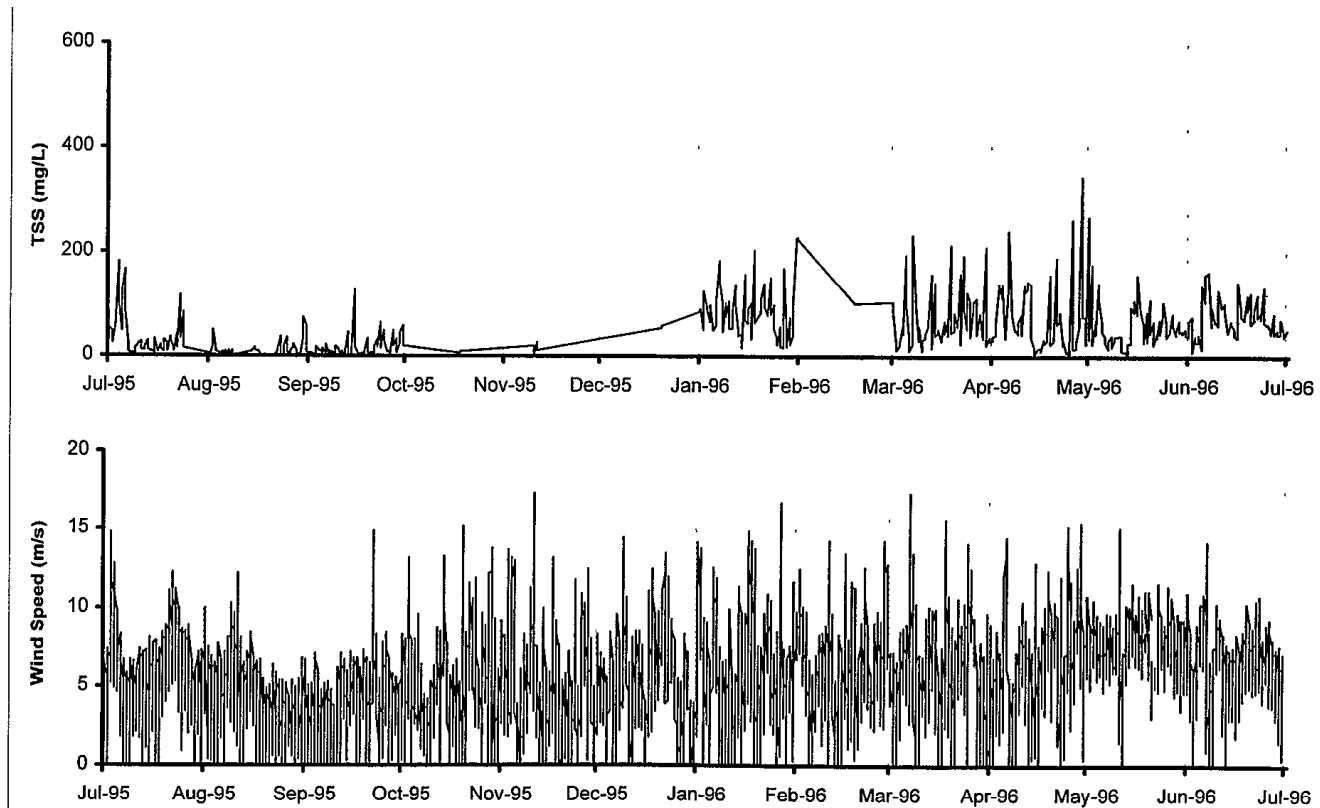


FIGURE 7-16
TIME SERIES OF TSS AT ULM3 AND WIND SPEED AT S. BIRD ISLAND

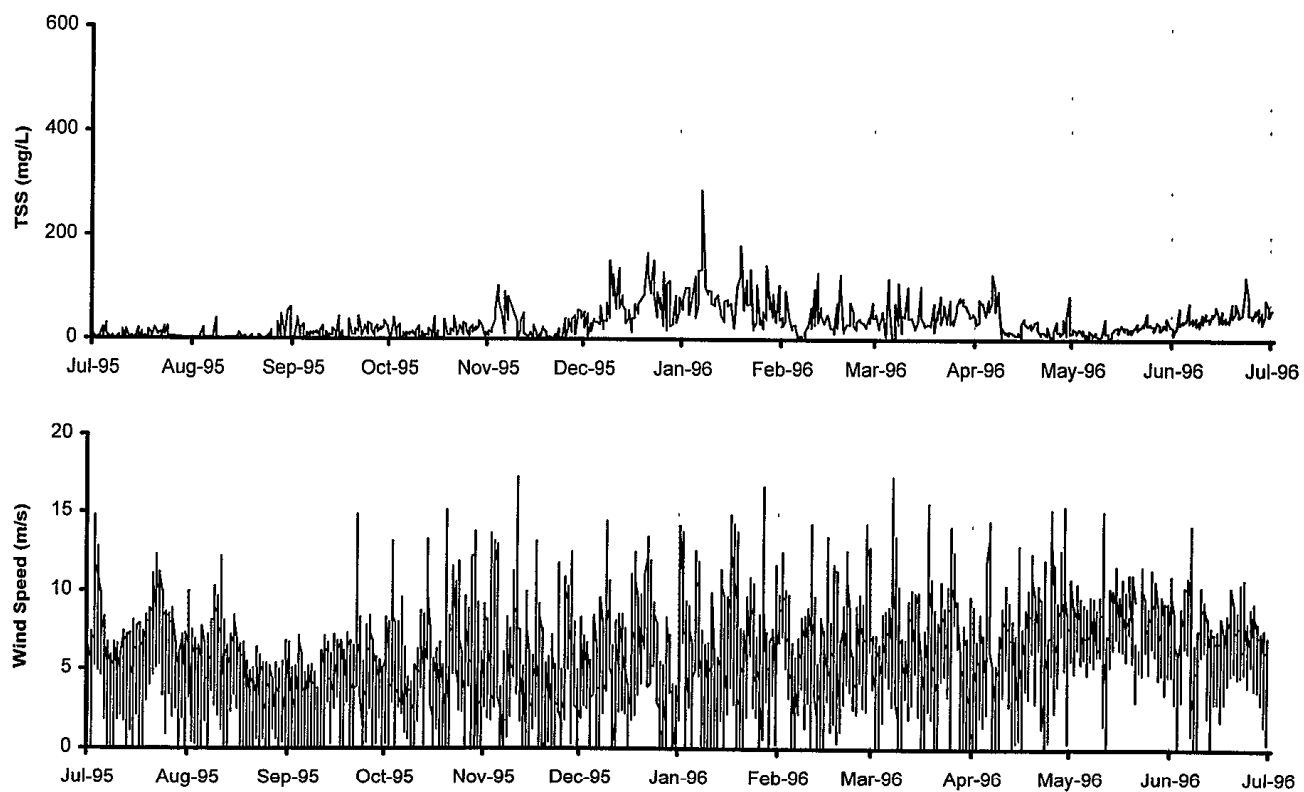


Fig7-12&16.xls Plot 8/2/99 12 46 PM YCS

PBS&J

The question immediately arises whether standard statistical tests might resolve an association between TSS and either current or wind that is indiscernible to the eye. Figures 7-17 through 7-20 display the scatterplots of current component and wind speed, each versus TSS, for the days/times for which TSS data were taken. In summary, there is no significant statistical relation. The very best relationship, between TSS and wind speed at LLM1, produces an explained variance of only 24%. The fact that there is no statistical relation does not mean that there is no relation, but if there is a relation, it appears to be for "events", i.e. the relation exists between the high excursions in TSS and the associated high excursions in current or wind. Most of the time, when TSS is low, or wind and currents are normal, the noise in their variation is uncorrelated. Since figures 7-17 *et seq.* plot all of the data, of which only a small minority correspond to hydrometeorological "events", the statistical correlation is nil.

Generally, there seems to be an association between wind speed excursions and TSS responses in the Lower Laguna and in lower Corpus Christi Bay. It is tempting to posit a causal forcing of TSS increases by the wind. However, the actual mechanism by which this operates remains elusive. While stronger winds, especially those that accompany the passage of a front, certainly generate waves that could resuspend fine bottom sediments, there should be some accompanying signature in the current, such as markedly increased variance in the measurement. The precise, high-time-resolution current measurements of this study do not correlate high currents with the increased TSS values. There does seem to be an association between the TSS spikes and the direction of the current, but this is weak. It seems most likely to us that the increases in TSS monitored at these platforms may be in response to resuspension elsewhere in the system (perhaps in the windward shallows) and transport into the platform area by wind-driven local circulations, so that the TSS response at a platform also depends upon the hydrometeorological "history." In the interior of the Upper Laguna, i.e., at stations ULM2 and ULM3, the association of TSS and currents, as well as TSS and wind, is less evident (or, if one prefers, more complex).

7.2 PREDOMINANT CIRCULATIONS AND PREFERENTIAL TRANSPORT DIRECTIONS

In tidal waterways, the direction of current vectors at a fixed station often follows a preferred trajectory, directed up the trajectory on the flood and down the trajectory on the ebb. Plotting the current over a tidal cycle leads to a scattering of points along the axis of the preferred trajectory. External forcing such as the rotation of the earth or the constraint of bathymetry or shorelines can convert this back-and-forth distribution into an open curve, an elongate closed oval, referred to as the current "ellipse." Turbulence and non-oscillatory variations contribute to scatter about this pattern, but scatterplots of current still will evidence a preferential axis of distribution. Such current ellipses are especially common in coastal and harbor regions, and their behavior has been analyzed for over a century in coastal engineering. While most of the experience has been with tidal-induced currents, any regular oscillatory variation that induces a storage and depletion of water through exchange with the sea will create the same elliptical scatter as a tide. So in the

FIGURE 7-17
TSS VERSUS CURRENT COMPONENTS AND WIND SPEED AT LLM1

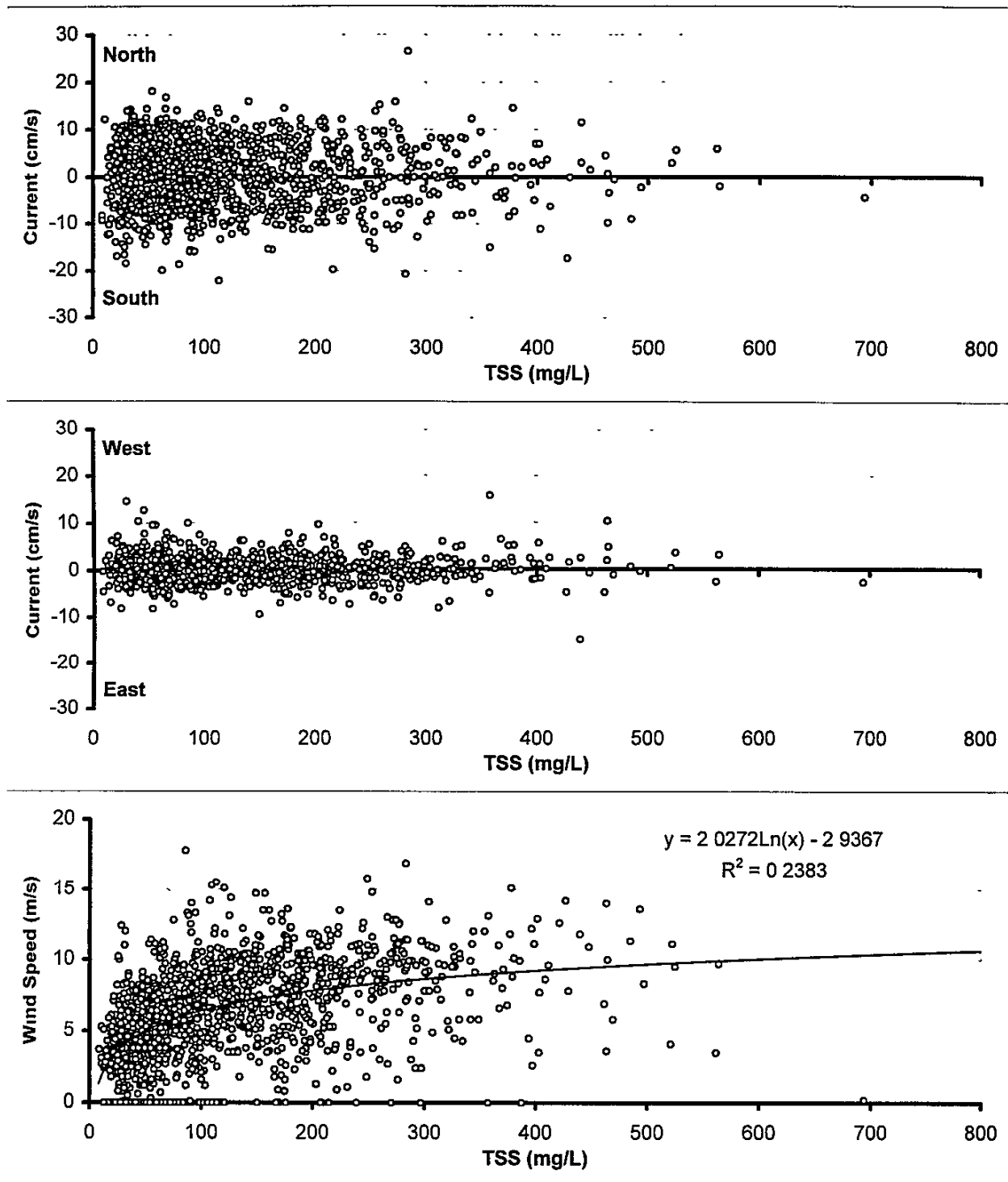


FIGURE 7-18
TSS VERSUS CURRENT COMPONENTS AND WIND SPEED AT ULM1

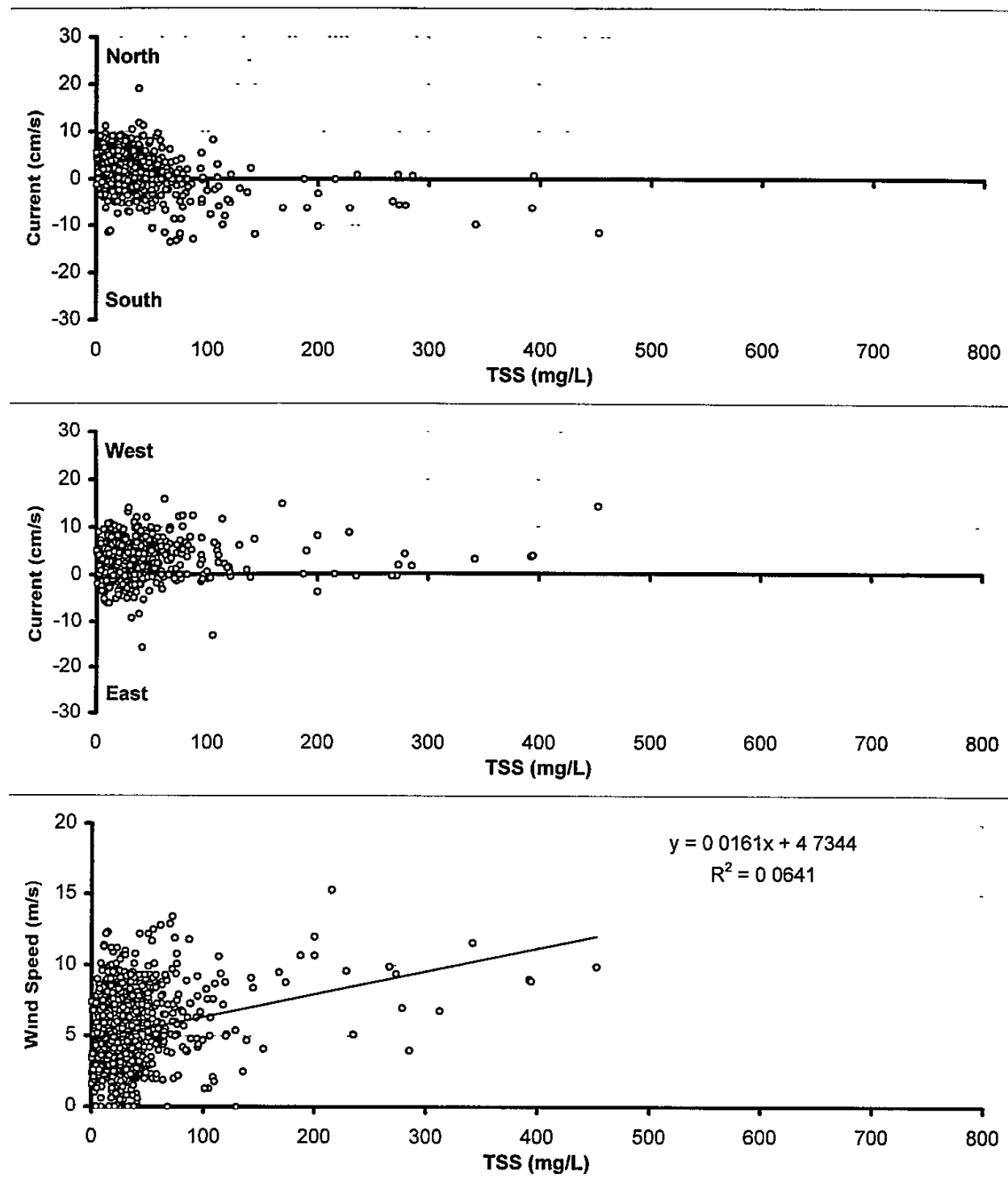


FIGURE 7-19
TSS VERSUS CURRENT COMPONENTS AND WIND SPEED AT ULM2

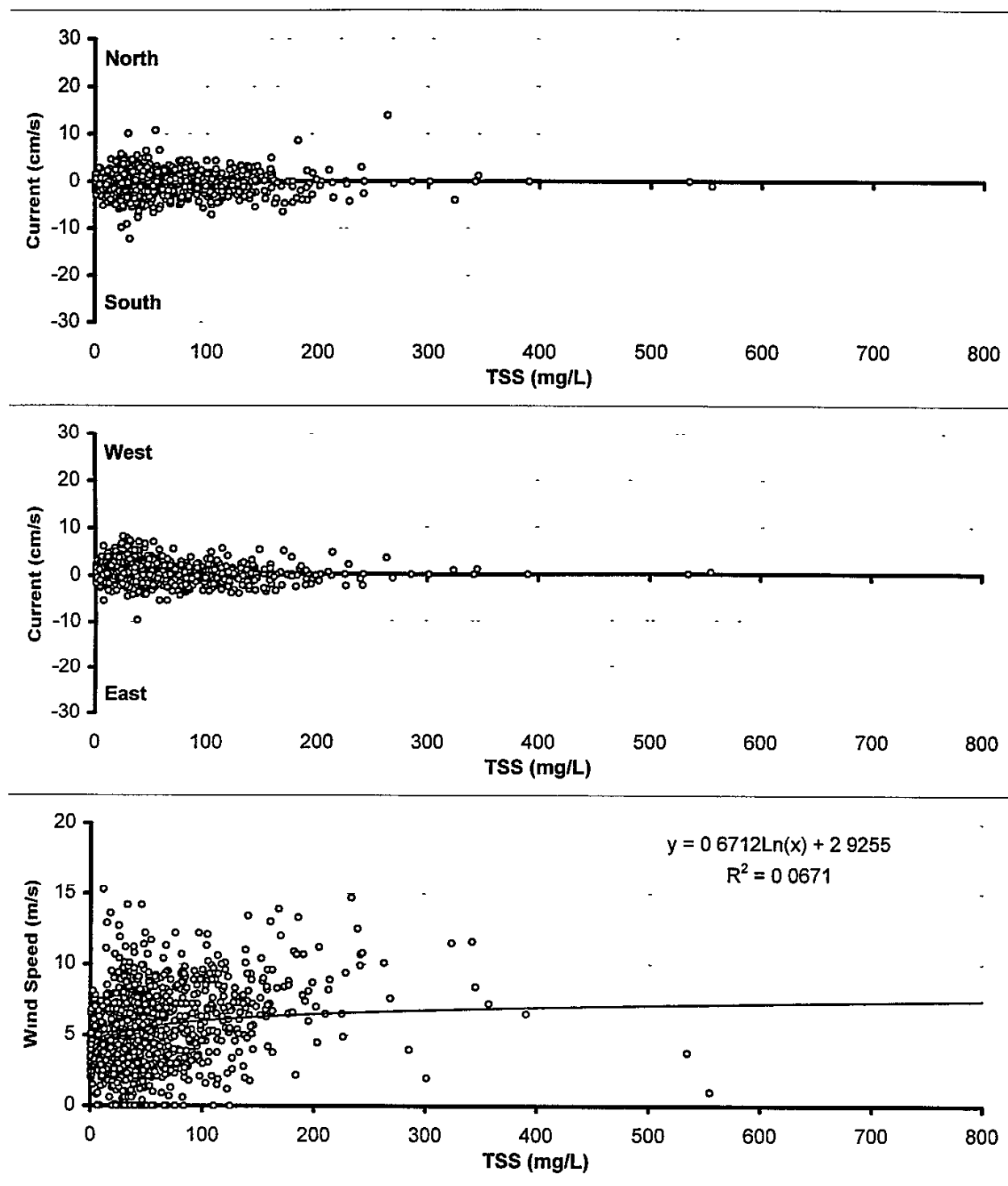
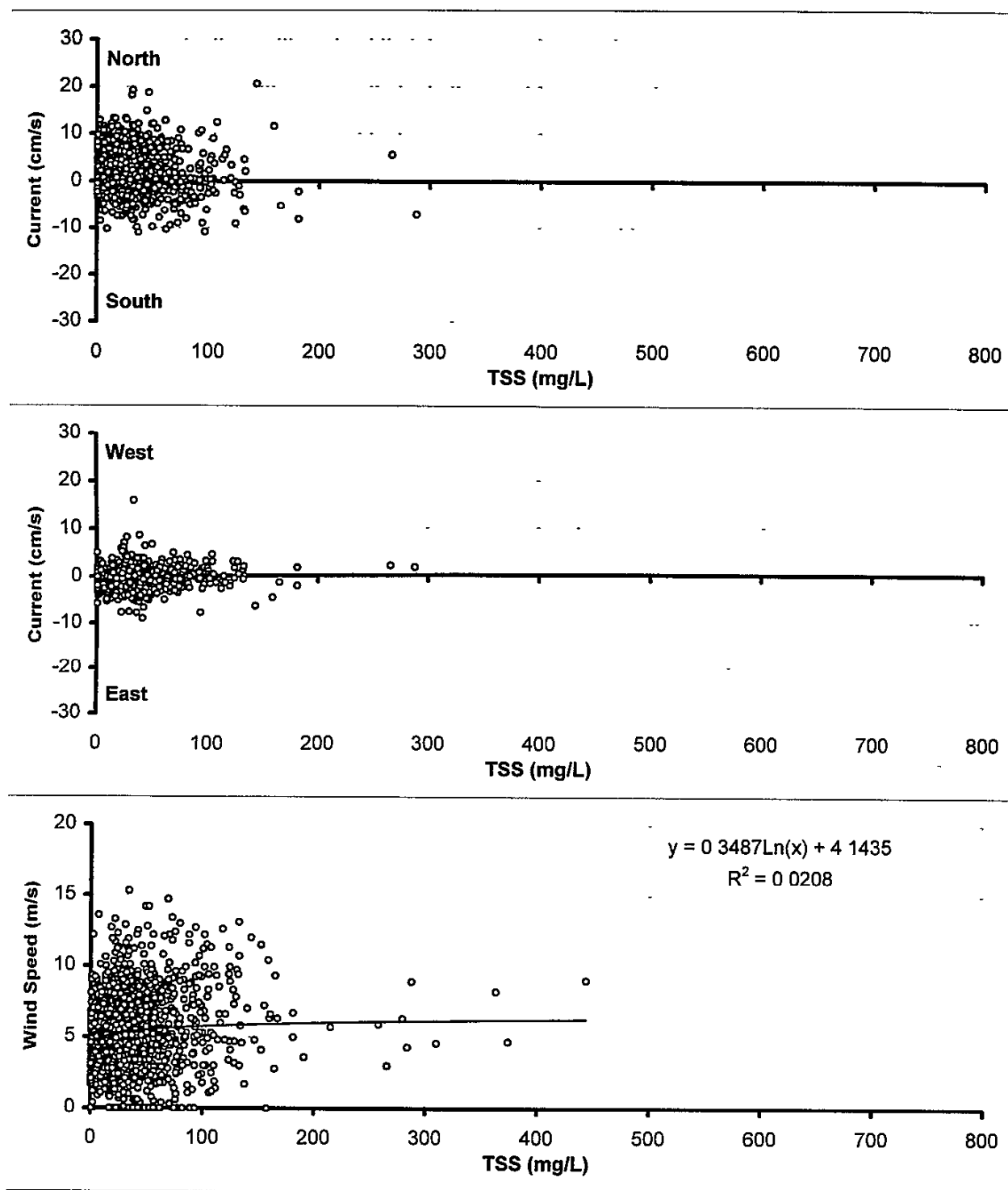


FIGURE 7-20
TSS VERSUS CURRENT COMPONENTS AND WIND SPEED AT ULM3



case of the Laguna Madre, both tides and the seabreeze oscillation could be expected to create such current ellipses in the data. This, indeed, is demonstrated in the preferred axes shown in both the scatterplots of figures 5-7 *et seq.* and the companion current roses of figures 5-18 *et seq.*, addressed earlier.

Brown and Kraus (1997) presented scatterplots for Station LLM1 similar to those of figures 5-7 through 5-9, in which the currents seem to scatter along a preferred axis of variation that runs approximately SSW-NNE and therefore crosses the GIWW at an acute angle. As discussed in the following section, this is a potentially significant observation because it offers an explanation of the high maintenance dredging historically required in this reach of the GIWW, and suggests some corrective actions. They further observed that this cross-channel component corresponds to a region of slightly deeper water (depths greater than 3.5 feet) and proposed that it is the direction of this bathymetric depression that forces the cross channel current.

The more extensive current data from the complete monitoring program reinforces the propensity of currents in this region to align along an axis clockwise from S-N and therefore crossing the GIWW at an angle. This is evident in the series of scatterplots of figures 5-7 *et seq.* as well as the current roses, figures 5-18 *et seq.* However, the actual situation proved to be more complex. The first clue to this complexity was the scatterplot from March 1998 at LLM2, in Figure 5-11. This shows two clear axes, one at 45° E of N and the other at 120°, neither of which corresponds to the distribution of currents monitored earlier at this station, which tracked more along a line 20°-30° E of N. The fact that this was early data from the re-equipped platforms of Data Set IV strongly suggested that this might be a measurement artifact or a processing error. Examination of the raw data disclosed that the March 1998 record was interrupted by a one-week outage, resuming after a service call at the platform, see Figure 7-21. The phasing of the current components clearly changed during the outage, resulting in a different preferred axis. A re-plot of this figure, using symbols to identify the data taken before and after the outage, demonstrates the change in current distribution, Figure 7-22. An examination of data from Station LLM1 in Figure 5-10, taken using the original instrumentation (Data Set III) followed by the new instrumentation (Data Set IV), showed a very different preferred axis for the former compared to the latter. The former lay along a general N-S axis, the latter along a SW-NE axis, therefore crossing the GIWW perpendicularly. This further confirmed our initial reaction that we were seeing a measurement anomaly.

This reaction proved premature. A closer inspection of earlier monthly scatterplots from this station disclosed evidence of these same preferred axes, though not with the clear shift from one to the other as manifested in the March 1998 data. Moreover, when earlier data from Station LLM1 were examined, e.g., November 1995 in Figure 5-9, it was evident that the same SW-NE axis was followed in some of the data from that month. These measurements, from Data Set II, were made using the original instrumentation. This eliminated the possibility that some kind of measurement anomaly had been introduced with the new

FIGURE 7-21
TIME PLOT OF COMPONENT CURRENTS AND WATER LEVEL AT LLM2, MARCH 1998

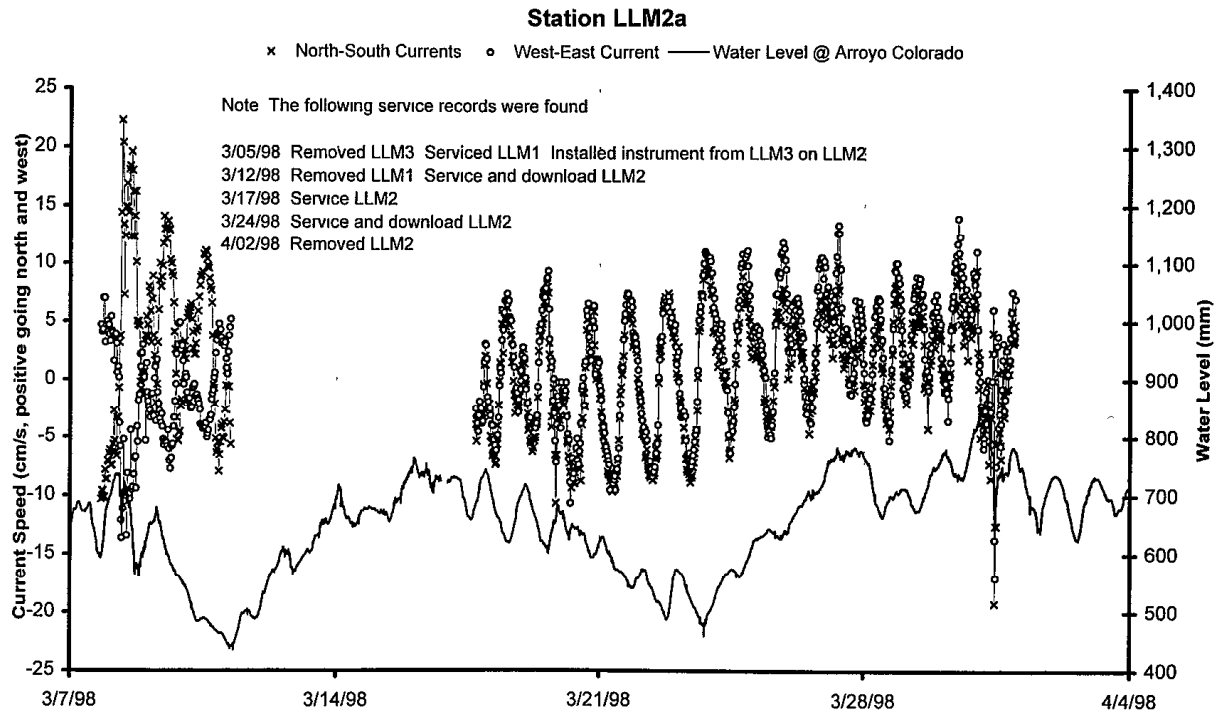
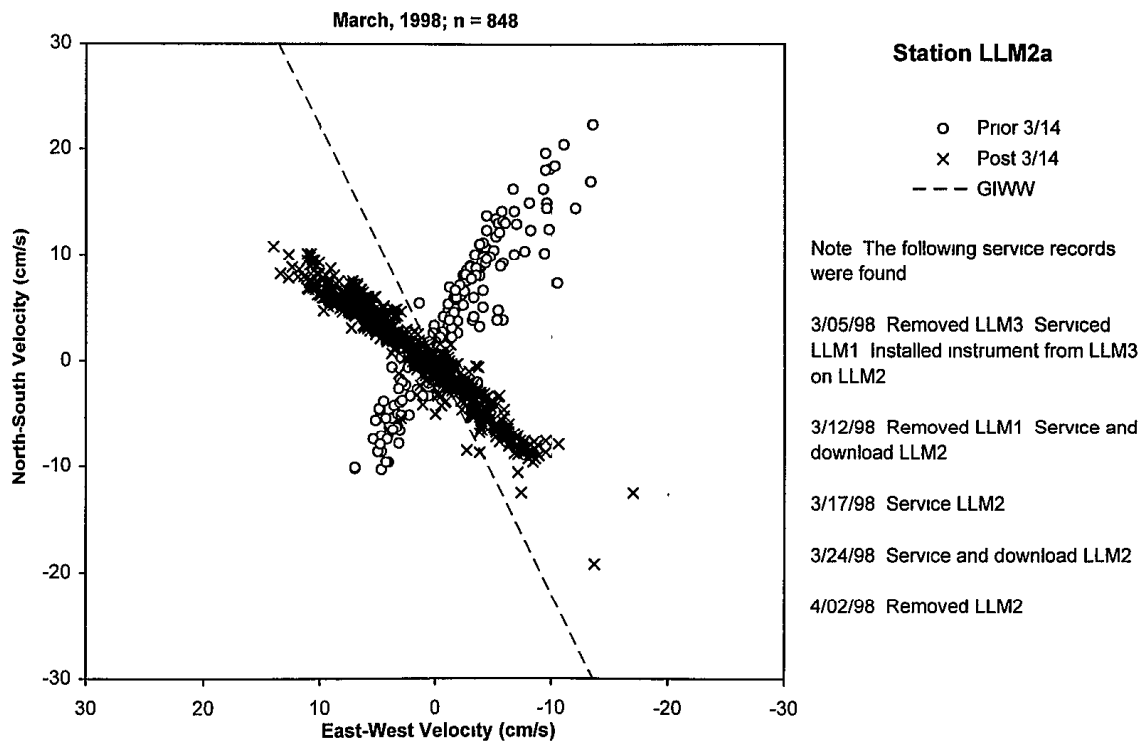


FIGURE 7-22
SCATTERPLOT OF LLM2 CURRENTS FOR MARCH 1998, DIFFERENTIATING BEFORE AND AFTER 12-17 MARCH OUTAGE



7-29

Data Set IV equipment Nor was this behavior confined to the Lower Laguna. In Corpus Christi Bay at ULM1, Figure 5-14 shows a preferred axis lying SW-NE in January 1997 (original instrumentation) and lying WNW-ESE in December 1997 (new instrumentation). But in February 1997 (old instrumentation) both axes are evident in the scatterplot. A careful inspection of the patterns of scatter in the scatterplots from the Upper Laguna ULM2 and ULM3 disclosed the same sort of behavior. We carried out an extensive examination of the data, trying to correlate changes in current distribution from one axis to another with service trips or instrument adjustments. As service trips to each platform were made often, see Appendix SR, there were frequent occasions when a change in current distribution occurred within a day or two of the service visit. But there were also occasions when a change in current distribution did not appear to correlate at all with service calls.

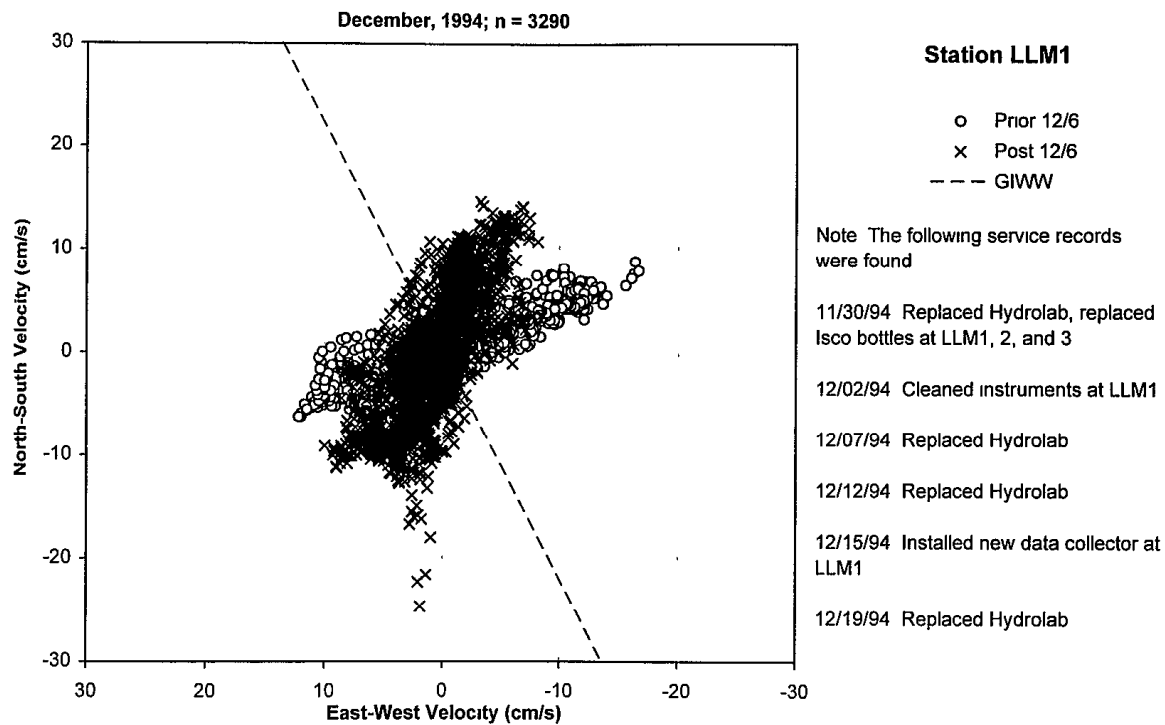
As each hypothesis of a measurement or processing artifact was floated and tested, then eliminated, we began to face the possibility that these shifts from one preferred axis to another might be a real phenomenon. A processing routine was written to read through a current data file, separating the data into 25-hour segments and computing the *normal* least-squares line through each such segment of data. The *ordinary* least-squares regression, which is known and loved by everyone, computes the straight-line that minimizes the sum of squares of the distance between the dependent variable, *u*, say, and the line at each point for the independent variable, *v*. A different line is obtained if the dependent and independent variables are interchanged. The normal-least-squares line, in contrast, minimizes the summed squares of perpendicular distance between each data point pair, *u,v*, say, and the line (Madansky, 1959). It is a statistical fit to the principal axis of a cloud of data points. Though rarely used in statistics, it is exactly the computation needed to determine this principal axis.

As an example of this analysis, we first consider the data at LLM1 for December 1994, see Figure 5-7. This is one of the data sets examined by Brown and Kraus (1997). There appear to be two separate preferred axes, one slightly clockwise from S-N and another nearly perpendicular to the GIWW. A preliminary inspection of these data suggested that the data shifted from one to the other around 6 December, as the plot of Figure 7-23 suggests. Note that there was no servicing of the current meter instrumentation during this period. The slopes of the normal-least-squares straight-line fit for individual 25-hour periods are shown in Figure 7-24. The two regression lines are computed to have slopes around 15° and 70°. A similar analysis for the same station a year later is shown in Figure 7-25. Virtually, the same two axes emerge from the data. In both cases, the system seems to acquire one preferred axis, maintaining that for 5-10 tidal cycles, then abruptly shifts to the other.

The same sorts of analyses were applied to simultaneous records from ULM1 (in lower Corpus Christi Bay) and ULM2 in the Upper Laguna, for July 1995, shown in figures 7-26 and 7-27, resp. Two principal axes emerge from the analysis for both stations. These axes are not apparent at all in the

FIGURE 7-23

SCATTERPLOT OF LLM1 CURRENTS FOR DECEMBER 1994, DIFFERENTIATING 6 DECEMBER TRANSITION



7-31

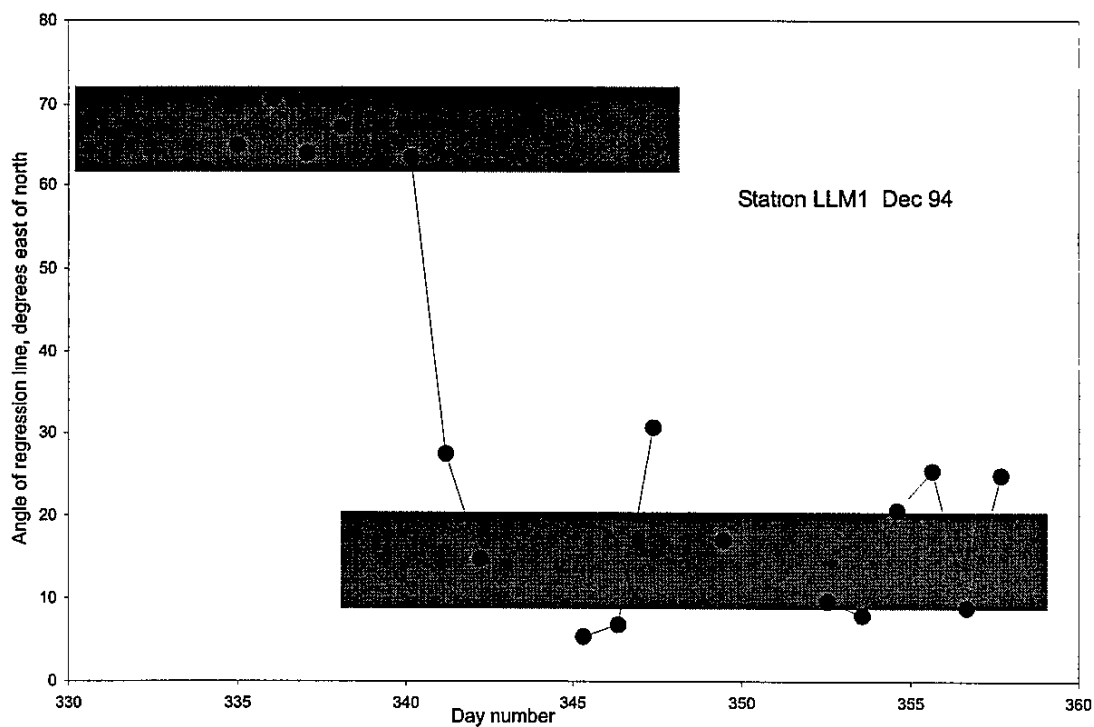


Figure 7-24. Computed slope of straight-line fit to current scatterplot by 25-hour intervals, LLM1 December 1994

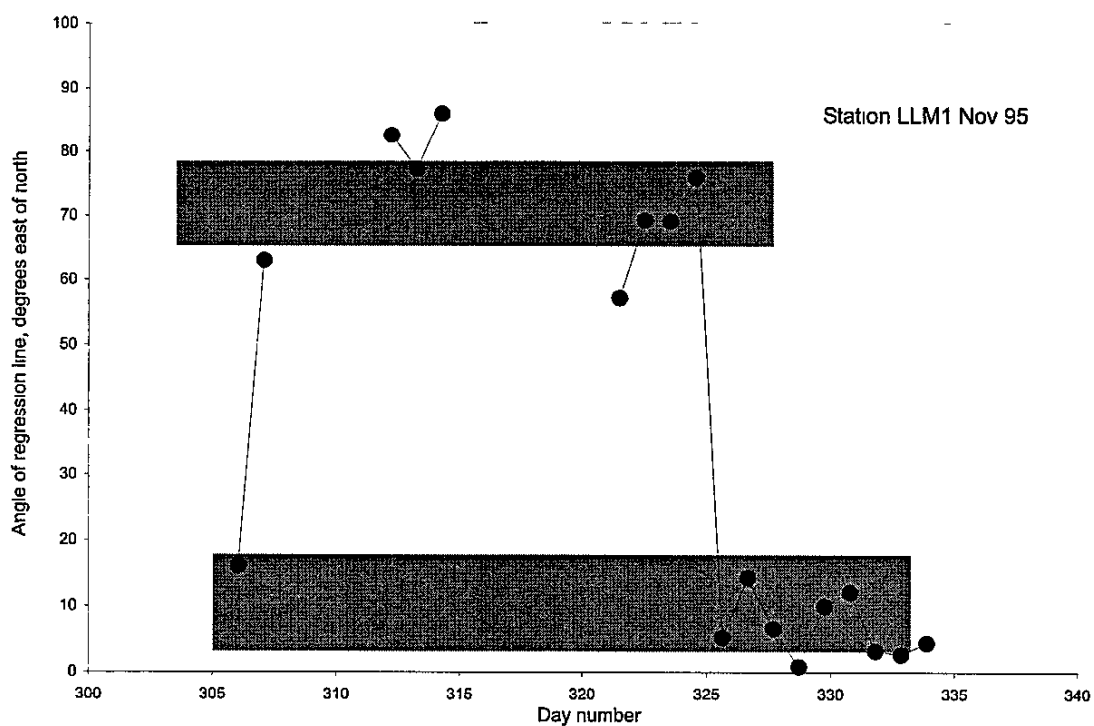


Figure 7-25. Computed slope of straight-line fit to current scatterplot by 25-hour intervals, LLM1 November 1995

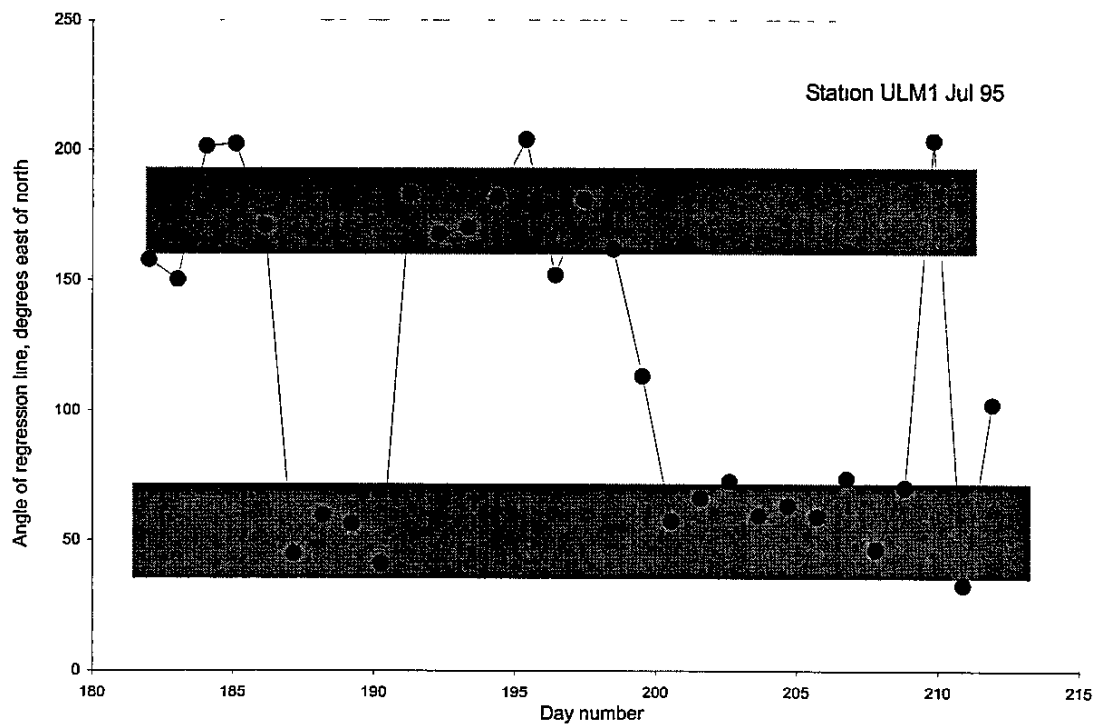


Figure 7-26 Computed slope of straight-line fit to current scatterplot by 25-hour intervals, ULM1 July 1995

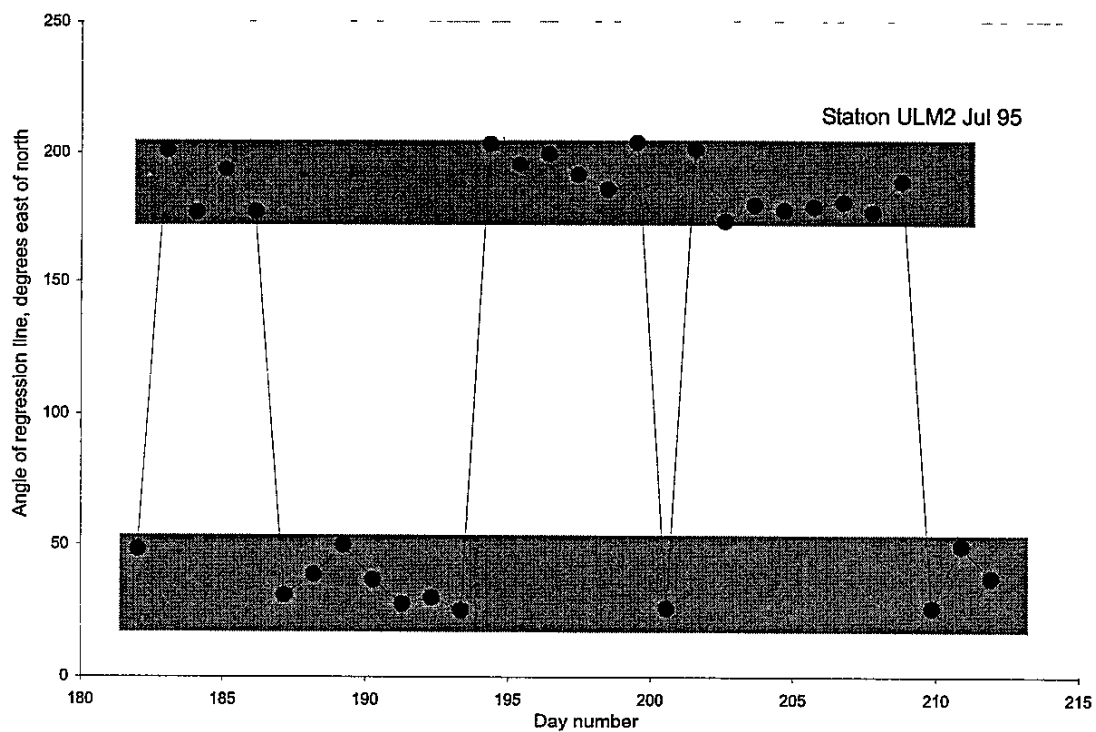


Figure 7-27 Computed slope of straight-line fit to current scatterplot by 25-hour intervals, ULM2 July 1995

current rose for ULM1, Figure 5-23, and they are only hinted at in the scatterplot, Figure 5-12, because the currents vacillate between the two without any extremes in speeds to bring out preferred directions in either format of these vector plots. But the two preferred axes are clearly established by the normal-least-squares fit. These two figures, 7-26 and 7-27, should be examined together. There is a close, but not exact, synchrony in the shifts from one axis to another. The shifts on Day 187, Day 200 and Day 209 occur together at both stations. The shift at ULM1 on Day 191 is followed at ULM2 three days later. While both stations shift together on Day 200, ULM1 in Corpus Christi Bay continues to follow the (new) 50° axis, while ULM2 immediately reverts back to the preceding 180° axis. This quasi-synchronous shifts suggest that they are precipitated by some external forcing of the system. (However, there was no obvious hydrographic event associated with any one of these axis shifts.)

This sort of analysis is beyond the scope of the present project, so it was impossible within the project resources to carry out such a preferred-axis determination for every month and every station in the monitoring data record. From these few examples, we pose the following provisional observations:

- (1) There is more than one preferred axis at these platforms, presumably corresponding to modes of circulation.
- (2) The circulation appears to be metastable, following a given preferred axis for a number of tidal cycles, the shifting to another axis.
- (3) Shifts from one axis to another are more-or-less synchronous in different regions of the system, indicating a large-scale systemic shift from one circulation regime to another. The mechanism that forces this shift is not clear from the few months of data analyzed here.
- (4) In lower Corpus Christi Bay, i.e. at ULM1, one preferred axis is along a N-S trajectory, and the other is along a line about 50° E of N. The former corresponds to flow in and out of Bulkhead Flats, while the latter roughly parallels the shoreline (and bayward margin of Bulkhead Flats).
- (5) At the mouth of Baffin Bay, i.e. at ULM2, one preferred axis is 10° (i.e., 190°) E of N, approximately the axis of the GIWW, and the other is 50° E of N, the direction of the entrance to Baffin Bay.
- (6) In the Lower Laguna, at LLM1 there are two preferred axes, at 15° and 70° E of N, the former being the one identified by Brown and Kraus (1997) from their

scatterplots. At least two axes are indicated at LLM2, at about 45° and 120° E of N (based upon Figure 7-22).

Thus, there seem to be obvious physiographic constraints dictating the axes of flow in lower Corpus Christi Bay and the Upper Laguna, but in the Lower Laguna, there is no such obvious physiographic constraint. (This is addressed further in the following section) Also, the lack of a clear triggering mechanism for the shift from one to the other is puzzling. It is possible that this trigger may involve interactions between the Laguna and the adjacent Gulf of Mexico, and meteorology may play a role as well. Inspection of the scatterplots and current roses of Chapter 5 (as well as the appendices) make it clear that some fundamental shift in the circulation of the system occurred in the monitoring hiatus between the termination of measurements with the original instrumentation (Data Set III) and their resumption with the new instrumentation (Data Set IV). It is clear that this phenomenon requires much more thorough analysis than could be indulged in the present project

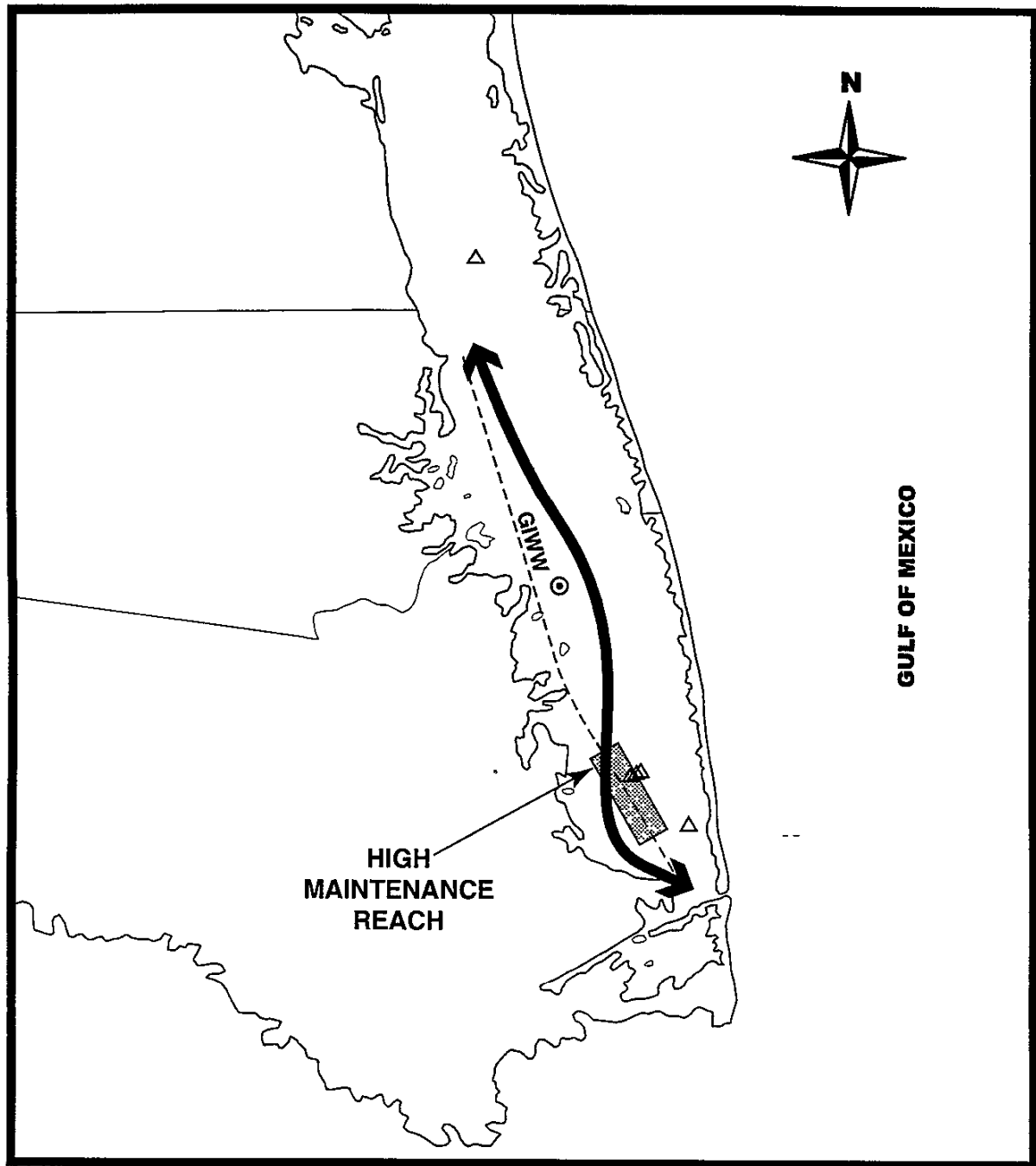
7.3 HYDROGRAPHIC PROCESSES AND SEDIMENT TRANSPORT

For the past 50 years, the reach of the GIWW crossing the Lower Laguna has exhibited very high shoaling (as measured by the volume of maintenance dredging) in a 5-km subreach extending from Cullen Bay almost to Port Isabel, see Atturio *et al.* (1976), James *et al.* (1977), and Militello and Kraus (1994). This region of high shoaling is indicated on the map of Figure 7-28. The platform LLM1 was placed about midway along this high-maintenance reach, and in their study of the scatterplot current vectors in the Year-1 report, Brown and Kraus (1997) noted that there is a component of the current across the axis of the GIWW. They proposed that it is this cross-channel flow in association with the practice of disposing of the dredged material to either side of the GIWW that is responsible for the high maintenance rates. This proposal was supported, albeit anecdotally, by the inferred current trajectories of James, *et al.* (1977) based upon what appear to be suspended sediment patterns in several remote imagery shots from the 1970s. In this earlier report, based on their analysis of the satellite images in conjunction with tide and wind data, James *et al.* (1977) had suggested that in the region of relatively high shoaling rates, previously identified by Atturio, *et al.* (1976), there was generally flow at an acute angle across the GIWW. The general trajectory of currents proposed by James *et al.* (1977) and later by Militello and Kraus (1994) and Brown and Kraus (1997), is shown as the bold curve in Figure 7-28. One of the figures, a LANDSAT image, showing turbidity contrasts in the Lower Laguna, was reproduced from the James *et al.* (1977) report in Brown and Kraus (1997), as their Figure 5.2

The present current vector analyses in one respect confirm the suggestions of these earlier authors, that there is indeed a prominent cross-channel component of current in this reach of the GIWW. Such a cross-channel component will be a significant mechanism for transport of suspended sediment across

FIGURE 7-28

LOWER LAGUNA MADRE SHOWING HIGH MAINTENANCE REACH
AND CURRENT TRAJECTRY PROPOSED BY JAMES et al. (1977)



I:\projects\h01\coe\449708\cad\figure7-28 au

5 0 5 10 15 20 25 Miles

⊙ TCOON Stations
△ CBI Stations

the GIWW, where a proportion of the sediments will settle out in the deeper water, thus contributing to the shoaling in the channel. The present results indicate, however, that there is more than one preferred axis of this transport, a second axis being directed almost perpendicular to the GIWW. Moreover, at each of the platform stations maintained during this study there is a mode of transport across the GIWW indicated in the current data (A qualified exception is Station LLM2, which is too distant from the GIWW, about 2 km east, to directly indicate currents there. However, if the preferred axes exhibited at this station are applied as well to the GIWW just north of the Queen Isabella Causeway, this would imply substantial cross-channel transport in this vicinity as well.)

The question may occur as to why the second cross-channel circulation is not manifested in the remote imagery. Part of the answer lies in the difficulty of interpreting imagery such as that assembled by James *et al.* (1977). This topic is beyond the present scope and cannot be explored here, but it is worthwhile to note several points:

- (1) In imagery such as this, suspended sediment in the water column, other light absorbing or reflecting matter in the water, and bed forms in the shallows appear very similar; they can be unambiguously differentiated only by cross comparing several images under various hydrographic conditions. (In fact, LANDSAT imagery is very poor for this kind of determination because its resolution is so coarse.)
- (2) It appears that much of the sinuosity indicated in the turbidity patterns of the imagery in James *et al.* (1977) is due to the distribution of shoals and the presence/absence of seagrasses, rather than sediment in suspension. The seagrass map of Kaldy and Dunton (1997), shown as Figure 7.2 in Brown and Kraus (1997), should be compared to the dark regions in the LANDSAT imagery of James *et al.* (1977), for example Figure 5-2 in Brown and Kraus (1997). They agree almost exactly.
- (3) The tidal excursion is only a couple of km in the Lower Laguna and less in other regions of the study area. To depict the current sinuosity as a trajectory (such as Figure 7-28) is therefore misleading, suggesting large-scale movement along the trajectory in a tidal cycle. The actual current excursion will be only a fraction of the length of the trajectory.

Brown and Kraus (1997) propose that the bathymetric depression crossing the axis of the GIWW in this vicinity is responsible for the cross-channel direction of currents. A more likely explanation is that the direction of currents is determined by other factors, and the depression is the expression of erosion and transport by currents in this dominant direction. Morton *et al.* (1998) reported a careful analysis of

historical aerial photos of Placement Area 233, which is in the northern half of the high-maintenance reach, to the west of the GIWW. They found depositional zones due to reworked sediment building to the west and south, which is consistent with the preferred axes of transport indicated in Section 7.2 for this area. The relation between disposal sediment reworking and physiography determined by Morton *et al* (1998) is straightforward: there is greater reworking for those placement areas (PAs) located in deeper water. Such PAs are more exposed to waves and currents. In the shallower areas, much of the PAs are subaerial, and after the fine sediments are winnowed by wind, these become armored by a lag of coarser sediments. The general correlation between wind and TSS in the Lower Laguna, and lack of same at the other stations, supports the role of currents and waves in reworking the disposed sediment. More sediment mobilized in this way from PA 233 and 234 (adjacent to the high maintenance reach) means more available to be transported across the GIWW and to settle out as maintenance material.

The data collection enterprise on the Laguna Madre has acquired a wealth of hydrodynamic and hydrographic data. The primary purpose of this project was to evaluate, correct and compile this data into files of "scrubbed" measurements, then carry out the same level of analysis on these complete data sets as performed in the Year-1 reports, Brown and Kraus (1997) and Brown (1997). Conclusions based upon the data recovery aspect of the work are as follows

- (1) Data anomalies are a ubiquitous feature of these robot data acquisition systems. While there is no way to avoid their occurrence, these anomalies will corrupt analyses of the data and must be eliminated before analysis.
- (2) Among the anomalies encountered in the data records from this project are data gaps, zero values, time discontinuities, anomalous or "freak" values, quantum jumps in the time history of a variable, and flatlines. Most of these required a degree of manual editing to detect and correct.
- (3) The data sets analyzed in the Year-1 reports in fact also contained undetected anomalies, which have been expunged in the present work.
- (4) In addition to the normal sources of anomalous records from an automated system, the data holdings suffered further from hardware problems in the data archive.

Archival digital copies of the final "cleaned" data files are transmitted separately. Because of the principle of diminishing returns, there remain unresolved anomalies in these files, but these are considered to be in such a minority that corruption of the analysis is minimal.

With respect to data analysis, various displays, statistics and tabular depictions of the data sets have been developed. A selection has been presented in previous chapters, and the full sets are given in separate Appendices. A number of conclusions have been drawn, as follows:

- (1) The annual wind roses are dominated by prevailing SE winds from the Gulf of Mexico. There is year-to-year variation in the annual winds. Monthly wind roses display a shift from predominantly southeasterly wind regimes in summer to bimodal in winter, i.e. alternating southeasterly and northerly winds resulting from frontal passages.

- (2) Power spectra of wind are characterized by a prominent spike at exactly 1 cpd, i.e. period 24 hours. This is the signal from the seabreeze. The seabreeze spike is present throughout the year, minimal during the winter months, and maximal in the period June - September. The greatest seabreeze energy is in the E-W component, transverse to the coastline.
- (3) Several lower frequency signals, particularly around 3- and 6-day periodicities appear in the wind spectra for the fall through spring period, being maximal in winter. These are the result of frontal passages during the winter and equinoctial seasons. Most of the energy of the frontal-passage periodicities is in the N-S component.
- (4) Power spectra of water level in the study area contain energy deriving from both tides and winds, as well as longer period variation due to meteorology (notably, frontal passages). In the annual spectra, there are prominent peaks at approximate periods of 12, 12.4, 24 and 25.5 hrs. Wind forcing is responsible for the 24-hr spike, mainly the seabreeze. This conclusion is reinforced by the coherency between wind and water level at this period, and by the seasonal increase of the energy in the 24-hr signal, being greatest during the summer.
- (5) The tidal semidiurnal and diurnal signals from the Gulf of Mexico are substantially filtered with passage through the inlets into the Laguna Madre. The semidiurnal tide is nearly eliminated from both the Upper and Lower Lagunas, being evident only as a minor peak in the annual power spectra. The diurnal tide is attenuated, but is detectable in the power spectra in both systems. Longer period water level variations, mainly the fortnightly associated with the cycle of lunar declination, and the seasonal semi-annual variation, are the most important sources of regular water level variation, but they raise and lower the Laguna waters so slowly that their effect on currents is negligible.
- (6) The current measurements performed at the platforms offer a direct index to mechanisms that may have a role in mobilization and transport of sediment. The original instrumentation measured the three components, including the vertical. Most important are the horizontal components of the current. The data for the vertical component appear spuriously large, and were given no further attention in this analysis.

- (7) The long-term statistics of measured currents indicate that each station exhibits a propensity for net flow. In the Lower Laguna, at both LLM1 and LLM2, there is a northward component in the net flow, which may be the result of a mean wind-driven circulation entering the Lower Laguna through Brazos Santiago and exiting through Mansfield Pass. In the Upper Laguna, station ULM2 does not set north-south as one might anticipate from the geometry of the Laguna, and as is exhibited by ULM3 farther south, but has a significant component directed into Baffin Bay. Station ULM1 in Corpus Christi Bay just north of Bulkhead Flats shows predominantly westerly currents, paralleling the trend of the south shoreline and the bayward margin of the Flats. Current speeds are lowest in the interior of the Upper Laguna, compared to Corpus Christi Bay (ULM1) or the Lower Laguna.
- (8) The energy in the power spectra of (horizontal) currents is greatest in the Lower Laguna at LLM1 and lowest in the Upper Laguna. The peaks in the power spectra are at solar diurnal, and lunar diurnal and semidiurnal periods, though the relative importance of these is highly variable from platform to platform.
- (9) There is considerable month-to-month variation in spectra at some of these stations, as well as year-to-year variation. Energy in the lower frequency (longer period) portion of the spectrum is more prominent during the winter months than in the summer, and is more prominent in the Upper Laguna than in the Lower. This is the part of the spectrum that is dominated by meteorological forcing at 3-7 day periods, hence the prominence in the winter months, and the greater influence in the Upper Laguna.
- (10) The detailed behavior of the current vector was analyzed by constructing monthly scatterplots and current roses. These are complementary plots that should be studied as companion diagrams. The scatterplots preserve all of the vector information of the individual measurements, and the distribution of the data points can give a visual impression of the speed/direction variation of the data, but biased toward the extreme values, because the smaller currents are overplotted as a massive cluster. The rose on the other hand is a statistical summary in graphical format, in which currents are sorted into bins of directional and speed ranges. These diagrams are analyzed for
- (i) extent of bi-directionality
 - (ii) prevalence of noncompensating directions, indicating a net nonzero flow component

- (iii) asymmetry in current speeds
 - (iv) prevalence of favorable axes, versus more omnidirectional distributions
 - (v) alignment with physiographic constraints such as bathymetry or shoreline
- (11) These vector displays disclosed that the currents do seem to exhibit movement along a preferred axis. This is consistent with the back-and-forth type of forcing typical of bays and estuaries, usually driven by tides, which produce the classical "current ellipse". However, in the Laguna Madre data, this behavior is much more complex. By a detailed study of a few station/months selected from these data holdings, employing a special-purpose analysis to fit a "normal least squares" to the data by 25-hr-duration steps, we determined:
- (a) There is more than one preferred axis at each of these platforms, presumably corresponding to modes of large-scale circulation
 - (b) The circulation appears to be metastable, following a given preferred axis for a number of tidal cycles, then shifting to another axis.
 - (c) Shifts from one axis to another are more-or-less synchronous in different regions of the system, indicating a large-scale systemic shift from one circulation regime to another. The mechanism that forces this shift is not clear from the few months of data analyzed here
 - (d) In lower Corpus Christi Bay, i.e. at ULM1, one preferred axis is along a N-S trajectory, and the other is along a line about 50° E of N. The former corresponds to flow in and out of Bulkhead Flats, while the latter roughly parallels the shoreline (and bayward margin of Bulkhead Flats).
 - (e) At the mouth of Baffin Bay, i.e. at ULM2, one preferred axis is 10° (i.e., 190°) E of N, approximately the axis of the GIWW, and the other is 50° E of N, the direction of the entrance to Baffin Bay
 - (f) In the Lower Laguna, at LLM1 there are two preferred axes, at 15° and 70° E of N, the former being the one identified by Brown and Kraus (1997) from their scatterplots. At least two axes are indicated at LLM2, at about 45° and 120° E of N.

- (12) Dredging contracts were active in the early months of the data collection. In the Lower Laguna, there is a tendency for higher TSS magnitudes during the dredging periods than prior to the contract or (one year) after the contract. While dredging would appear to be a factor, there are clearly other processes operating, because the TSS magnitudes are nearly as large in spring of 1996 when no dredging was underway. In the Upper Laguna, there is no clear difference between "dredging" and "post-dredging" periods partly due to the fact that the contract dredging period, very early in the data collection, was not well sampled.
- (13) Two measures of suspended sediments were made in the data collection program. Total suspended solids (TSS), a filtration determination, was measured on water samples collected at 12-hr intervals, and turbidity was measured automatically at the same interval as the current measurements using an optical backscatter (OBS) sensor on the platform. The OBS was a bold experiment to determine sediment concentrations on the same fine time-resolution as the other robot measurements, which, if successful, would allow direct computation of several important parameters relating to sediment mobilization and transport. Because the OBS sensor is sensitive to biofouling, the data proved untrustworthy, and could not be used quantitatively in this study.
- (14) There is no clear association between current velocity and the surges of TSS. The statistical relation between the two is nil, however the majority of data are low current speeds and low TSS, whose lack of correlation dominates the statistics. There may be relations between extremes of current and extremes of TSS. Where there is an association, it seems to be more governed by current direction than current speed. Longer rises in TSS seem to be associated with a direction of current, e.g. a mean northward set accompanies the higher TSS values observed in the Lower Laguna during April-May 1996.
- (15) In the Lower Laguna, at LLM1, there is an association between wind speeds and TSS, with elevated TSS values during periods of sustained higher winds, notable July and August 1995, and April and May 1996, and clear correspondences between spikes of TSS and spikes in wind speed, especially for those wind spikes exceeding 12 m/s. This is also the case in Corpus Christi Bay, ULM1, though the values of TSS are lower than in the Lower Laguna, and the clearest association is for wind speed spikes.

exceeding 14 m/s. In the Upper Laguna, there is no clear relation, though the TSS values are generally higher in summer of 1996 than summer of 1995, and wind speeds were also higher in 1996 than 1995.

- (16) In the Year-1 report, Brown and Kraus (1997) gave special attention to the reach of the GIWW crossing the Lower Laguna that for 50 years has exhibited high shoaling rates in a 5-km subreach extending from Cullen Bay almost to Port Isabel, midway in which platform LLM1 was placed. From current vector scatterplots, Brown and Kraus (1997) identified a component of the current at an acute angle across the axis of the GIWW, and proposed that this cross-channel flow in association with the practice of disposing of the dredged material to either side of the GIWW is responsible for the high maintenance rates. The present analyses confirm that there is indeed a prominent cross-channel component of current in this reach of the GIWW in the direction identified by Brown and Kraus (1997). The present results indicate, however, that there is more than one preferred axis of this transport at this station, a second axis being directed almost perpendicular to the GIWW. Moreover, at each of the platform stations maintained during this study there is at least one mode of transport across the GIWW indicated in the current data.
- (17) In an earlier study of the high-maintenance reach of the GIWW, James, *et al.* (1977) inferred current trajectories from the patterns of turbidity in several LANDSAT images from the 1970's, and proposed that there was generally flow at an acute angle across the GIWW in the center of the high-dredging reach. This general trajectory of currents agrees with the directions inferred by Brown and Kraus (1997) from scatterplot current diagrams. It is the conclusion of the present study that this is only one of at least two preferred current directions, effecting cross-channel transport, and the current trajectory proposed by James *et al.* (1977) is based in part upon misinterpreting the patterns of shoals and seagrasses also visible in the LANDSAT image. This conclusion in no way undermines the inferred importance of the cross-channel transport as a factor in the high maintenance of this reach. It does underscore that cross-channel transport occurs more broadly and in other preferred directions in this vicinity. The solution, which might occur to some readers based upon the proposed current trajectory of James *et al.* (1977), of moving the present PAs 233 and 234 a short distance north or south to be out of the main cross-channel trajectory, would be ineffective.

The initial data collection effort and the present data recovery and analysis are, foremost, research projects. As such, as many questions about the mechanisms of hydrography and sediment transport in the Laguna have been raised as answered, and additional work is needed. The following specific recommendations are proffered:

- (1) In any data collection enterprise such as that of the Conrad Blucher Institute (CBI), a major strategic issue is how much effort and resources to invest in the processing and quality-assurance tasks before archiving the data. The CBI provides a major service to agencies and researchers in the Texas coastal zone in the collection, archiving and dissemination of data from its TCOON system, and the users generally understand that this data must be evaluated and subjected to Q/A procedures before using. We generally concur with the procedures employed by CBI, but offer two recommendation(s).
 - (i) that preliminary screening of the data be carried to identify quantum shifts in variables, time slips, and flatlines (especially zero values)
 - (ii) that field maintenance protocols include in situ measurements of the same variables monitored by the platform, e.g. current velocity, salinity, temperature

Many problems with data acquisition at the platform are in principle detectable and capable of correction if such early screening methods are employed; this, in turn, would reduce irrecoverable data loss

- (2) A surprising finding of this project is the existence of multiple preferred axes of current direction, and that these seem to evidence larger-scale metastable modes of circulation in the Laguna Madre and Corpus Christi Bay. We recommend that the type of analyses initiated here for a selection of the data base be made more rigorous and be applied to the entire data base to better determine the nature of these circulation modes. These analyses should include companion data on meteorology and Gulf of Mexico hydrography, as potential trigger mechanisms for forcing the shift from one mode to another. This result would not only be of intrinsic scientific interest, but would be of potential practical value in at least two respects: (a) identifying a hydrodynamic feature of the Laguna Madre that could serve as a

suitable crucial test for validating hydrodynamic models; (b) identifying the conditions under which favorable or adverse sediment transport occurs, thereby providing guidance to scheduling and methods of dredged material placement.

- (3) The OBS offered promising technology for detailed measurement of important sediment transport processes. That it failed in the present project only underscores the fact that this is new technology which will require additional effort to develop into a practical and reliable methodology. Recent experiments with transparent antibiofouling compounds by the staff at the Blucher Institute may indicate a way to control this problem. We recommend continued experimentation with the OBS at CBI
- (4) The fact that there is no correlation between TSS and currents in either the Upper or the Lower Laguna, but there may be an association between extremes of wind and extremes of TSS, raises questions about the causal mechanism. We speculate that the increases in TSS monitored at these platforms may be in response to sediment resuspended elsewhere in the system (perhaps increased windwave activity in the windward shallows) and transported into the platform area by local circulations. The fact the spikes in TSS seem to be more associated with the direction of current than the speed adds support to this interpretation. Additional analysis and modeling using the data collected in this program, supplemented by TCOON data and archival remote sensing, are recommended to better determine the processes leading to these surges in TSS
- (5) Cross-channel currents in the high-maintenance reach of the Lower Laguna were confirmed in the present analysis. These can be a significant mechanism for transport of suspended sediment across the GIWW, where a proportion of the sediments will settle out in the deeper water, thus contributing to the shoaling in the channel. Brown and Kraus (1997) recommended placement of the dredged material from the high maintenance reaches, presently being placed in Areas 233 and 234, in confined or upland areas to prevent their transport back into the GIWW. In effect, this means stabilizing or abandoning these placement areas for future disposal. We concur with this recommendation, noting that Morton *et al* (1998) found shallow-water or subaerial placement areas to be less exposed to windwave remobilization and the GIWW reaches using such PAs to be low-maintenance.

- Atturio, J., D Basco, and W. James 1976 Shoaling characteristics of the Gulf Intracoastal Waterway in Texas. Report TAMU-SG-76-207, Texas A&M University Sea Grant, College Station
- Behrens, E.W. 1966 Surface Salinities for Baffin Bay and Laguna Madre, Texas, April 1964 - March 1966 *Publs Inst Ma. Sci.*, 11, pp 168-173
- Bloomfield, P 1976. *Fourier analysis of time series: an introduction*. New York: John Wiley
- Breuer, J P 1961 Life history studies of the marine flora of the lower Laguna Madre area Job Completion Rep M-9-R-3, Job No E-4, Dept. Coastal Fish., Texas Parks & Wildlife
- _____. 1962. An ecological survey of the lower Laguna Madre of Texas, 1953-1959 *Pub. Inst. Marine Sci.*, Vol. 8, 153-183
- Brown, C 1997. Data Report September 1994 - May 1997, Environmental monitoring of dredging and processes in Upper Laguna Madre, Texas Conrad Blucher Institute, Texas A&M University—Corpus Christi.
- Brown, C. and N Kraus. 1997 Environmental monitoring of dredging and processes in Lower Laguna Madre, Texas Tech. Rep. TAMU-CC-CBI-96-01, Conrad Blucher Institute, Texas A&M University—Corpus Christi.
- Collier, A and J. Hedgpeth. 1950. An Introduction to the Hydrography of Tidal Waters of Texas *Publ. Ins. Mar. Sci* , 1 (2), pp 120-194
- Espey, Huston & Associates, Inc. (EH&A) 1998a Benthic macroinfaunal analysis of dredged material placement areas in the Laguna Madre, Texas - spring and fall surveys EH&A Document No. 970740: 90 pp. + appendices. Austin, Texas.
- _____. 1998b Laguna Madre, Contaminant assessment EH&A Document No 971410. Austin, Texas
- James, W., S. Giesler, R. DeOtte, and M Inoue 1977. Environmental considerations relating to the operation and maintenance of the Texas Gulf Intracoastal Waterway. Report TAMU-SG-204, Sea Grant Program, Texas A&M University, College Station
- Kaldy, J and K. Dunton. 1996 Light attenuation processes in the lower Laguna Madre of Texas. In C A Brown and N.C Kraus (eds), environmental monitoring of dredging and processes in the lower Laguna Madre. Final Report to the U.S. Army Corps of Engineers. 118 pp
- _____. 1997 Light attenuation Chap 6 in Brown and Kraus (1977), pp 62-73.
- Kraus, N.C., A. Lohmann, and R. Cabrera. 1994. New Acoustic Meter for Measuring 3D Laboratory Flows *Journal of Hydraulic Engineering*, 120(3), 406-412
- Lee, K.L. 1997. *Time series analysis of salinity with unequally spaced observations in Galveston Bay* Ph.D Dissertation, Dept Civil Engr , University of Texas at Austin.

- Lee Wilson & Associates, Inc. (LW&A). 1998a Characterization of dredged material, Laguna Madre, Texas. LW&A Document No. EP556014 Santa Fe, New Mexico.
- Lyles, S., L. Hickman, and H. Debaugh. 1988 Sea level variations for the United States, 1855-1986 National Oceanic and Atmospheric Administration, National Ocean Service, Rockville, Maryland
- Madansky, A 1959 The fitting of straight lines when both variables are subject to error. *Am Stat. Assoc. Jnl.* 54 (285), pp. 173-205.
- Militello, A. and N. Kraus. 1994. Reconnaissance investigation of the current and sediment movement in the lower Laguna Madre between Port Isabel and Port Mansfield, Texas. TAMU-CC-CBI-94-04, Conrad Blucher Institute, Texas A&M University—Corpus Christi.
- Militello, A , N C Kraus, and R.D Kite 11 Environmental Monitoring of Dredging and Processes in the Upper Laguna Madre, Texas. U.S. Army Corps of Engineers, Galveston District
- Morgan, G., D Brunkow, and R. Beebe, 1975 *Climatology of surface fronts* Circ 122, Illinois State Water Survey, Urbana.
- Morton, R., W. White, R Nava and G. Ward 1998. *Sediment budget analysis for Laguna Madre, Texas, an examination of sediment characteristics, history and recent transport*. Report to Galveston District Corps of Engineers, Bureau of Economic Geology, University of Texas at Austin
- National Oceanic and Atmospheric Administration. 1983 Laguna Madre. Technical Report, prepared for the Texas General Land Office by Tides and Water Level Branch, NOAA.
- Onuf, C.P 1994. Seagrass, dredging and light in Laguna Madre, Texas, U.S.A. *Est., Coastal Shelf Sci.*, 39, pp 75-91
- Pejrup, M 1986. Parameters affecting fine-grained suspended sediment concentrations in a shallow micro-tidal estuary, Ho Bugt, Denmark *Est., Coastal Shelf Sci.*, 22, pp 241-254.
- Priestley, M.B. 1981 *Spectral analysis and time series* (2 vols) London: Academic Press.
- Pugh, D.T. 1987. *Tides, surges and mean sea-level*. Chichester John Wiley & Sons.
- Quammen, M. and C Onuf. 1993. Laguna Madre. Seagrass changes continue decades after salinity reduction. *Estuaries*, 16 (2), pp 302-310.
- Schoellhammer, D.H. 1995 Sediment resuspension mechanisms in Old Tampa Bay, Florida. *Est., Coastal & Shelf Sci* , 40, pp 603-620.
- Shepard, F and G. Rusnak 1957 Texas bay sediments. *Publ. Inst. Marine Sci.*, 4 (2), pp 5-13.
- Sheridan, P. 1998. Colonization of dredged material placement areas by shoalgrass in Lower Laguna Madre, Texas, and the habitat value of these sites for fishery species. Final Report to the U S. Army Corps of Engineers, Galveston District, Galveston, Texas

- Shideler, G L 1984 Suspended sediment responses in a wind-dominated estuary of the Texas Gulf coast. *J. Sed. Petrol.* 54 (3), pp 0731-0745.
- Smith, N.P. 1978 Intracoastal tides of upper Laguna Madre, Texas. *Texas Journal of Science*, 30 (1), pp 85-95.
- Texas Department of Water Resources 1979 *The influence of freshwater inflows upon the major bays and estuaries of the Texas Gulf Coast* Report LP-115 TDWR, Austin
- U.S. Army Corps of Engineers 1998
- Ussery, S 1997. Data Report, Environmental monitoring of dredging and processes in Upper Laguna Madre, Texas. Conrad Blucher Institute, Texas A&M University—Corpus Christi
- _____. 1998 Addendum to Data Report (Ussery, 1997), corrected analyses for ULM3 1995-1996 Conrad Blucher Institute, Texas A&M University—Corpus Christi.
- Ward, G. and C Montague. 1996. Estuaries Chapter 12, *Handbook of Water Resources* (L. Mays, ed) New York McGraw-Hill
- Ward, G.H 1981. *Intensive Inflow Study. Laguna Madre of Texas, July 1980*. Doc No. 81013, Espey, Huston & Assoc., Austin, Texas.
- _____. 1993. Dredge and fill activities in Galveston Bay. Doc. GBNEP-28, Galveston Bay National Estuary Program, Texas Natural Resource Conservation Commission, Austin.
- _____. 1997 *Processes and trends of circulation within the Corpus Christi Bay National Estuary Program Study Area* Report CCBNEP-21, Corpus Christi Bay National Estuary Program, Corpus Christi, Texas
- Ward, L., W Kemp, and W Boynton. 1984. The influence of waves and seagrass communities on suspended particulates in an estuarine embayment *Marine Geology*, 59, pp 85-103